# DEVELOPMENT OF SEISMIC VELOCITY ANALYSIS SOFTWARE

by

EMIL KHALIL SAID

Thesis submitted for the degree of Master of Science (by research) at the University of Glasgow, Department of Geology and Applied Geology, September 1990.



ProQuest LLC.
789 East Eisenhower Parkway
P.O. Box 1346
Ann Arbor, MI 48106 – 1346

*To my parents; with all my love and respect*

# DECLARATION

The material presented in this thesis is the results of independent research by the author undertaken between October 1987 and June 1990 at the Department of Geology and Applied Geology, University of Glasgow. Any published or unpublished results of other works have been given full acknowledgment in the text.

Department of Geology and Applied Geology,
University of Glasgow,
Glasgow,

# ACKNOWLEDGEMENTS

My first thanks must be to the *Iraqi Government* for the scholarship which made my studies possible.

The completion of this thesis would not have been possible without the assistance of a number of people, particularly those mentioned below.

I would like to thank my supervisor, Dr. J. J. Doody, for his guidance and generous sharing of expertise throughout this project. Thanks are due to Professor B. Leake for making available the facilities and resources of the department and to Dr. C. Farrow for his advice and assistance regarding the complexities of the computer system. Professor D. K. Smythe is also thanked for his cooperation and advice.

I am indebted to Mr. R. Morrison for supplying, almost, everything he can, to Eddie for accommodating my needs regarding departmental transport, and to Bob for providing technical assistance and an enlightened grasp of the English language. My thanks also go to my friend and colleague Zayd for his help and stimulating discussions on matters scientific and social, and to Ursilla for providing me with the best coffee and water of life ever I had.

Last, but not, least my special thanks to my family : to my parents for their unfailing love, encouragement and concern, to my brother Nabil for his financial and emotional support during my studies and to my sisters, and to my wife and children for their patience, love and understanding during the ups and downs of the last three years.

# Table of Contents

# ABSTRACT

Seismic velocity analysis software was developed. The main program was written in FORTRAN77 and mounted on a SUN workstation. Options for the users include three types of time correction (reflection, refraction, and continuous velocity increase with depth) and five methods to compute the coherency coefficient value (semblance, energy normalised crosscorrelation sum, statistical normalised crosscorrelation sum, unnormalised crosscorrelation, and the mean amplitude summation). Four S-Macros were written to display the results in the form of contour lines, window peak power, maximum coherency coefficient, and velocity spectrum. The software was tested using synthetic and field data. Two sets of field data were used, the first was recorded for this project using blasts at Newburgh quarry as the source and was called dataset A. The second was data from the South West England Seismic Experiment (SWESE) and was called dataset B.

Results obtained, by the software, from dataset A match that of the regression analysis showing two segments of velocities, the first with 5.24 km/s at time intercept of 0.02 s and the second at greater offsets with a velocity of 4.55 km/s at a time intercept of -0.01 s. Some results, of dataset B, obtained by the software confirm a previous interpretation of the data while some other did not.

It was concluded that the software could be a useful support tool in guiding or confirming other methods of interpretation, but that the conditions of use had to be carefully evaluated.

# INTRODUCTION

The aim of the project was to design seismic velocity analysis software which would correct the arrival time of seismic data according to an assumed travel time function using one of three expressions, as requested. Then, a coherency coefficient value is computed employing one of five methods. Finally, the results would be displayed, in the time-velocity domain, in four types of plots.

A large volume of synthetic seismic data was constructed for this project to test the performance of the software in dealing with common cases of events.

Testing the software on field data followed two paths. One profile was recorded specifically for this project in simple area which has been well studied. The software was tested also on a pre-existing sparse wide-angle data to examine the benefits of the software for such data.

In the first chapter a general review of principles and theories used will be discussed. A description of the software will be presented in chapter two. Chapter three will deal with synthetic trace tests. In chapter four, the acquisition and digitisation of the test field data will be presented. Chapter five will discuss results obtained from these field data. Finally, conclusions and recommendations will be given in chapter six. For ease of reference, the numerous figures of chapters three, four, and five are placed at the end of each chapter.

# Chapter 1

# GENERAL REVIEW : PRINCIPLES AND THEORY

## 1.1. Introduction

Seismic data processing has grown very rapidly as a branch of time series analysis during the last twenty-five years with the help of computers. All steps of processing have been affected. Many factors outwith the processing stage may affect the results of processing strongly: for example, field acquisition parameters and equipment, geological conditions, environmental and demographic restrictions.

The aim of seismic processing is to detect and extract signals from a seismogram which are related to the subsurface structure, and to eliminate (or suppress) all other signals, commonly known as *noise*. Noise is generated by seismic equipment, nonseismic sources or passing through other than the desired path (Silverman 1967).

Signals can be expressed in two forms as a time function: continuous, representing the amplitude of the signal as a function of time ( analogue form), or as a series of numbers each of which represents the amplitude of the signal at equal increments of time (digital form). The process of converting from analogue to digital form is called "digitisation" (Robinson & Treitel 1964, Silverman 1967).

In the processing stage, which is the middle stage between recording the data in the field and interpreting it to obtain useful geological information, many techniques can help to achieve the task. These include filtering, stacking, velocity analysis, trace corrections, migration, common depth point composition, plotting,

(e.g. Silverman 1967, Dobrin 1976).

Velocity analysis, in exploration seismology, is well known and widely employed for reflected events. In this project it was employed for direct and refracted, as well as reflected, events. That was accomplished by employing different expressions to correct the time of the data before computing coherency coefficients.

Aspects of velocity analysis, which is the aim of this project, will be discussed. Theoretical background will be summarized for time corrections and coherency measures employed in this work. Frequency filtering, which was used as a pre-velocity analysis option, will be presented briefly.

## 1.2. Velocity studies

In situ velocity can be determined either by a borehole sonic log, which represents direct measurement of the velocity with which a seismic wave travels in the earth as a function of depth, or from seismic data, which provide an indirect measurement of velocity. Velocity is an important parameter in seismic processing and controls the processing quality (Al-Sadi 1980). In the seismic method three types of ray path exist by which energy may travel from a near-surface source to a receiver on the surface (Kearey & Brooks, 1984).

[1] *Direct :* in which the energy travels directly, in a straight line, from the source to the receiver. It is the first arrival at offsets less than the "cross over" distance, which is the offset distance where the direct ray is overtaken by a refracted ray.

[2] *Refracted :* in which the energy travels obliquely down and meets an interface at the critical angle, the angle of incidence for which the refracted ray grazes the surface of contact between the two media (Sheriff 1968), travels along the interface and returns to the surface at the same critical angle.

[3] *Reflected :* in which the energy travels down to an interface and is reflected back to the surface. There must be a difference in the acoustic impedance, the product of density and compressional velocity, of the layers either side of the interface.

Velocity may be expressed in a variety of ways :

[1] Apparent Velocity : the reciprocal of the gradient of the travel-time curve.

[2] Interval Velocity: the velocity of a seismic wave in a single homogeneous layer

[3] Average Velocity : the mean velocity of the wavelet averaged over travel time, and used to convert from travel-time to depth.

[4] Normal Moveout Velocity : the velocity used to calculate the normal moveout.

[5] Root Mean Square Velocity : the weighted root mean square of layer interval velocities, the weights being determined by the thickness of the layer.

[6] Stacking Velocity : the velocity which gives the optimum stack, or the highest coherency measure, when used for NMO correction.

### 1.3. Velocity Analysis

Velocities estimated from seismic data require data at different non zero offsets. Thus seismic waves arrive at different detectors at different travel times, which is the interval between the shot instant and the arrival of the energy at a receiver (Sheriff & Geldart, 1982). Using estimated seismic velocities one can correct travel time to that at a reference offset which, in this study, is taken to be at zero distance. The necessary correction is henceforth referred to as "*Time correction*".

#### 1.3.1. Time Corrections

The goal of time correction, in this work, is to remove from seismic traces

that time difference caused by offset differences. Summation, following such correction, of the traces in an array will lead to enhancement of any signal crossing the array with the parameters specified in the correction formula (see below). Hence velocity analysis can be carried out on the dataset.

Three expressions for reflection, refraction, and continuous velocity increase with depth, were used in this project to compute time correction.

[1] *Time Correction for Reflection data :*

Time correction for such data is widely known as *Normal Move Out (NMO).* Consider the simple case of a single horizontal layer (Fig. 1.1).

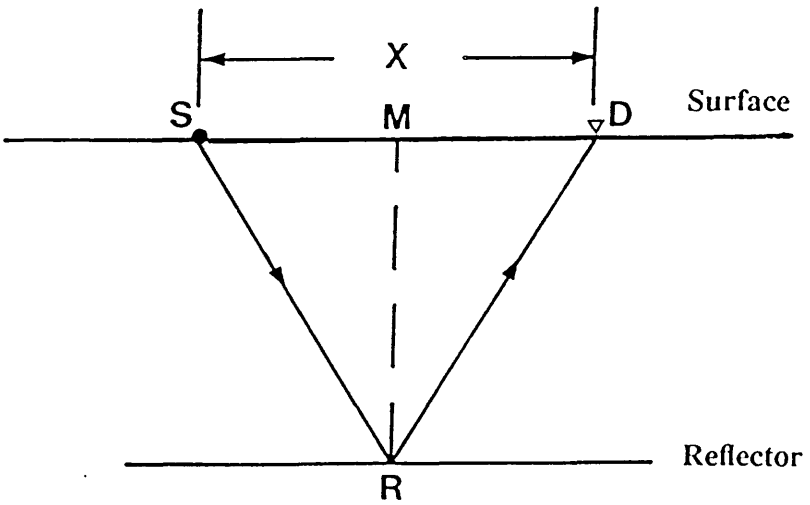


Fig.1.1 Time correction (NMO) geometry, for reflection data.

The travel time along the ray path from the source S to the reflection point R then to detector D is $T_x$ and the travel time equation as a function of offset, using Pythagoras Theorem, is

$$T_x^2 = T_o^2 + \frac{X^2}{V^2} \tag{1-1}$$

where

$T_o$ is two way normal travel time to the reflector

$X$ is the offset

$V$ is the velocity of the medium above the reflector

So the travel time curve as a function of the offset for single horizontal reflector is a hyperbola (eq. 1-1), the equation velocity may be referred to as the NMO velocity and (as stated above) is equal to that of the layer. In the case of a dipping layer the NMO velocity is the velocity of the layer divided by the cosine of the dip angle (Levin 1971, Montalbetti 1971). In the case of horizontal multi-layer strata (Fig. 1.2),

$$T_{o,n} = \sum_{i=1}^{i=n} t_i \tag{1-2}$$

$$= \sum_{i=1}^{i=n} \frac{d_i}{v_i} \tag{1-3}$$

$$V_{a,n} = \frac{\sum_{i=1}^{i=n} v_i \; t_i}{T_{o,n}} \tag{1-4}$$

where

$v_i$ is the interval velocity at i-th layer

$d_i$ is the thickness of i-th layer

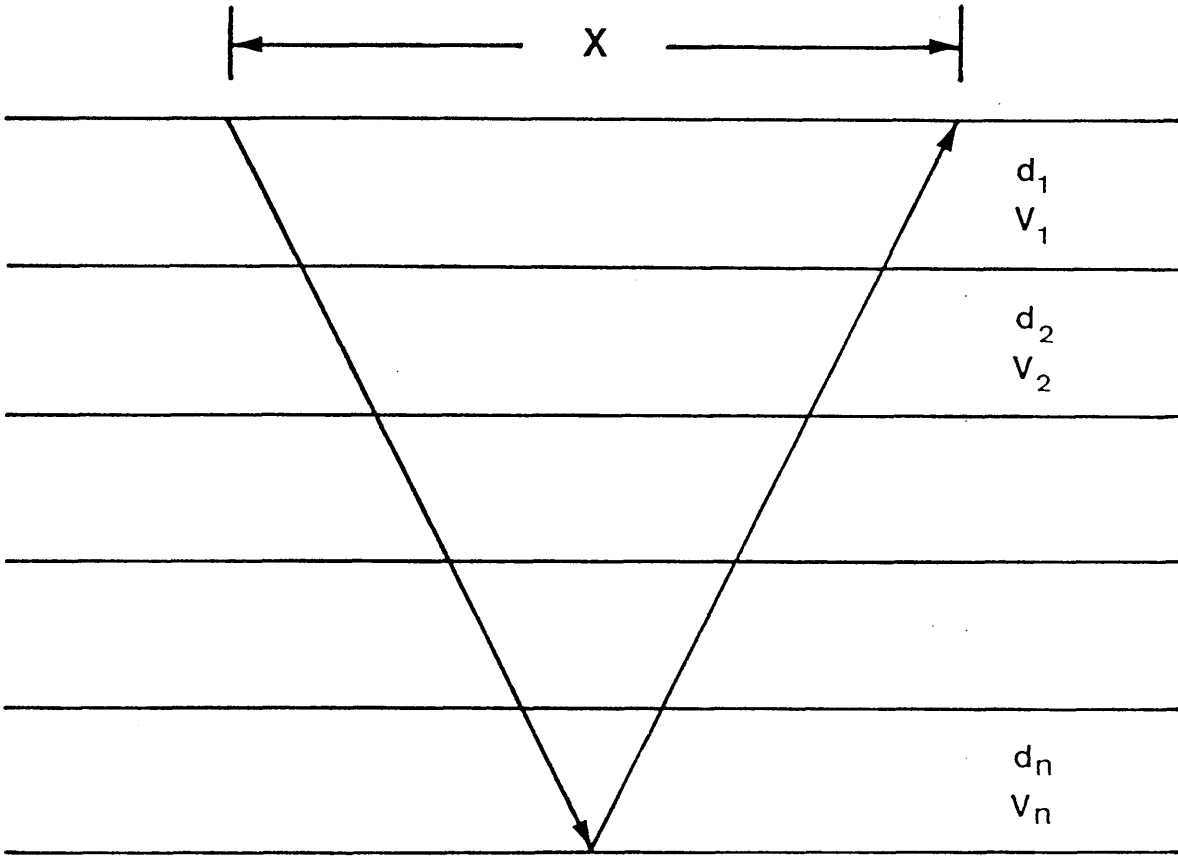


Fig.1.2 Straight ray analysis in a horizontally layered medium (after Taner & Koehler 1969).

$t_i$ is the two-way travel time within the i-th layer

$x$ is the offset

$T_{o,n}$ is the two-way normal travel time to the base of n-th layer

$V_{a,n}$ is the average velocity to the base of n-th layer

Assuming that a wavefront travels along the shortest path ( distance ) between the source, reflector and the receiver the travel time is given by,

$$T_{x,n}^2 = T_{o,n}^2 + \frac{X^2}{V_{a,n}^2} \tag{1-5}$$

According to Fermat's principle, the wavefront will travel along the shortest time path (Fig. 1.3). Thus the arrival time at a receiver at offset X from the energy source after travelling to an interface n is given by the infinite series :

$$T_{x,n}^2 = C_1 + C_2X^2 + C_3X^4 + \ldots + C_jX^{2j-2} + \ldots \tag{1-6}$$

where the coefficients $C_1$, $C_2$, $C_3$, .... depend on layer thickness and the interval velocity (see appendix A of Taner & Koehler 1969). They showed that

$$C_1 = a_1^2 \tag{1-7}$$

$$C_2 = \frac{a_1}{a_2} \tag{1-8}$$

$$C_3 = \frac{a_2^2 - a_1 a_3}{4 a_2^4} \tag{1-9}$$

where

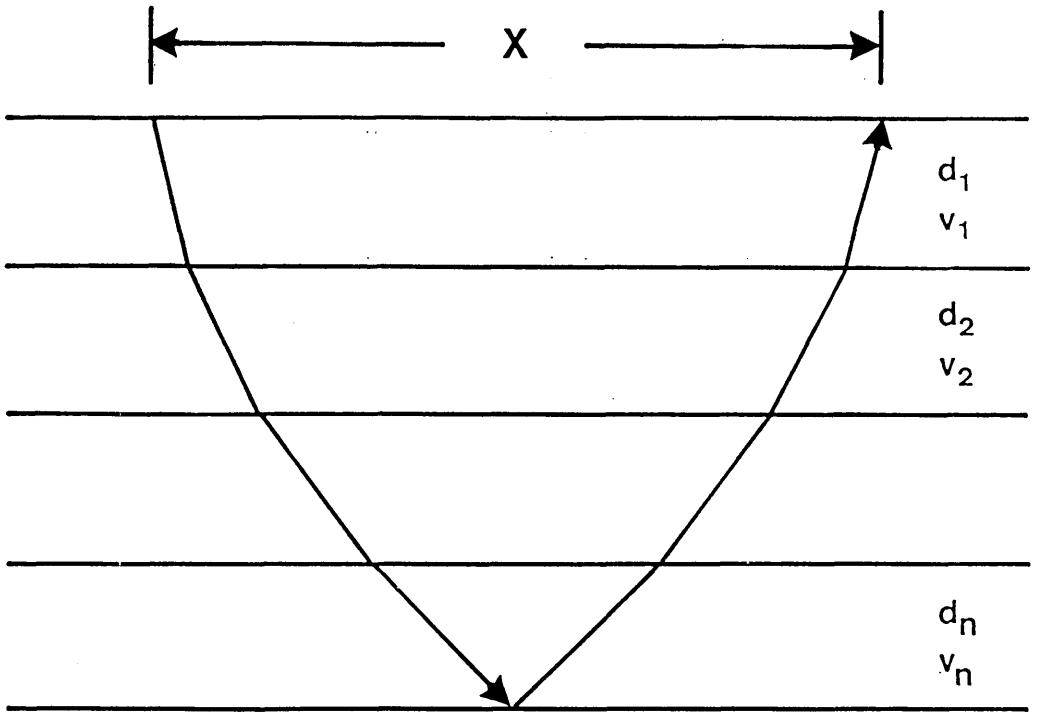


Fig.1.3 Snell's Law ray analysis in a horizontally layered medium (after Taner & Koehler 1969).

$$a_m = 2 \sum_{k=1}^{k=n} v_k^{(2m-3)} d_k \qquad (1\text{-}10)$$

where m = 1, 2, 3, . . . .

Taner & Koehler explain that $C_3$ is always negative except when $v_1 = v_2 = v_3 = \ . \ . \ . = v_n$ then its value is zero and that the convergence of eq. 1-6 has been found to be quite rapid for all values of X of interest, therefore the first two terms give sufficient accuracy for practical purposes in a great many cases. So the travel time equation may be expressed as

$$T_x^2 = C_1 + C_2 X^2 \qquad (1\text{-}11)$$

$$= \left( \sum_{i=1}^{i=k} t_i \right)^2 + \frac{\sum_{i=1}^{i=k} t_i}{\sum_{i=1}^{i=k} t_i \ v_k^2} \ X^2 \qquad (1\text{-}12)$$

$$= T_o^2 + \frac{X^2}{V_n^2} \qquad (1\text{-}13)$$

where $V_n$ is the apparent time weighted velocity and is the same velocity as given by Dix (1955), commonly known as the root mean square velocity :

$$v_{rms}^2 = \frac{\sum_{i=1}^{i=n} v_i^2 t_i}{\sum_{i=1}^{i=n} t_i} \qquad (1\text{-}14)$$

where $v_i$ is the interval velocity of the i-th layer.

For areas of gentle dip the time correction can be computed reasonably accurately by

$$\delta T_n = \sqrt{T_{o,n}^2 + \frac{X^2}{V_n^2}} - T_{o,n} \qquad (1\text{-}15)$$

where

$$\delta T_n = T_{x,n} - T_{o,n} \tag{1-16}$$

Taner & Koehler (1969) confirmed that experiments using different dips and interval velocities indicate that arrival time distance relations remain nearly hyperbolic. Because of that they suggest that in the dipping bed cases NMO corrections should be applied just as they would be in horizontal bed areas. In the same manner Yilmaz (1987) mentioned that, by making the spread small and assuming small dips, moveout is hyperbolic for all cases and given by:

$$T_x^2 = T_o^2 + \frac{X^2}{V_{NMO}^2} \tag{1-17}$$

Al-Chalabi (1973) proved that the time produced by a two term truncation of eq. 1-6 is always greater than the true travel time, except where the ground is homogeneous then they will be equal. According to that rms velocity estimated using travel time computed by eq.(1-11) is less than true velocity.

May & Straley (1979) mentioned that Taner & Koehler's second order polynomial works well for the bulk of seismic reflection data analysis. However, for ray tracing, depending critically on accurate knowledge of moveout curves for calculations of interval velocity and depth, and for high resolution data they suggest the use of higher-than second order orthogonal polynomials, whose coefficients are determined independently to compute the travel time.

Since paths to far receivers are more oblique and relatively more high velocity material is encountered than along paths to nearer receivers, so velocity spectra for far traces exhibit higher stacking velocity than the nearer traces for a given reflection event, (Taner *et al.* 1970). In this case, where NMO equation is a hyperbolic function, the value of $\delta T$ required will vary from sample to sample.

That will cause a frequency deformation, called NMO *stretching*. The effect of NMO stretching becomes large when the rate of NMO ( $\delta T / T_o$ ) is large, in other words it is large at large offsets and shallow times, see (Fig. 1.4). To overcome such disadvantage, in this work, the window length was fixed for near and far traces (D. K. Smythe 1989, pers. comm.).

Equation 1-17 was used, in this work, to correct the data for reflection events before coherency coefficient measures.

[2] *Time Correction for refraction data :*

The basis of the refraction method has been discussed by many authors (e.g. Dobrin 1976, Sheriff & Geldart 1982, Kearey & Brooks 1984). Consider the case of two homogeneous layers where the velocity of each layer is constant and the velocity of the lower layer is greater than that of the upper one. The ray path of a direct wavefront travelling from near surface source S to receiver R will be SR, while for a refracted wavefront traveling from the source S to the receiver R will be SABR (Fig. 1.5). The direct wavefront will travel with velocity equal $V_1$ and the refracted with velocity equal $V_1$ from S to A and from B to R and with velocity equal $V_2$ from A to B. Therefore the total travel time, for the direct will be $T = T_{SR}$,

$$T_{SR} = \frac{X}{V_1} \qquad (1\text{-}18)$$

where

$X$ is the offset

$V_1$ is the velocity of the first layer

and for the refracted wavefront will be,

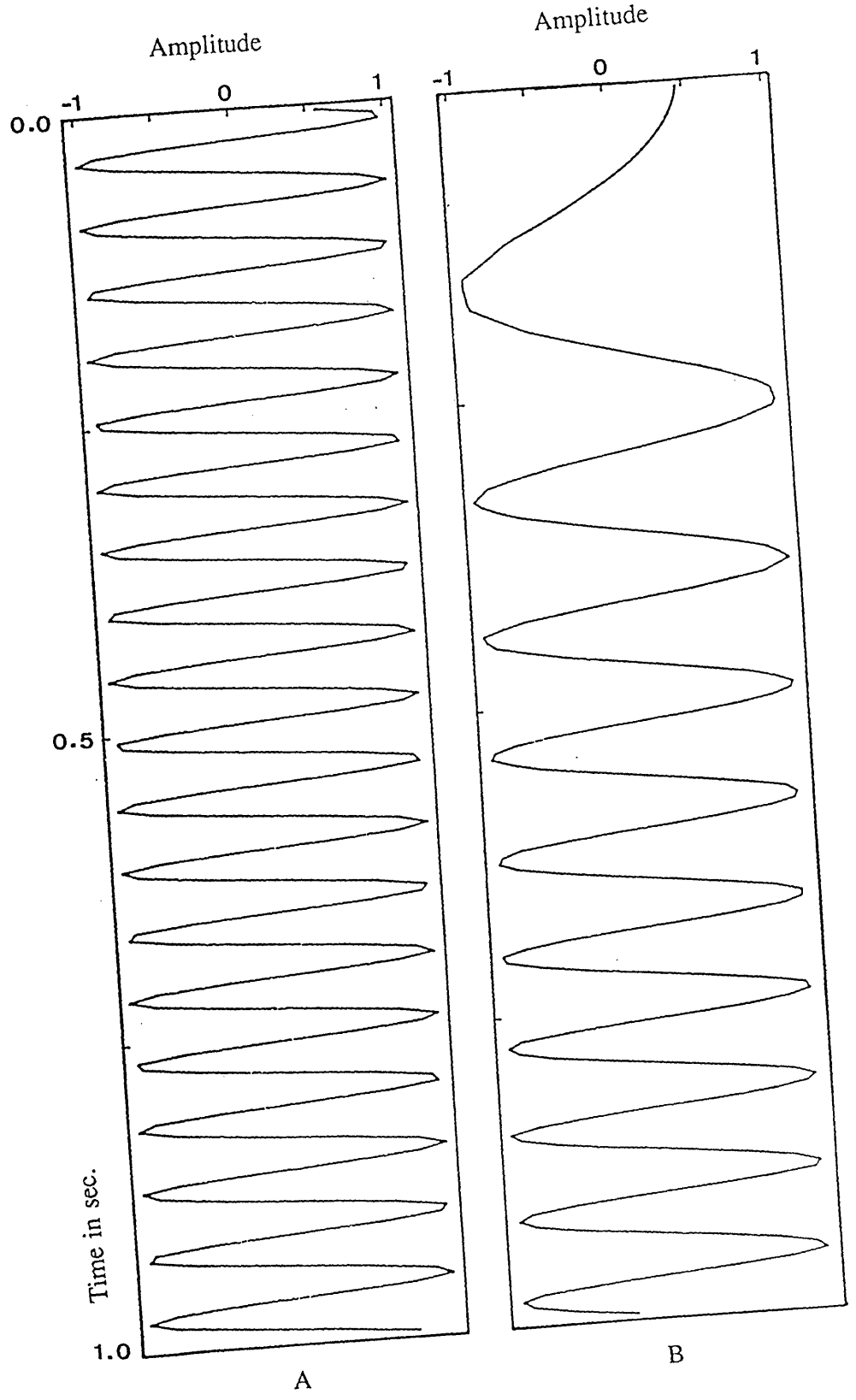


Fig.1.4 NMO stretching using eq.1-17 with offset 3.0 km and velocity 4.0 km/s.
A) before NMO correction, B) after correction.

$$T = T_{SA} + T_{AB} + T_{BR} \tag{1-19}$$

If the interface is horizontal, then $T_{SA} = T_{BR}$ .

The refracted headwave which travels along the described ray path satisfies Snell's law, applied to critical refraction :

$$\sin\theta = \frac{V_1}{V_2} \qquad \textit{Snell's Law} \tag{1-20}$$

Alternatively,

$$\cos\theta = \left\{ 1 - \frac{V_1^2}{V_2^2} \right\}^{1/2} \tag{1-21}$$

where

$\theta$ is the critical angle

$V_i$ is the velocity of the i-th layer

Travel time can be computed by the expression,

$$T_x = X \frac{\sin\theta}{V_1} + 2Z \frac{\cos\theta}{V_1} \tag{1-22}$$

or

$$T_x = \frac{X}{V_2} + 2Z \frac{\cos\theta}{V_1} \tag{1-23}$$

where

$\theta$, $V_i$ as above.

$Z$ is the depth of the interface

$X$ is the offset

Therefore, on a graph of travel time vs. distance (Fig. 1.6), a plot of a refracted arrival has the form :

$$T_x = T_i + \frac{X}{v_i} \tag{1-24}$$

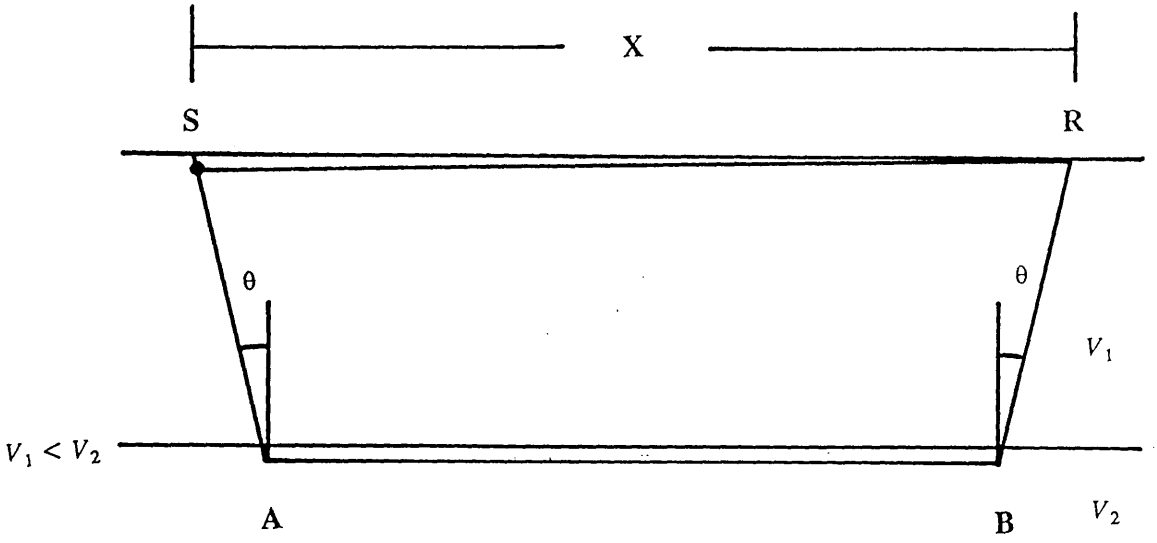


Fig.1.5 Ray path of a direct and a refracted wavefront in a two layer case with homogeneous layers and horizontal interface.

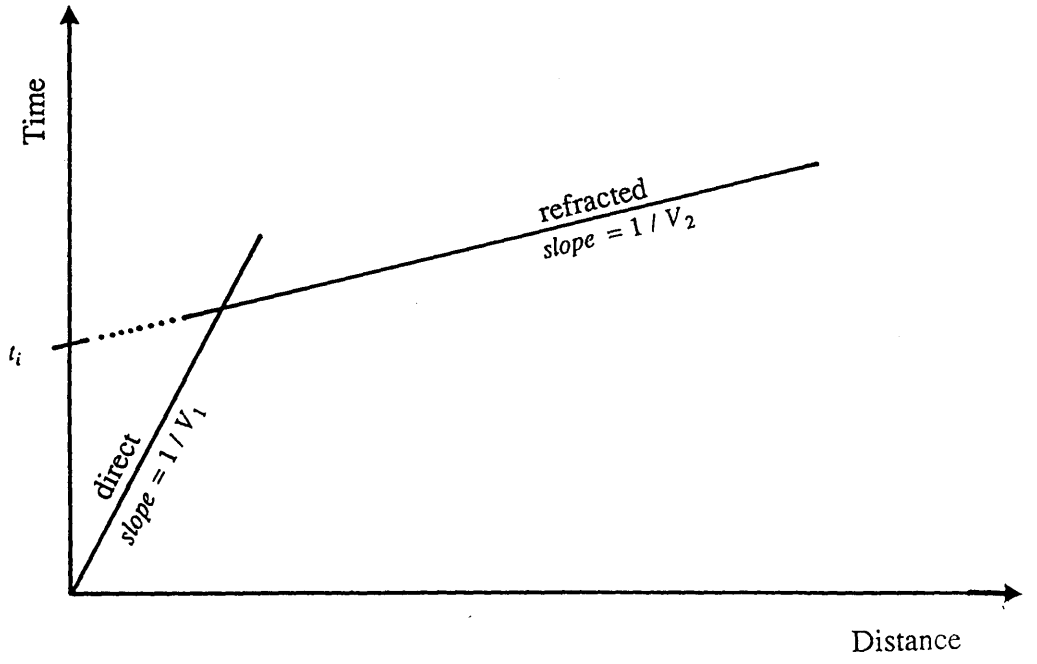


Fig.1.6 Time-distance curve for a two layer earth.

where $v_i$ is the observed (apparent) velocity of the refracting medium and $T_i$ is the intercept on the time axis, which can be computed by

$$T_i = \frac{2\,Z\,\sqrt{v_2^2 - v_1^2}}{v_1\,v_2} \tag{1-25}$$

While the depth of the refractor, Z, is given by,

$$Z = \frac{T_i\,v_1\,v_2}{2\,\sqrt{v_2^2 - v_1^2}} \tag{1-26}$$

Equations of travel time in cases of more than two layers are available in many textbooks. The travel time required for a headwave to travel from the source to an offset x can be computed by,

$$T_{x_n} = T_{i_n} + \delta T_{x_n} \tag{1-27}$$

$$\delta T_{x_n} = \frac{x}{v_i} \tag{1-28}$$

where

$x$ is the offset

$v_i$ is the velocity of the i-th layer

In this work, we are concerned with the basic equation of time correction, $\delta T = T_x - T_i$, where $T_x$ is the total travel time, to receiver at an offset $x$, and $T_i$ is the time intercept. In Figure 1.7 $t_{i_o}$ is the time intercept of the direct arrivals (travels through the first layer) and equal to zero always, $t_{i_1}$ and $t_{i_2}$ are the time intercept of first and second interface, respectively. While $\delta t_{i_o}$, $\delta t_{x_1}$ and $\delta t_{x_2}$ are the time correction of offsets $x_o$, $x_1$ and $x_2$ consequently. Equation 1-27 was used, in this project, to correct the data for direct and refraction events before the meas-

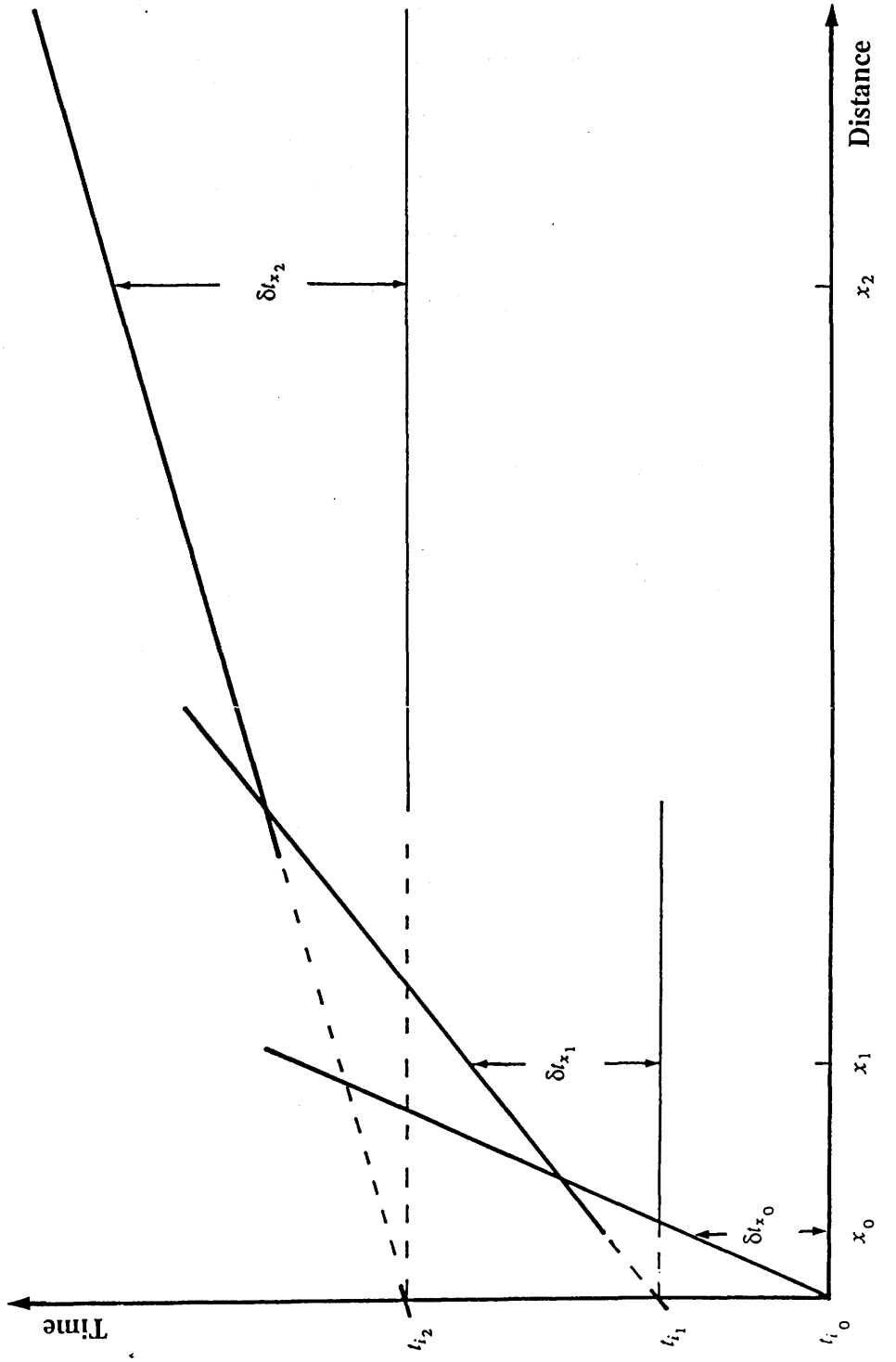


Fig.1.7 Time correction for direct and refracted data.

urement of the coherency coefficient.

[3] *Time Correction for Continuous Velocity Increase :*

In some areas the direct arrivals travelling through the first layer will form a curve on the time-distance plot, instead of a straight line. This indicates that the subsurface velocity is varying with depth. This is a common feature in the Midland Valley (Davidson 1986, Dentith 1987 and Kamaliddin 1988), where trial data were acquired for this work. The ray paths and time-distance curve for a linear velocity increase with depth are illustrated in Fig. 1.8. This Figure shows that the ray path in this case will describe arcs of circles and the deepest point is known as its turning point (Kearey & Brooks 1984).

Travel time equations exist for a variety of velocity-depth functions. For a linear increase with depth,

$$V = V_o + K\ Z \tag{1-29}$$

where

$V_o$ is the velocity at the surface

$Z$ is the depth

$K$ is a constant represents the increase in velocity per unit depth

$V$ is the velocity at depth $Z$

The maximum depth reached for a circular ray, see Fig. 1.8, to an offset X is,

$$Z_{max.} = \frac{V_o}{K} \left\{ \left[ 1 + \left[ \frac{K\ X}{2\ V_o} \right]^2 \right]^{½} - 1 \right\} \tag{1-30}$$

and the total travel time is,

$$T = \frac{2}{K} \sinh^{-1} \frac{K\ X}{2\ V_o} \tag{1-31}$$

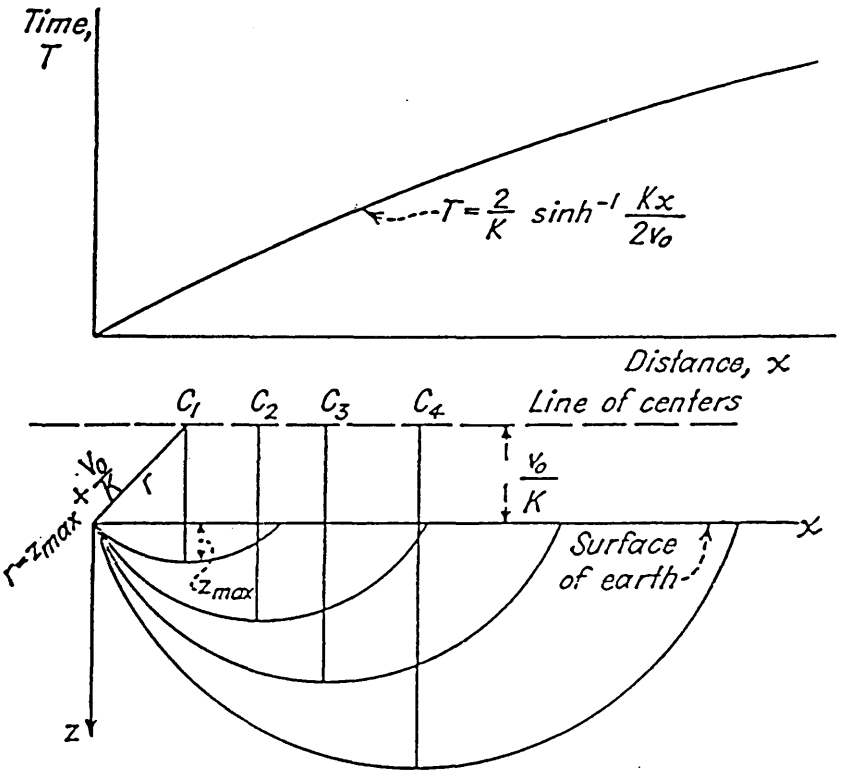


Fig.1.8 Ray paths and time-distance curves for linear increase of velocity with depth (after Dobrin 1976).

Since, in this case, the correction is achieved for a special type of the *direct* arrivals the correction time value is the entire travel time

The general form of the time correction :-

$$T_o = T_x - \delta T \qquad (1\text{-}32)$$

$\delta T$ is obtained from (eq. 1-17 for reflection, eq. 1-27 for direct and refraction, and eq. 1-31 for continuous velocity increase with depth) to correct the data to remove the effect of the difference in the offsets, before computing a coherency coefficient. This is repeated over the required range of velocities.

### 1.3.2. Coherency measurements

In velocity analysis the aim of coherency (degree of match) measures is to determine how well a time correction process will fit a path (Fig. 1.9). In turn, the parameters of a best fit time correction can be used as attributes of an observed arrival across the receiver array. In this project hyperbolic (reflection) and straight line trajectories (direct and refracted), were considered, as a function of $T_o$ and $V$. For the case of velocity increase with depth $K$ and $V_o$ were considered. Different forms of coherency measure exist. Five expressions were tested and employed in this project to achieve the computation of the coherency coefficient after applying time correction to the data : unnormalised crosscorrelation (Schneider & Backus 1968), energy normalised crosscorrelation, statistical normalised crosscorrelation sum (Neidell & Taner 1971), semblance (Taner Koehler & 1969) and mean amplitude summation (Garotta & Michon 1967).

A coherency measure will give a maximum value if the signal was corrected properly before the coherency computation, i.e for the optimum combination of $T_o$ and $V$ or $K$ and $V_S$ used in time correction.

Each digitised seismic trace may be defined as $f_{i,j}$ where i is the trace

Velocity Spectra

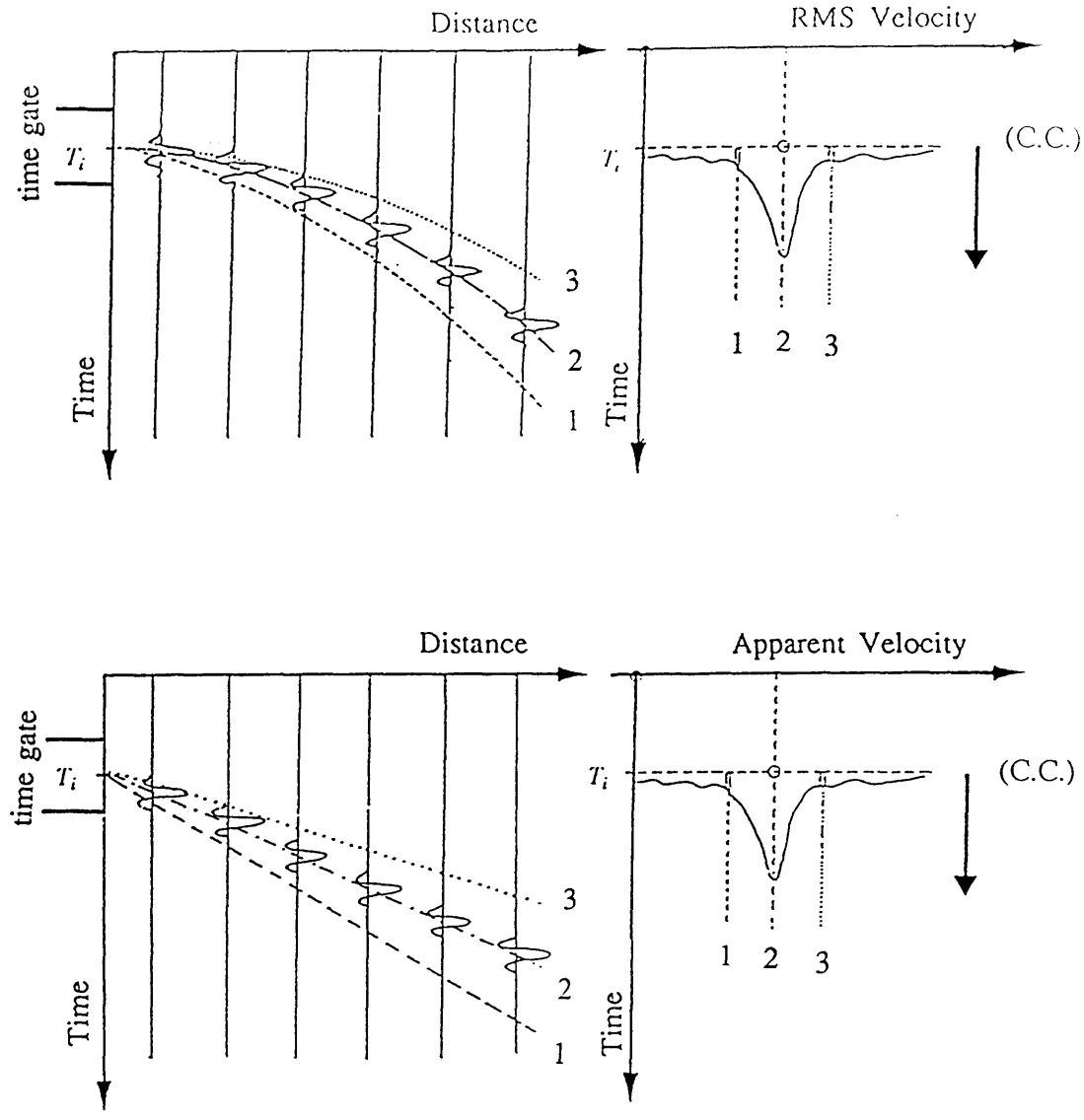


Fig.1.9 Schematic velocity spectra for A) reflection data and B) refraction data (modified after Taner & Koehler 1969). These diagrams show the trajectories involved in calculating coherency coefficients, here for a range of velocities with a fixed time intercept ( $T_i$). The window, or time gate, illustrated in A shows conceptually the portion of data on one of the traces used to calculate the coefficient for a given trajectory (here 2).

* The resulting variation in coherency coefficient (C.C.) is shown on the right.

number and j is the sample number, such that $f_{i,j}$ is the amplitude of the j-th sample in the i-th trace. Assume a coherent signal crossing M number of traces following a lag path. A time gate (window) of length N+1 samples may be considered, such that its samples are symmetrically distributed around an index sample K in a trace. The coherency measures utilised can be expressed as follows :

[1] *Mean Amplitude Summation ( MAS ) :* as a coherency measure MAS is given by,

$$CC_{MAS} = \sum_{i=1}^{i=M} \frac{1}{(N+1)} \sum_{j=k-(N/2)}^{j=k+(N/2)} f_{i,j} \tag{1-33}$$

The above expression can be normalised in terms of absolute amplitude variation to give a unity value if all traces involved in the computation have the same phase and zero if they are completely out of phase.

$$CC_{norm.} = \frac{\left| CC_{MAS} \right|}{\sum_{i=1}^{i=M} \frac{1}{N+1} \left| \sum_{j=k-(N/2)}^{j=k+(N/2)} f_{i,j} \right|} \tag{1-34}$$

[2] *Unnormalised crosscorrelation :* is used as a coherency measure in many applications such that for each combination ($T_o$ and $V$, or $K$ and $V_s$) a zero lag crosscorrelation sum is computed to give a coherency measure. An unnormalised crosscorrelation sum for M traces is computed by expression (1-35).

$$CC_{unnorm.} = \sum_{p=1}^{p=M-1} \sum_{i=1}^{i=M-P} \frac{1}{N+1} \sum_{j=k-(N/2)}^{j=k+(N/2)} f_{i,j} f_{i+p,j} \tag{1-35}$$

where $p$ is trace index units apart.

Neidell & Taner (1971) emphasised that "The unnormalised crosscorrelation sum of [eq.(1-35)] is exactly equivalent to half an energy difference, or

$$\sum_{j=k-(N/2)}^{j=k+(N/2)} \sum_{p=1}^{p=M-1} \sum_{i=1}^{i=M-P} f_{i,j}\, f_{(i+p),j} = \frac{1}{2} \sum_{j=k-(N/2)}^{j=k+(N/2)} \left\{ \left\{ \sum_{i=1}^{i=M} f_{i,j} \right\}^2 - \sum_{i=1}^{i=M} f_{i,j}^2 \right\} \qquad (1\text{-}36)$$

They pointed out that "the unnormalised crosscorrelation sum [is] equal to half the difference between an output energy and the gate input energy". They also mentioned that "the unnormalised crosscorrelation sum of [eq. 1-35] is exactly equivalent to [eq. 1-36]". However, we would like to mention here that it was found that, for the same input traces using exactly the same number of samples, computing the value of the unnormalised crosscorrelation sum by eq. 1-36 is greater than by eq. 1-35 by a factor of N+1.

[3] *Normalised crosscorrelation sum :* The normalised form for eq. (1-35), from a statistical approach, is given by

$$CC_{norm.} = \frac{2}{M(M-1)} \sum_{j=k-(N/2)}^{j=k+(N/2)} \sum_{p=1}^{p=M-1} \sum_{i=1}^{i=p} \frac{f_{i,j}\, f_{i+p,j}}{\sqrt{\sum_{j=k-(N/2)}^{j=k+(N/2)} f_{i,j}^2 \sum_{j=k-(N/2)}^{j=k+(N/2)} f_{(i+p),j}^2}} \qquad (1\text{-}37)$$

Neidell & Taner (1971) developed an alternative normalisation for the crosscorrelation. They used the trace average energy and a constant $\frac{M(M-1)}{2}$ times the common trace input energy (which is the output value of eq. 1-36 when input amplitudes are equal) to normalise eq. 1-36. Then the energy normalised crosscorrelation sum would be,

$$CC_{norm.} = \frac{\sum_{j=k-(N/2)}^{j=k+(N/2)} \left\{ \left\{ \sum_{i=1}^{i=M} f_{i,j} \right\}^2 - \sum_{i=1}^{i=M} f_{i,j}^2 \right\}}{(M-1) \sum_{j=k-(N/2)}^{j=k+(N/2)} \sum_{i=1}^{i=M} f_{i,j}^2} \qquad (1\text{-}38)$$

Computationally eq. 1-38 requires $\frac{M}{2}$ less multiplications than eq. 1-37. Moreover eq. 1-37 will give unit correlation even when the rms amplitude of a signal is varying from trace to trace, provided its phase and shape are identical, whereas eq. 1-38 is sensitive to amplitude differences. The output value of eq. 1-37 will vary in the range of $-1 \leq CC \leq 1$, while that of eq. 1-38 will be in the range $\frac{-1}{M-1} \leq CC \leq 1$.

[4] *Semblance :* is defined to be a normalised output/input energy ratio, and is often used in multi-channel seismic reflection velocity analysis as a coherency measure. It was introduced by Taner and Koehler (1969).

The ratio of output/input energy along a time period, N+1, is defined by eq. (1-39).

$$S = \frac{\sum_{j=k-(N/2)}^{j=k+(N/2)} \left\{ \sum_{i=1}^{i=M} f_{i,j} \right\}^2}{\sum_{j=K-(N/2)}^{j=k+(N/2)} \sum_{i=1}^{i=M} f_{i,j}^2} \qquad (1\text{-}39)$$

For M identical of traces,

$$S = \frac{M^2 \sum_{j=k-(N/2)}^{j=k+(N/2)} f_{i,j}^2}{M \sum_{j=k-(N/2)}^{j=k+(N/2)} f_{i,j}^2} = M \qquad (1\text{-}40)$$

Thus a normalised form of eq. 1-39 is,

$$S = \frac{\sum_{j=k-(N/2)}^{j=k+(N/2)} \left\{ \sum_{i=1}^{i=M} f_{i,j} \right\}^2}{M \sum_{j=K-(N/2)}^{j=k+(N/2)} \sum_{i=1}^{i=M} f_{i,j}^2} \qquad (1\text{-}41)$$

Semblance has values in the range $0 \leq S \leq 1$. It will exhibit a unity value if the signal of all traces have the same phase and amplitude (are identical) and zero if they are totally out of phase. Semblance is related to the energy normalised crosscorrelation sum by eq.( 1-42).

$$CC_{cros} = \frac{1}{M-1} (M\ S - 1) \qquad (1\text{-}42)$$

In the case of a simple linear signal-noise model, assuming that the noise sum over all traces at any time is zero, Neidell & Taner (1971) showed that the semblance coefficient will be the ratio of signal energy to the total energy.

## 1.4. Frequency Filtering

Filtering is a process by which a given input signal is converted to an output signal. The operator that transforms the input signal into an output signal is called a "filter" (Kulhanek 1976). A common measure for the filtering capacity, the effect of the filter, is the filter response for an impulse input (Fig. 1.10) (Al-Sadi 1980).

A digital filter is represented by a series of weighting coefficients, and its output is obtained by convolving the digitised input trace with the weighting coefficients (Robinson & Treitel 1980).

A filter can be considered as a part of a system which discriminates against some of the information entering it. The discrimination can be on the basis of frequency, wavelength, moveout or other bases of discrimination (Sheriff 1968).

Digital filtering applications in geophysical data processing are very often to improve signal to noise ratio ( s/n ), which is the energy of a desired event divided by all remaining energy (noise) at that time (Sheriff 1968), or otherwise to improve the signal character (Kearey & Brooks 1984). The term, filtering, must be qualified : for example, band-pass filtering, anti-alias filtering, velocity filtering and so on. Filter design may be dependent or independent of data. In data independent filters, such as frequency filters, the filter operator is not derived from the data to be filtered. In the case of data dependent filtering, such as Wiener filtering, the characteristics of the filter are derived from the data to be filtered (Hatton *et al.* 1986).

Filters, in general, have a disadvantage in that they necessarily distort the shape of the signal. In particular the pulse is lengthened and, moreover, its phase is shifted, that is, characteristics such as crests and troughs are displaced in time (Parasnis 1979). The application of a frequency filter in frequency or time domain yields identical results. In practice, the time domain approach is favoured, because convolution involving a short array, such as a filter operator, is more economical than doing Fourier transforms (Yilmaz 1987).

The concept of the Fourier transform is that any arbitrary function can be represented by simple trigonometric series. In other words, any time series, such as a seismic trace, can be uniquely and completely described as a sum of sinusoids, each with a unique peak amplitude, frequency and phase-lag. This concept is illustrated in Fig. 1.11. The continuous amplitude and phase spectra in A were divided into sixteen individual sinusoidal waves of different frequency and phase (B) and the sum of these waves is shown by the waveform in C.

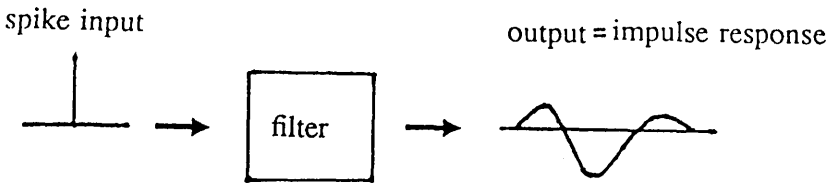


Fig.1.10 The impluse response of a filter (after Kearey & Brooks 1984).

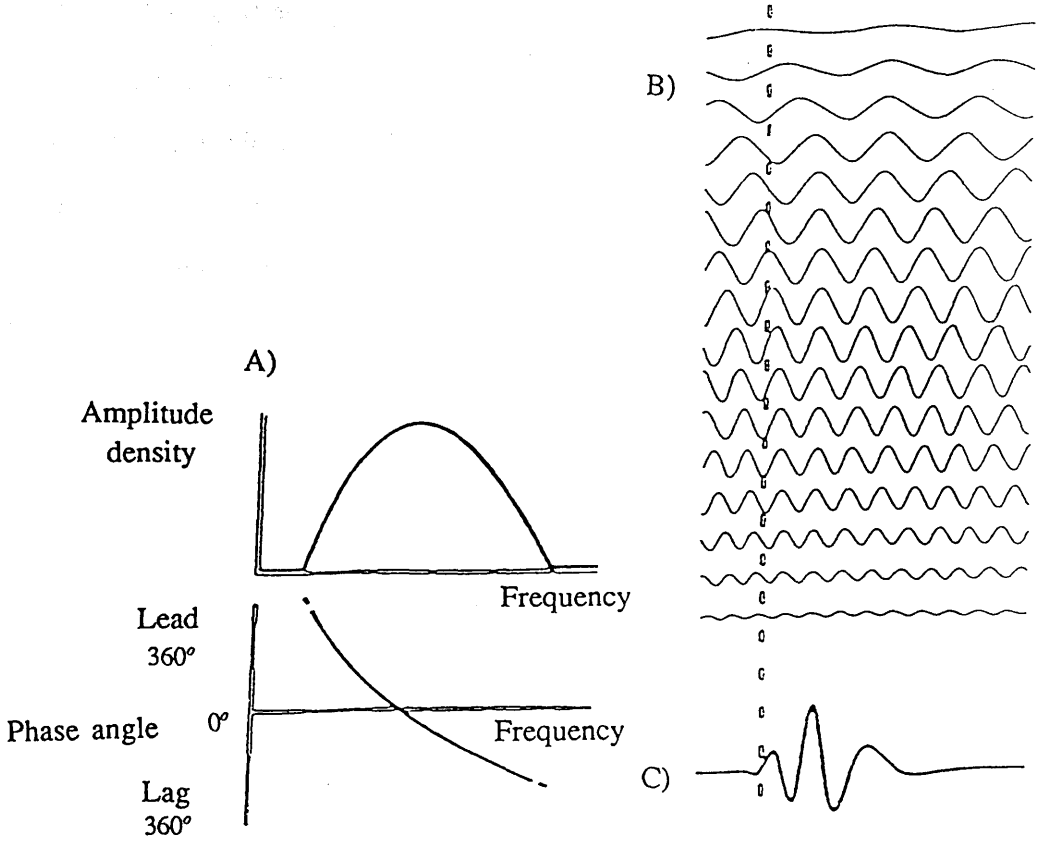


Fig.1.11 Fourier representation of a seismic wave: A) amplitude and phase spectrum. B) sinusoidal waves having amplitudes and time shifts corresponding to the spectra in (A). C) simple stacking of the waves in (B). (after Anstey 1970).

Two properties of the noise used commonly as a basis for separating it from the signal are its frequency and apparent velocity. Frequency filtering can be carried out on a single trace. Filtering based on apparent velocity requires the use of multi-channel data.

In frequency filtering the greater the difference between desired and unwanted frequencies the better they can be separated by filtering (Silverman 1967). This kind of filter is designed on an arbitrary basis of passing or rejecting specific frequencies. The aim will be to remove high amplitude noise, such as ground roll or wind noise, that occurs at frequencies different to those the of the signal (Hatton *et al.* 1986).

The time domain representation of a zero-phase band-limited wavelet can be used to filter a seismic trace, such that the output trace contains only those frequencies that make up the wavelet, by convolving the described wavelet and seismic trace. The coefficients of the operator are the individual time samples (Yilmaz 1987).

Frequency filters are described in terms of their form of frequency response (Fig. 1.12). The low pass, or high cut-off, filter will pass only frequencies less than a defined frequency (cut-off frequency) and reject other frequencies. The band pass filter will allow all frequencies within the pass band to transmit without any distortion and to infinitely attenuate frequencies outside that band. A high pass filter, also known as a low cut-off filter, will allow all frequencies greater than the cut-off frequency to pass without any distortion and reject other frequencies. Usually a seismic trace contains unwanted noise at frequencies lower and higher than the signal, so band pass filtering is widely used in seismic data processing. Band pass filtering is performed at different stages in seismic data processing for different purposes. It is useful before computing cross correlations during construction of velocity spectrum for improved velocity picking.

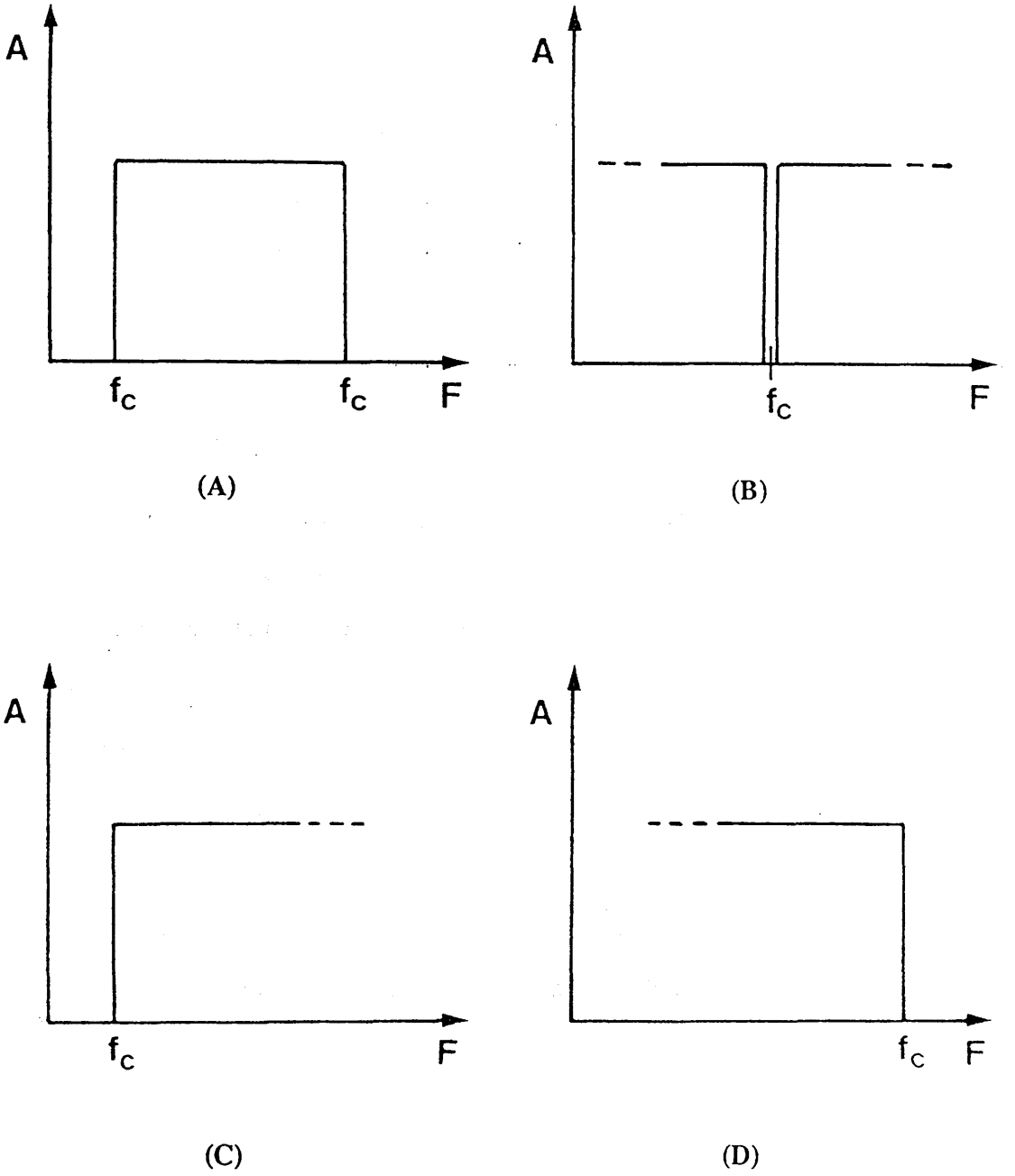


Fig.1.12 Frequency response of frequency filters: A) band-pass, B) notch, C) high-pass filter, D) low-pass .

From the above it appears that designing a frequency filter can be done by defining the desired amplitude spectrum for the filter operator with the cut-off frequencies, known as the boxcar amplitude spectrum (eq. 1-43).

$$A(f) = \begin{cases} 1 & f_1 < f < f_2 \\ 0 & elsewhere, \end{cases} \tag{1-43}$$

where $f_1$ , $f_2$ are the cut off frequencies.

Such an operator is infinitely long for an ideal frequency filter and, therefore, it must be truncated for practical use as a convolution operator. Representing a boxcar with a finite number of Fourier coefficients will cause ripples in the wavelet and the actual amplitude spectrum will have ringy character, known as the *Gibbs phenomenon.*

The ripples of an operator also depend on the property of frequency filters:

[1] The broader the bandwidth, the more compressed the filter operator, i.e. fewer coefficients are required.

[2] The smaller the bandwidth ratio the greater ripples. Bandwidth ratio is the ratio of high-cut to low-cut frequency. In other words for two passbands having the same bandwidth, the one with a smaller bandwidth ratio will have an operator with greater ringyness .

Gibbs phenomenon is undesirable for two reasons; firstly some of the frequencies in the pass-band are amplified while others are depressed, secondly some of the rejected frequencies, on both sides, are passed. Therefore the band-pass must be defined as a trapezoid, a boxcar with slopes assigned on both sides, and it is recommended that a gentler slope be assigned on high-frequency side relative to the low-frequency side of the band-pass (Bracewell 1965, Hatton *et al* 1986, Yilmaz 1987).

Frequency filters are useless if the desired signal and noise have a similar frequency content. In this case one must use another kind of filter called the *optimum filter,* also referred to as *least squares* or *Wiener* filter, to achieve the separation of signals in the seismic record (Robinson & Treitel 1964).

# Chapter 2

# SOFTWARE DESCRIPTION

## 2.1. Introduction

This project was concerned with the analysis of digitised seismic traces (i.e. time series data), assuming that the signal of interest appears on a group of traces at different offset and travel times. In this chapter the software written for this project is described. All programs and subroutines written for the project are listed in Appendix 1.

The main program and all subroutines were written using the FORTRAN 77 programming language, since it is the most widely employed programming language in the field of time series analysis. Figure 2.1 shows the organisation of the software which was designed to correct the arrival time of the seismic data for an assumed travel time function, and then to compute a coherency coefficient and, finally, to plot the results using the "S" software package. Software operation can be split into five sections : reading and checking, frequency filtering (optional), time correction, coherency coefficient measurements and display.

## 2.2. Reading and checking:

The program reads all processing parameters requested from a control system file and checks for any incorrect input. It then reads, from the same file, the names of the files containing the seismic data to be processed. The program was designed to read GLAMK2 seismic data files digitised on the PDP-11/23 PLUS at the Geol-

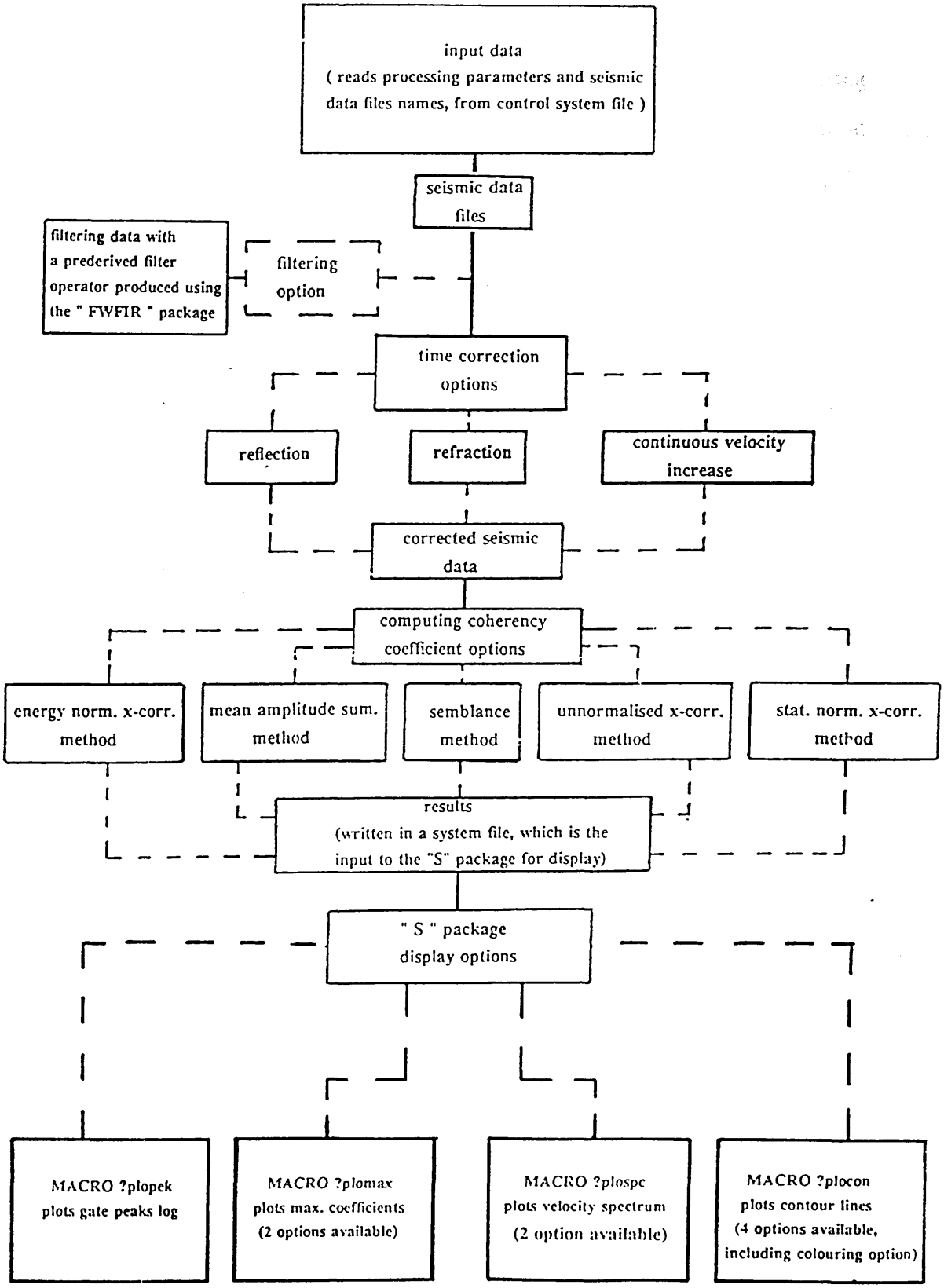


Fig.2.1 Software organisation diagram, dashed lines represent optional functions.

ogy and Applied Geology Department, Glasgow University. However, it can also read GEOSTORE seismic data files digitised on the Global Seismology digitising system at the British Geological Survey and MARS seismic data files digitised at University College, Cardiff.

### 2.3. Frequency filtering:

This is an optional stage allowing the user to apply a frequency filter to the seismic data. The objective of frequency filtering is to improve s/n ratio.

Filtering of the seismic data requires the construction of a filter operator, which can be designed to fulfil the requirements of the user by the "FWFIR" filter design package. The "FWFIR" package was designed to write, after construction, the desired filter operator to a system file called "fwk1", which our software will read and convolve with each input seismic trace. The "FWFIR" package and all subroutines utilised to filter the data in this software are available in the "geophysical computer library" on the departmental computer at the Geology and Applied Geology Department, Glasgow University. The "FWFIR" package is capable of designing low-pass, high-pass, band-pass, and band stop filters. In each case different types of window can be applied.

### 2.4. Time correction:

Time correction is achieved, at this stage, using one of three expressions provided, according to the option requested in the control file. Eq. 1-17 was used to correct data for reflected events, eq. 1-27 for refracted events. For continuous velocity increase with depth cases eq. 1-31 was used. The time correction value, for reflected and refracted events, will be computed once, at the centre of the window, for each combination of $T_o$ and $V$. In the case of continuous velocity increase time correction will be computed at zero time for each $K$ and $V_o$ combination, where $K$ is the velocity gradient and $V_o$ is the surface velocity. The next step is to check that, for every trace, the calculated window lies entirely within the

trace. If this is not the case the program will terminate that combination of ( $T_o$ and $V$, or $K$ and $V_o$) and start processing of the next given combination. The software then calculates the data value that occurs at each sample time of the window. The estimation is achieved by linear interpolation between two existing data samples, where necessary.

### 2.5. Coherency coefficient measurements:

Five different methods were used to measure coherency coefficients, for the corrected data. The main program calls a subroutine that applies the required method. The methods are the mean amplitude summation (eq. 1-33), unnormalised crosscorrelation sum (eq. 1-36), statistically normalised crosscorrelation (eq 1-37), energy normalised crosscorrelation (eq. 1-38) and semblance method (eq. 1-41). Results are written to a system file for the use in the next step.

### 2.6. Display

Display of the results is achieved using the "S" data analysis and graphics package. "S" is a very high-level language for specifying computations (Becker and Chambers 1984). Four interactive "MACRO"s were written. A MACRO is a sequence of "S" commands (instructions) which can be run (executed) using the Macro name and they have the additional facility of allowing the user to define arguments which are used to pass variable information to the command sequence, to modify its behaviour (C. Farrow 1989, pers. comm.).

All MACROs were written to read from two system files, one containing the processing parameters and the other the results of the FORTRAN program. Results, except for MACRO plopek, were displayed in the $T_o - V$ domain for reflected and refracted events, and in the case of continuous velocity increase results were displayed in the $K - V_o$ domain. MACROs designed for this project are listed in Appendix 2 and briefly described here.

[1] MACRO plopek :

This MACRO will extract the maximum coherency coefficient for each window time and dispay it as a peaks log in the time-coherency coefficient domain, (Fig. 2.2). It is the only MACRO which hase no options. The following three MACROs (plocon, plomax and plospc ) will also display this log on a smaller scale.

[2] MACRO plocon :

This MACRO was written to display the results as contour lines and window peaks power, with four options (Fig. 2.3). The first option gives the user the choice of which coherency coefficients to contour and display :-

i) all coefficients.

ii) coefficients > arithmetic mean of all coefficients.

iii) coefficients > { ( arithmetic mean + maximum coefficient) / 2 }

This option provides the opportunity to display significant coherency coefficients only. A second option allows the user to define an approximate number of contour lines to be plotted. Printing values on contour lines is the object of the third option. Finally, the fourth option controls the method of plotting the contour lines. Three different colours can be used on plotters with such facilities. On other plotters contour lines are plotted with three different types of lines: solid, dashed and dotted.

[3] MACRO plomax :

The task of this MACRO is to display the maximum coherency coefficient and the power for each window time in the results (Fig. 2.4). Two options are available. The first is the same as the first option of MACRO plocon, see the previous section. The second option was for the type of plotting: lines, points or both.

[4] MACRO plospc

Results are displayed as a typical velocity spectrum and window power by this MACRO, which have two options (Fig. 2.5). The first is the same as the first option of MACRO plocon, see section [2]. Scaling of the spectrum was the goal of the second option.

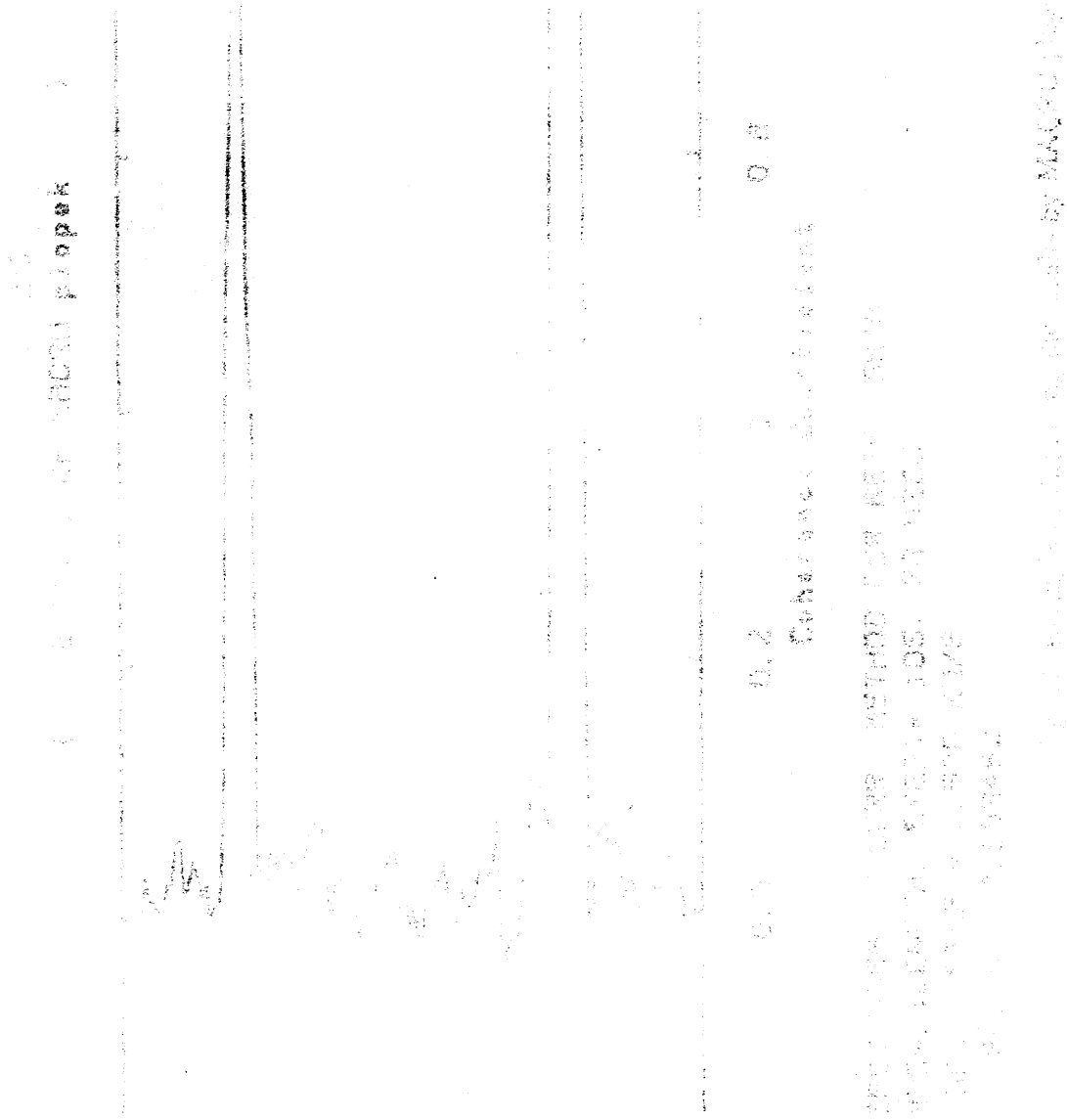

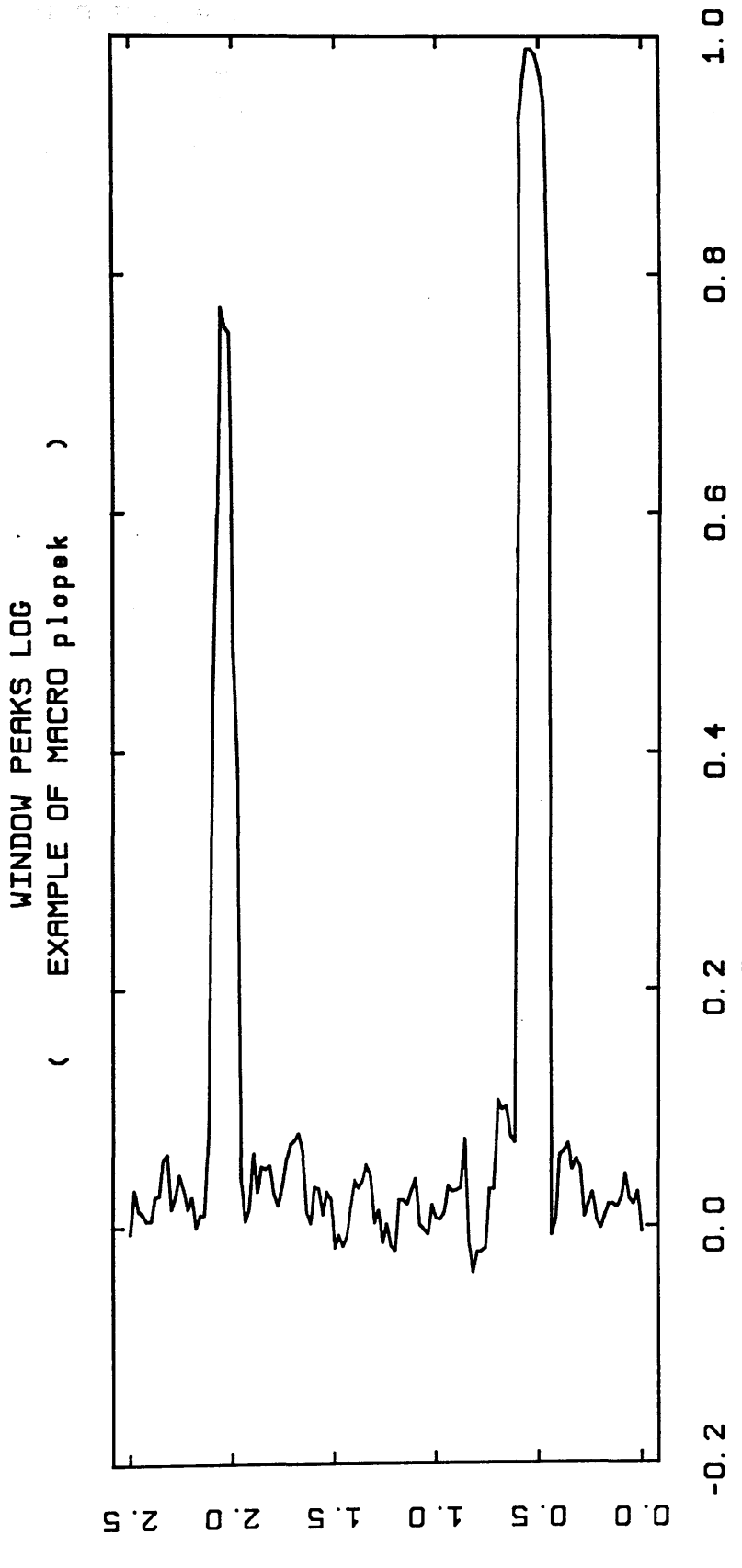


Fig.2.2 Example of displaying the results by MACRO plopek.

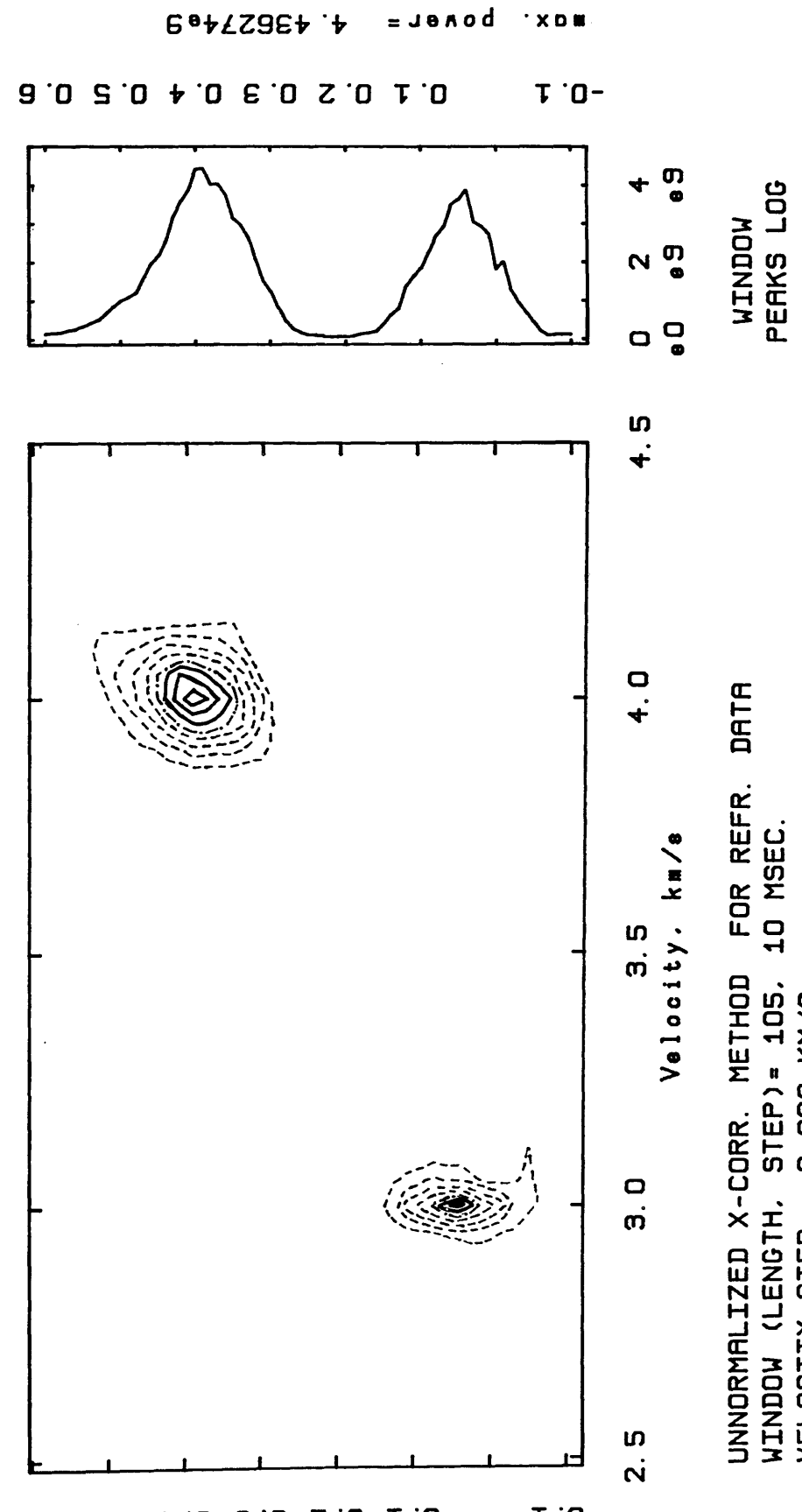


Fig.2.3 Example of displaying the results by MACRO plocon.

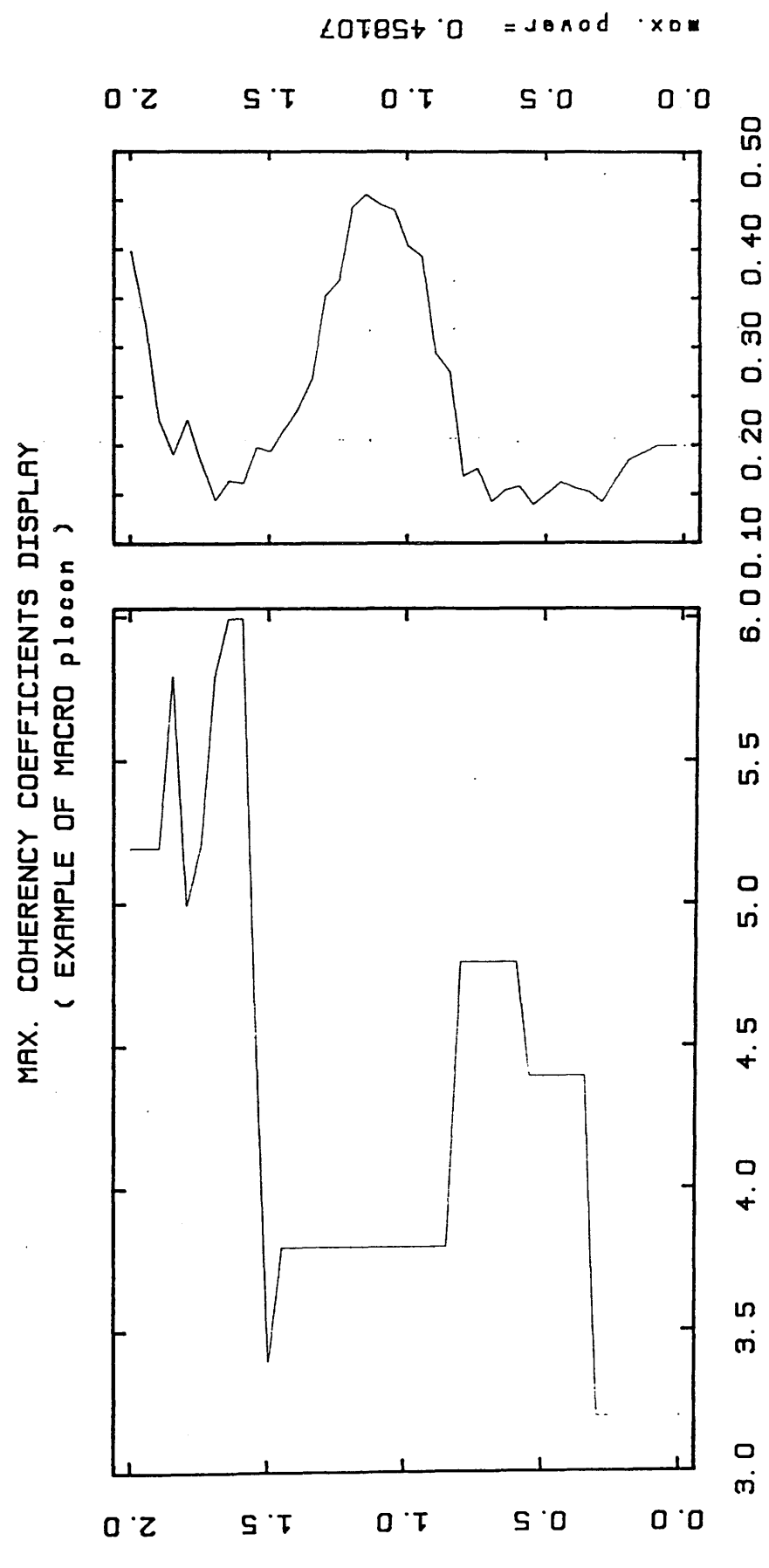


Fig.2.4 Example of displaying the results by MACRO plomax.

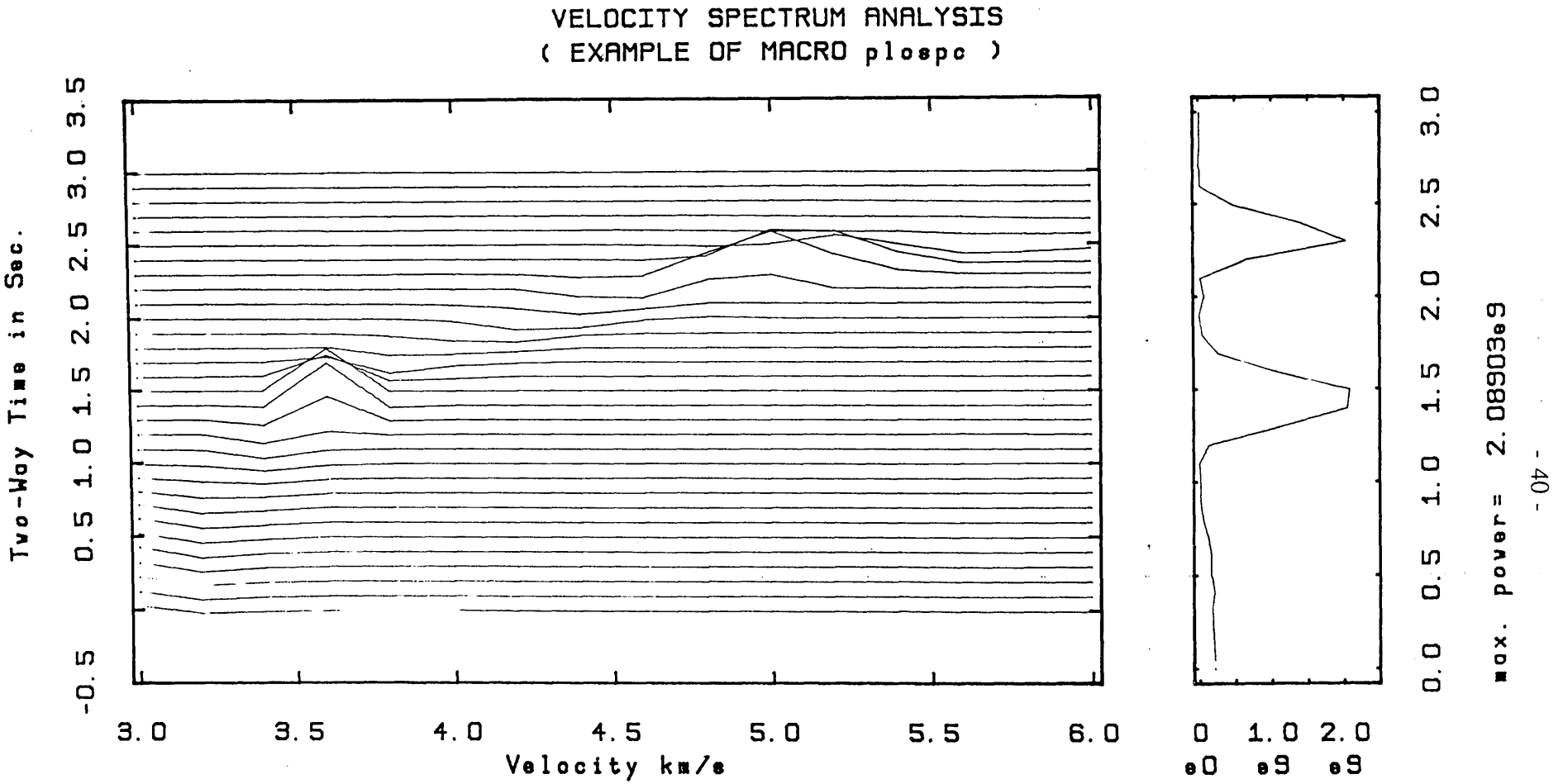


Fig.2.5 Example of displaying the results by MACRO plospc.

# Chapter 3

# SYNTHETIC TRACE TESTS

## 3.1. Introduction

Five different types of tests were carried out. These concerned the coherency method, parameters of event and processing, signal interference, combination of events, and finally a test for scattering of arrival time. Testing of the software was carried out using synthetic traces throughout the project period. However, at the early stages of the project, the aim of testing the software was to ensure that it is computing the required time correction and coherency coefficient properly.

For the above tests synthetic traces were constructed using program SYNTH.f which was designed to generate random noise by calling the "S" MACRO "noise" and to construct a truncated sine wave for the desired signal for a specified arrival time, frequency, time length, maximum amplitude and sample rate. All synthetic traces were written in GLAMK2 format. Events on synthetic seismic traces, except one set, have no scatter of arrival times, i.e. they have ideal travel times.

It is difficult to compute S/N ratio for real seismic data, while it is much easier to calculate for synthetic data (Anderson & McMechan 1989). Amplitude ratio was used, in this work, to determine S/N ratio for synthetic traces instead of energy ratio. In most cases, a set of synthetic traces was constructed with a uniform S/N ratio for its traces. In one set the S/N ratio was varied from trace to trace.

Synthetic traces fall into two classes. The first class has only events of an truncated sine wave shape and the second is contaminated with noise. The latter was achieved by stacking two traces, one containing the signal and a noisy trace, using program STK.f, which was designed to stack a given number of traces to construct one stacked trace using $\frac{1}{N}$ as a normalising factor where $N$ is number of input traces.

### 3.2. Comparison of the coherency methods :

A set of ten synthetic seismic traces was constructed, rr1 - rr10 (see Fig. 3.1), containing two refracted events. Table 3.1 shows the parameters of each event:

Table 3.1 Parameters of events on synthetic traces rr 1 - rr 10.

| | First event | Second event |
|---|---|---|
| Time intercept (sec.) | 0.5 | 2.0 |
| Velocity (km/sec.) | 4.0 | 5.0 |
| Frequency (Hz) | 14 | 14 |
| Event span (msec.) | 70 | 70 |
| S/N | 5 | 1 |

The program was executed for each method of coherency measure using the same processing parameters. Results are displayed in two types of plot, coloured contour lines and velocity spectrum analysis, for each method : Fig. 3.2 for semblance, Fig. 3.3 for unnormalised cross correlation, Fig. 3.4 for energy normalised cross correlation, Fig. 3.5 for statistically normalised cross correlation and, finally, Fig. 3.6 for mean amplitude summation

From the results it is clear that **all** methods perform well for the first event

which has a high S/N ratio. However, two methods (unnormalised cross correlation and the mean amplitude summation) did not detect the low amplitude second event as well as the other three methods. Three methods (semblance, statistical normalised crosscorrelation and energy normalised cross correlation) displayed very similar results.

However, the statistical normalised crosscorrelation method required a long computer time, compared with the other methods, to finish the task. As an example executing the program for this test took 06:36 minutes to finish the job employing the statistical normalised x-correlation method, while it needed only 01:35 minutes when the semblance method was employed, with the same load on the same computer. Semblance and energy normalised x-correlation methods displayed almost the same results with a small advantage to the semblance in that the maximum coherency coefficient was a little higher, being 0.991 compared to 0.989 for the energy normalised x-correlation method.

All methods perform well for poor data (second event) if high S/N ratio data (here the first event) are absent. Later tests reveal particular circumstances in which a given method excels.

### 3.3. Testing of event and processing parameters :

Five tests were carried out to illustrate the effect of various parameters. Three tests were of parameters of the seismic event: the S/N ratio, frequency content and trace polarity. The other two were for the processing parameters: time window length, and time, velocity steps.

#### 3.3.1. S/N ratio test :

Semblance is a good coherency measure between traces even at low S/N ratio (Douze & Laster 1979). Given this view and the comparison test of section 3.2, different methods were used to test S/N ratio. Three tests were carried out, the first for a very poor S/N ratio; the second for two events which are identical in all

parameters except the S/N ratio; thirdly, the variation of S/N ratio of an event within a set of seismic traces was tested in the final test.

A) Poor S/N ratio

A set of ten synthetic seismic traces, ali 1 - ali 10 (Fig. 3.7), was constructed containing one reflected event. The two way normal time of the event was 1.0 sec and its velocity was 3.8 km/sec; frequency was 14 Hz and its span 145 msec. The ratio of peak signal amplitude to peak noise amplitude was 1. Each trace was stacked with a noise only trace to construct a set of traces, alno 1 - alno 10 (Fig. 3.8), which contains the same event but with S/N ratio less than 1 (approx. 0.5). Frequency analysis of traces alno 1 - alno 10 is displayed in Fig. 3.9, which clearly shows that there is no dominant frequency in that set of traces. Results of executing the software over a velocity range of 3.0 - 5.0 km/sec. and a time range of 0.0 - 2.0 sec. are displayed in Fig. 3.10. It is clear from the results that both methods used, semblance and unnormalised crosscorrelation, were capable of extracting events with poor S/N ratio.

B) Different S/N ratio

The aim of this test was to assess the change in performance of the coherency methods as the S/N ratio of the dataset varies. Six sets each of six noise-free synthetic traces (sig2, sig1, sig0.5, sig0.3, sig0.2 and sig0.1) containing refracted signals with the same parameters, except the amplitude of the event, were constructed, see Fig. 3.11 which shows only one trace from each set (as a sample). Table 3.2 shows the parameters of the signals. Six datasets were created by summing these with the set of noise traces (noise1 - noise6) of maximum amplitude equal to 1, shown in Fig. 3.12. To ensure that any characteristics of the noise did not influence the results, a second group of datasets was created using the noise traces noi1 - noi6 shown in Fig. 3.13. Again the maximum amplitude on a trace was equal to 1.

Frequency analysis of both sets of noise, displayed in Figs 3.12b and 3.13b, shows clearly that there is no dominant frequency.

The dataset groups are termed "snf" and "sns" respectively and are illustrated in Fig. 3.14. Note that a given dataset is called "snf*", where * denotes the amplitude value of the event, e.g. sns1 is the dataset formed from noise traces noi1 - noi6 and noise-free dataset sig1. Within dataset sns1 the traces are called sns11 - sns16 with increasing offset.

Table 3.2 Parameters of events on synthetic trace sets sig2 to sig0.1 .

| | sig2 | sig1 | sig0.5 | sig0.3 | sig0.2 | sig0.1 |
|---|---|---|---|---|---|---|
| Time Intercept (sec.) | 0.5 | 0.5 | 0.5 | 0.5 | 0.5 | 0.5 |
| Velocity (km/sec.) | 5.0 | 5.0 | 5.0 | 5.0 | 5.0 | 5.0 |
| Frequency (Hz) | 14 | 14 | 14 | 14 | 14 | 14 |
| Span of event (msec.) | 145 | 145 | 145 | 145 | 145 | 145 |
| * Signal amplitude * | 2 | 1 | 0.5 | 0.3 | 0.2 | 0.1 |

For each dataset, including the noise only sets, the software was executed five times, once for each coherency method available, with the same processing parameters. Results are listed in Tables 3.3a and 3.3b for groups snf and sns respectively (see footnote of this page). The maximum coherency coefficient measured and its relevant combination of time and velocity are shown for each dataset. For comparison, the coherency coefficient of each method was normalised to its maximum for each group. These are listed in Table 3.4 (see foot note of this page) and displayed in Fig. 3.15.

Abbreviations of the methods used in Tables 3.3 and 3.4 are :- SEMB.-semblance, UNCR-unnormalised x-corr, CROS-energy normalised x-corr, STCR.-statistical normalised x-corr and SUMS-mean amplitude summation.

The performance of the mean amplitude summation method was very poor even at the highest S/N ratio (2) where it located the event 120 msec earlier than the correct time. Moreover, at a S/N ratio of 1 it failed to pick the event for the first group entirely. The rate of change of the unnormalised crosscorrelation method for both groups was higher than the others, this indicates that it is the most appropriate for high S/N ratio events. The results of the other three methods (semblance, energy and statistical normalised crosscorrelation) were similar, with small variation in locating the time but identical in velocity. The rate of change of the semblance coherency coefficient with S/N was the lowest of all methods in both datasets groups. As mentioned in section 3.2 the statistical normalised crosscorrelation method required much longer time to finish the task. The differences in the performance of the methods, between the groups, highlighted the great effect of the noise on the accuracy of picking an event at its proper combination of time and velocity. However, for S/N ratio less than 0.5 performance of all methods was poor and unreliable.

Table 3.3a Results of different S/N ratio ( snf ).

| Set name | | SEMB. | UNCR. | CROS. | STCR. | SUMS |
|---|---|---|---|---|---|---|
| snf2 | CC. | 0.877 | 3.654657e9 | 0.852 | 0.854 | 3659 |
| | T sec. | 0.580 | 0.580 | 0.580 | 0.580 | 0.460 |
| | V km/s | 5.0 | 5.0 | 5.0 | 5.0 | 5.0 |
| snf1 | CC. | 0.616 | 6.89366e8 | 0.539 | 0.505 | 1467 |
| | T sec. | 0.580 | 0.580 | 0.560 | 0.520 | 0.02 |
| | V km/s | 4.95 | 5.0 | 4.95 | 4.95 | 4.4 |
| snf0.5 | CC. | 0.500 | 2.50888e8 | 0.400 | 0.403 | 1594 |
| | T sec. | 0.540 | 0.540 | 0.540 | 0.540 | 0.140 |
| | V km/s | 4.95 | 4.95 | 4.95 | 4.95 | 5.2 |
| snf0.3 | CC. | 0.383 | 129338120 | 0.260 | 0.251 | 1594 |
| | T sec. | 0.50 | 0.540 | 0.500 | 0.540 | 0.140 |
| | V km/s | 4.95 | 4.95 | 4.95 | 4.95 | 5.20 |
| snf0.2 | CC. | 0.355 | 107258336 | 0.226 | 0.248 | 1594 |
| | T sec. | 0.480 | 0.480 | 0.480 | 0.480 | 0.140 |
| | V km/s | 4.80 | 4.80 | 4.80 | 4.80 | 5.20 |
| snf0.1 | CC. | 0.348 | 98827472 | 0.218 | 0.248 | 1594 |
| | T sec. | 0.480 | 0.480 | 0.480 | 0.480 | 0.140 |
| | V km/s | 4.80 | 4.80 | 4.80 | 4.80 | 5.20 |
| noise | CC. | 0.339 | 91159864 | 0.206 | 0.220 | 1594 |
| | T sec. | 0.480 | 0.480 | 0.480 | 0.480 | 0.140 |
| | V km/s | 4.80 | 4.80 | 4.80 | 4.80 | 5.20 |

Table 3.3b Results of different S/N ratio ( sns ).

| Set name | | SEMB. | UNCR. | CROS. | STCR. | SUMS |
|---|---|---|---|---|---|---|
| sns2 | CC. | 0.871 | 3.546008e9 | 0.846 | 0.849 | 3757 |
| | T sec. | 0.560 | 0.580 | 0.560 | 0.560 | 0.460 |
| | V km/s | 5.00 | 5.00 | 5.00 | 5.00 | 5.00 |
| sns1 | CC. | 0.678 | 8.72096e8 | 0.614 | 0.625 | 2016 |
| | T sec. | 0.580 | 0.580 | 0.580 | 0.560 | 0.520 |
| | V km/s | 5.05 | 5.00 | 5.05 | 5.05 | 4.90 |
| sns0.5 | CC. | 0.412 | 203874384 | 0.295 | 0.302 | 1341 |
| | T sec. | 0.58 | 0.58 | 0.58 | 0.58 | 0.36 |
| | V km/s | 5.05 | 5.00 | 5.05 | 5.05 | 4.05 |
| sns0.3 | CC. | 0.358 | 97208696 | 0.230 | 0.222 | 1279 |
| | T sec. | 0.12 | 0.12 | 0.12 | 0.12 | 0.36 |
| | V km/s | 5.60 | 5.55 | 5.60 | 5.60 | 4.05 |
| sns0.2 | CC. | 0.358 | 97208696 | 0.230 | 0.222 | 1257 |
| | T sec. | 0.12 | 0.12 | 0.12 | 0.12 | 0.74 |
| | V km/s | 5.60 | 5.55 | 5.60 | 5.60 | 5.95 |
| sns0.1 | CC. | 0.358 | 97208696 | 0.230 | 0.222 | 1303 |
| | T sec. | 0.12 | 0.12 | 0.12 | 0.12 | 0.74 |
| | V km/s | 5.60 | 5.55 | 5.60 | 5.60 | 5.95 |
| noi | CC. | 0.358 | 97208696 | 0.230 | 0.222 | 1349 |
| | T sec. | 0.12 | 0.12 | 0.12 | 0.12 | 0.74 |
| | V km/s | 5.60 | 5.55 | 5.60 | 5.60 | 5.95 |

Table 3.4a Results of normalising the results listed in Table 3.3a

| | SEMB. | UNCR. | CROS. | STCR. | SUMS. |
|---|---|---|---|---|---|
| snf2 | 1 | 1 | 1 | 1 | 1 |
| snf1 | 0.702 | 0.189 | 0.633 | 0.591 | 0.401 |
| snf0.5 | 0.570 | 0.068 | 0.469 | 0.472 | 0.436 |
| snf0.3 | 0.437 | 0.035 | 0.305 | 0.294 | 0.436 |
| snf0.2 | 0.405 | 0.029 | 0.265 | 0.290 | 0.436 |
| snf0.1 | 0.397 | 0.027 | 0.256 | 0.290 | 0.436 |
| noise | 0.387 | 0.025 | 0.242 | 0.258 | 0.436 |

Table 3.4b Results of normalising the results listed in Table 3.3b

| | SEMB. | UNCR. | CROS. | STCR. | SUMS. |
|---|---|---|---|---|---|
| sns2 | 1 | 1 | 1 | 1 | 1 |
| sns1 | 0.778 | 0.246 | 0.726 | 0.736 | 0.537 |
| sns0.5 | 0.473 | 0.057 | 0.349 | 0.356 | 0.357 |
| sns0.3 | 0.411 | 0.027 | 0.272 | 0.261 | 0.340 |
| sns0.2 | 0.411 | 0.027 | 0.272 | 0.261 | 0.335 |
| sns0.1 | 0.411 | 0.027 | 0.272 | 0.261 | 0.347 |
| noi | 0.411 | 0.027 | 0.272 | 0.261 | 0.359 |

c) Variation of S/N ratio within a dataset:

A set of nine synthetic seismic traces (signoi2 - signoi10, Fig. 3.16a) of variable S/N ratio was constructed to illustrate the effect of such variation on the coherency coefficient measurements. A set of synthetic seismic traces

(dsn 2 - dsn 20, Fig. 3.16b) containing a refracted event was constructed. The time intercept of the event was 1.0 sec; and its velocity was 5.0 km/s, frequency was 14 Hz and its span 75 msec; with different S/N ratio. The value of the ratio was taken as a factor $\frac{3}{X}$ where $X$ is the offset. Each trace was stacked with a noisy trace to form the test dataset. All methods (semblance, unnormalised crosscorrelation, energy normalised cross correlation, statistical normalised crosscorrelation, and mean amplitude summation) were employed in this test (Fig. 3.17).

All methods performed well in locating the event to its time and velocity. However, the highest coherency coefficient for the normalised methods was of the statistical normalised crosscorrelation method, which was expected since it was mentioned in section 1.3.2 that this method is not sensitive to amplitude variation between traces. Because of the requirement of long computer time when employing the above method the unnormalised crosscorrelation method seems more appropriate since it displayed similar results, see Figs 3.17b and 3.17d.

### 3.3.2. Event frequency test :

Two sets each of six traces (Fig 3.18) were constructed with refracted events having the same parameters except the frequency, which was 14 Hz in set ff1 and 28 Hz in ff2. Table 3.5 shows the parameters of the signals.

To provide two sets of seismic synthetic traces which are equivalent in all parameters except the frequency both sets were stacked with the same set of noisy synthetic traces (Fig 3.11) to construct the two sets frq1 1 - frq1 6 and frq2 1 - frq2 6, displayed in Fig 3.19.

Two methods were applied to each dataset, semblance and the unnormalised crosscorrelation methods. All tests showed the maximum coherency coefficient at $T_o$=0.625 sec., which is the centre of the event, and $V$= 5.0 km/sec (Fig 3.20). The

window peaks power for the unnormalised cross correlation method was sharper than that of the semblance method. Both methods showed a high density of contour lines for the second set (frq2 1 - frq2 6) at two other combinations of $T_o$ and $V$. That phenomenon is called *velocity aliasing,* which will be discussed later in section 3.7.

Table 3.5 Parameters of event of synthetic traces ff1 - ff2.

| | ff1 | ff2 |
|---|---|---|
| Time intercept (sec.) | 0.5 | 0.5 |
| Velocity (km/sec.) | 5.0 | 5.0 |
| * Frequency (Hz) * | 28 | 14 |
| span of event(msec.) | 250 | 250 |
| Signal amplitude | 5 | 5 |

Since the energy in both events is the same so semblance, which is the ratio of signal energy to total energy in a time gate, showed a similar coherency coefficient (0.965). However, the relationship between the length of an event and the window length will be discussed in section 3.3.4.

### 3.3.3. Trace polarity test :

A test was carried out to illustrate the effect of a reverse polarity trace, or traces, occurring within a set of seismic traces. The set of ten synthetic seismic traces ( rr 1 - rr 10, Fig. 3.1), which was used in section 3.2, was employed in this test. The result of employing the semblance and the mean amplitude summation methods on a set of traces all of normal polarity was shown in Figs. 3.2. and 3.5. Both methods were used in three more runs, employing the same processing parameters, after reversing the polarity of one, two, and three traces. All results

are listed in Table 3.6, but only one case is displayed, after reversing the polarity of three traces, in Figs. 3.21a and b for semblance and MAS respectively.

Table 3.6 Results for reverse polarity test.

| | SEMBLANCE | | | MEAN AMPLITUDE SUMMATION | | |
|---|---|---|---|---|---|---|
| No. of reverse polarity traces | Max. coherency coefficient | Velocity km/s | Time sec. | Max. coherency coefficient | Velocity km/s | Time sec. |
| 0 | 0.9905 | 4.0 | 0.560 | 10671 | 4.0 | 0.48 |
| 1 | 0.6345 | 4.0 | 0.560 | 8281 | 4.0 | 0.48 |
| 2 | 0.5481 | 4.05 | 0.620 | 6357 | 3.95 | 0.46 |
| 3 | 0.4277 | 3.95 | 0.440 | 4964 | 4.25 | 0.62 |

It is obvious, from the results, that the maximum power of the coherency coefficient was decreasing rapidly and the resolution was reduced.

### 3.3.4. Window length test :

The set of seismic traces, frq1 1 - frq1 6, used in section 3.3.2 was utilised in this test. Results for a window length of 225 msec ( 45 samples ) are already displayed in Fig. 3.20a, employing semblance method. Eight other values of window length were employed and results are listed in Table 3.7, which exhibits the maximum coherency coefficients in each test and the relevant combination of time and velocity. Illustrative results for window lengths of 35, 55 and 505 msec. are displayed in Fig. 3.22a, b and c respectively, and should be examined with Fig. 3.20a.

From Figs 3.20a and 3.22 and Table 3.7 it is obvious that all executed window lengths extracted the event properly. However, the highest maximum coherency coefficient shown was when the window length employed was very

close to the period of the event (35 msec). Moreover, the smaller the window length the less computational time that is required.

Table 3.7 Window length test : results

| Window length (employed) | Maximum coherency coefficient | Time msec. | Velocity km/s |
|---|---|---|---|
| 35 | 0.9735 | 0.625 | 5.0 |
| 55 | 0.9730 | 0.675 | 4.975 |
| 105 | 0.9698 | 0.700 | 4.975 |
| 155 | 0.9663 | 0.625 | 5.0 |
| 205 | 0.9660 | 0.600 | 5.0 |
| 255 | 0.9655 | 0.625 | 5.0 |
| 305 | 0.9607 | 0.625 | 5.0 |
| 405 | 0.9498 | 0.625 | 5.0 |
| 505 | 0.9418 | 0.675 | 4.975 |

### 3.3.5. Time and velocity increments test :

To illustrate the effect of time and velocity increments the result of executing the software for the set of six synthetic traces frq1 1 - frq1 6, which was displayed in Fig. 3.20c, was made a reference for this test. Five more runs of the software were made. In two the time increment was altered and in three the velocity increment, fixing all processing parameters. The total computational time, which is the time to compute coherency coefficients and display the results, was seen to vary enormously. Results are shown in Table 3.8.

It was found that increments can degrade the results if chosen too large and can increase the computing cost when chosen too small. Therefore, time and velo-

city increments (steps) and ranges should be chosen very carefully, since they will affect both the resolution and computational time (cost). Moreover, ranges of time and velocity employed in the analysis must sweep the likely time and the velocity of an event of interest, so as to allow the software to extract that event. A good policy, in choosing increments, is to execute the software with a reasonable increment in an initial run to detect the events, then each event can be analysed separately with smaller increments to obtain more detail and accuracy.

Table 3.8 Time and velocity increments test : results

| Time increment (ms.) | Velocity increment (m/s) | Total computational time (min.) |
|---|---|---|
| 25 | 25 | 09:06 |
| 25 | 75 | 02:14 |
| 25 | 100 | 01:48 |
| 25 | 250 | 01:07 |
| 10 | 25 | 54:47 |
| 50 | 25 | 03:25 |

Note: the run with time increment 25 ms and velocity increment 25 m/s is the reference run referred to in the text.

### 3.4. Testing for Signal Interference :

Inevitably, seismograms will demonstrate significant overlapping of events, hence, interference. The software was tested for two types of events, reflected and refracted, to illustrate its performance in such a situation.

### 3.4.1. Reflection :

The aim of this test was to determine how well the software performed in distinguishing two interfering reflection events. Both events have the same frequency, span, and S/N ratio, but different velocity and normal two way time.

Two sets of traces, intf 1 - intf 10 (Fig. 3.23) and ints 1 - ints 10 (Fig. 3.24), were constructed with the same frequency ( 14 Hz), span (145 msec.) and S/N ratio (4). The event on the first set has a velocity of 3.8 km/sec and $T_o$ = 1.0 sec, while the event on the second set has a velocity of 5.3 km/sec and $T_o$ = 2.0 sec. Table 3.9 shows the offsets of the traces and the arrival times of the events on each trace. Stacking traces with common offsets was achieved to create the target set, int 1 - int 10 (Fig. 3.25).

Table 3.9 Offset & arrival times of events on intf & ints sets.

| Trace no. | Offset (km) | 1st event arrival time (sec.) traces (intf) | 2nd event arrival time (sec.) traces (ints) |
|---|---|---|---|
| 1 | 8.000 | 2.330 | 2.505 |
| 2 | 8.333 | 2.410 | 2.545 |
| 3 | 8.666 | 2.490 | 2.585 |
| 4 | 9.000 | 2.570 | 2.625 |
| 5 | 9.333 | 2.650 | 2.665 |
| 6 | 9.666 | 2.735 | 2.710 |
| 7 | 10.000 | 2.815 | 2.750 |
| 8 | 10.333 | 2.895 | 2.795 |
| 9 | 10.666 | 2.980 | 2.840 |
| 10 | 11.000 | 3.060 | 2.880 |

The execution of the software was nearly perfect (see Fig. 3.26) in locating each event to its corresponding time and velocity, despite the use of large increments and ranges of $T_o$ and velocity.

### 3.4.2. Refraction :

In the previous section it was found that the software was good in distinguishing between two interfering reflected events. The goal of this test was to find if the software is also good in the case of interfering refracted events. Two sets of synthetic seismic traces were constructed having two different events. The first set ( dir 2.5 - dir 7.0, see Fig. 3.27) contained a direct event of time intercept = 0.0 sec and velocity of 3.0 km/sec; the second set contained a refracted event ( refr 2.5 - refr 7.0, see Fig. 3.28) of time intercept = 0.34 sec and velocity = 4.0 km/s. Parameters of each event are shown in Table 3.10, while offsets and arrival times are listed in Table 3.11.

Table 3.10 Parameters of events on synthetic traces dir & refr

| | dir | refr |
|---|---|---|
| Time intercept (sec.) | 0.000 | 0.335 |
| Velocity (km/sec.) | 3.0 | 4.0 |
| Frequency (Hz.) | 20 | 16 |
| Span (msec.) | 100 | 125 |
| S/N | 3 | 3 |

The two sets, described above, were stacked to construct a set of synthetic seismic traces containing the desired events (dirf 2.5 - dirf 7.0, Fig. 3.29). The first execution of the software used large increments and ranges for time and velocity and, to take an extreme view, showed that both events were resolved fairly

well (Fig. 3.30). A second run was made zooming on the area of interest using smaller increments and ranges, to better illustrate the result of both methods used, semblance and unnormalised cross correlation (Fig. 3.31). The difference in the density of the contour lines of the events, which was expected, was due to the variation in the energy between the events, which was caused by the differences in the spans.

Table 3.11 Offset & arrival times of events on dir & refr sets.

| Trace no. | Offset (km) | Arrival times of the direct event in sec., synthetic traces (dir 2.5 - dir 7.0) | Arrival times of the refracted event in sec., synthetic traces (refr 2.5 - refr 7.0) |
|---|---|---|---|
| 1 | 2.5 | 0.835 | 0.960 |
| 2 | 3.0 | 1.000 | 1.085 |
| 3 | 3.5 | 1.165 | 1.210 |
| 4 | 4.0 | 1.335 | 1.335 |
| 5 | 4.5 | 1.500 | 1.460 |
| 6 | 5.0 | 1.665 | 1.585 |
| 7 | 5.5 | 1.835 | 1.710 |
| 8 | 6.0 | 2.000 | 1.835 |
| 9 | 6.5 | 2.165 | 1.960 |
| 10 | 7.0 | 2.335 | 2.085 |

## 3.5. Testing for a combination of events :

A simple two layer subsurface model was designed for this test. The first layer with surface velocity 3.0 km/sec and velocity gradient 0.5 km/sec/km and a

thickness of 2.0 km and a second layer with velocity 5.0 km/sec. Fig. 3.32 shows the result of raytracing through this model using the SEIS83 package. Three sets of synthetic seismic traces were constructed, the first for the direct event, the second for the reflected event from the interface and the last containing the refracted event. All three events have the same frequency (20 Hz), span (100 msec) and S/N ratio (3), see Fig. 3.33. The described sets were stacked to construct the desired set (mod 1 - mod 10),which is displayed in Fig. 3.34. Table 3.12 shows the arrival times, extracted from the raytracing model, for each event and the offset.

Table 3.12 Offset & arrival times of events on the mod 1 - mod 10 dataset.

| Offset (km) | Arrival time of the direct event in sec (direct 1 - direct 10) | Arrival time of the reflected event in sec. (reflected 1 - reflected 10) | Arrival time of the refracted event in sec (refracted 1 - refracted 1) |
|---|---|---|---|
| 1 | 0.335 | 1.185 | - |
| 2 | 0.660 | 1.281 | - |
| 3 | 0.985 | 1.430 | - |
| 4 | 1.310 | 1.615 | - |
| 5 | 1.620 | 1.825 | 1.818 |
| 6 | 1.925 | 2.055 | 2.020 |
| 7 | 2.215 | 2.290 | 2.215 |
| 8 | 2.495 | 2.535 | 2.415 |
| 9 | 2.770 | 2.785 | 2.610 |
| 10 | 3.030 | 3.035 | 2.810 |

The software was executed twice for each type of event, the first time with large increments in velocity and time to obtain a general view and the second, which depends on the results of the first, was with smaller ranges and increments in velocity and time. Results are shown in Figs. 3.35 to 3.37 for refracted, reflected, and continuous velocity increase data respectively, and show clearly that all events were extracted even when large increments of velocity and time were employed.

Aliasing, which was mentioned previously in section 3.3.2 and will be discussed later in section 3.7, of events appears on Fig. 3.35a where the execution was made for refracted data. Two closures, with low coherency coefficient, occur at combinations of time and velocity different to the proper combination. On Fig. 3.36a another closure can be seen at time 0.85 sec. and velocity 3.3 km/s, again with low coherency coefficient. Such combination, for hyperbolic trend, seems to be including energy from different events, regarding the window length employed in the processing was 100 msec; i.e. at offset 6.0 km it includes some energy from the direct event while at 7.0 km from the refracted event and at 3.0 km from the reflected event.

## 3.6. Scattering of arrival time test :

Arrival times of a seismic event across a suite of seismograms often deviate significantly from a perfect travel time trend. Generally there are two main reasons, in the limits of this project, for such deviation:

1) Geological reasons, due to either irregularity of the causal surface or variation of overlying structure.

2) Non-geological reasons, which include errors in the positions of the shots and/or the receivers (offset error), variation in the speed of recording and/or digitisation instruments.

Given the above, the set of ten seismic traces ints 1 - ints 10 shown in Fig.

3.24, was amended to be scattered randomly about the true reflection curve. Table 3.13 shows the static changes in the time of each trace. The resulting set was renamed scat 1 - scat 10 and is displayed in Fig. 3.38.

Table 3.13 Changes in arrival times of traces in the "scat" set compared to Table 3.9

| Trace no. | time shift (msec.) |
|---|---|
| 1 | -25 |
| 2 | +20 |
| 3 | -15 |
| 4 | -5 |
| 5 | +30 |
| 6 | -20 |
| 7 | 0 |
| 8 | -30 |
| 9 | +40 |
| 10 | +5 |

Note: The "-" sign is a shift to an earlier time.

The result of executing the software for the "perfect" event on the seismic set "ints" is shown in Fig. 3.39, and displays a perfect performance in extracting the event. On the other hand, execution for the scattered set "scat" shows an entirely different result (Fig. 3.40), which has little relation to the existing event. These two figures are providing a good evidence for the effect of the scattering.

The array used in this test occurs over an offset range of only 3km, which is quite small for a wide-angle experiment. To illustrate the effect of scattering over a long range the same set of synthetic traces was rearranged on a spread of 15 km,

keeping the offset of the first trace as before. The new set was named ss 1 - ss 10 and is displayed in Fig. 3.41. The result of applying the software (Fig. 3.42), shows that the effect of a given amount of scatter is less than that over a shorter range, but prevents the event being detected at the perfect time and velocity combination.

### 3.7. Aliasing velocity :

When the events consist of more than one cycle there may be combinations of velocity and intercept time, other than the true pair, which will exhibit a high coherency coefficient. The values of these velocities, called aliasing velocities, are related to: true velocity, inter receiver distance, and period of the event. The equation for time correction in the case of refracted or a normal direct event is a first order (straight line) equation. Fig. 3.43 shows how this may lead to the alignment of incorrect peaks in phase, which result in a high coherency coefficient. From Fig. 3.43 it is simple to compute the lower and higher aliasing velocities via eq. 3-1 and eq. 3-2,

$$V_{lo-alias} = \frac{D * V}{D + (V/F)} \tag{3-1}$$

or

$$V_{hi-alias} = \frac{D * V}{D - (V/F)} \tag{3-2}$$

where

$V_{lo-alias}$ & $V_{hi-alias}$ are the lower and higher aliasing velocities respectively.

$D$ is the inter receiver distance.

$V$ is the velocity of the event.

$F$ is the frequency of the event.

An example is already displayed in Figs 3.20b and d, which was the result of processing the set of synthetic seismic traces "frq2" shown in Fig. 3.19b. It shows that for an event of velocity 5 km/s, frequency 28 Hz and inter receiver distance 1 km there are higher and lower aliasing velocities which are, by eq. 3-1 and eq. 3-2, 6.09 and 4.24 km/s respectively. However, for the same event but with frequency 14 Hz, the set (frq1) shown in Fig. 3.19a, the higher and lower aliasing velocities, by the equations above, are 7.78 and 3.68 km/s respectively (Fig. 3.44).

Therefore analysis for refracted events should be made very carefully to avoid interpreting alias phenomena as real events, although the coherency coefficients are lower than that of the actual event. Predicting the lower and higher aliasing velocities by the two equations above is very helpful.

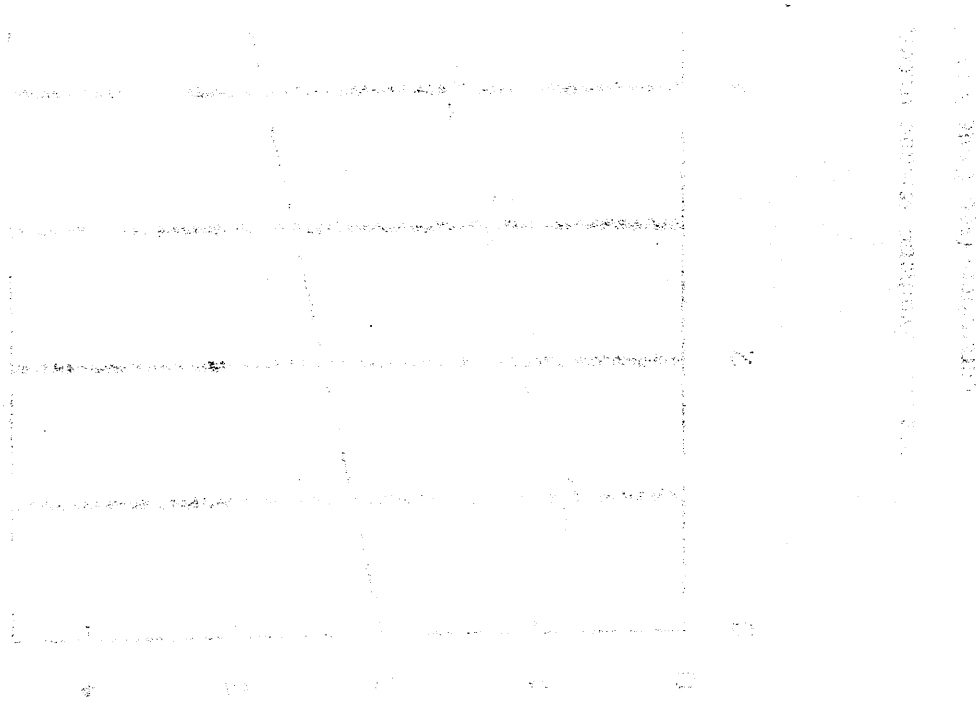

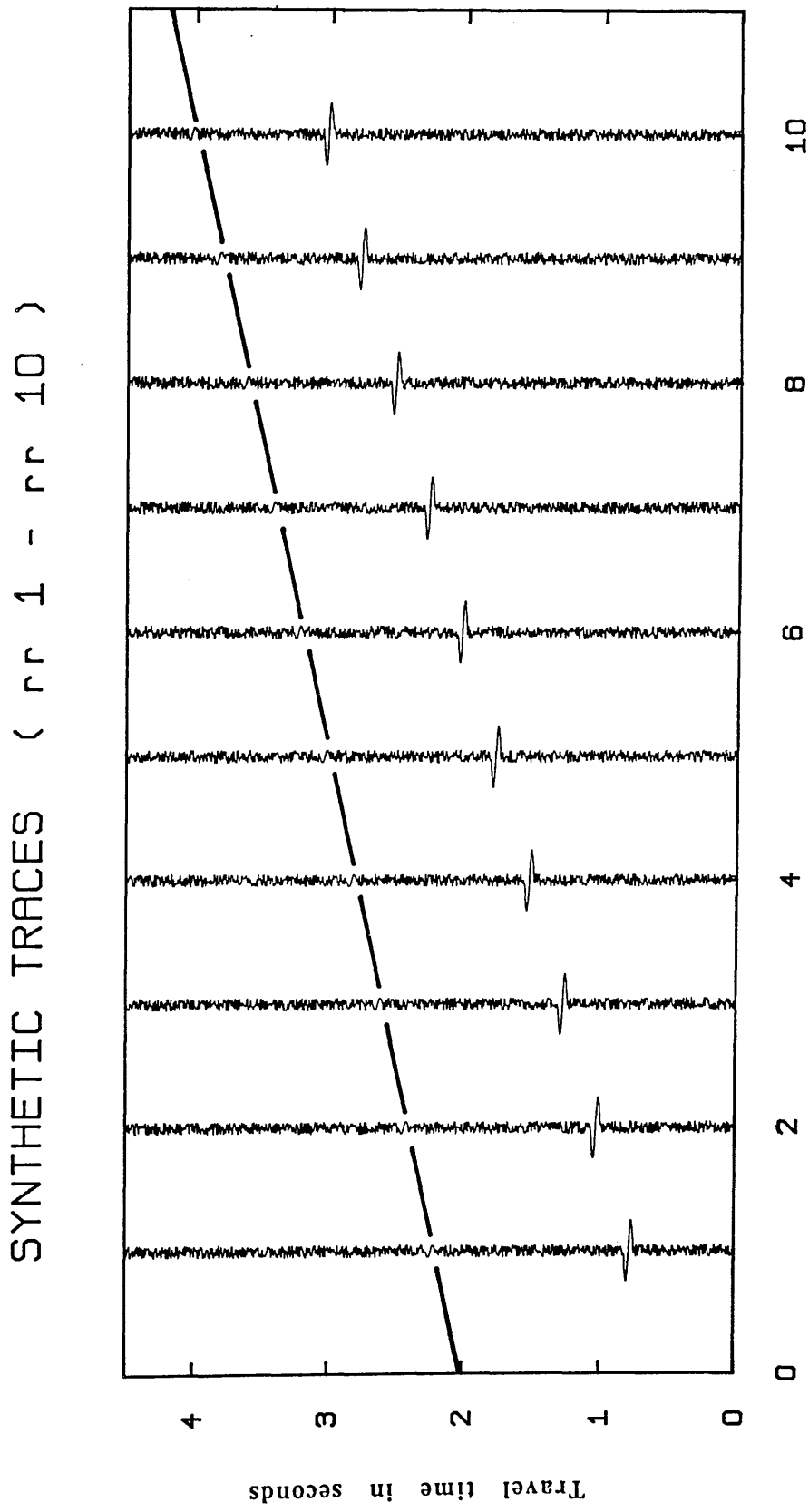


Fig.3.1 Synthetic seismic traces, set "rr", containing two refracted events with different parameters (see Table 3.1). The trajectory of the second event is highlighted.

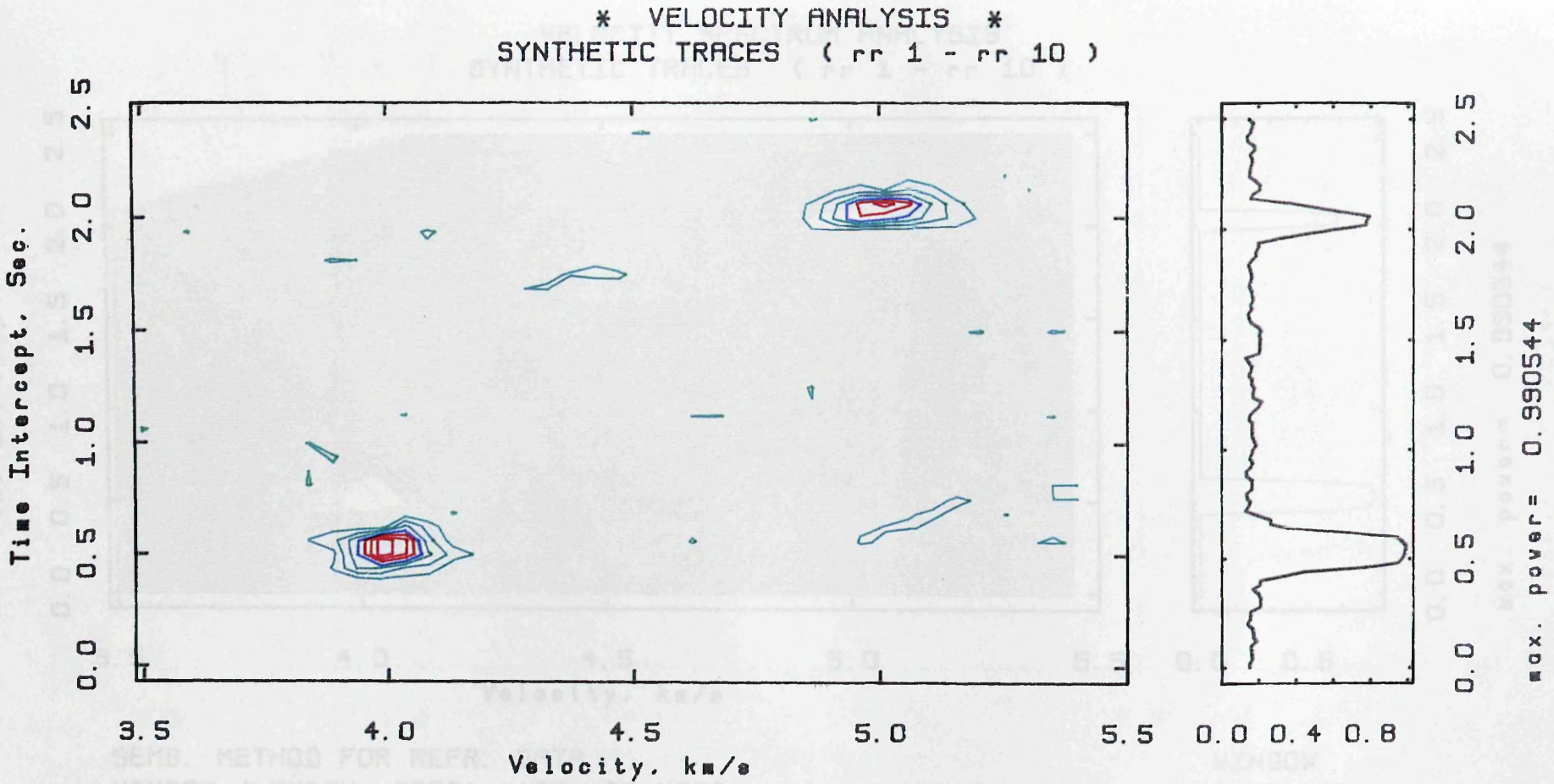


Fig.3.2a Results of applying the semblance method to dataset "rr" displayed in contour format.

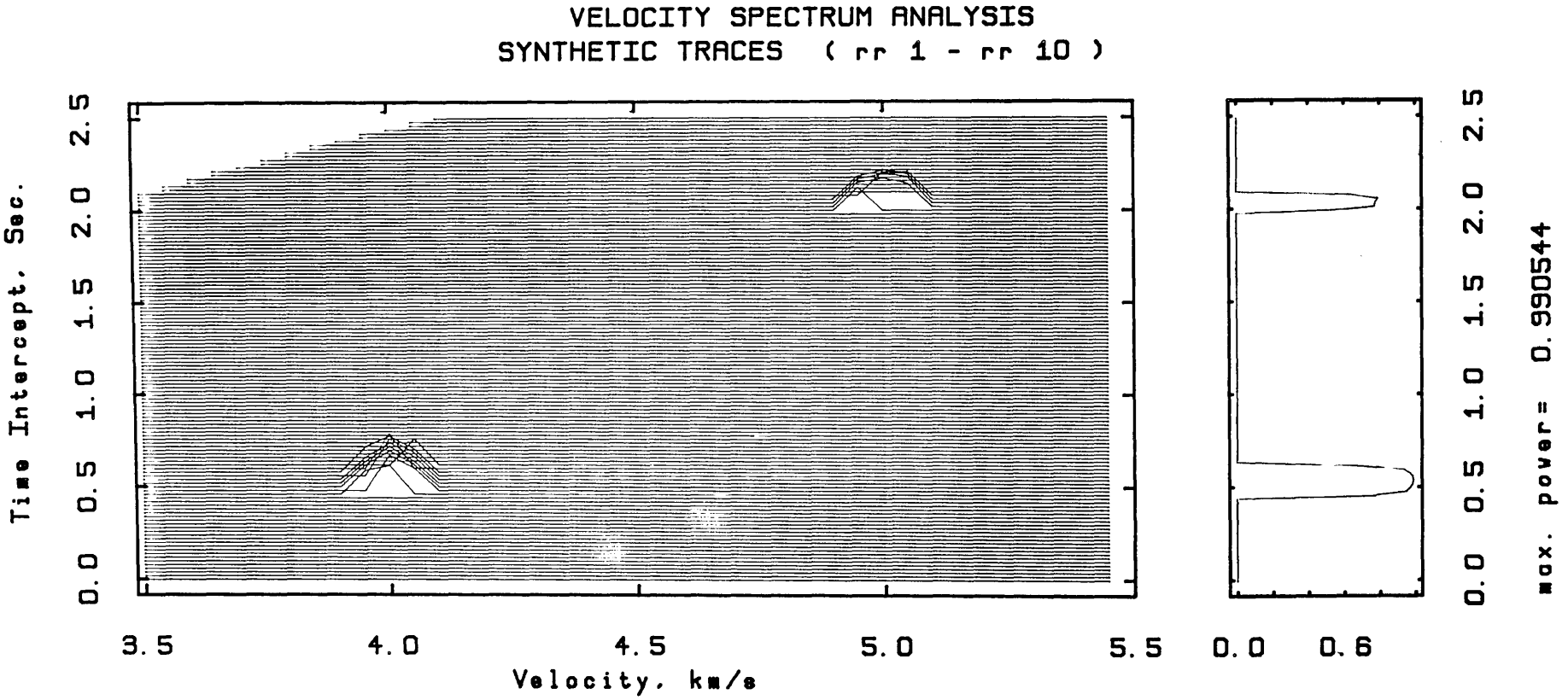


Fig.3.2b Results of applying the semblance method to dataset "rr" displayed in velocity spectrum form.

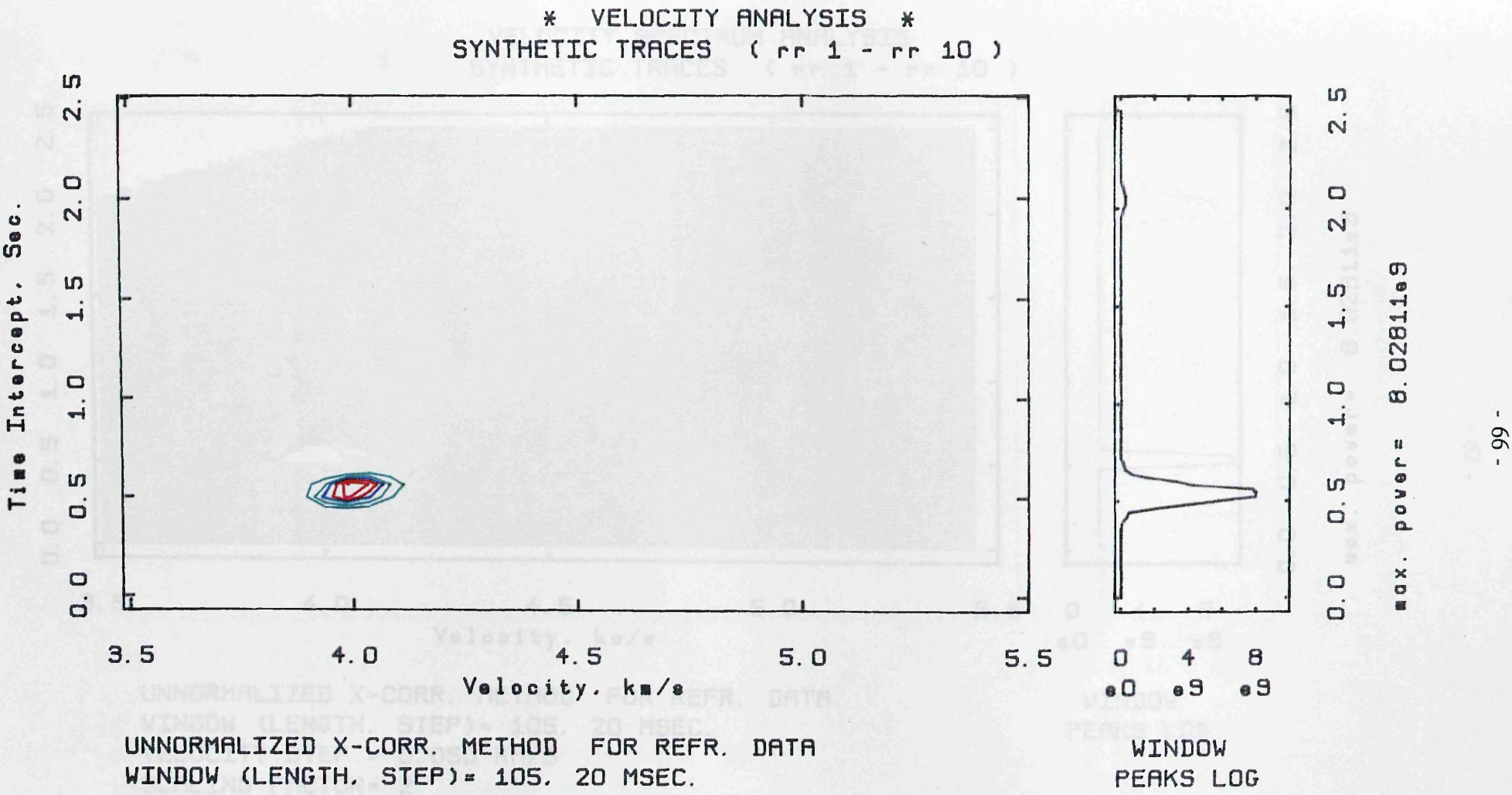


Fig.3.3a Results of applying the unnormalised crosscorrelation method to dataset "rr" displayed in contour format.

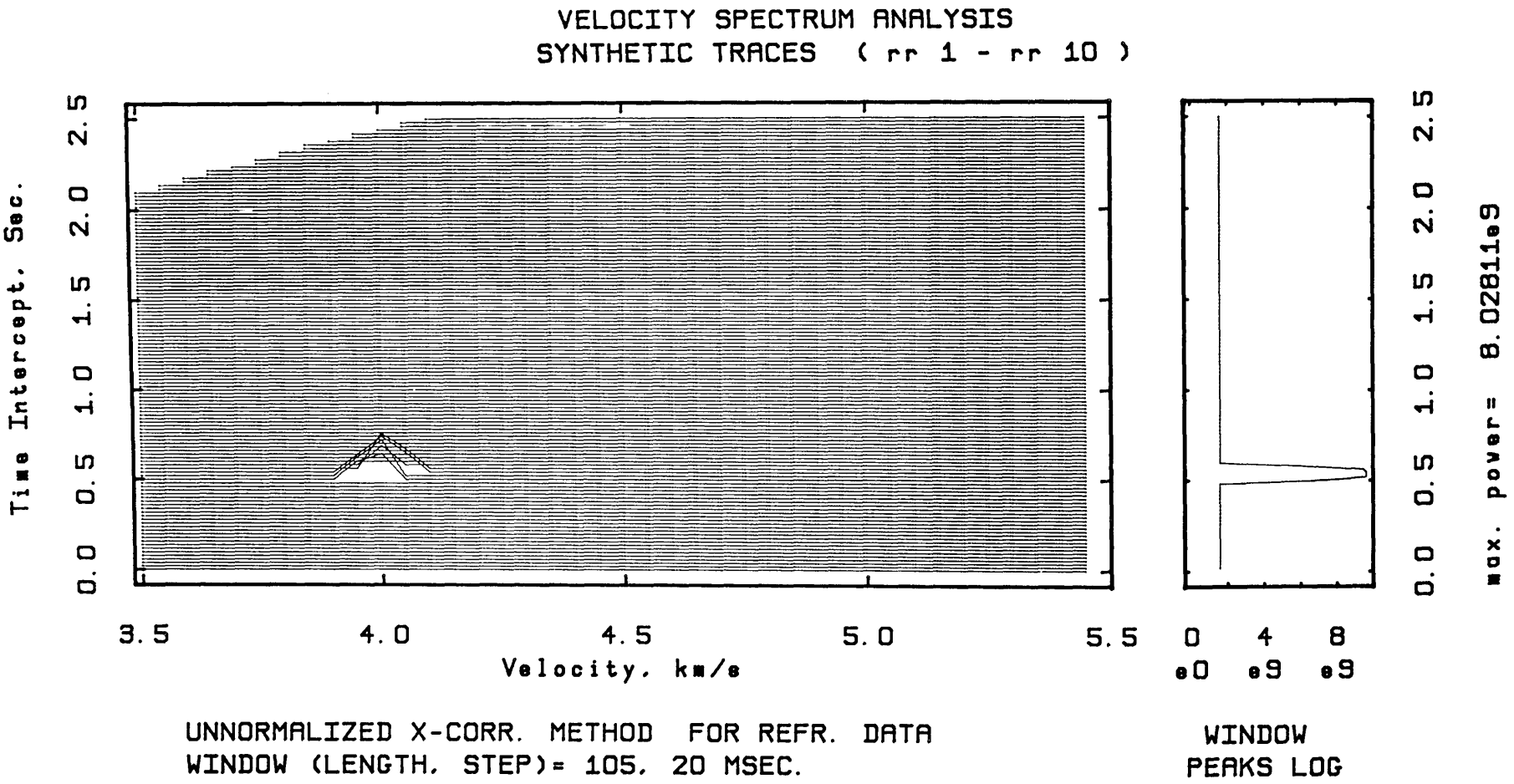


Fig.3.3b Results of applying the unnormalised crosscorrelation method to dataset "rr" displayed in velocity spectrum form.

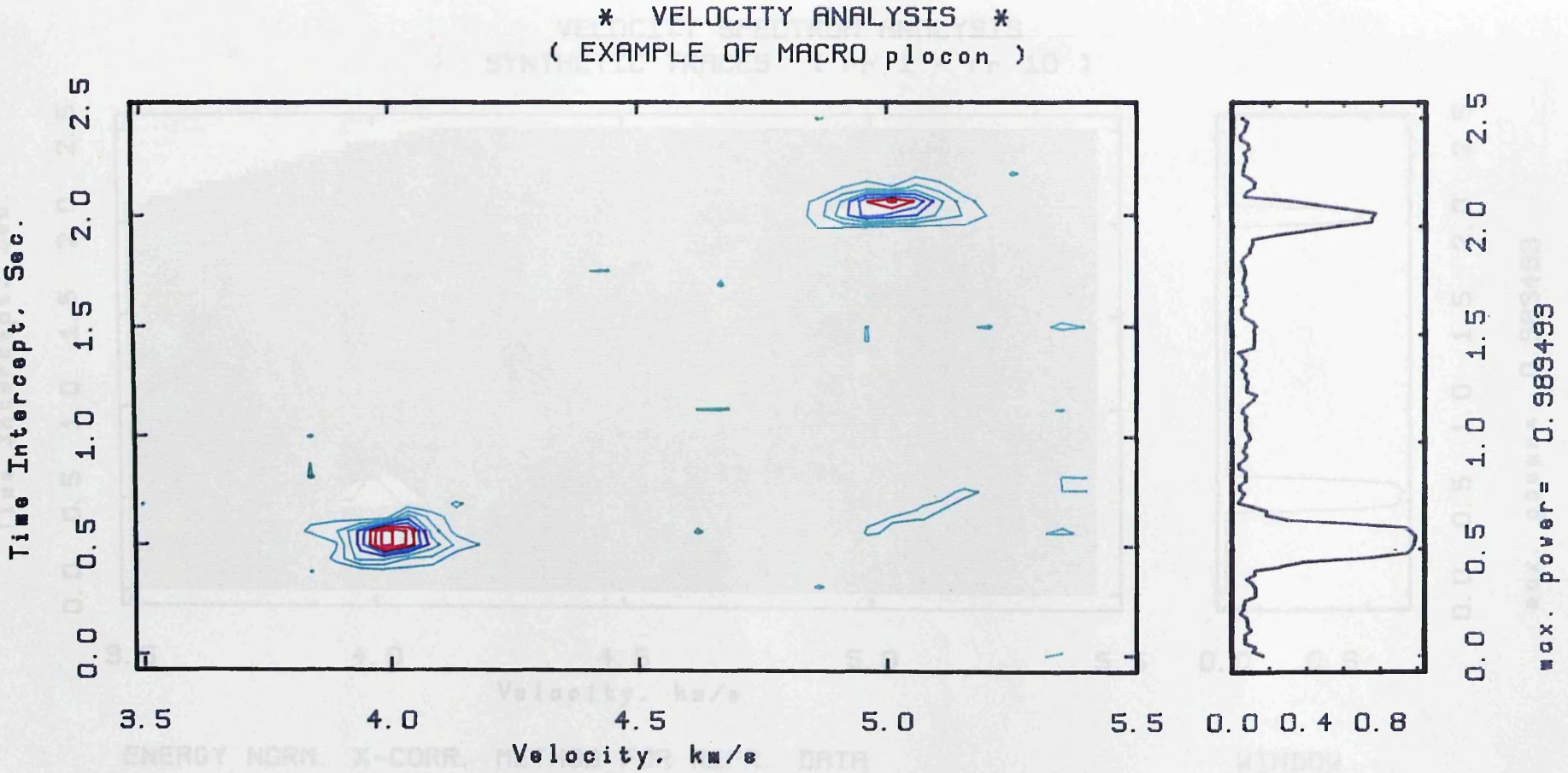


Fig.3.4a Results of applying the energy normalised crosscorrelation method to dataset "rr" displayed in contour format.

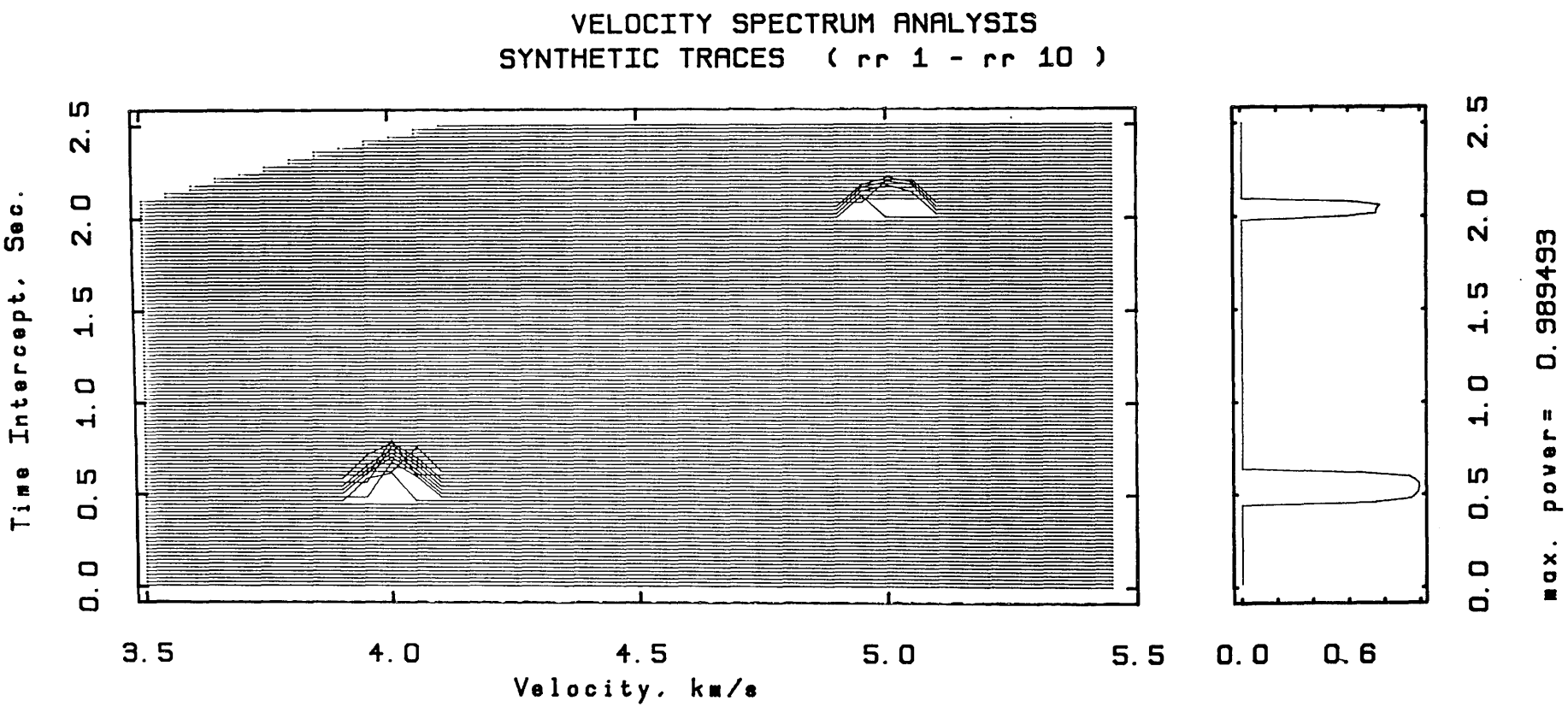


Fig.3.4b Results of applying the energy normalised crosscorrelation method to dataset "rr" displayed in velocity spectrum form.

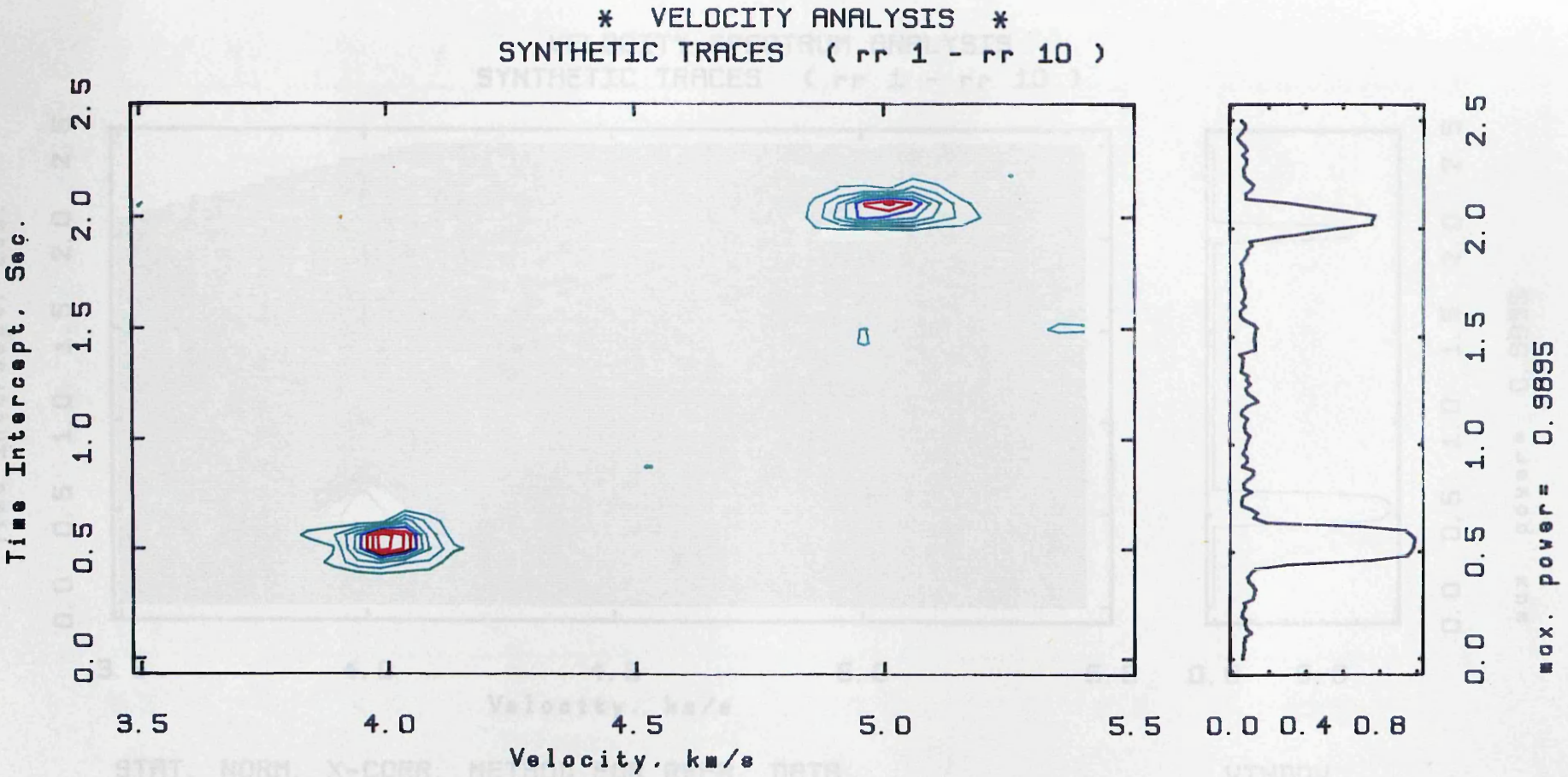


Fig.3.5a Results of applying the statistical normalised crosscorrelation method to dataset "rr" displayed in contour format.

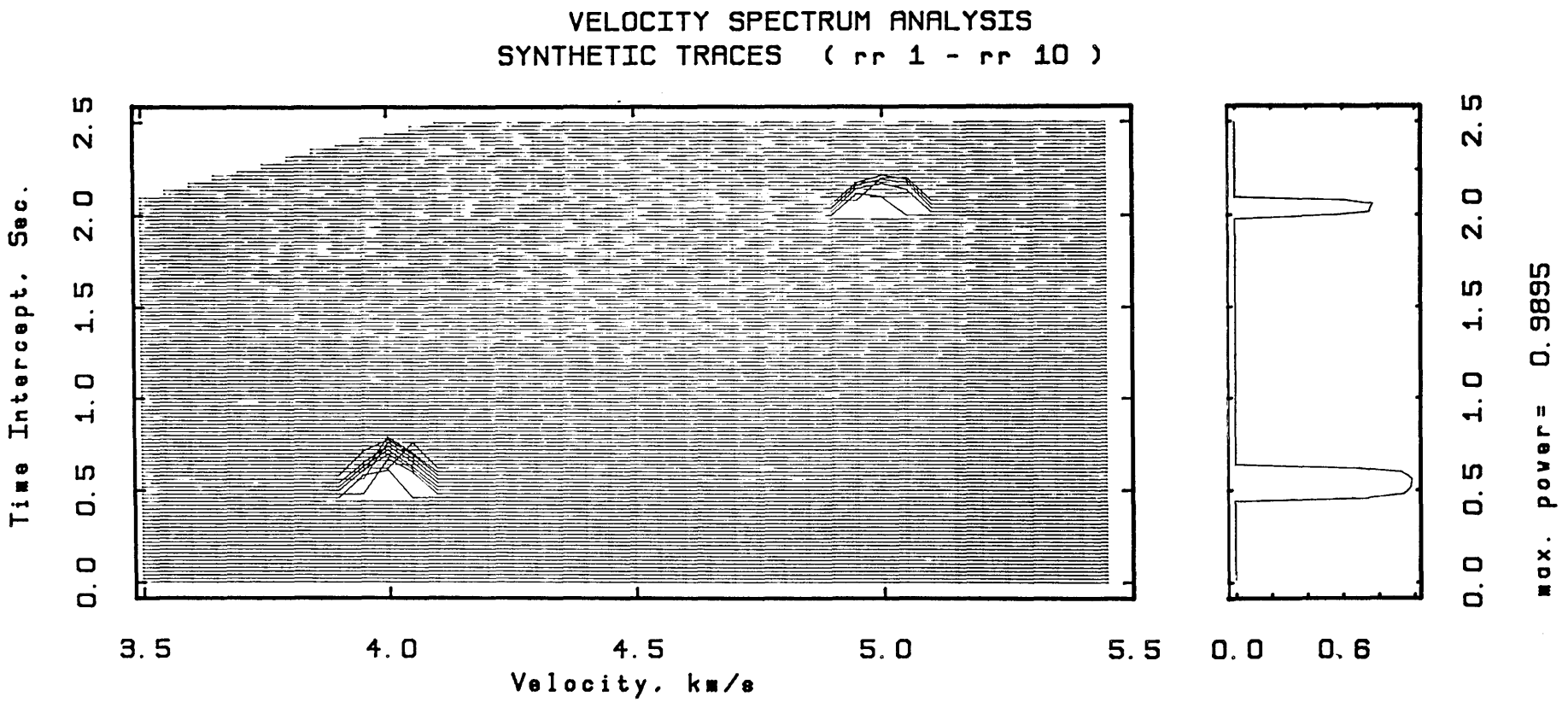


Fig.3.5b Results of applying the statistical normalised cross correlation method to dataset "rr" displayed in velocity spectrum form.

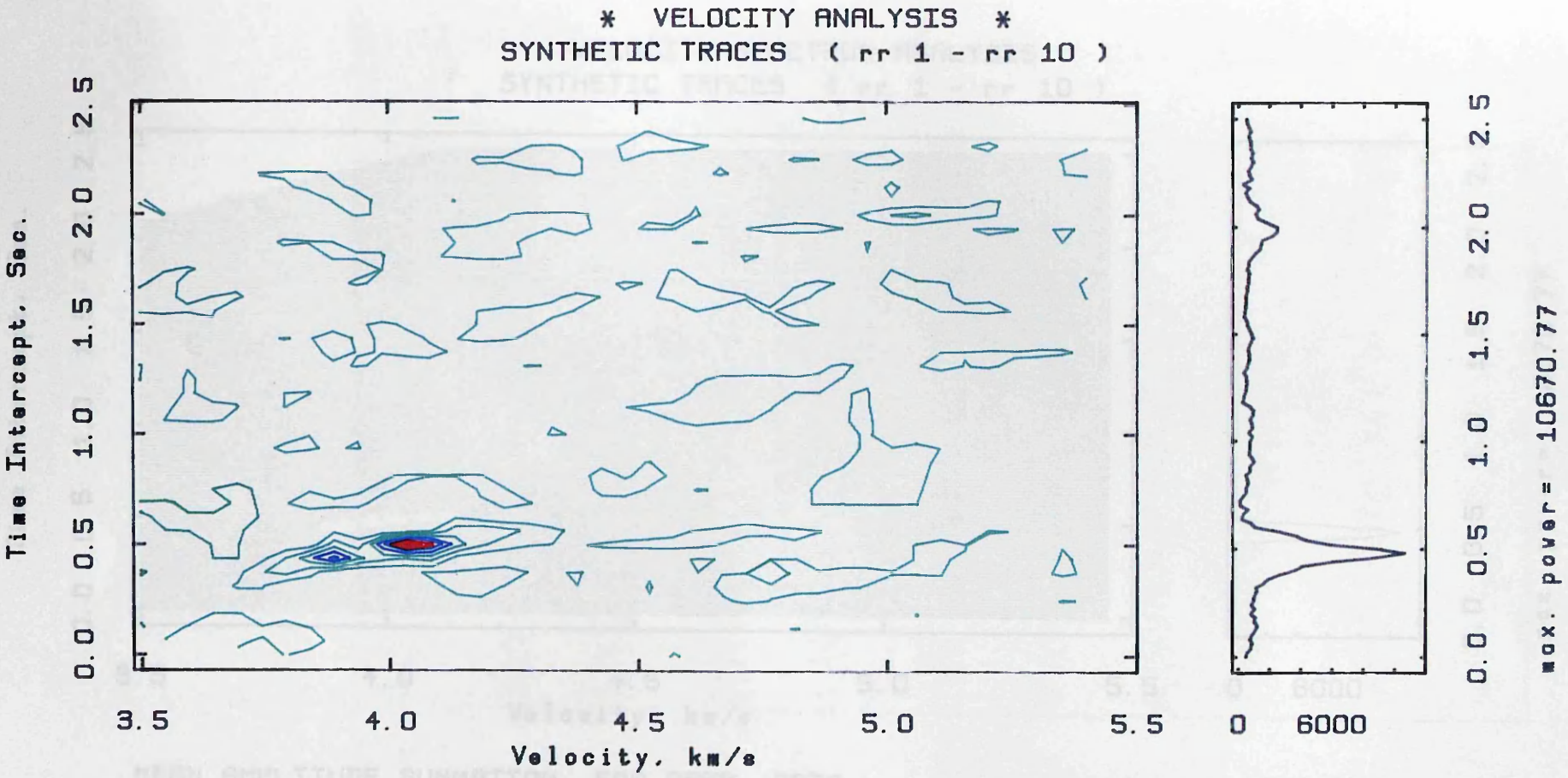


Fig.3.6a Results of applying the mean amplitude summation method to dataset "rr" displayed in contour format.

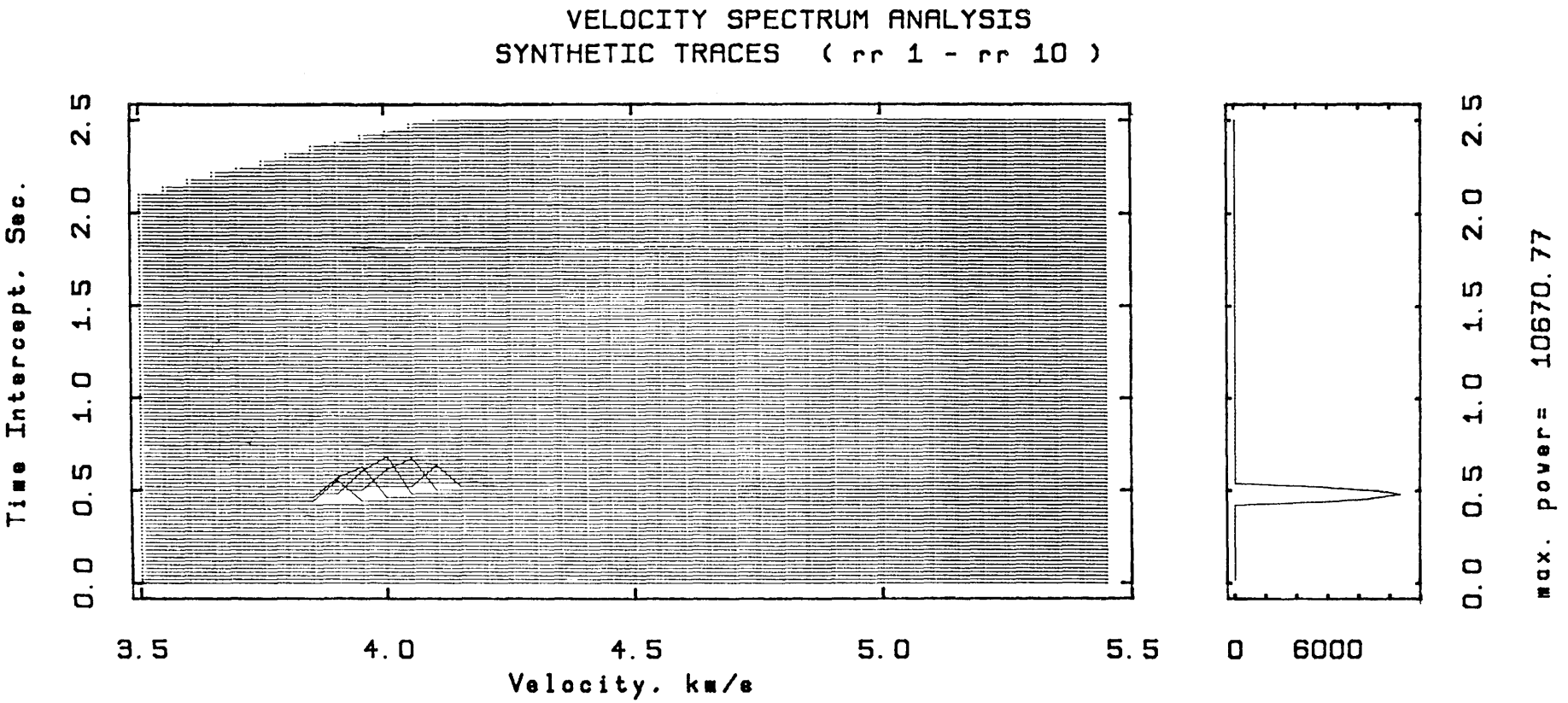


Fig.3.6b Results of applying the mean amplitude summation method to dataset "rr" displayed in velocity spectrum form.

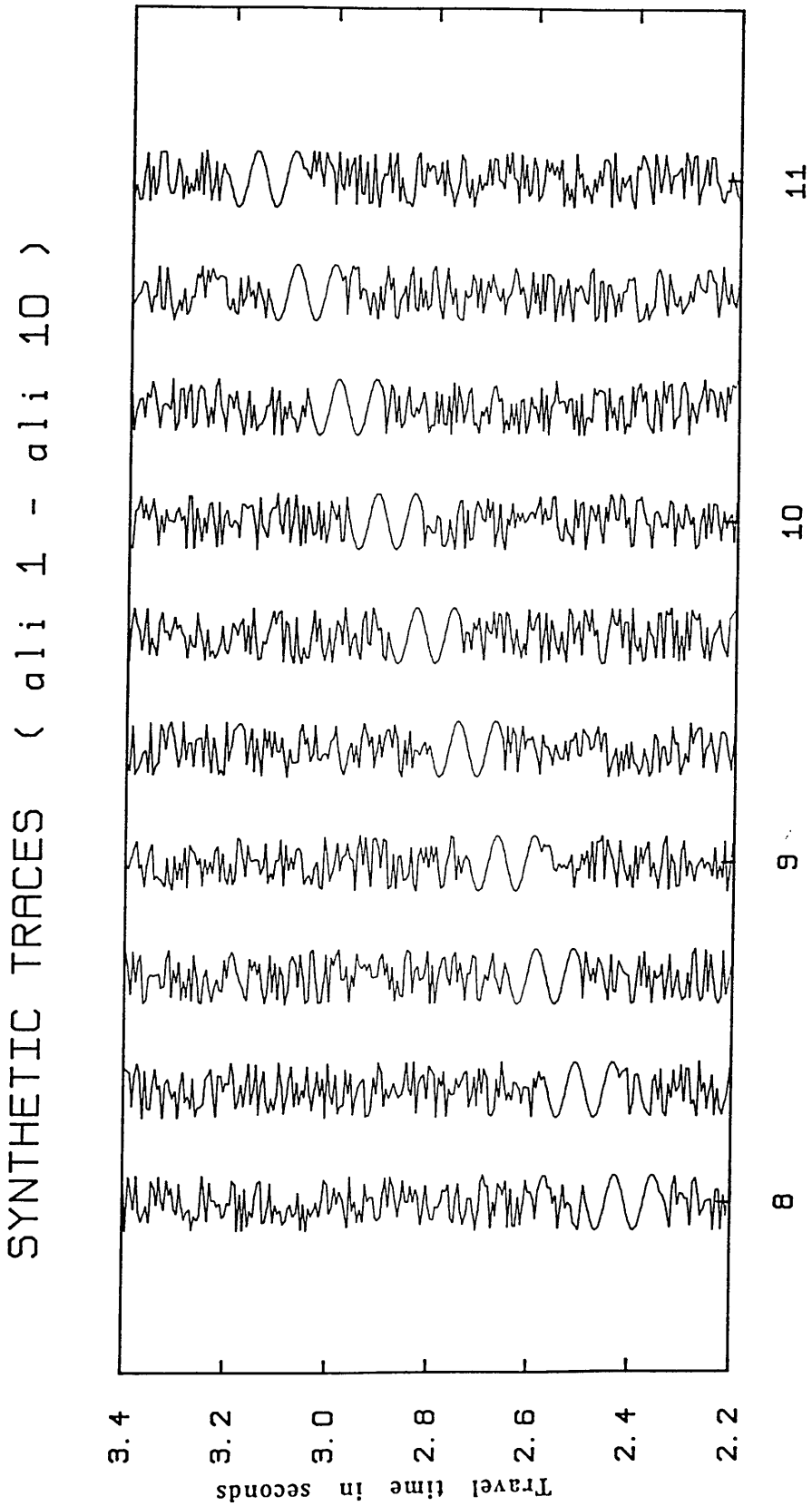


Fig.3.7 Synthetic seismic traces, set "ali", containing one reflected event of normal TWT =1.0 s, velocity =3.8 km/s, frequency =14 Hz, and span =145 msec.

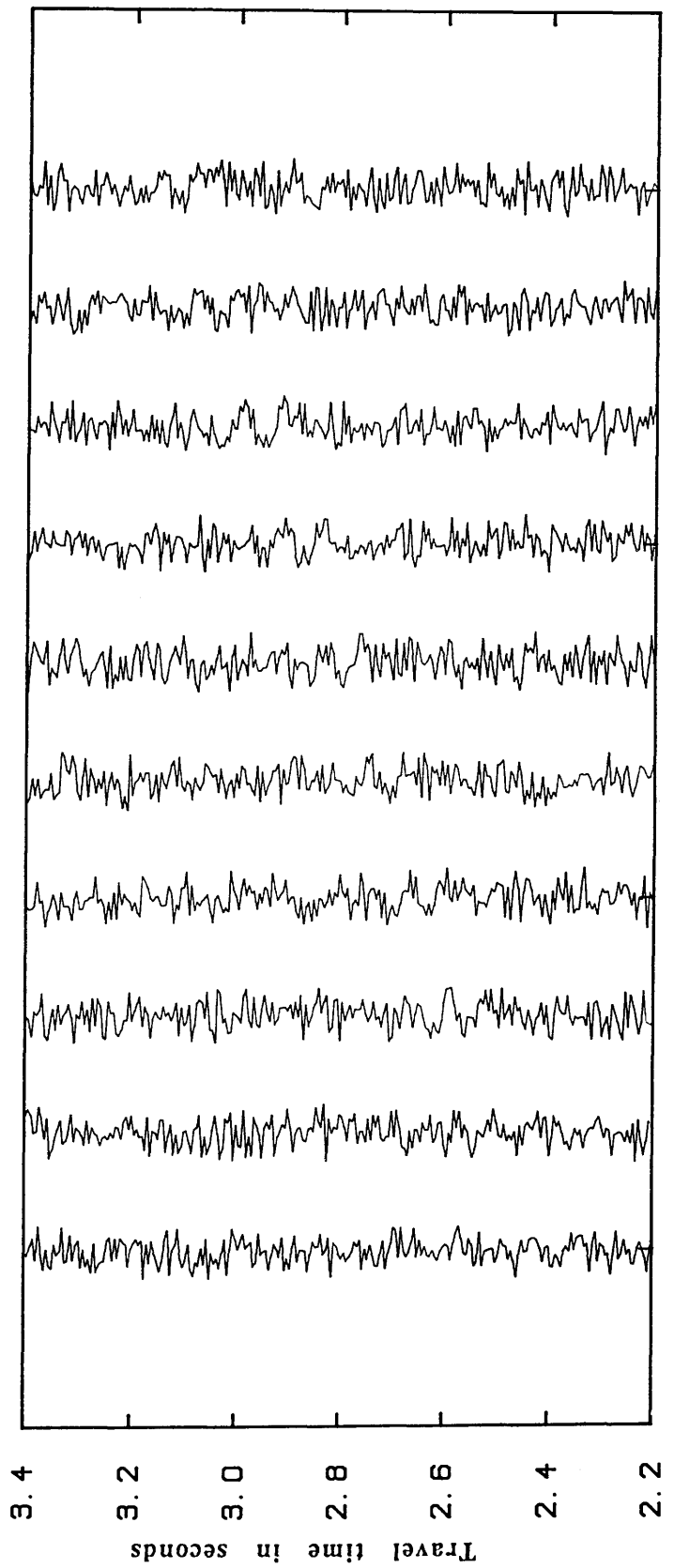


Fig.3.8 Synthetic seismic traces, set "alno", which was constructed by stacking traces of the set "ali", Fig. 3.7, with noisy traces.

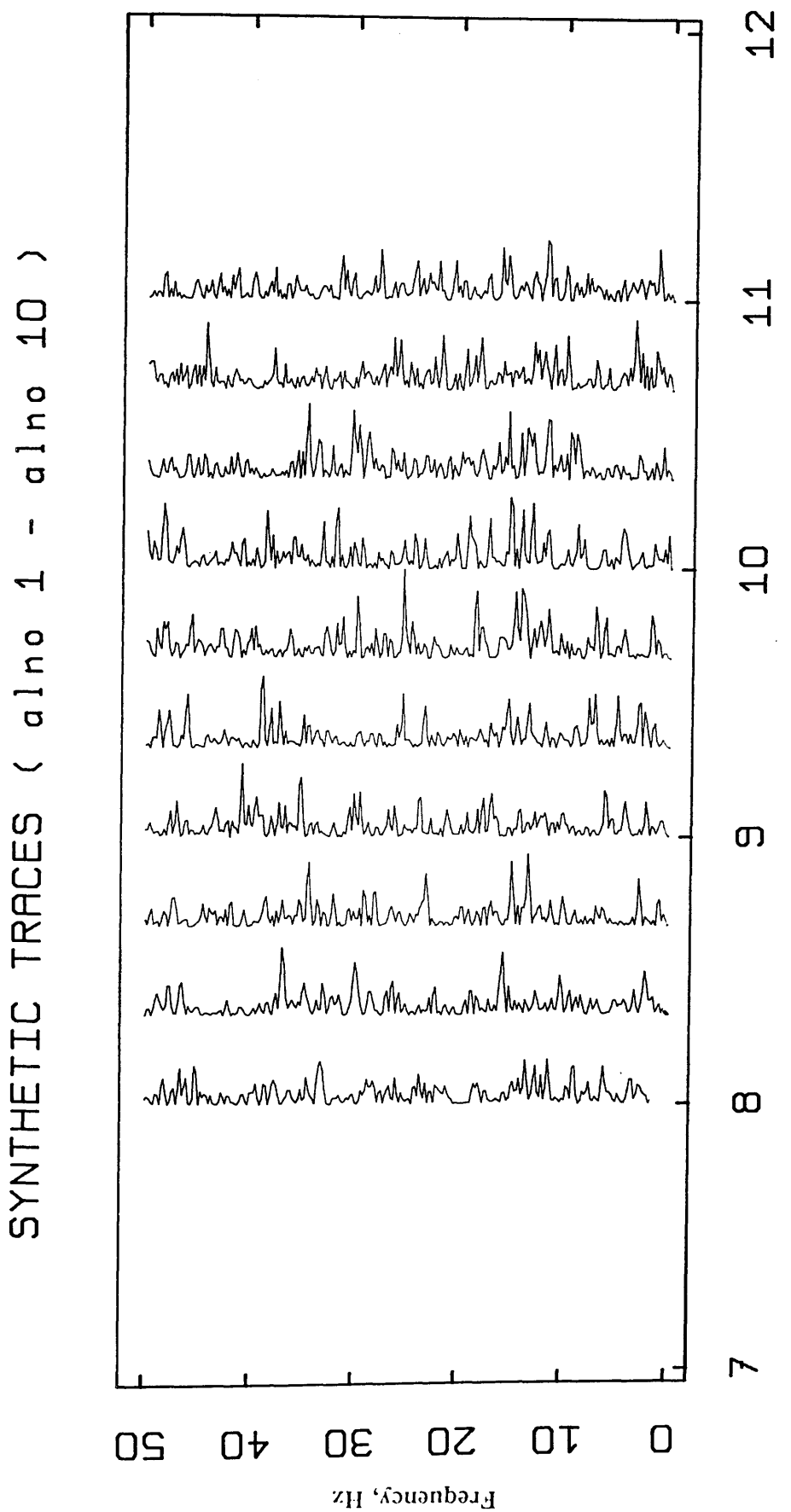


Fig.3.9 Frequency analysis of traces in the dataset "alno", Fig 3.8, showing that there is no dominant frequency in the set.

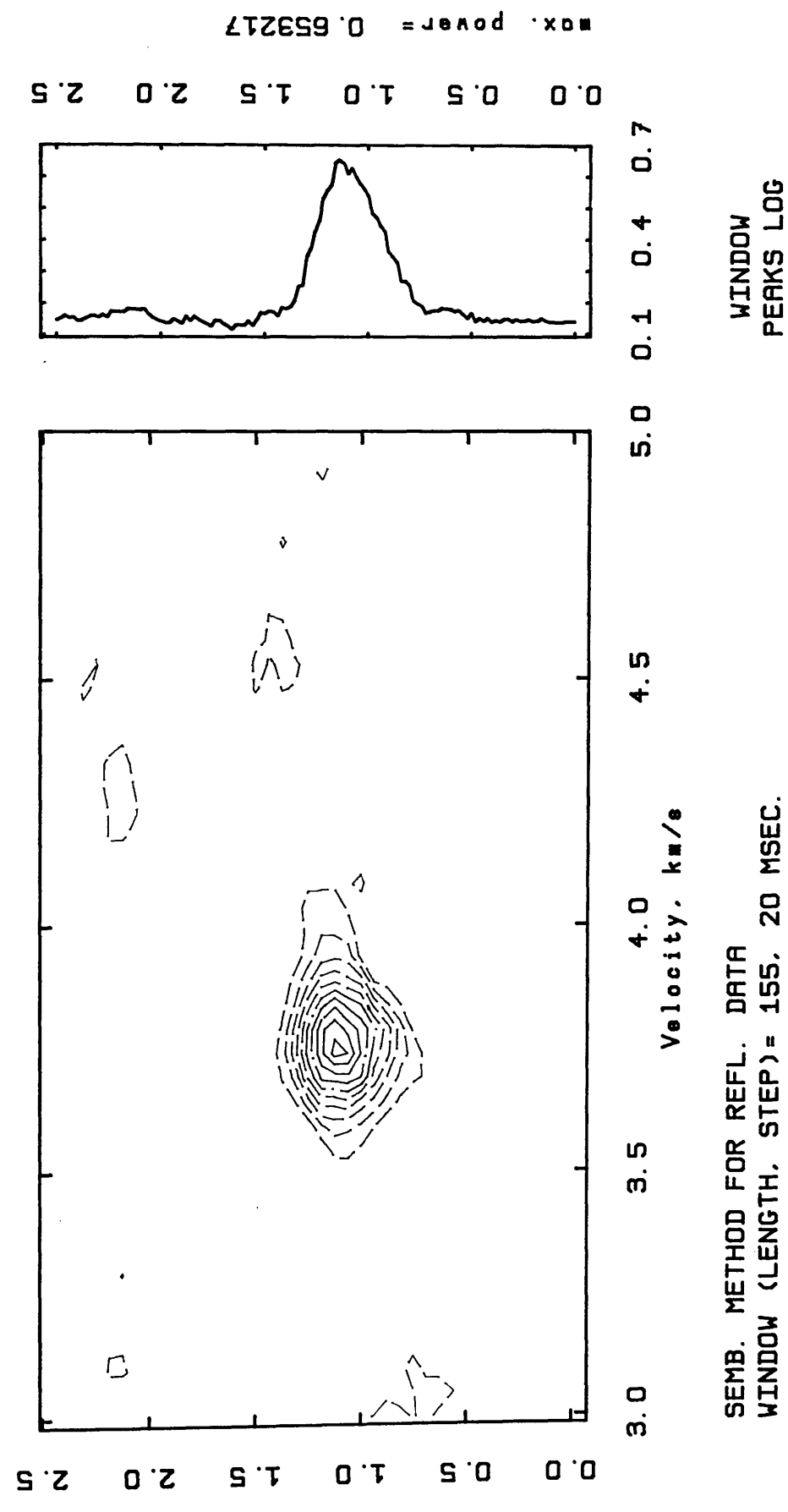


Fig.3.10a Results of applying the semblance method to dataset "alno" displayed in contour format.

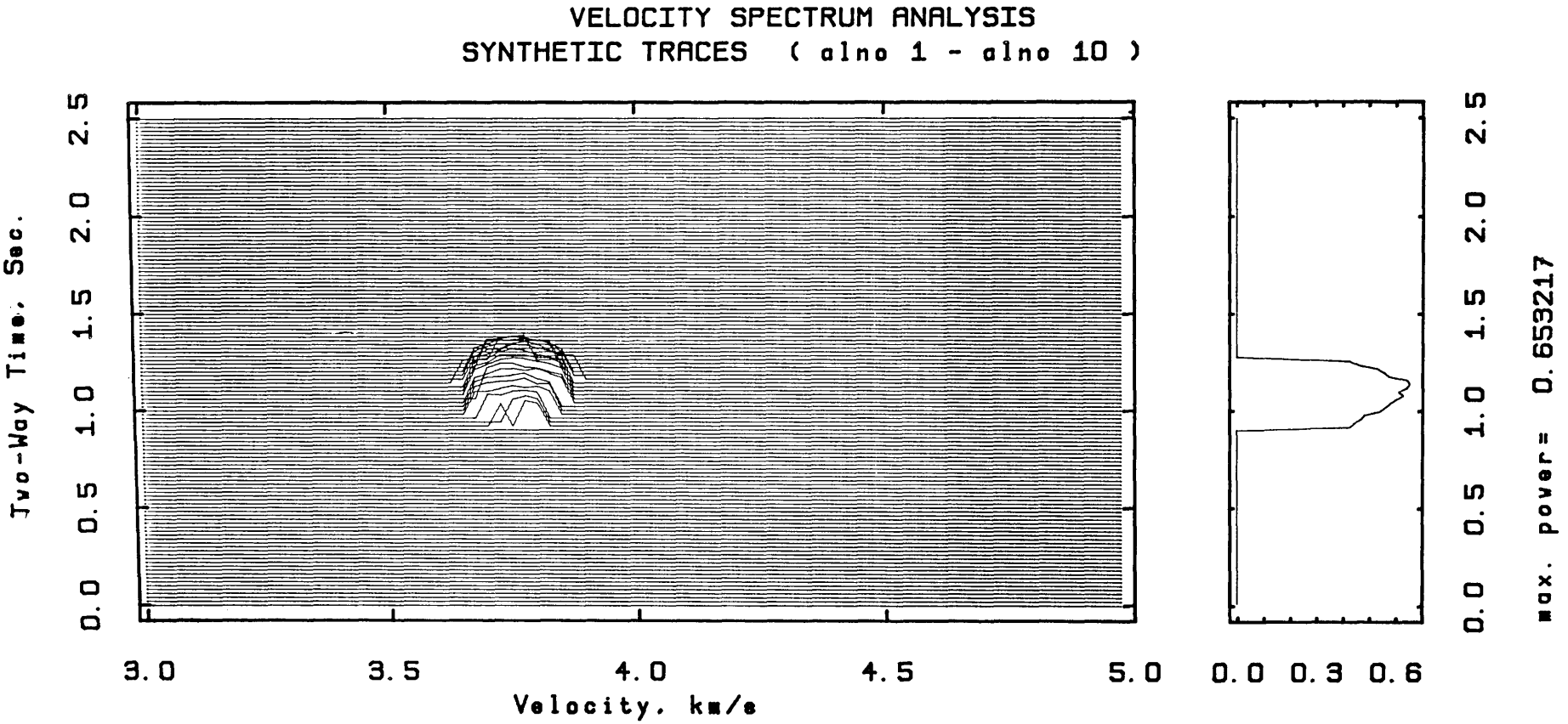


Fig.3.10b Results of applying the semblance method to the dataset "alno" displayed in velocity spectrum form.

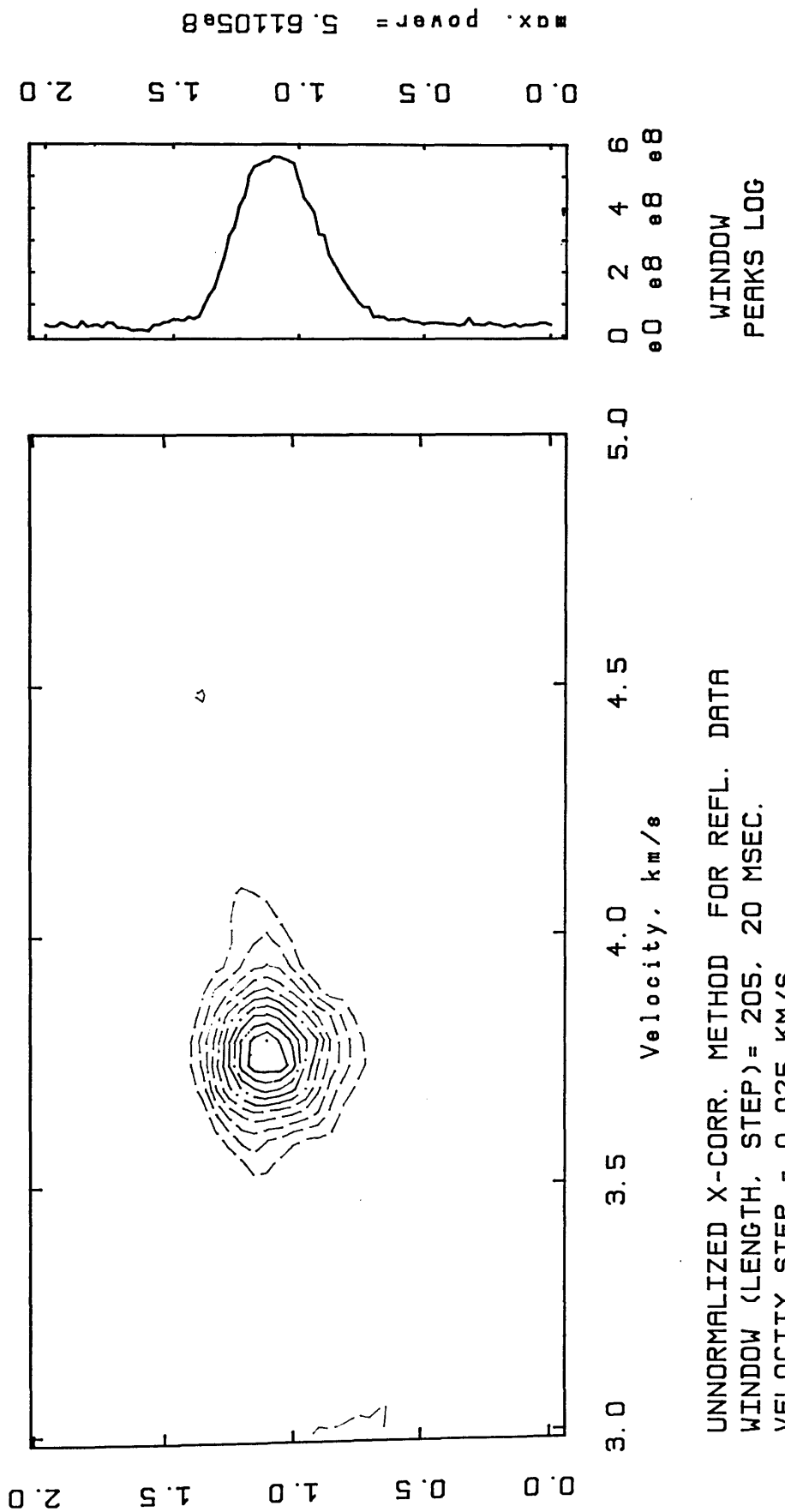


Fig.3.10c Results of applying the unnormalised crosscorrelation method to the dataset "alno" displayed in contour format.

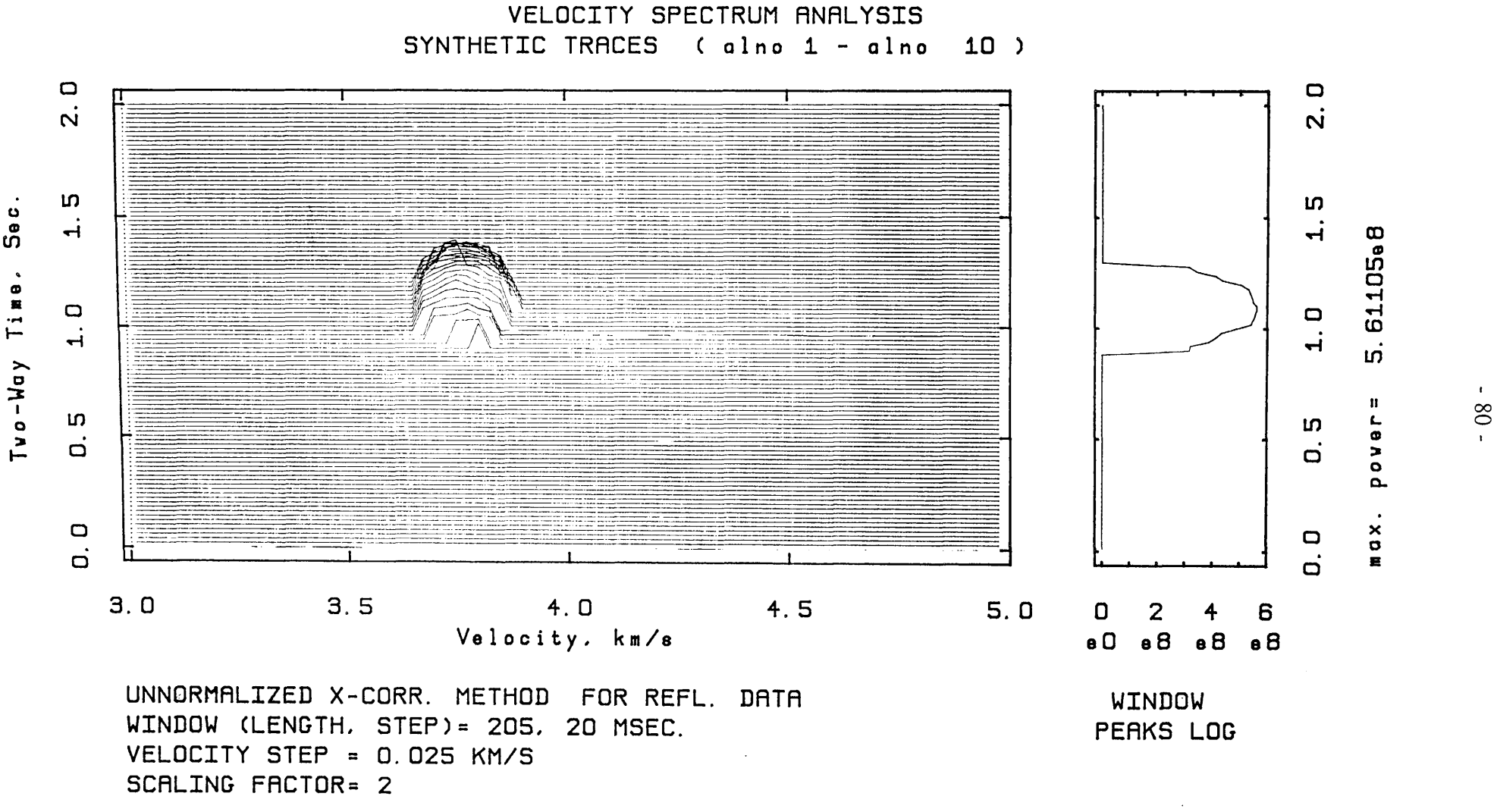


Fig.3.10d Results of applying the unnormalised crosscorrelation method to the dataset "alno" displayed in velocity spectrum form.

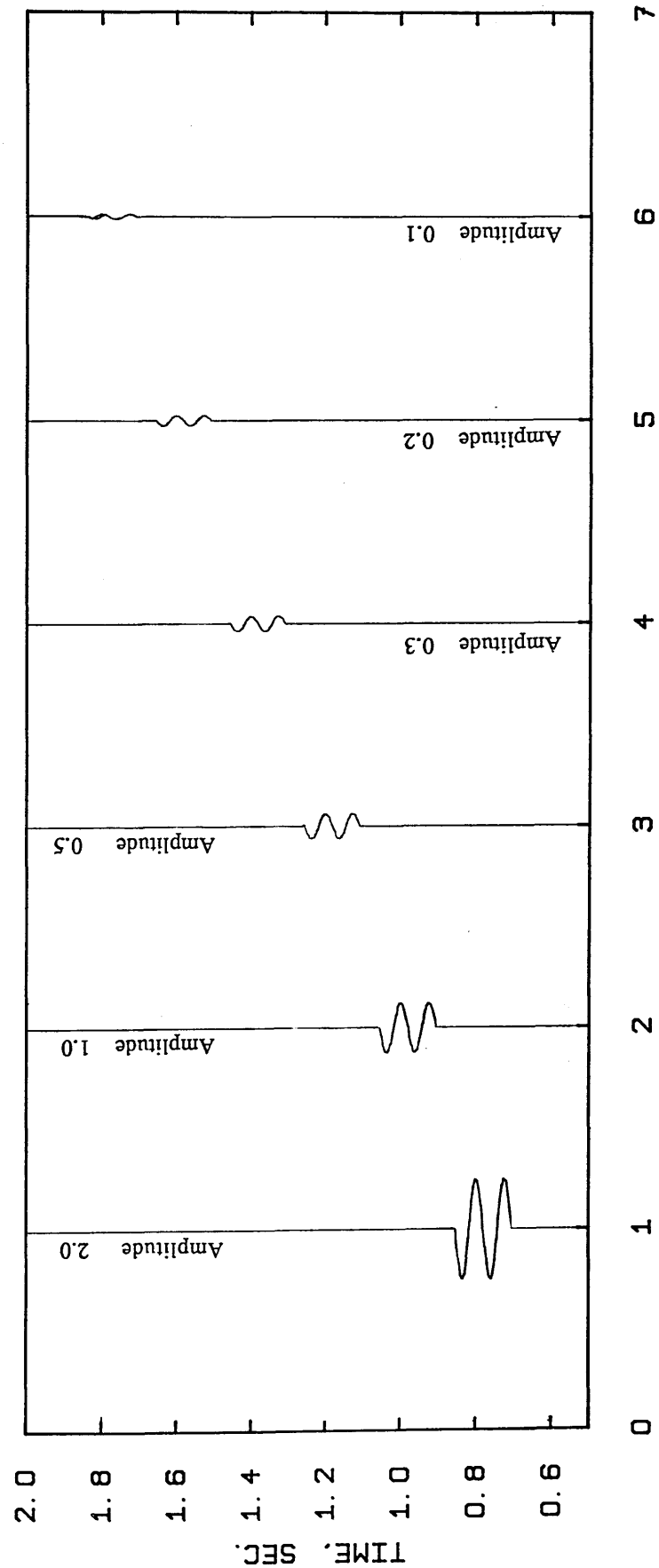


Fig.3.11 Six synthetic seismic traces displaying one trace only from each set of the "sig*" group. All sets contain the same event but with different amplitude.

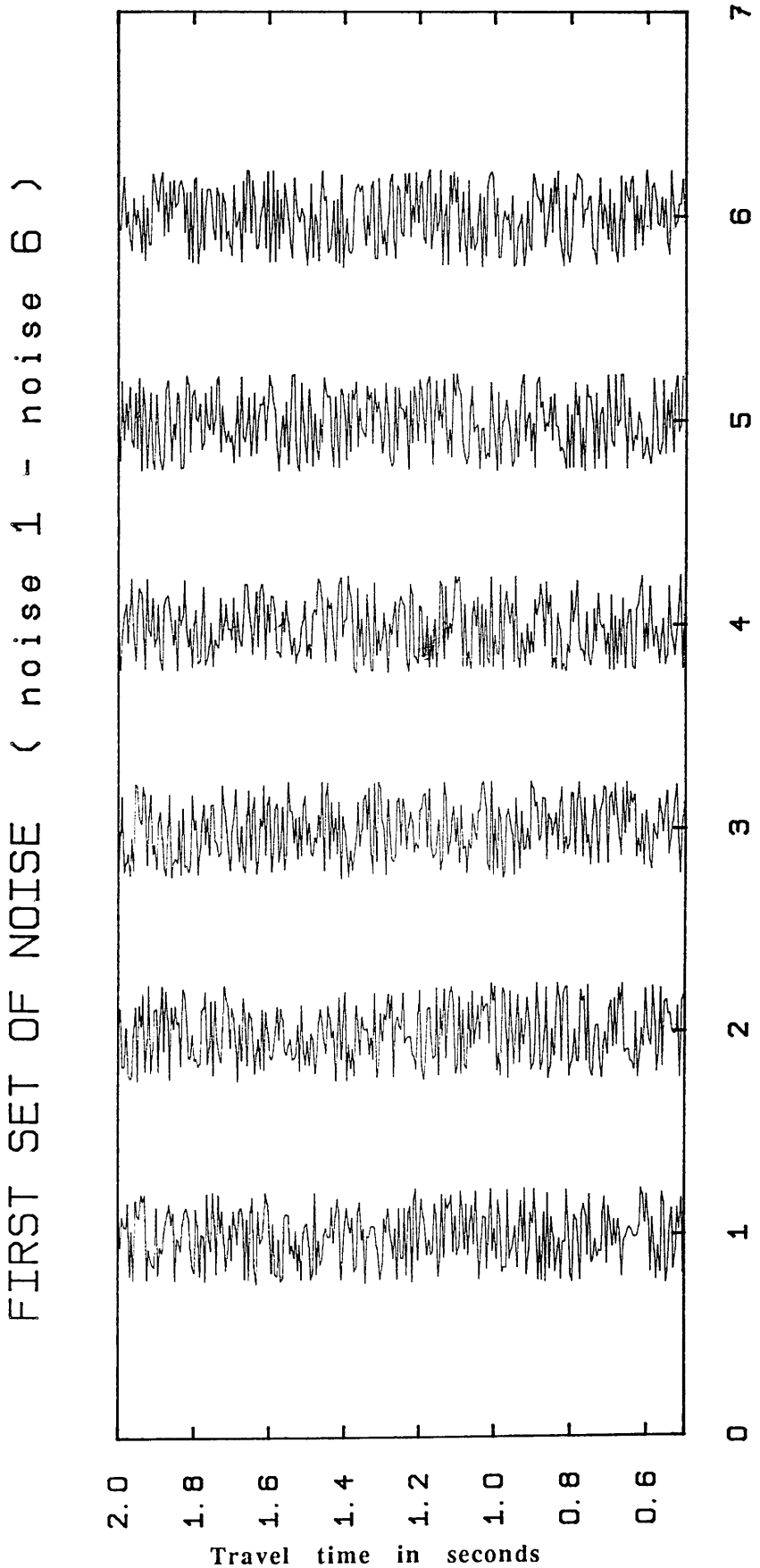


Fig.3.12a Set of six synthetic noisy traces "noise", maximum amplitude equal one.

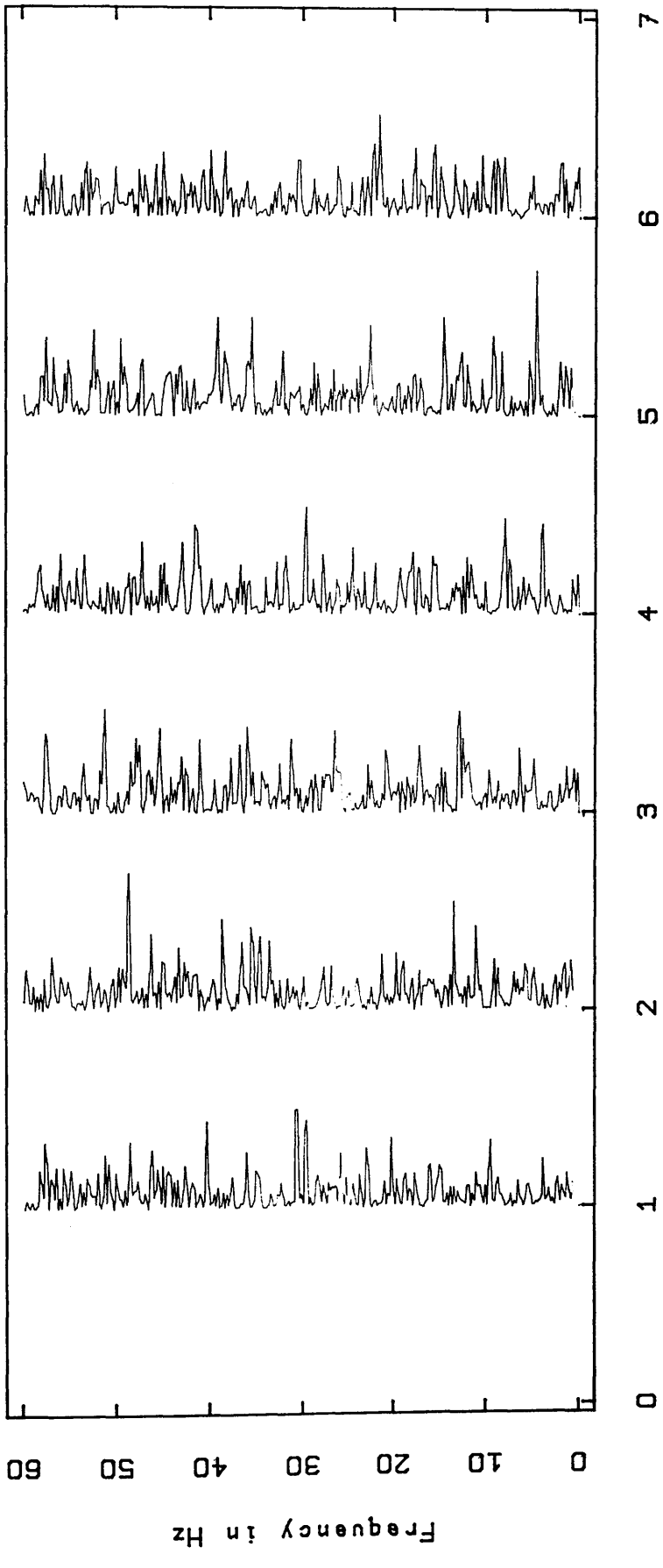


Fig.3.12b Frequency analysis of traces in the dataset "noise", Fig 3.12a, showing that there is no dominant frequency in the set.

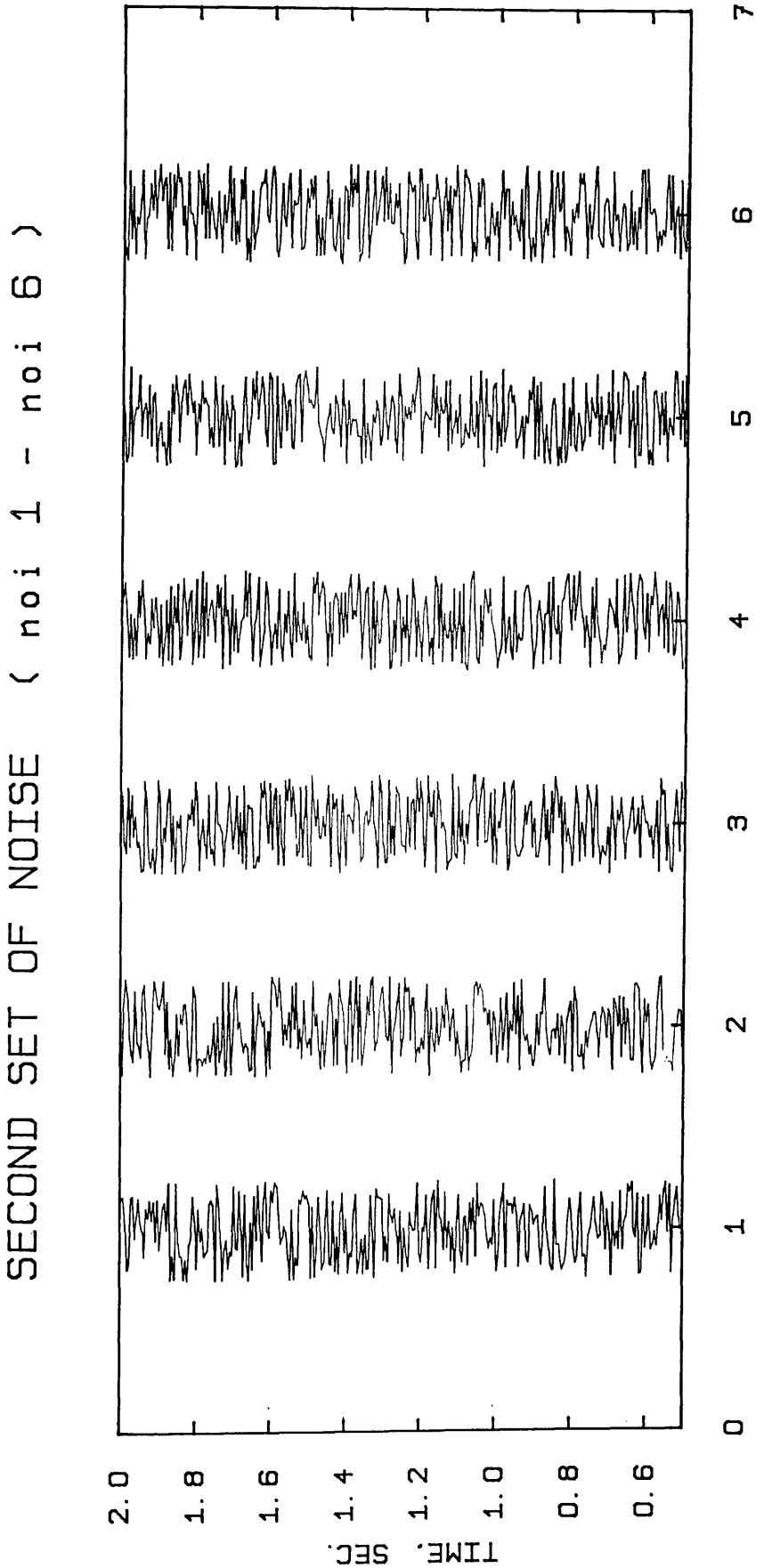


Fig.3.13a Set of six synthetic noisy traces "noi", maximum amplitude equal one.

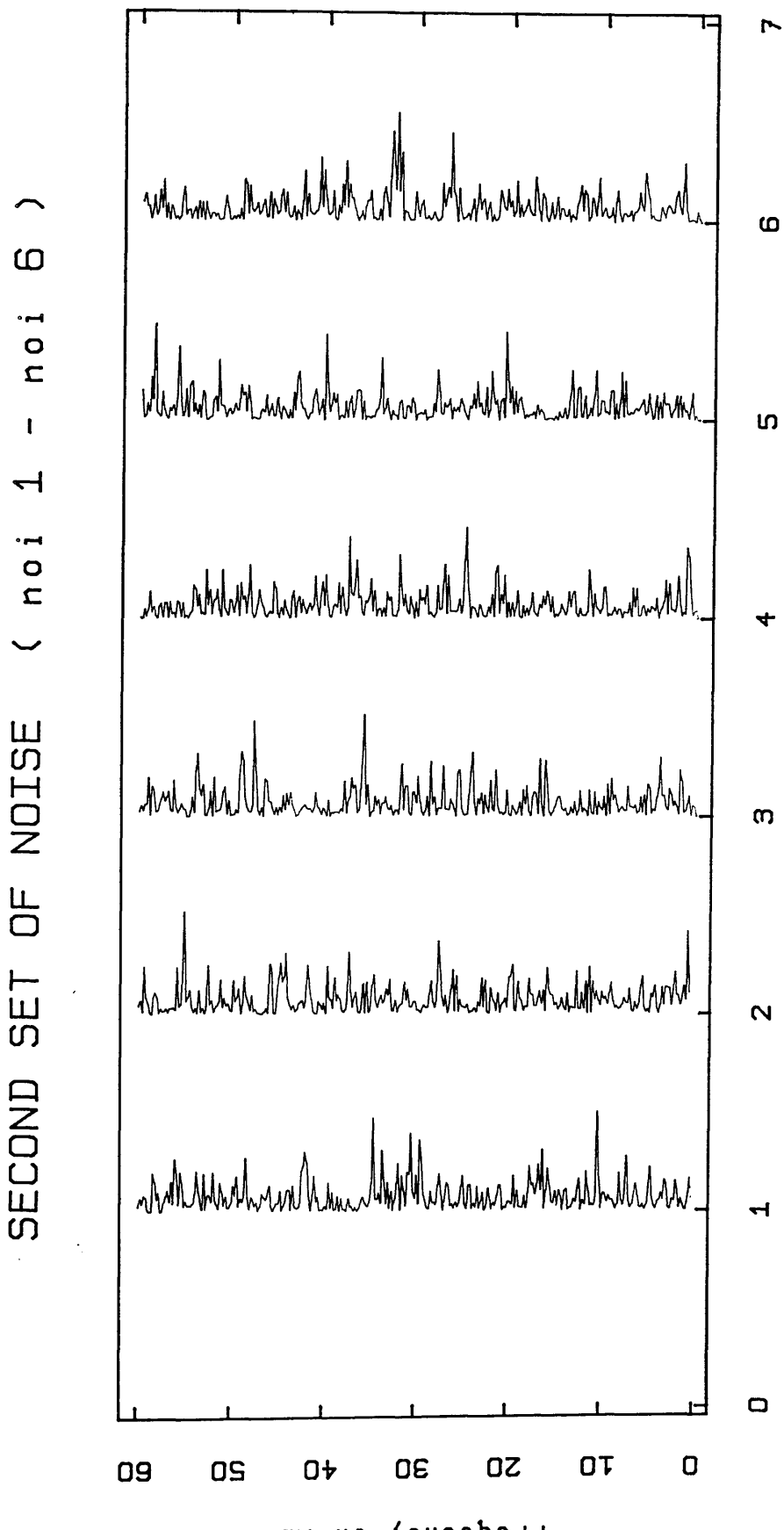


Fig.3.13b Frequency analysis of traces in the dataset "noi", Fig 3.13a, showing that there is no dominant frequency in the set.

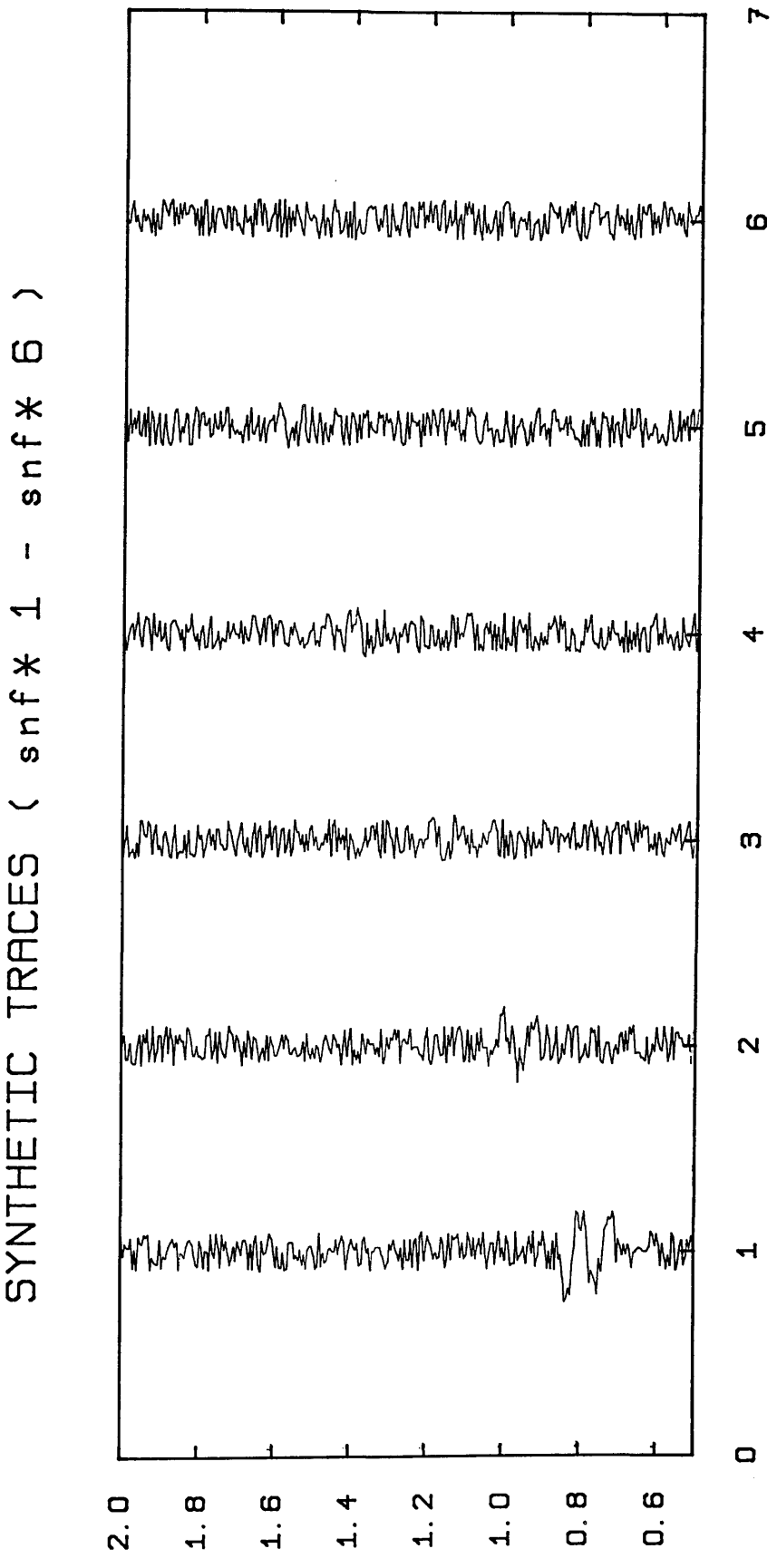


Fig.3.14a Six traces displaying one trace only from each set "snf*", which was constructed by stacking the sets "sig*" of Fig.3.11 with the noisy set "noise" of Fig. 3.12a.

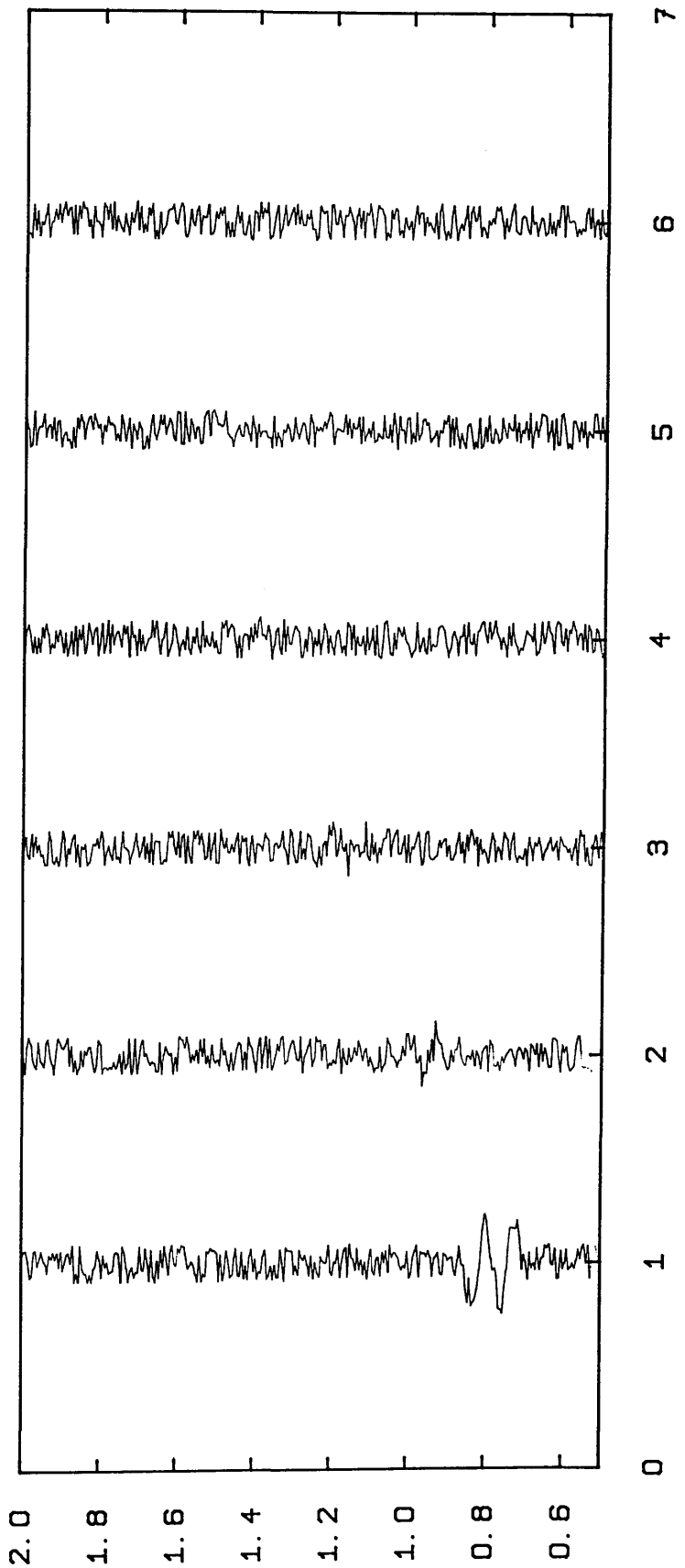


Fig.3.14b Six traces displaying one trace only from each set "sns*", which was constructed by stacking the sets "sig*" of Fig.3.11 with the noisy set "noi" of Fig. 3.13a.

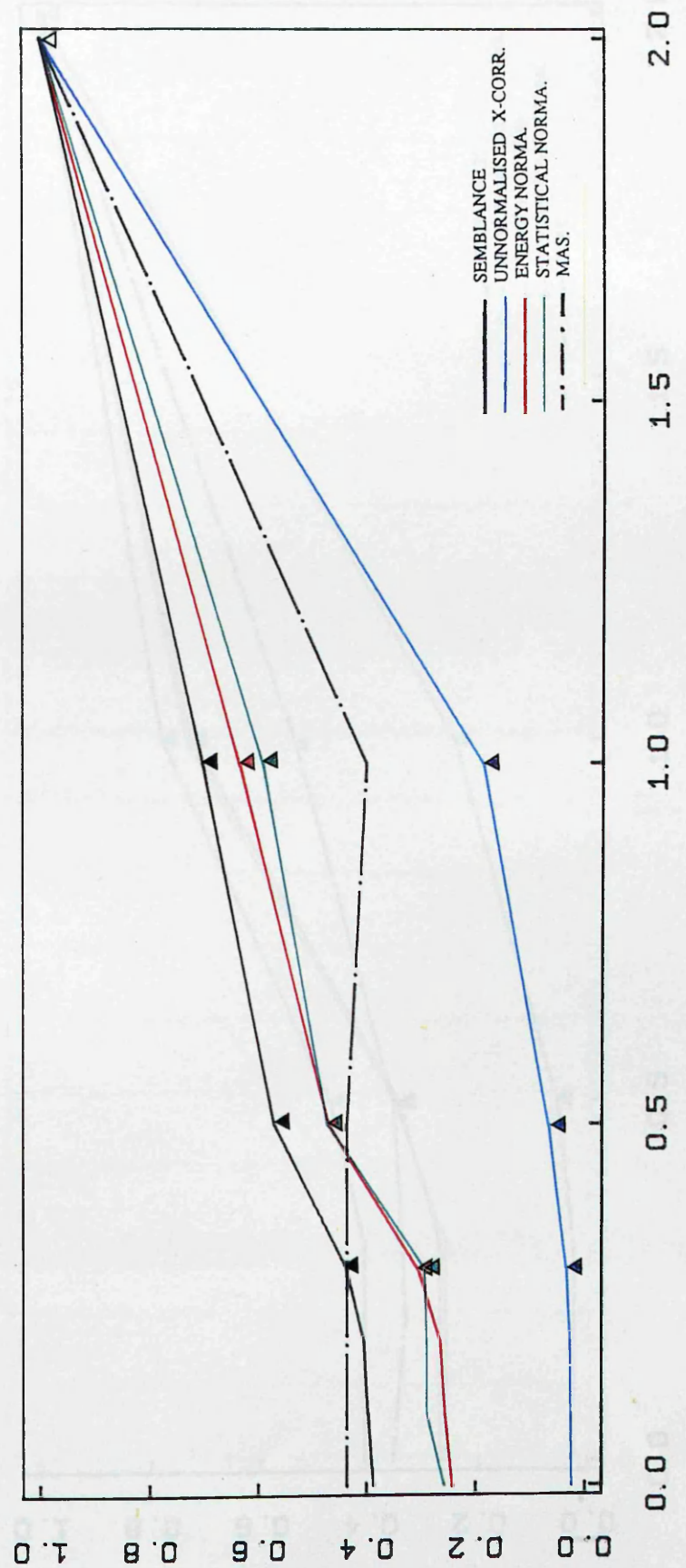


Fig.3.15a Normalised results of all methods employed to the datasets of the first group "snf", which are listed in Table 3.4a. The top of the triangles represent a proper combination of time and velocity.

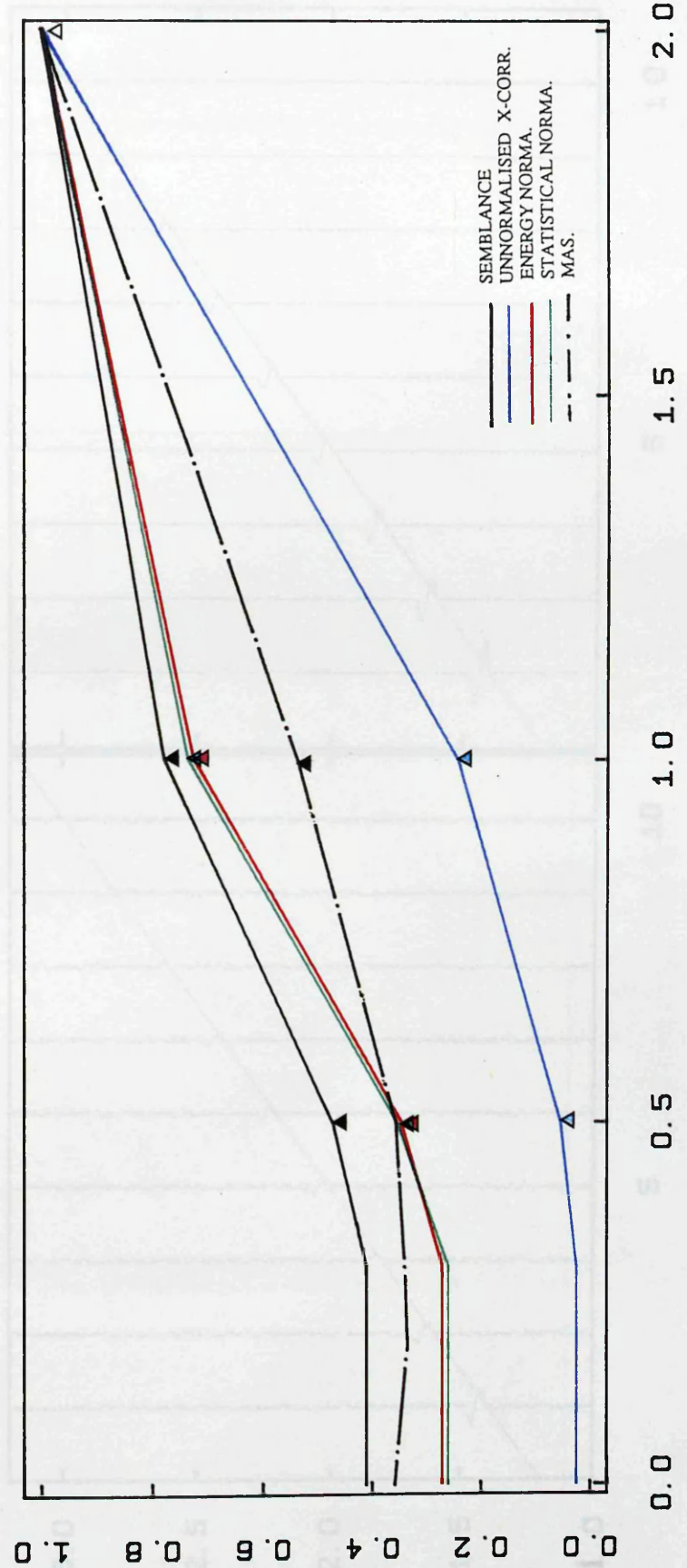


Fig.3.15b Normalised results of all methods employed to the datasets of the first group "sns", which are listed in Table 3.4b. The top of the triangles represent a proper combination of time and velocity.

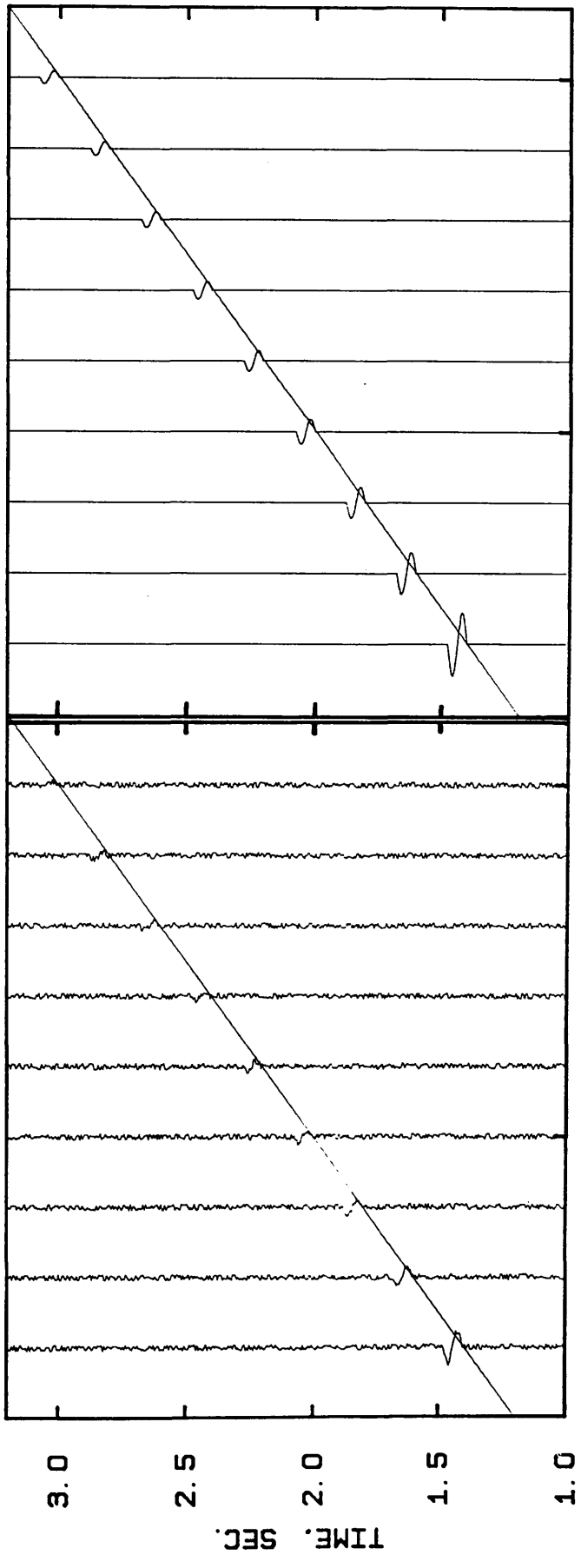


Fig.3.16 A) Synthetic seismic traces, set "signoi", which was constructed by stacking noisy traces with traces of the set "dsn". B) Synthetic noise-free traces "dsn" containing one refracted event with velocity =5.0 km/sec; time intercept =1 sec; frequency = 14 Hz and span =75 msec.

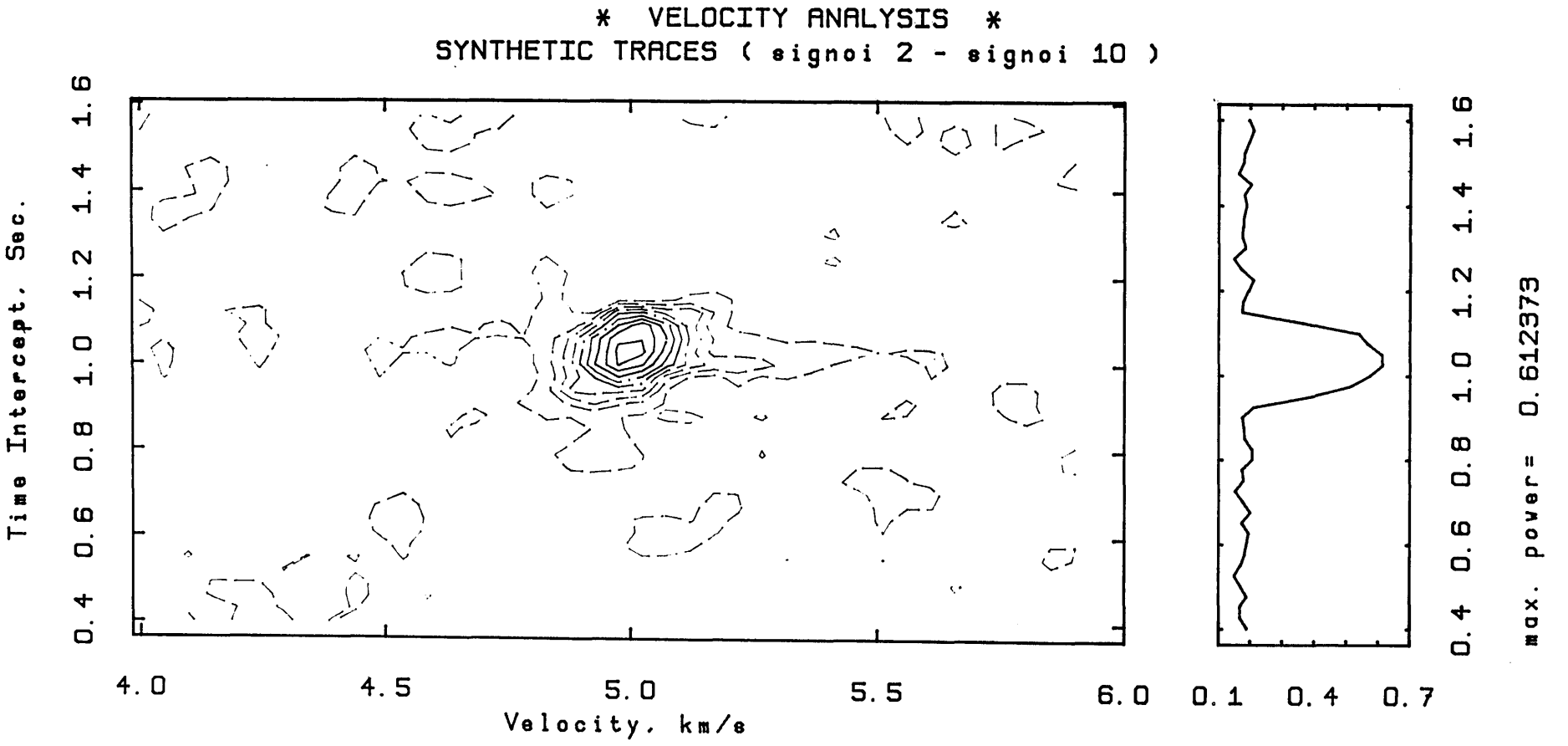


Fig.3.17a Results of applying the semblance method to dataset "signoi" displayed in contour format.

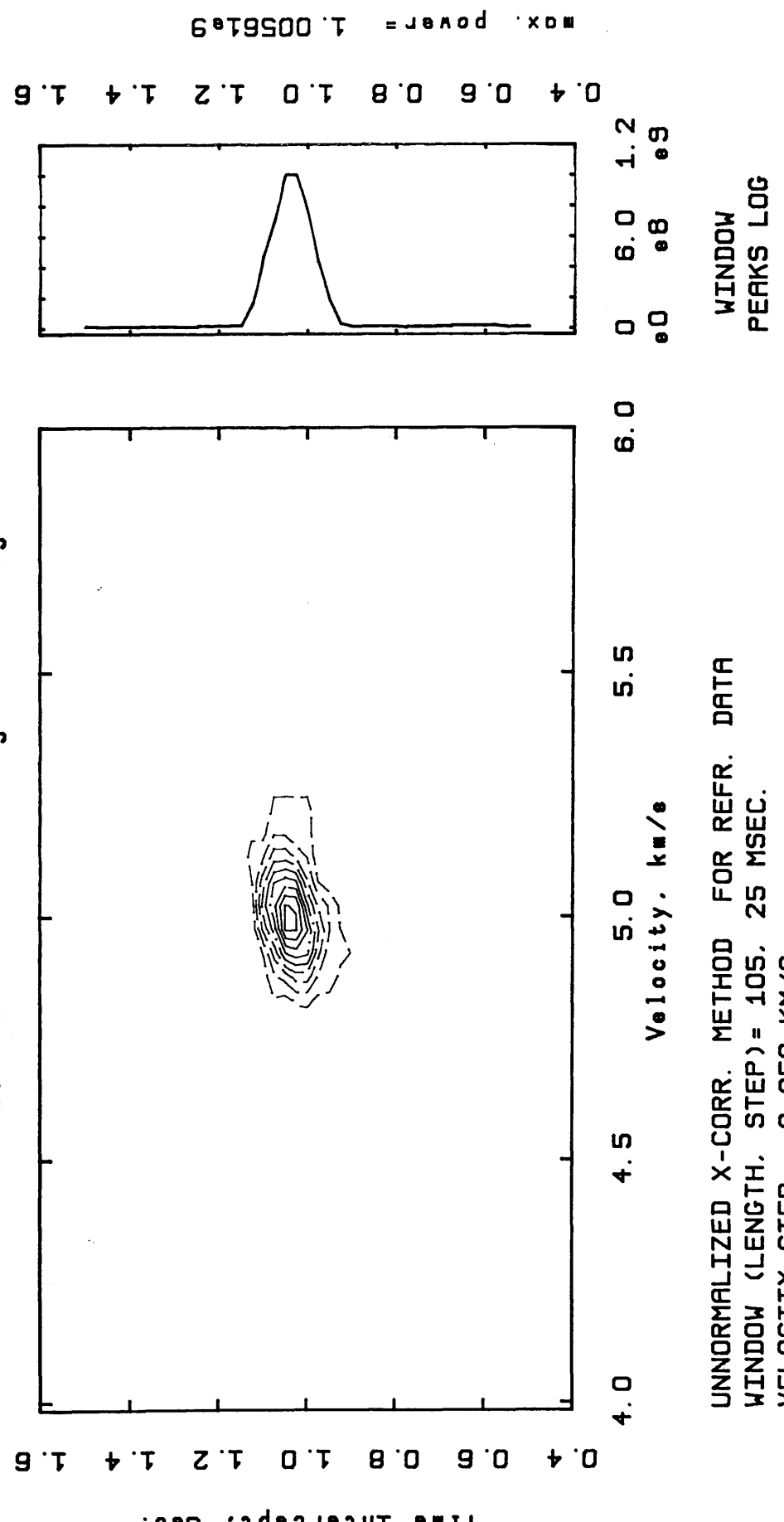


Fig.3.17b Results of applying the unnormalised crosscorrelation method to dataset "signoi" displayed in contour format.

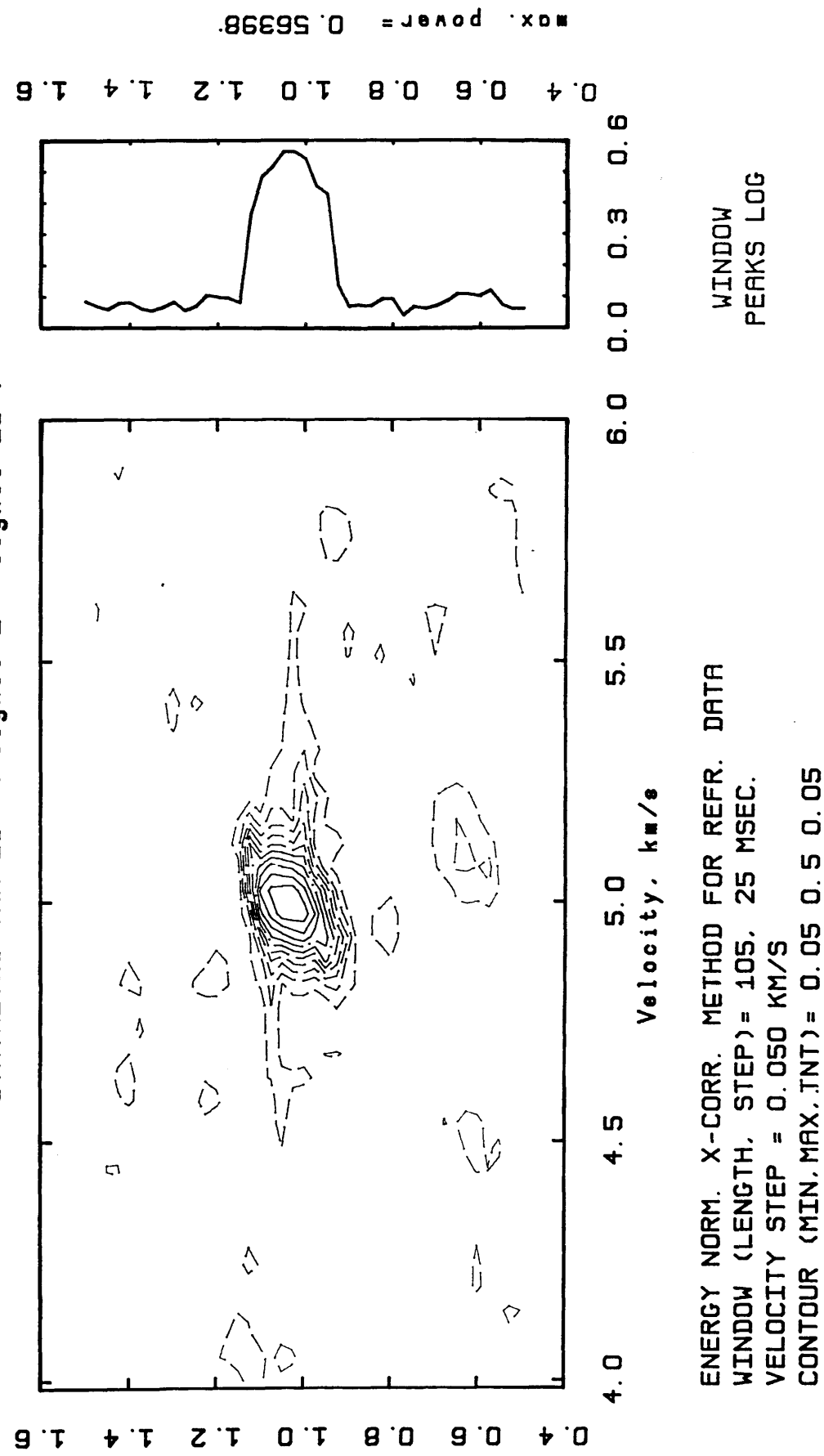


Fig.3.17c Results of applying the energy normalised crosscorrelation method to dataset "signoi" displayed in contour format.

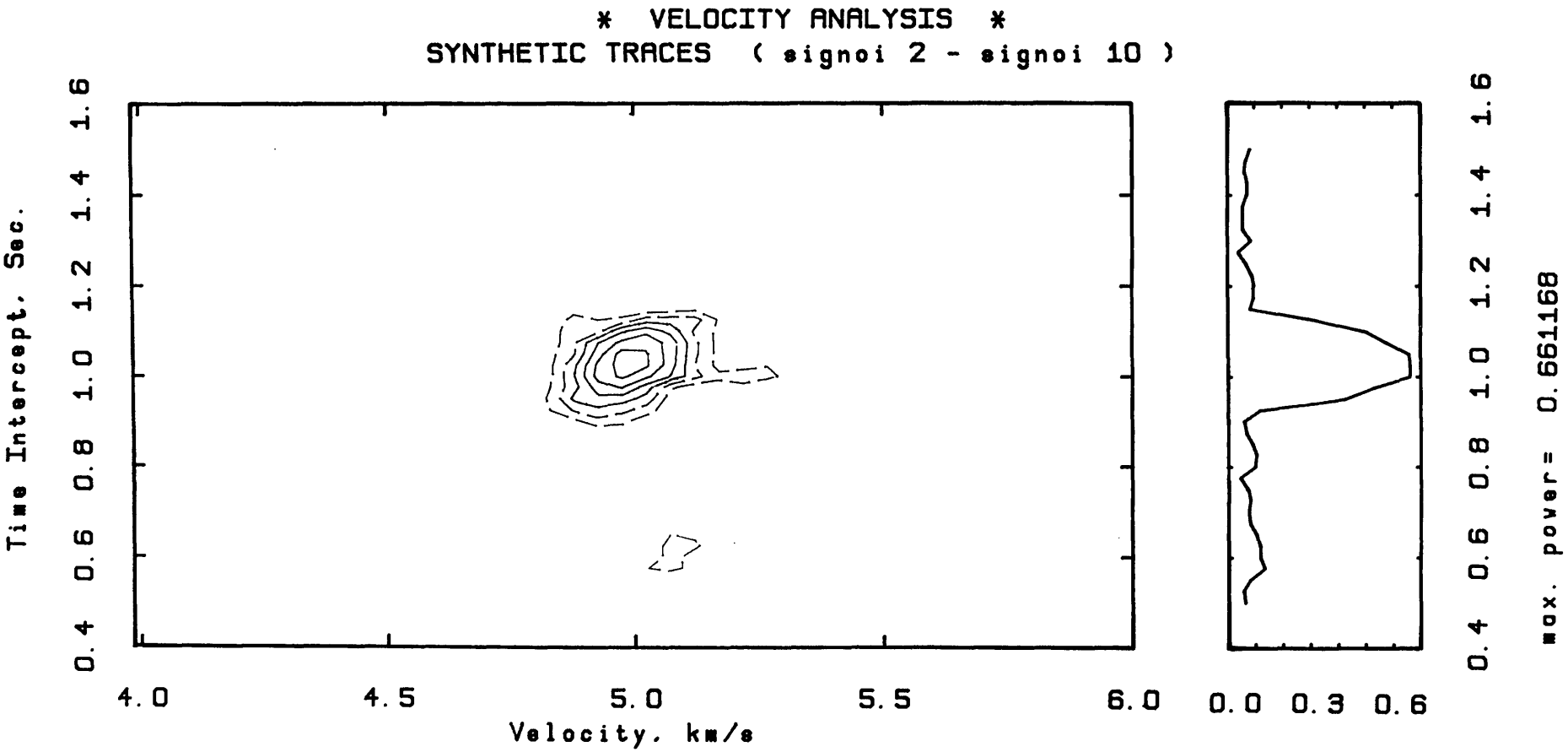


Fig.3.17d Results of applying the statistical normalised crosscorrelation method to dataset "signoi" displayed in contour format.

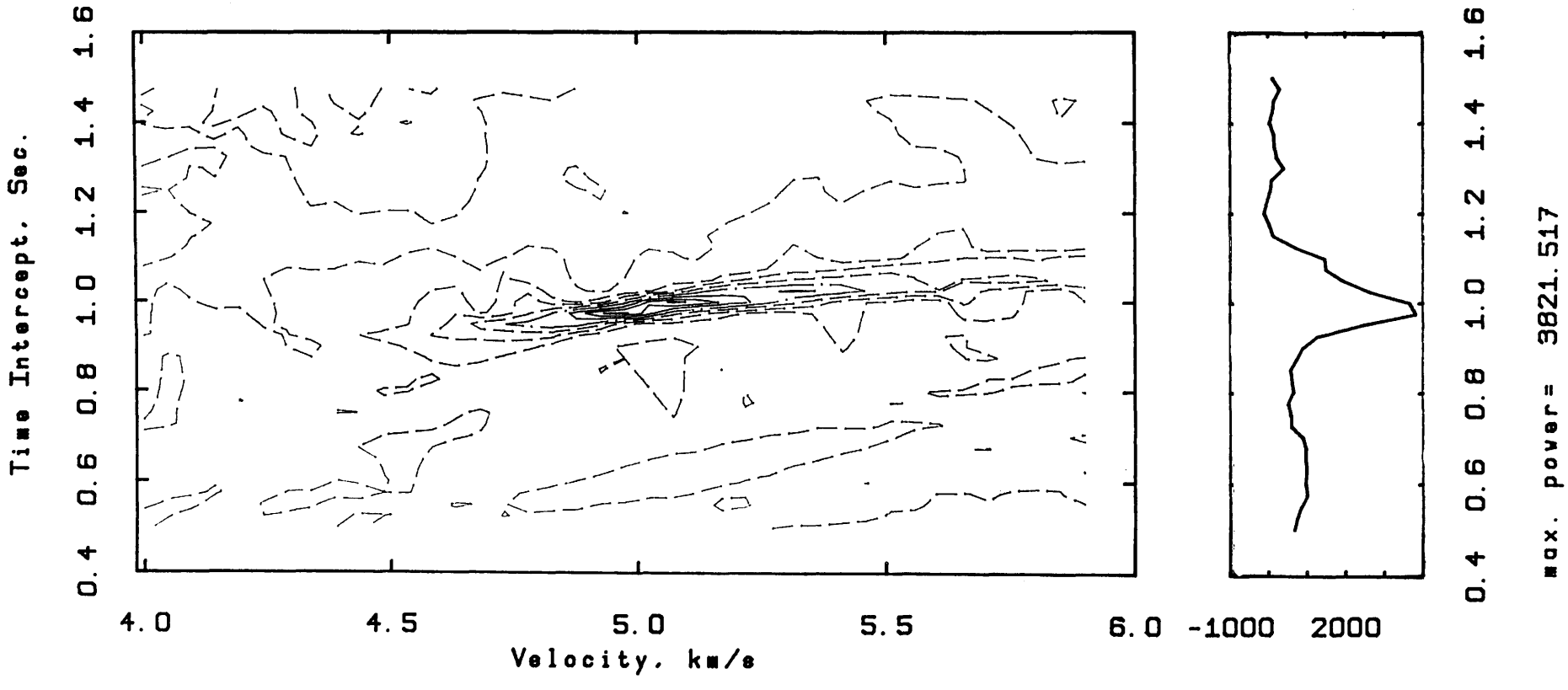


Fig.3.17e Results of applying the mean amplitude summation method to dataset "signoi" displayed in contour format.

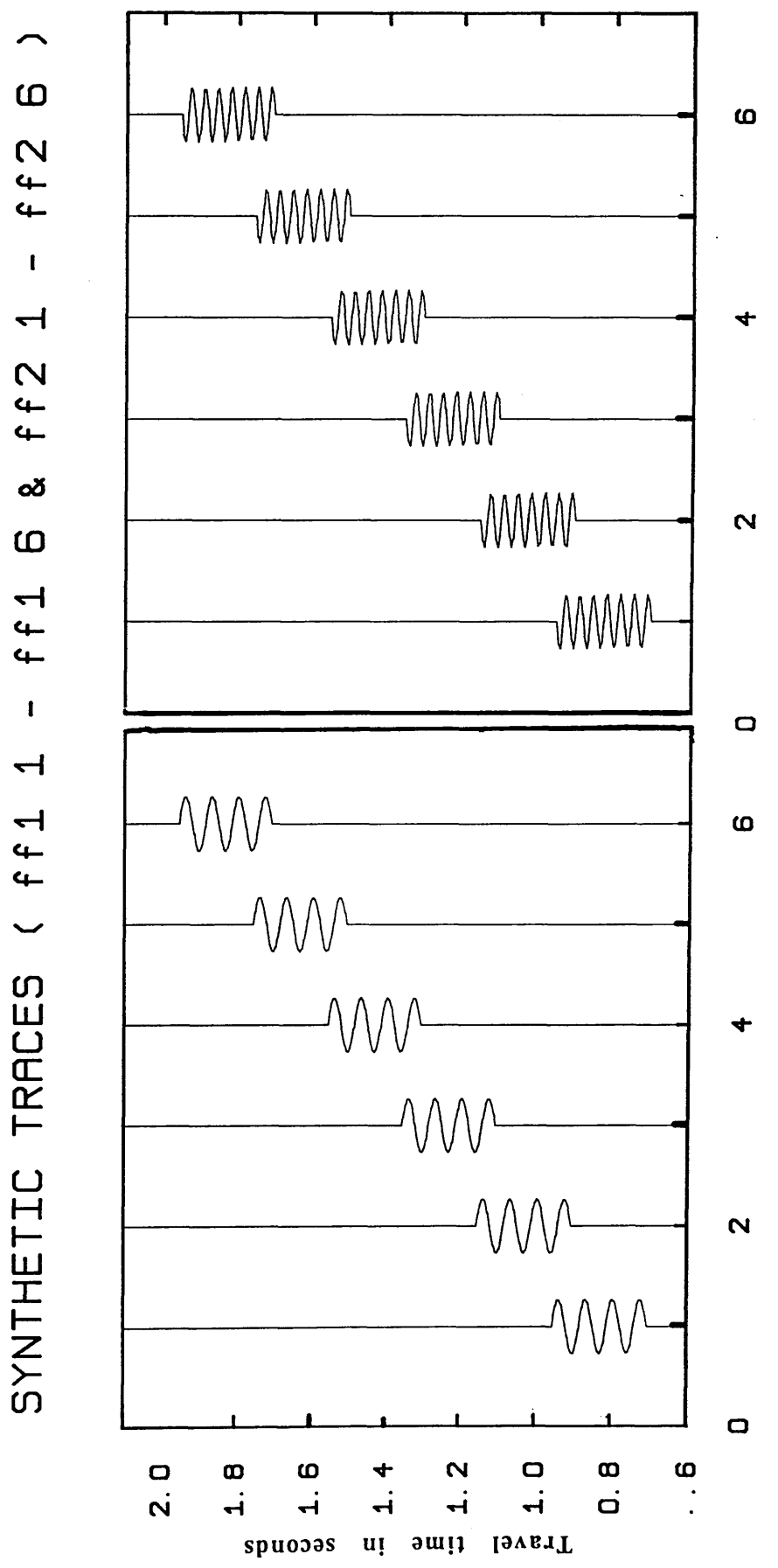


Fig.3.18 Two sets of synthetic traces having the same parameters except frequency. a) ff1 1 - ff1 6, with frequency =14 Hz b) ff2 1 - ff2 6, with frequency =28 Hz.

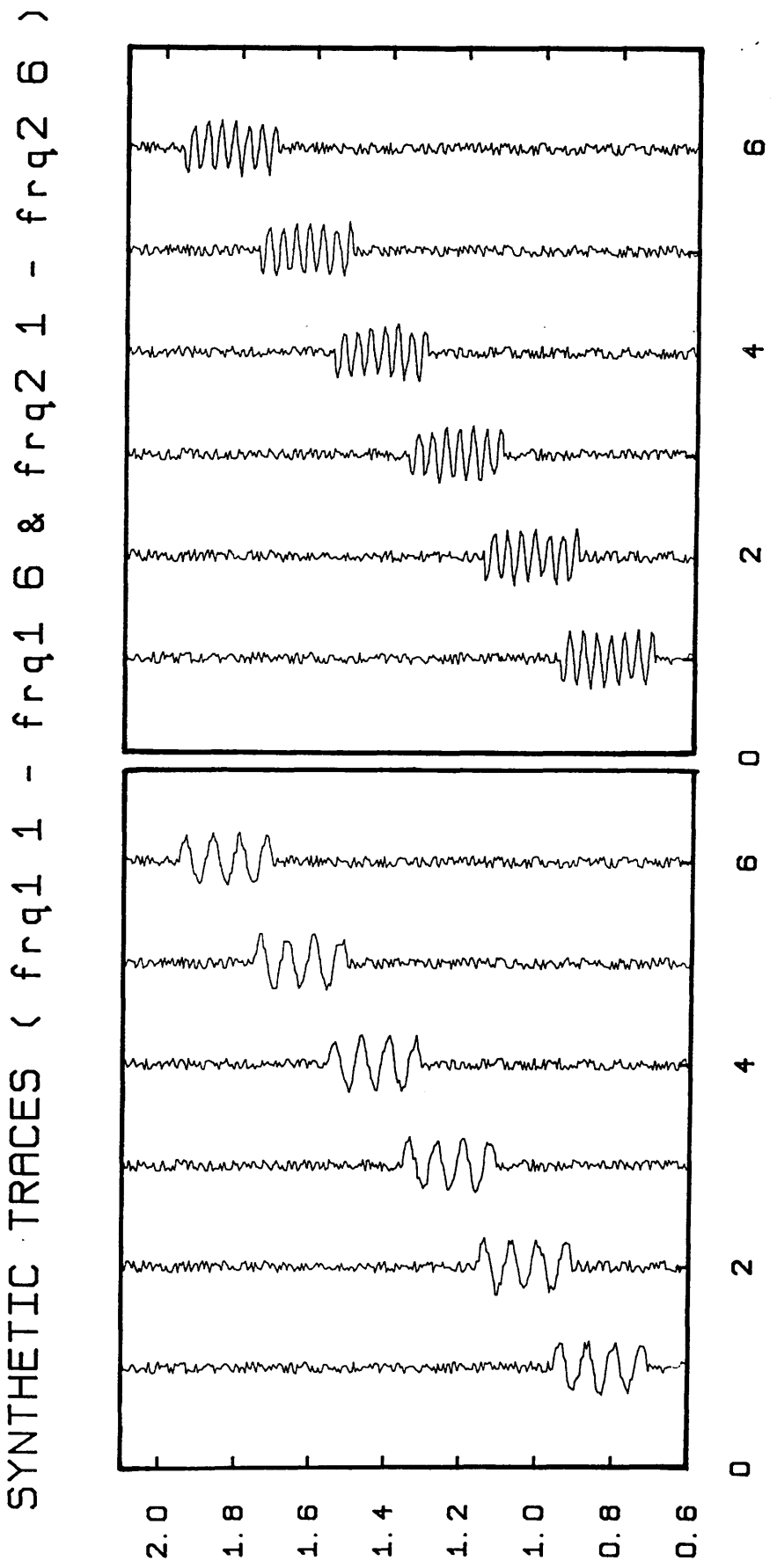


Fig.3.19 Synthetic seismic traces constructed by stacking traces of two sets "ff1 & ff2", Fig. 3.18, with the noisy traces of the set "noise", Fig. 3.12a. A) synthetic seismic set " frq1 1 - frq1 6 ", B) synthetic seismic set "frq2 1 - frq2 6".

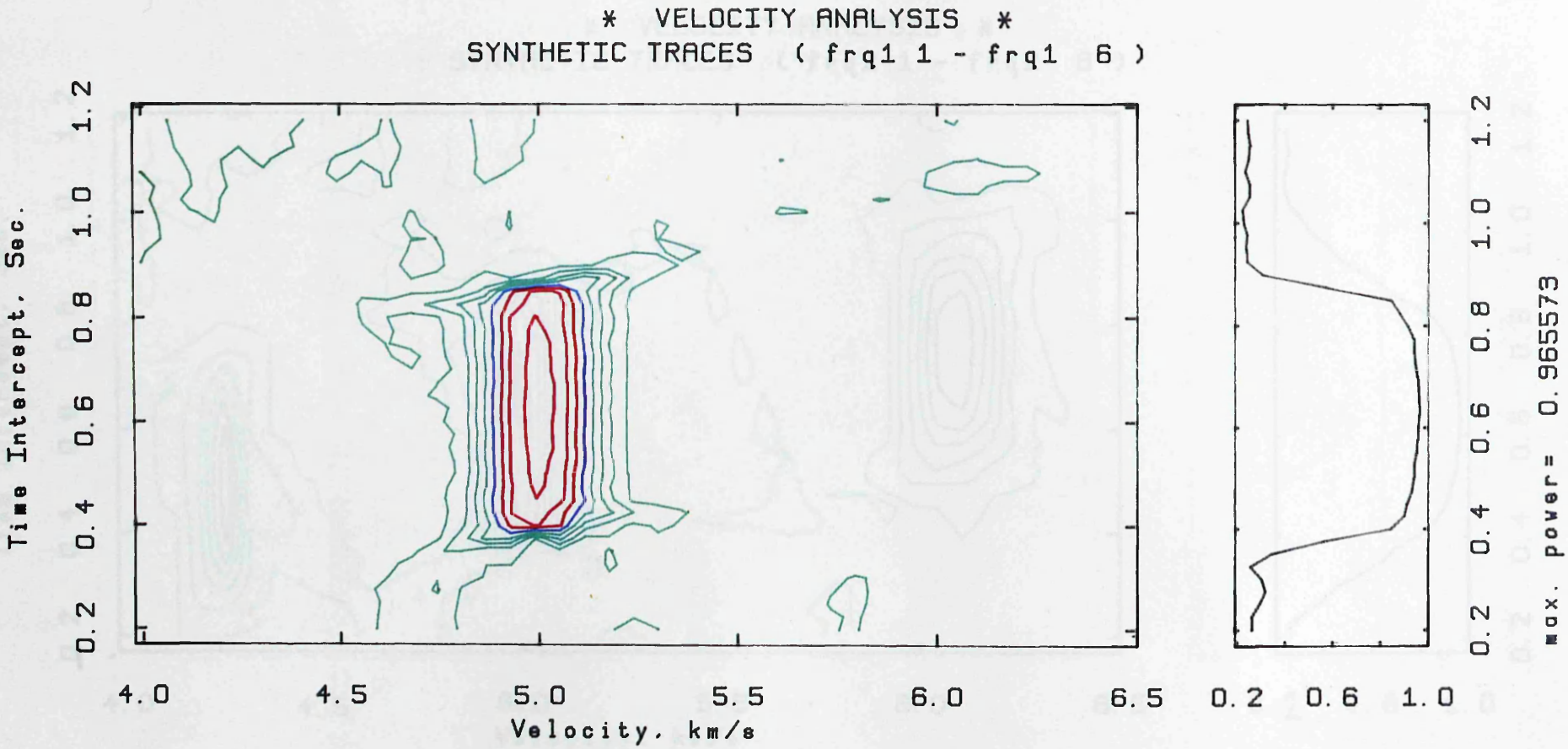


Fig.3.20a Results of applying the semblance method to dataset "frq1" displayed in contour format.

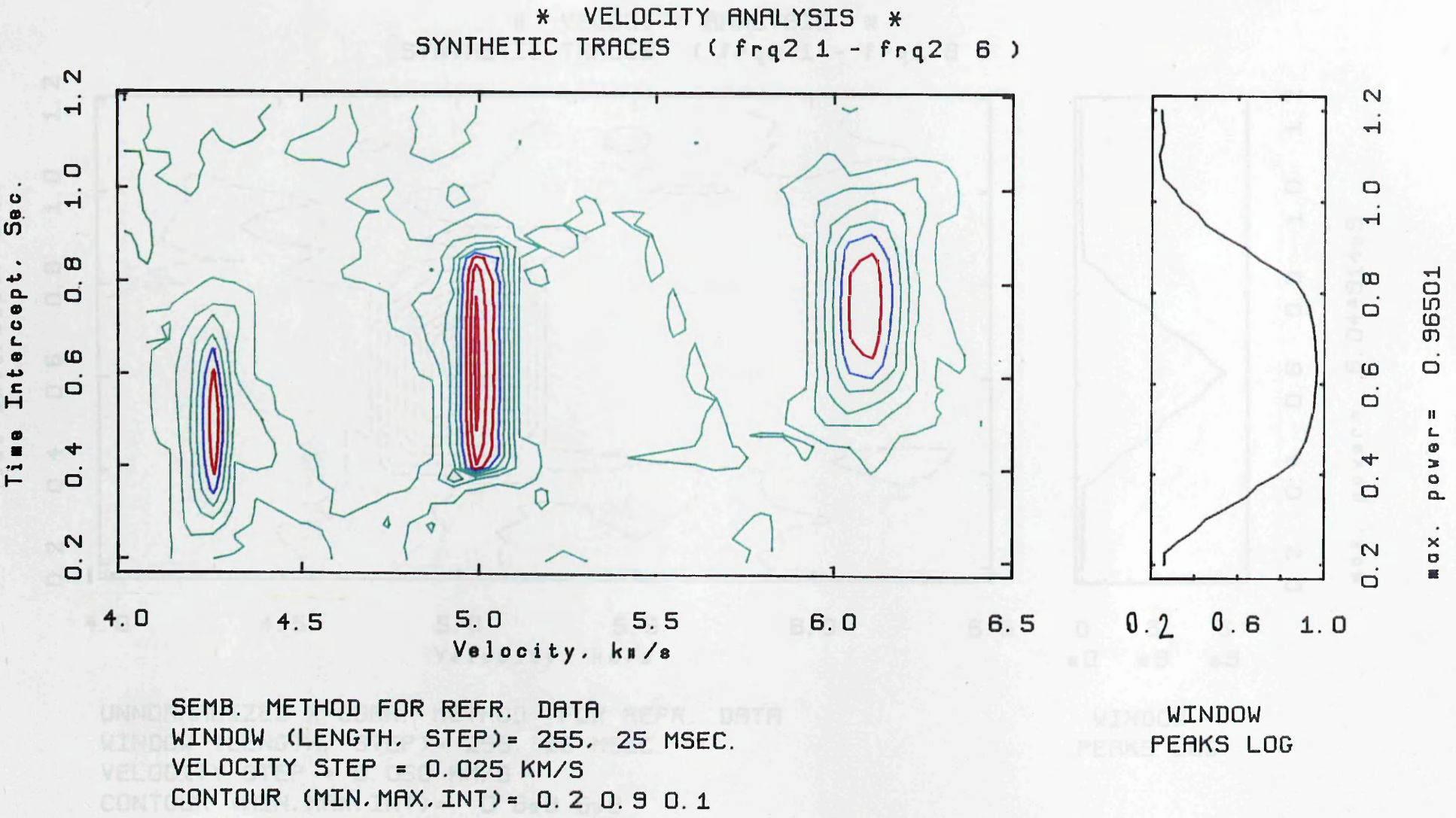


Fig.3.20b Results of applying the semblance method to dataset "frq2" displayed in contour format.

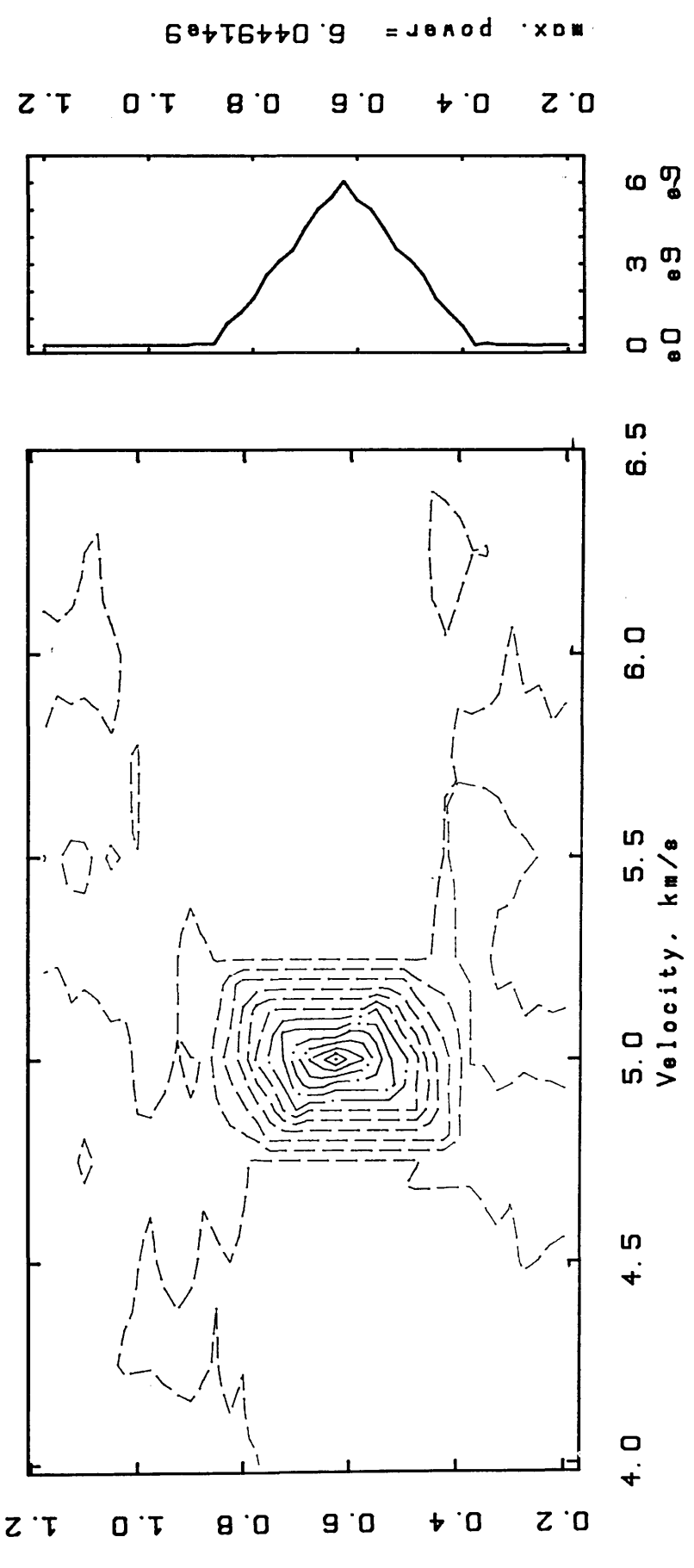


Fig.3.20c Results of applying the unnormalised crosscorrelation method to dataset "frq1" displayed in contour format.

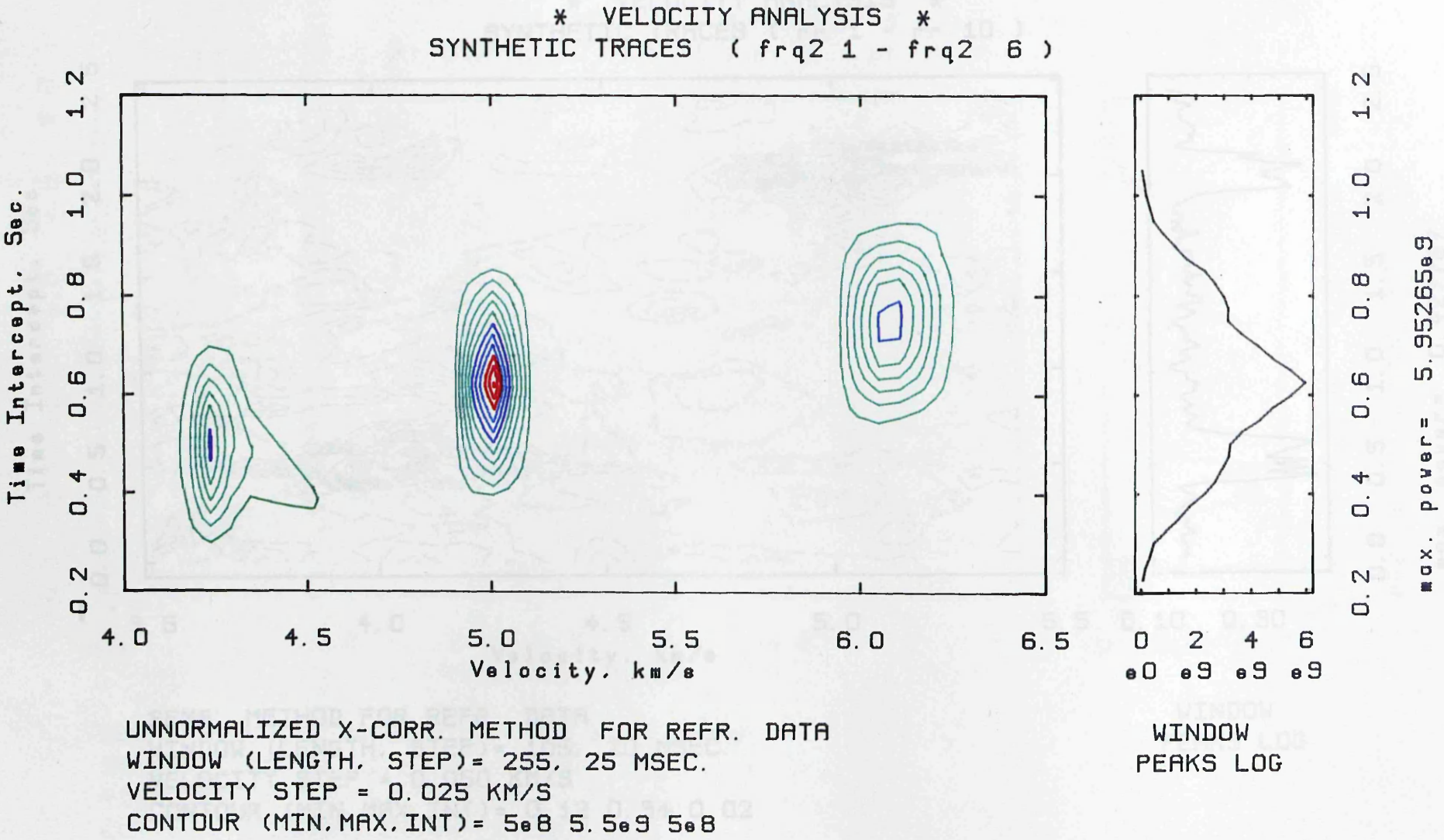


Fig.3.20d Results of applying the unnormalised crosscorrelation method to dataset "frq2" displayed in contour format.

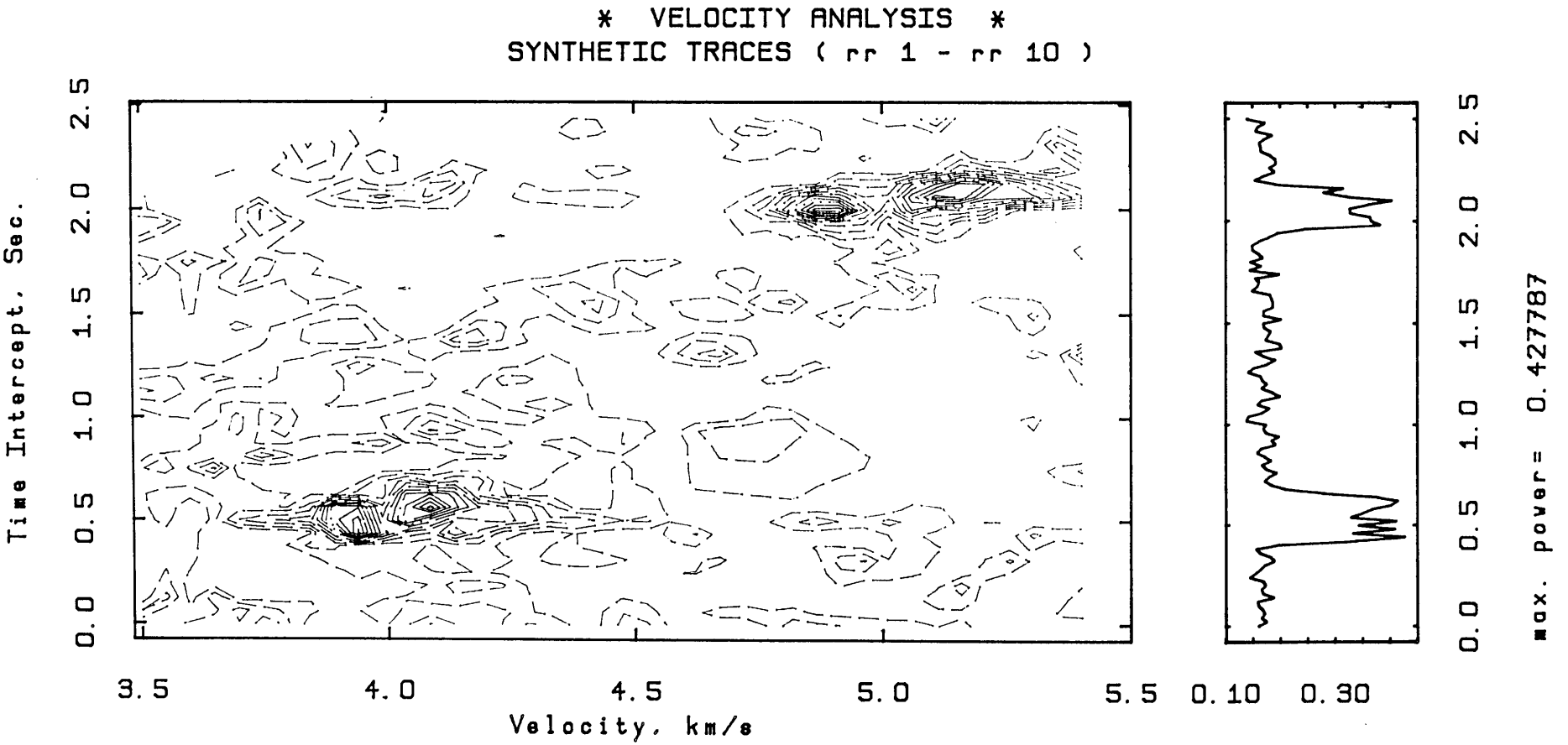


Fig.3.21a Results of applying the semblance method to dataset "rr" displayed in contour format, after reversing three traces.

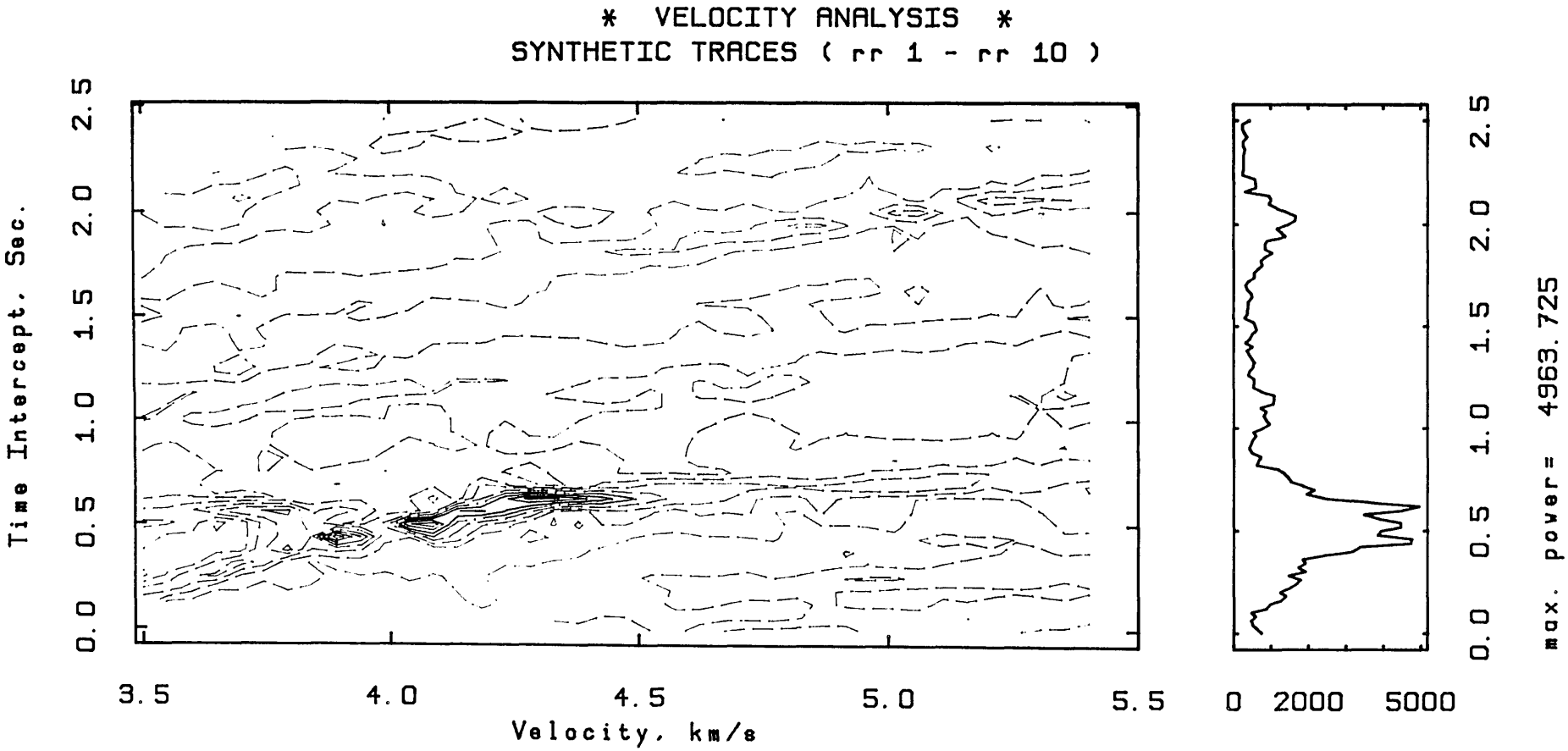


Fig.3.21b Results of applying the mean amplitude summation method to dataset "rr" displayed in contour format, after reversing three traces.

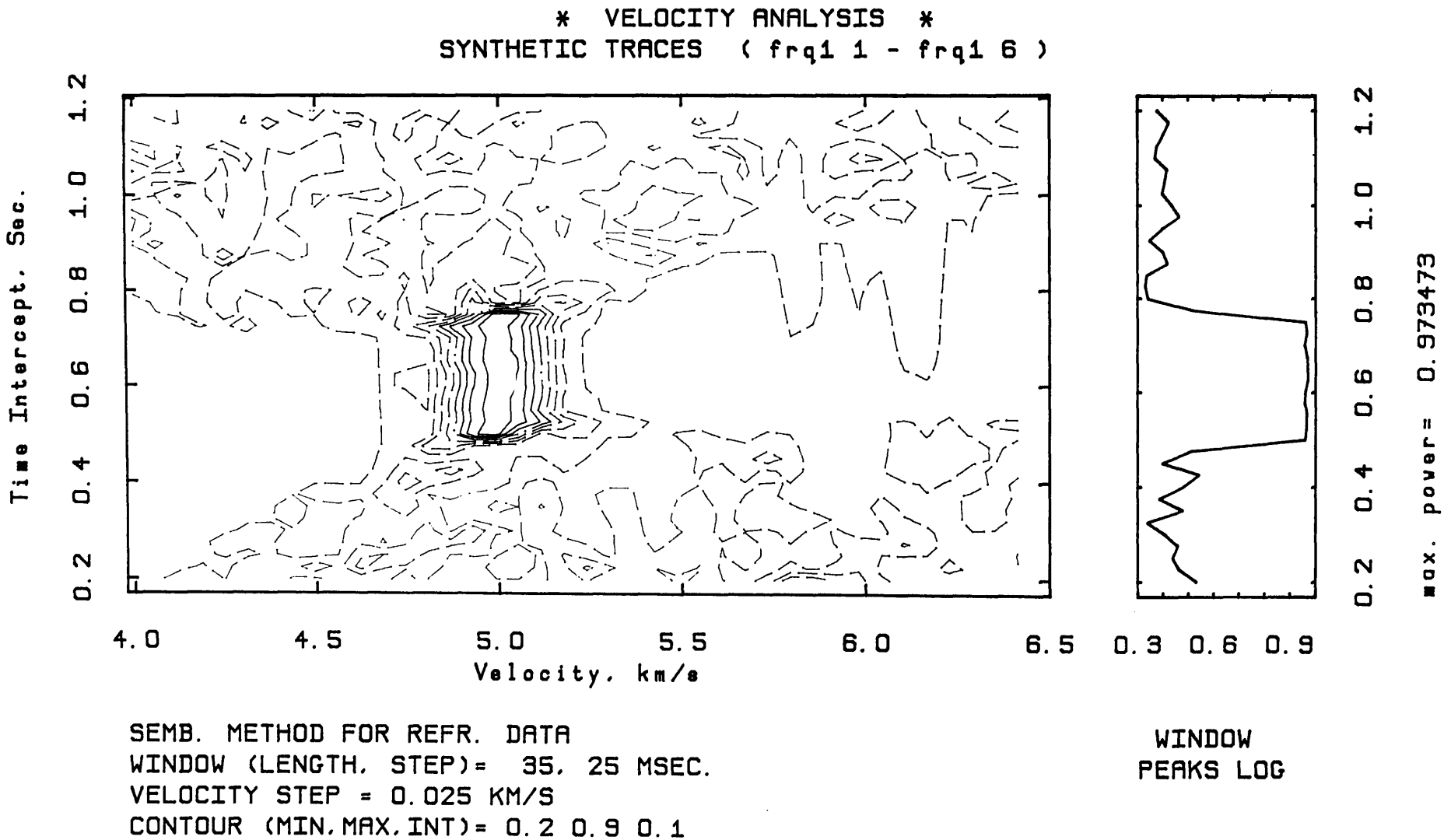


Fig.3.22a Results of applying applying the semblance method to dataset "frq1" displayed in contour format, employing window length (time gate) =35 ms.

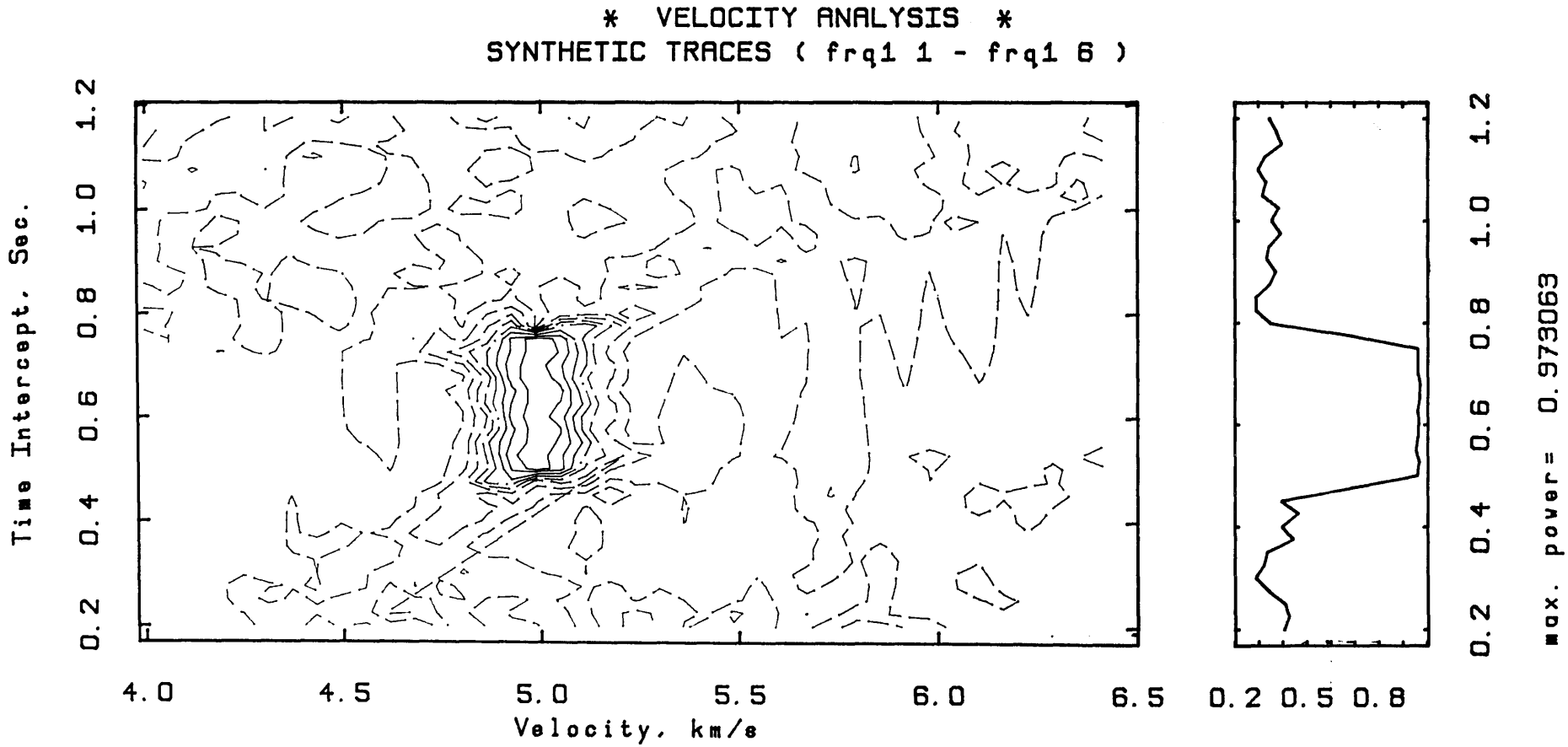


Fig.3.22b Results of applying applying the semblance method to dataset "frq1" displayed in contour format, employing window length (time gate) =55 ms.

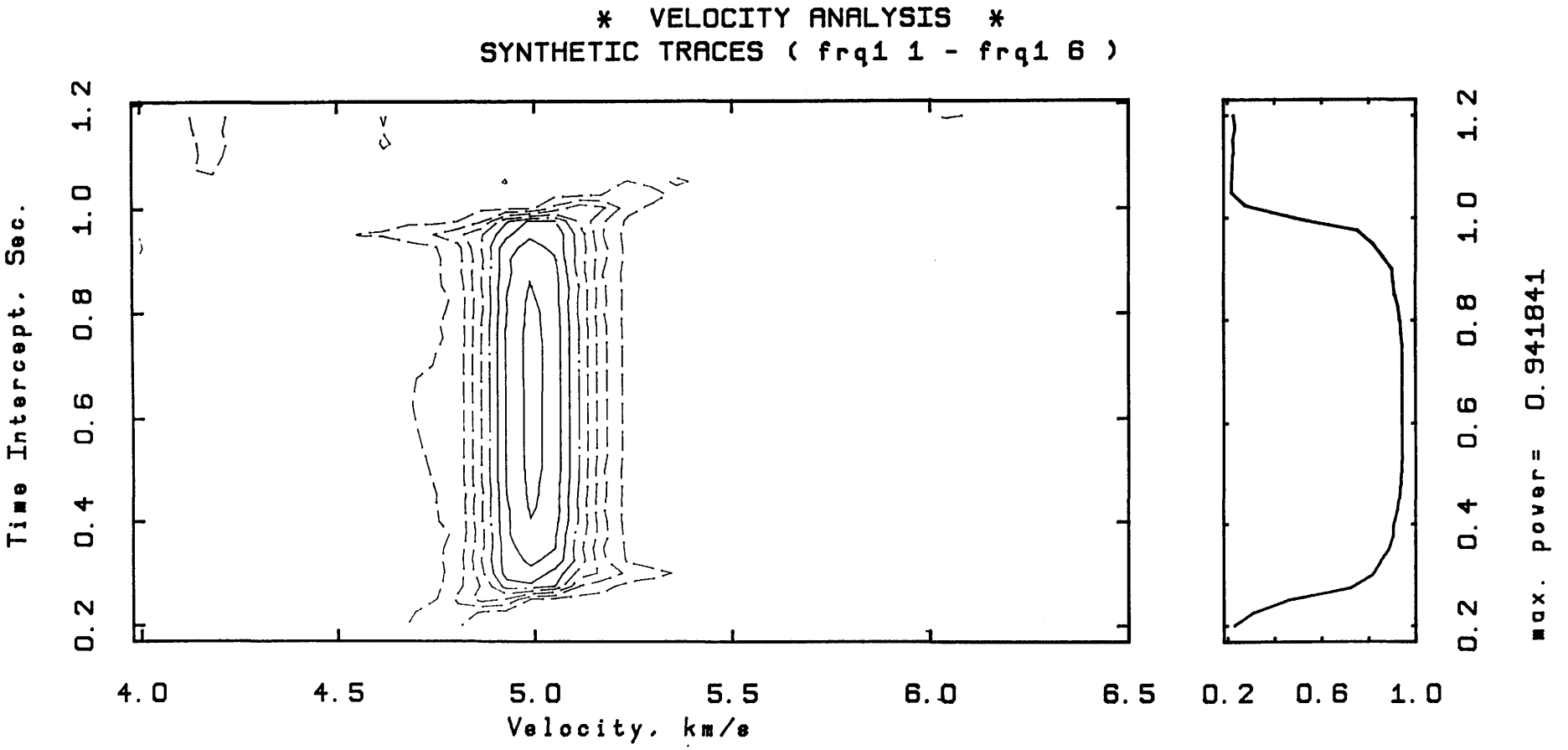


Fig.3.22c Results of applying the semblance method to dataset "frq1" displayed in contour format, employing window length (time gate)=505 ms.

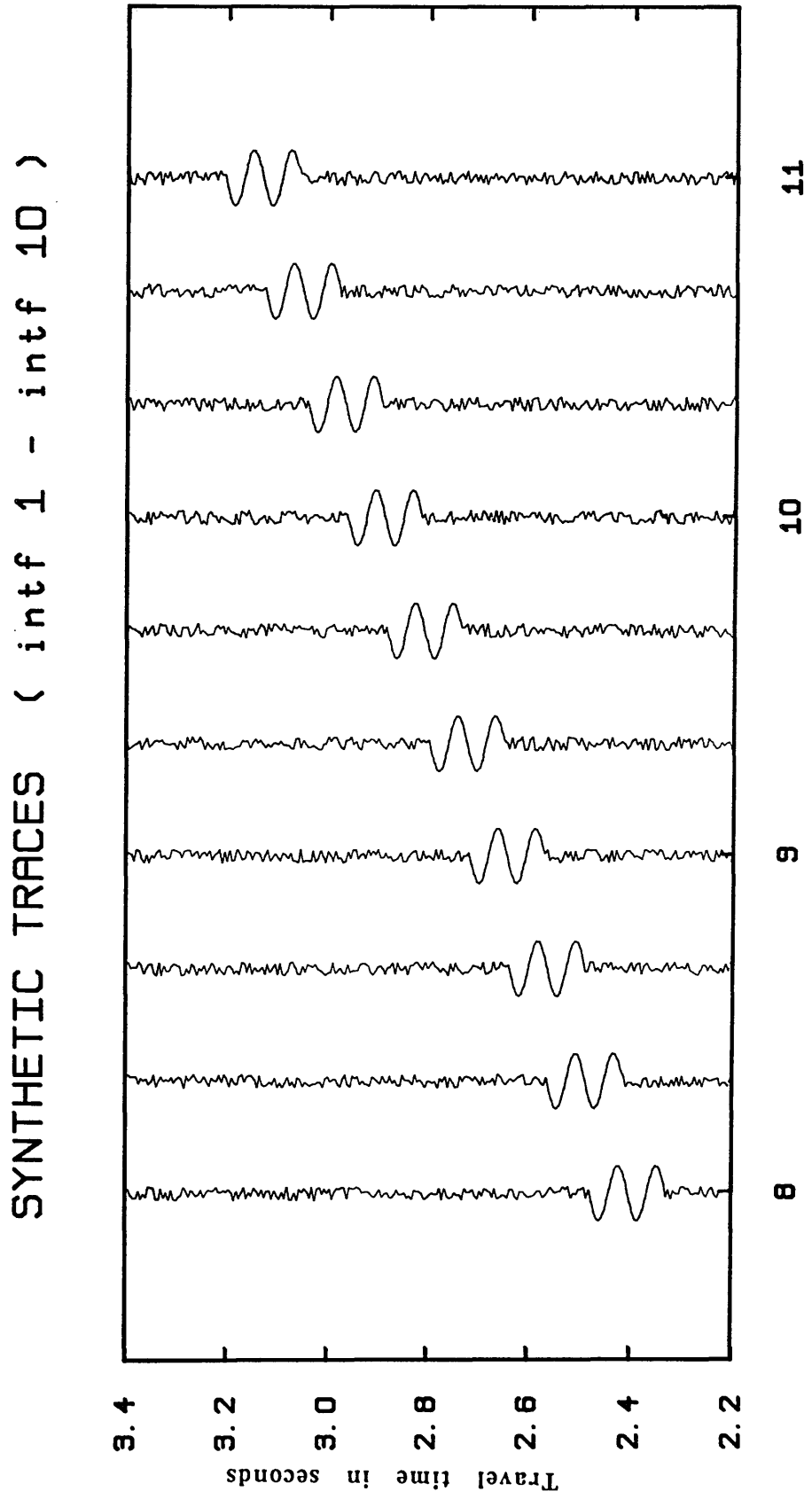


Fig.3.23 Synthetic seismic traces, set "intf", containing one reflected event with normal TWT =1.0s, velocity =3.8 km/s, frequency =14 Hz, peak amplitude =4, and span =145 msec.

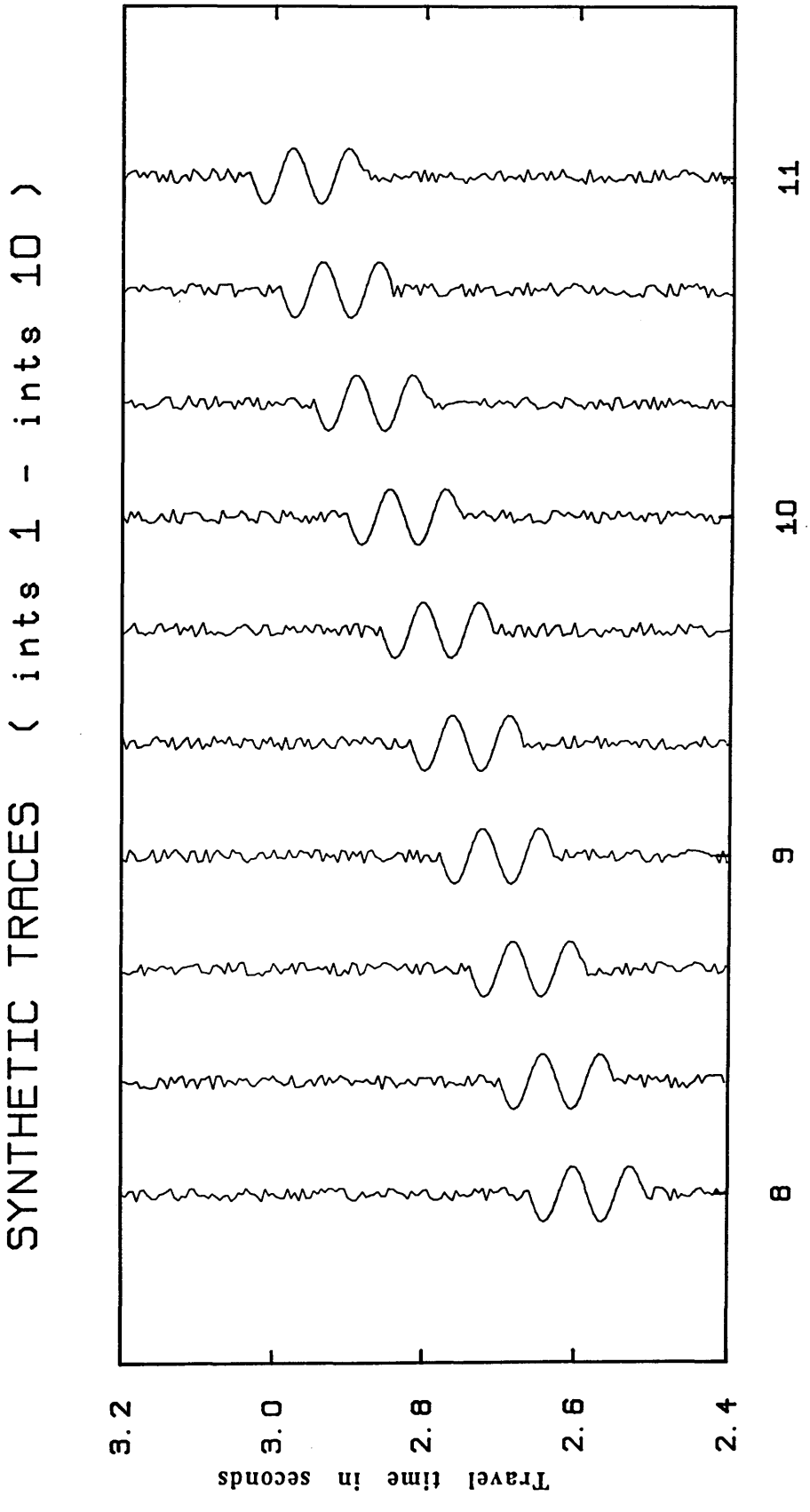


Fig.3.24 Synthetic seismic traces, set "ints", containing one reflected event with normal TWT =2.0s, velocity =5.3 km/s, frequency =14 Hz, peak amplitude =4, and span =145

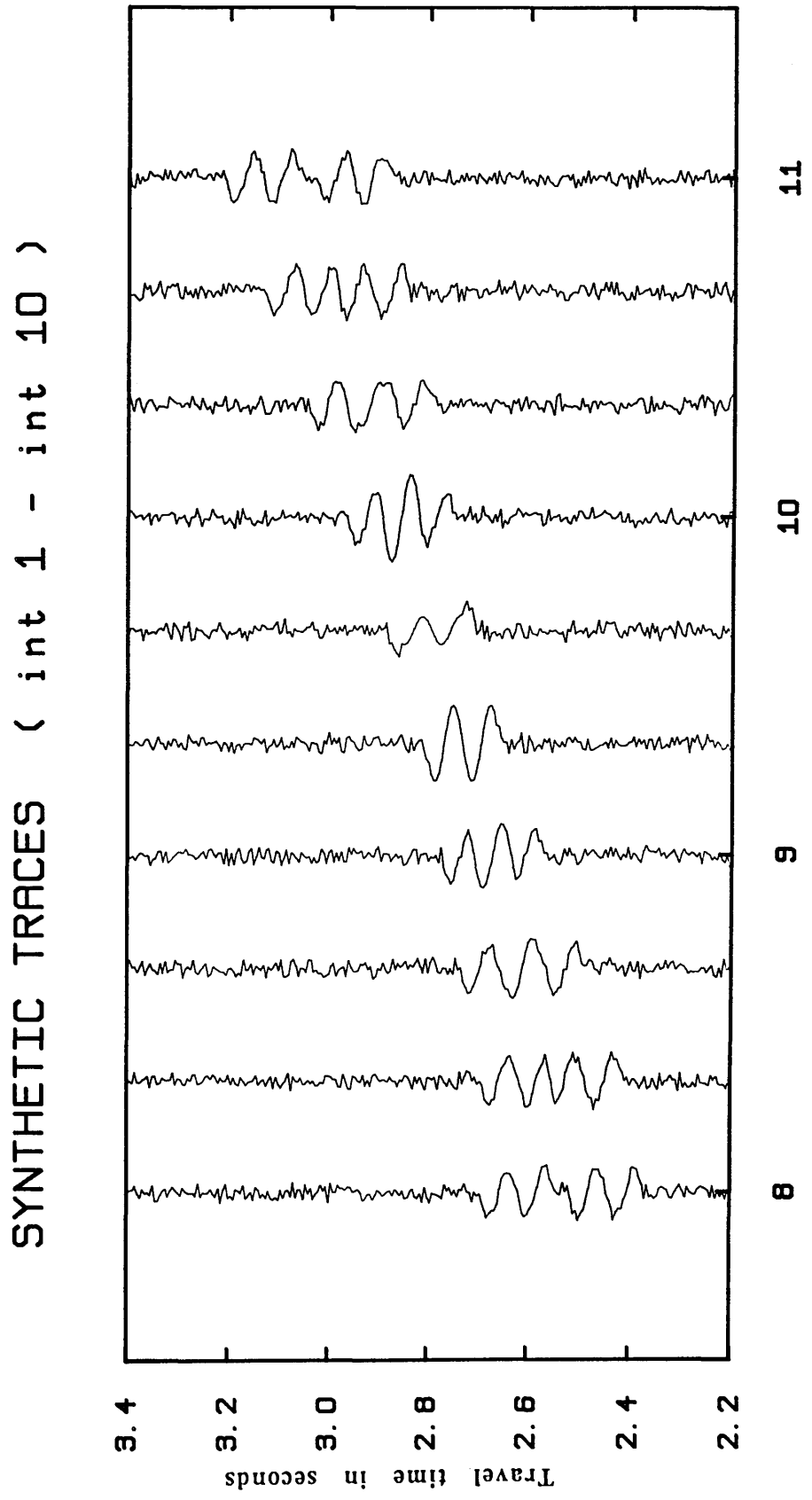


Fig.3.25 Synthetic seismic traces, set "int", which was constructed by stacking traces of the set "intf", Fig. 3.23, with traces of the set "ints", Fig. 3.24.

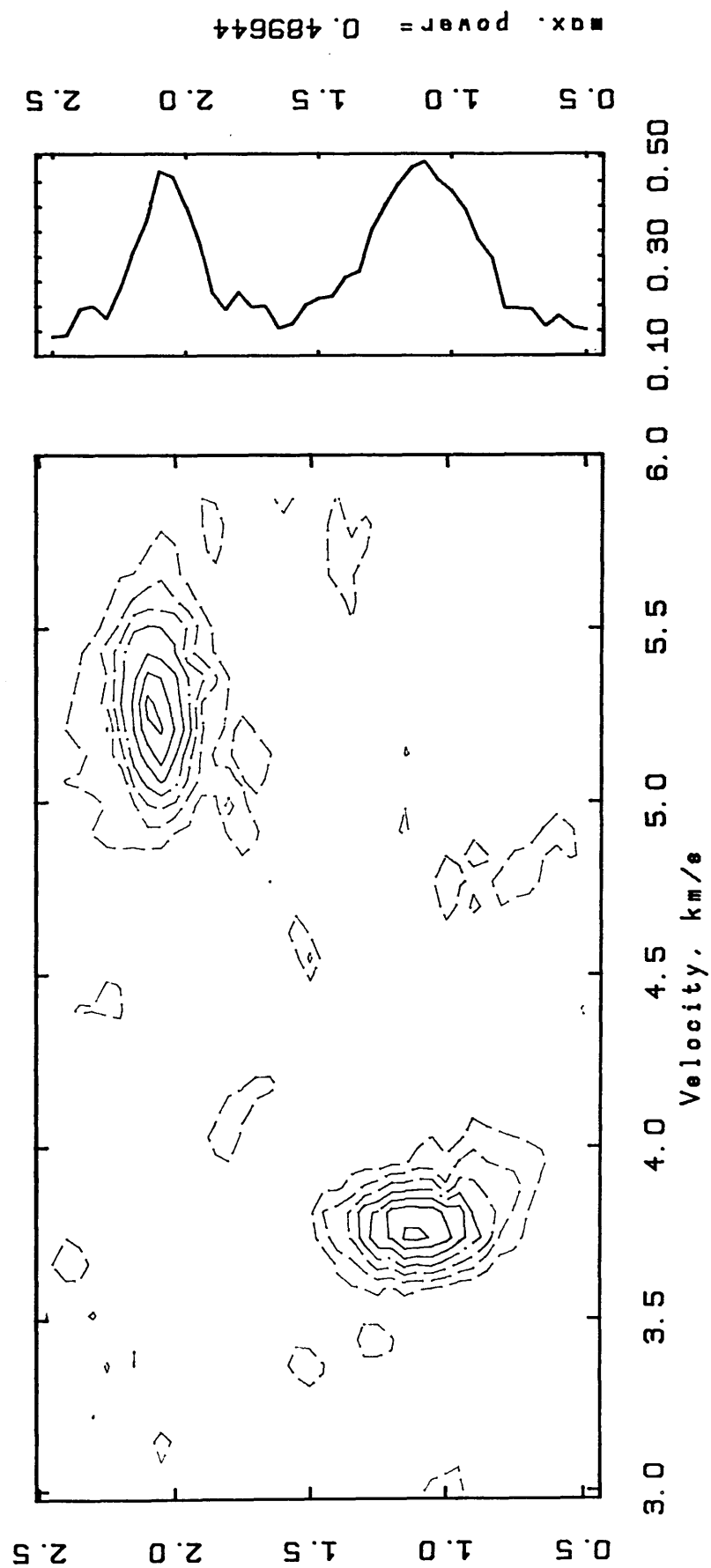


Fig.3.26 Results of applying the semblance method to dataset "int" displayed in contour format.

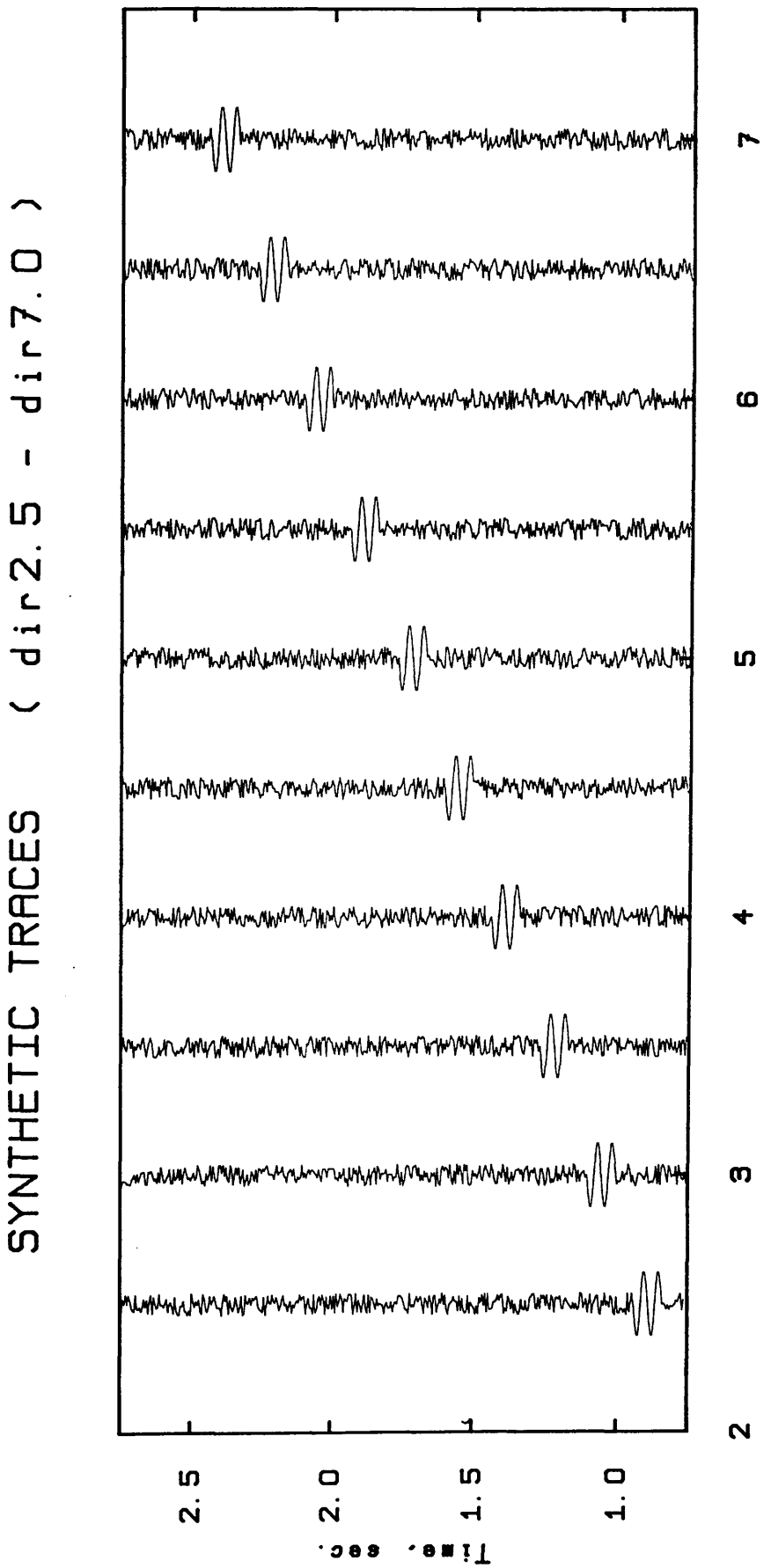


Fig.3.27 Synthetic seismic traces, set "dir", containing a direct event of time intercept =0.0s, velocity =3.0 km/s, span =100 ms, frequency =20 Hz, and peak amplitude =3.

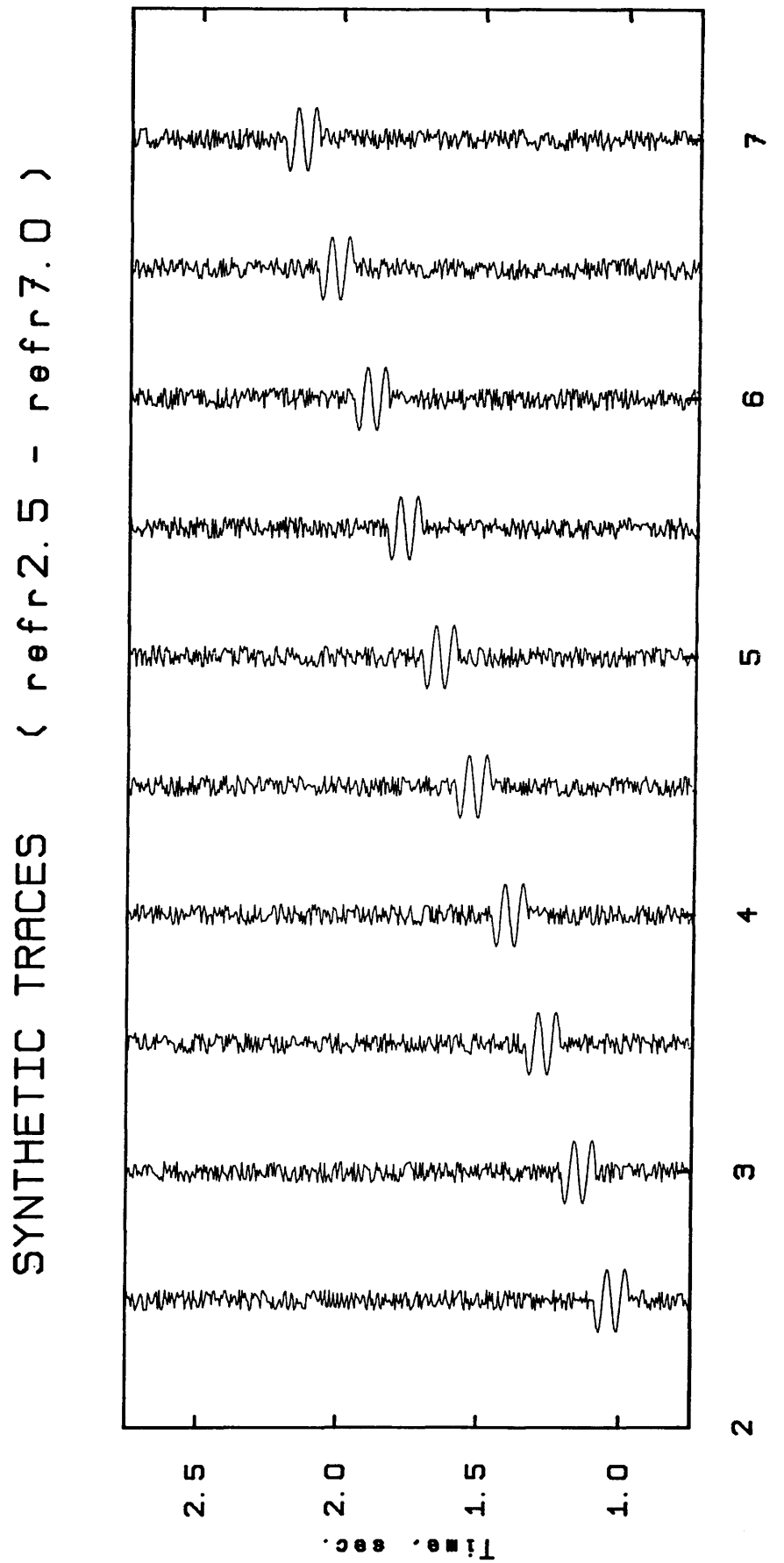


Fig.3.28 Synthetic seismic traces, set "refr", containing a refracted event with: time intercept =0.335 s, velocity =3.0 km/s, span =125 ms, frequency =16 Hz and peak amplitude =3.

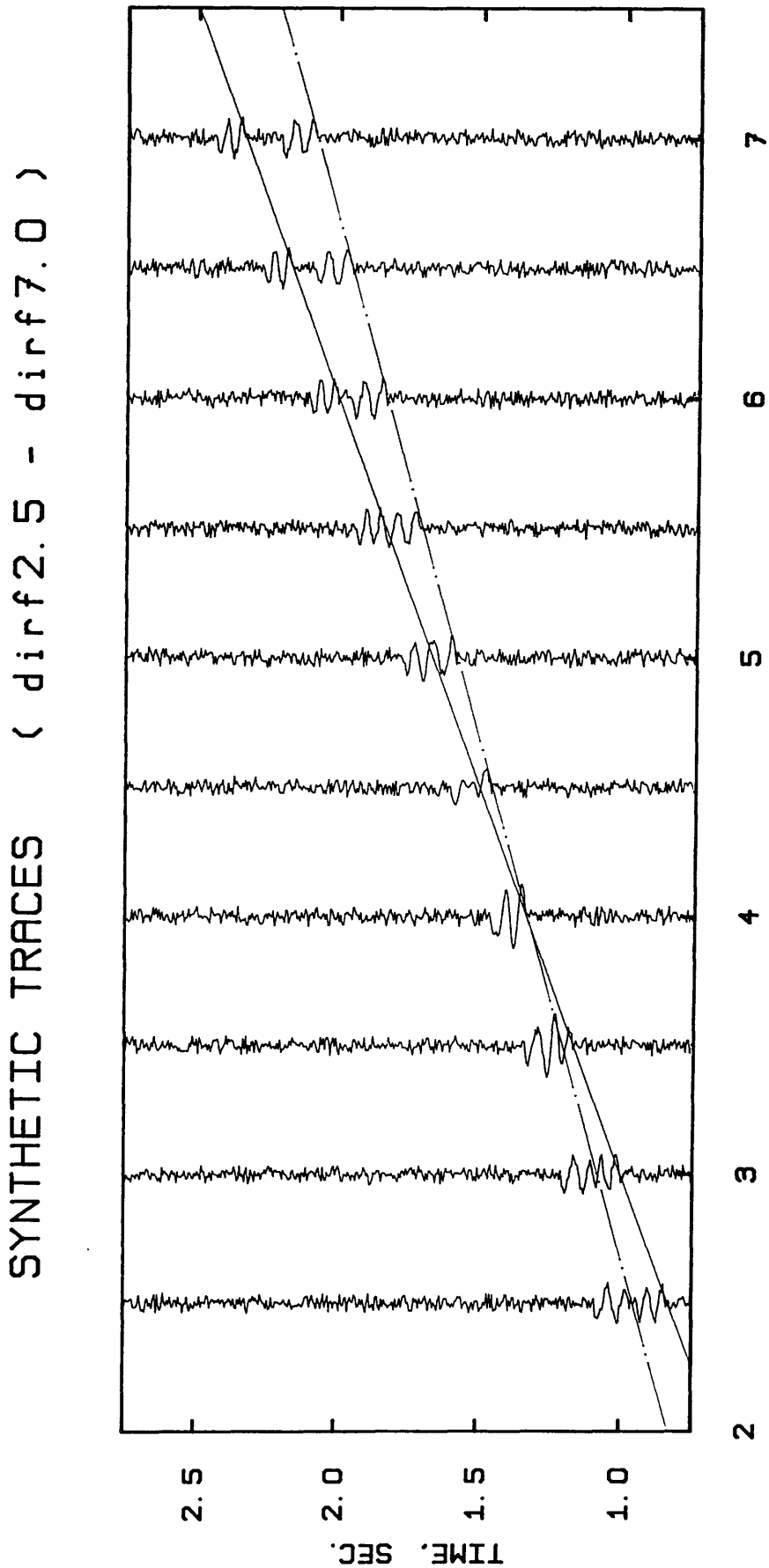


Fig.3.29 Synthetic seismic traces, set "dirf", which was constructed by stacking traces of the set "dir", Fig. 3.27, with traces of the set "refr", Fig. 3.28.

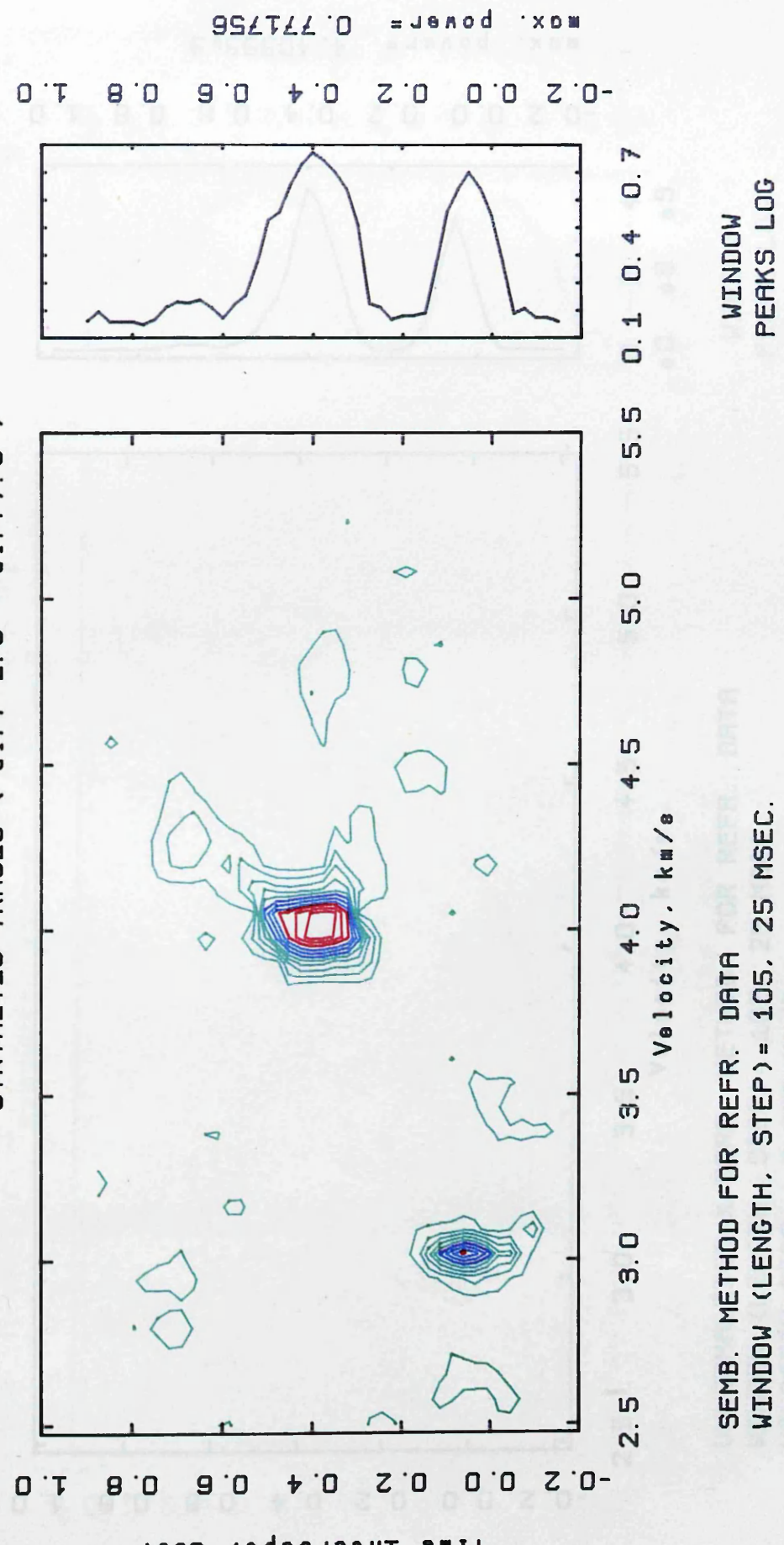


Fig.3.30a Results of applying the semblance method to dataset "dirf" displayed in contour format, employing **large** increments and ranges.

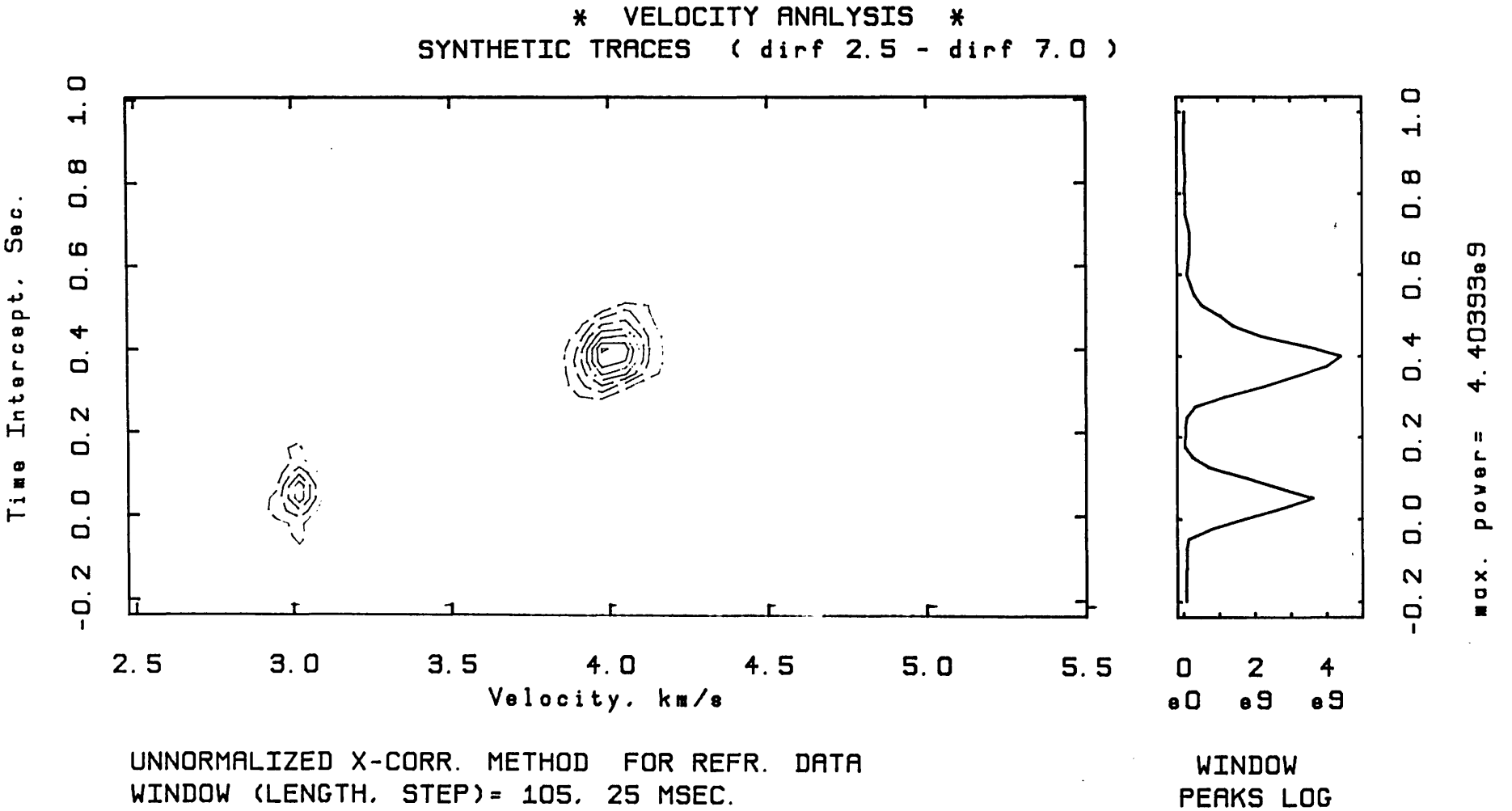


Fig.3.30b Results of applying the unnormalised crosscorrelation method to dataset "dirf" displayed in contour format, employing **large** increments and ranges.

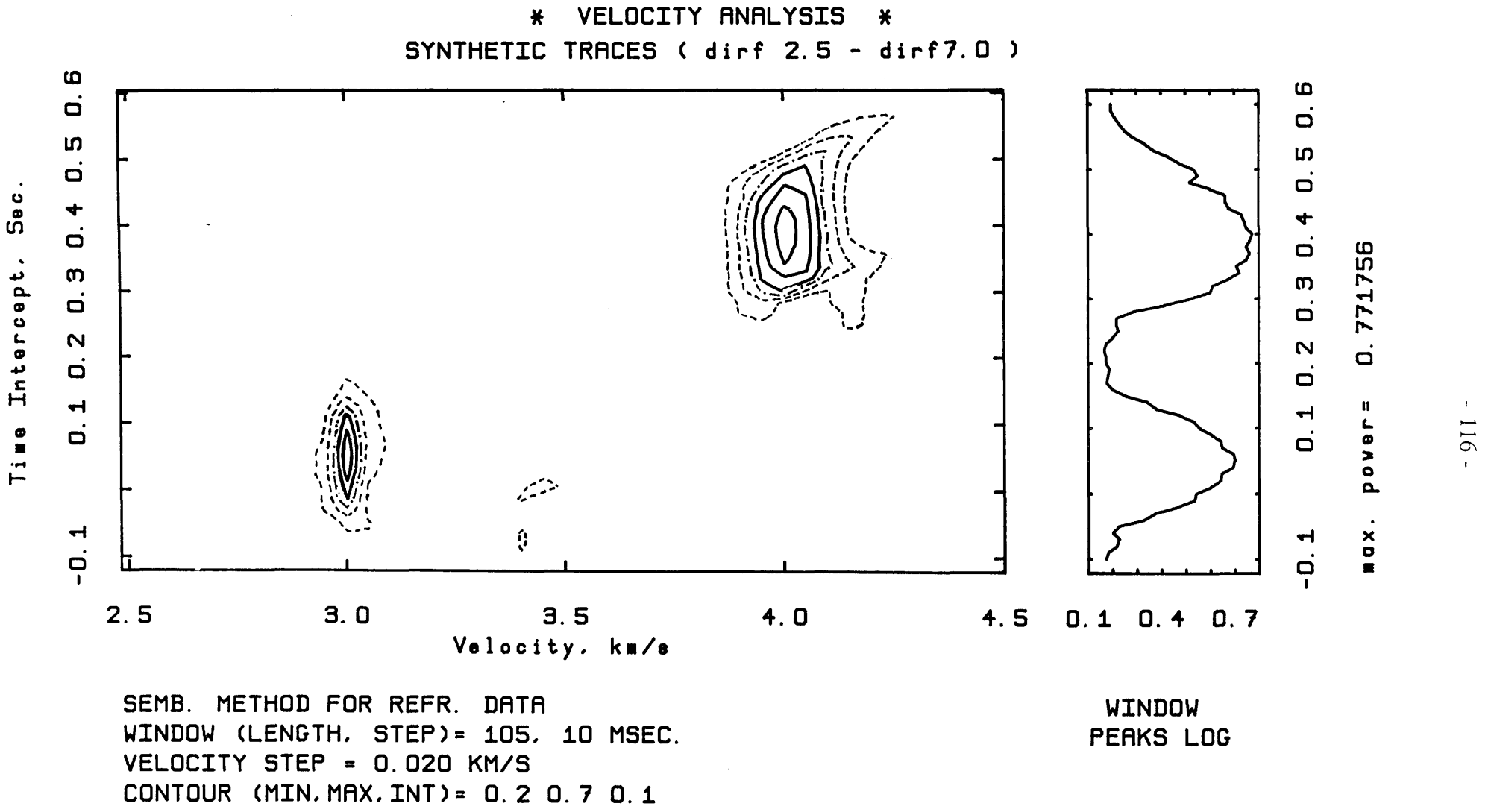


Fig.3.31a Results of applying the semblance method to dataset "dirf" displayed in contour format, employing **small** increments and ranges.

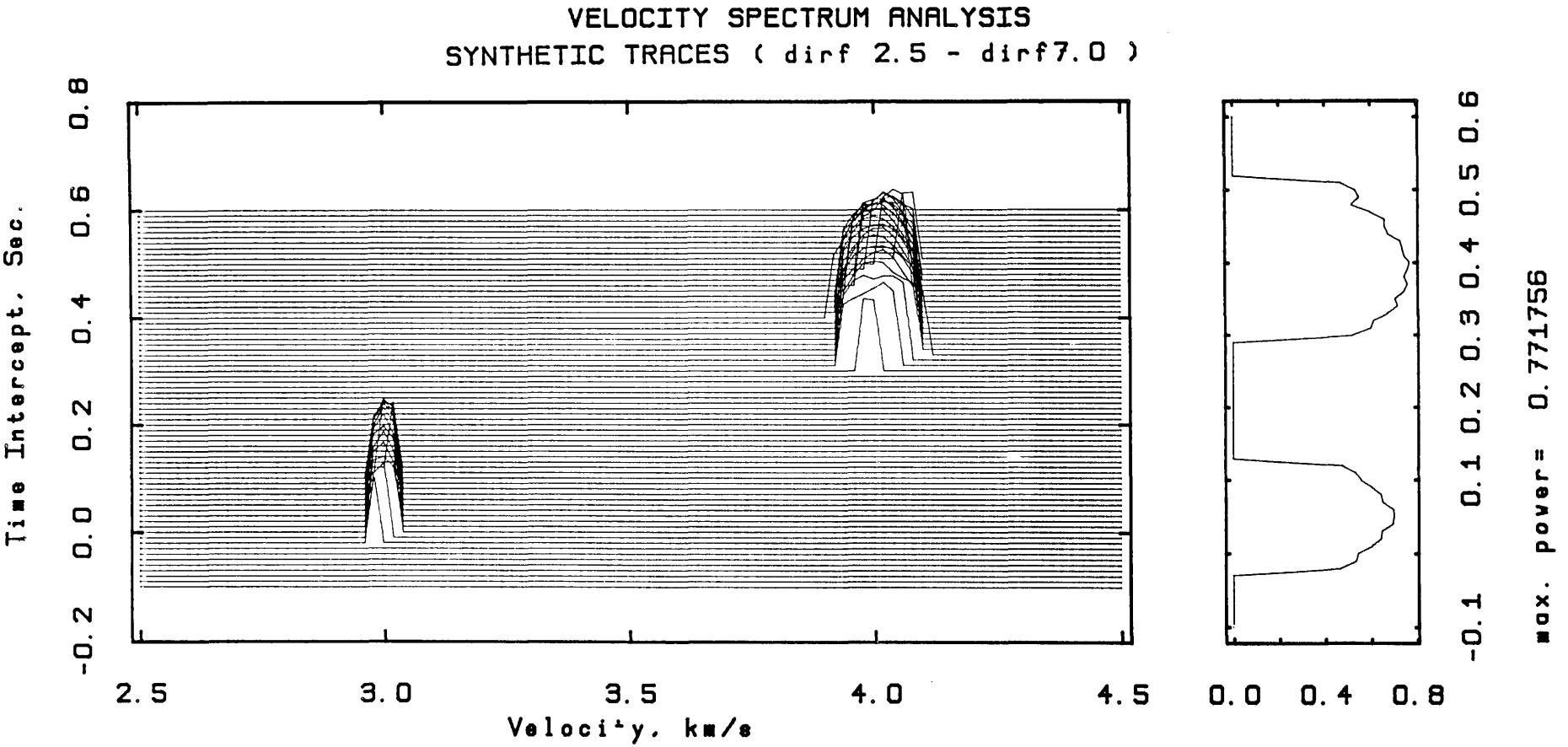


Fig.3.31b Results of applying the semblance method to dataset "dirf" displayed in spectrum analysis format.

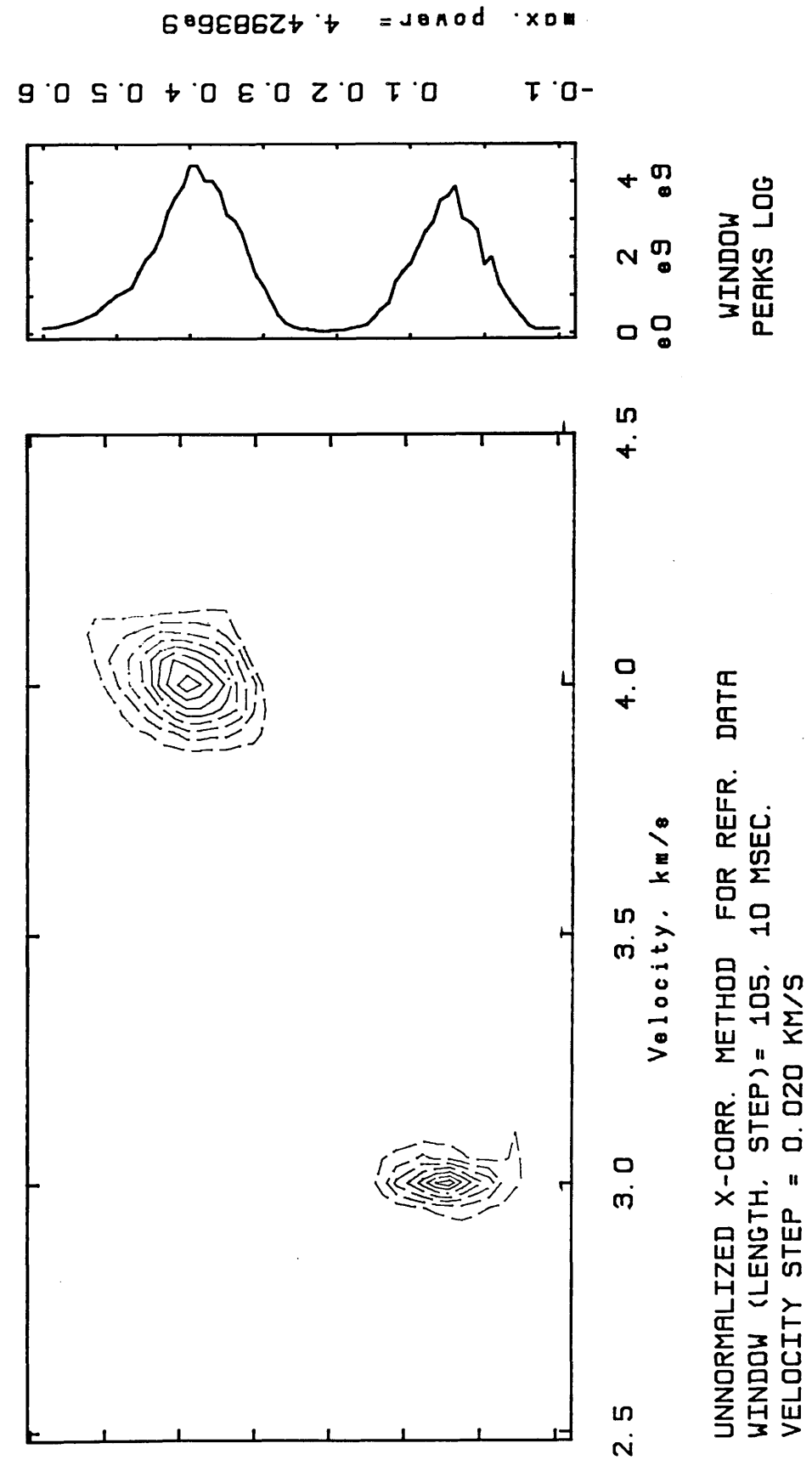


Fig.3.31c Results of applying the unnormalised crosscorrelation method to dataset "dirf" displayed in contour format, employing small increments and ranges.

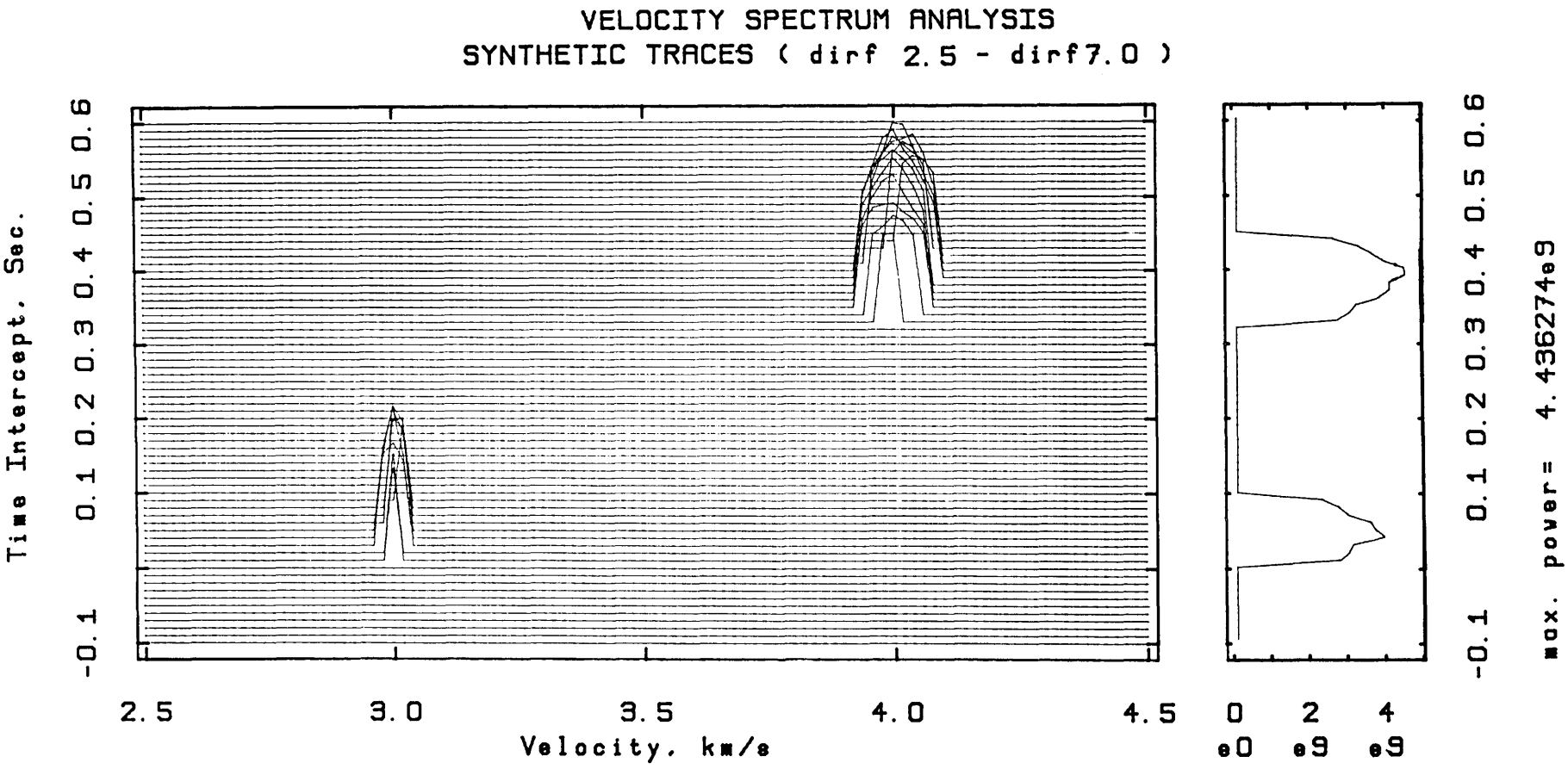


Fig.3.31d Results of applying the unnormalised crosscorrelation method to dataset "dirf" displayed in spectrum analysis format.

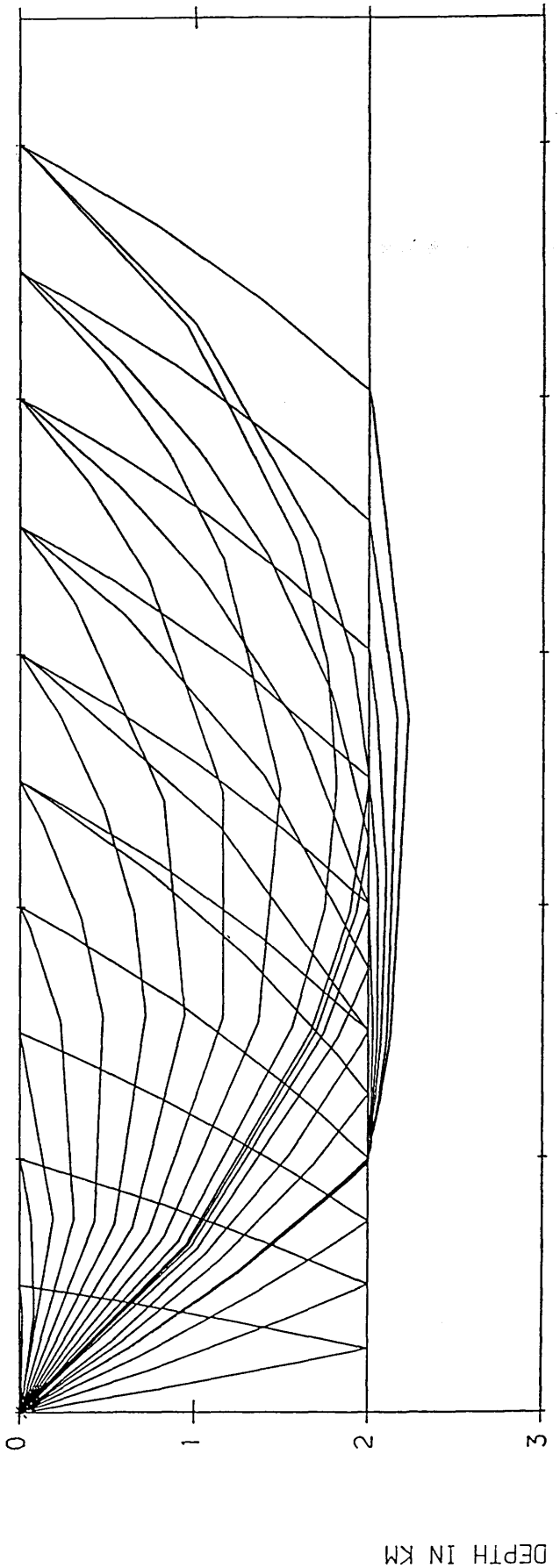


Fig.3.32 Raypaths for a simple two layer subsurface model. First layer: surface velocity =3.0 km/s and velocity gradient =0.5 km/s/km. Second layer velocity is =5.0 km/s and small velocity gradient.

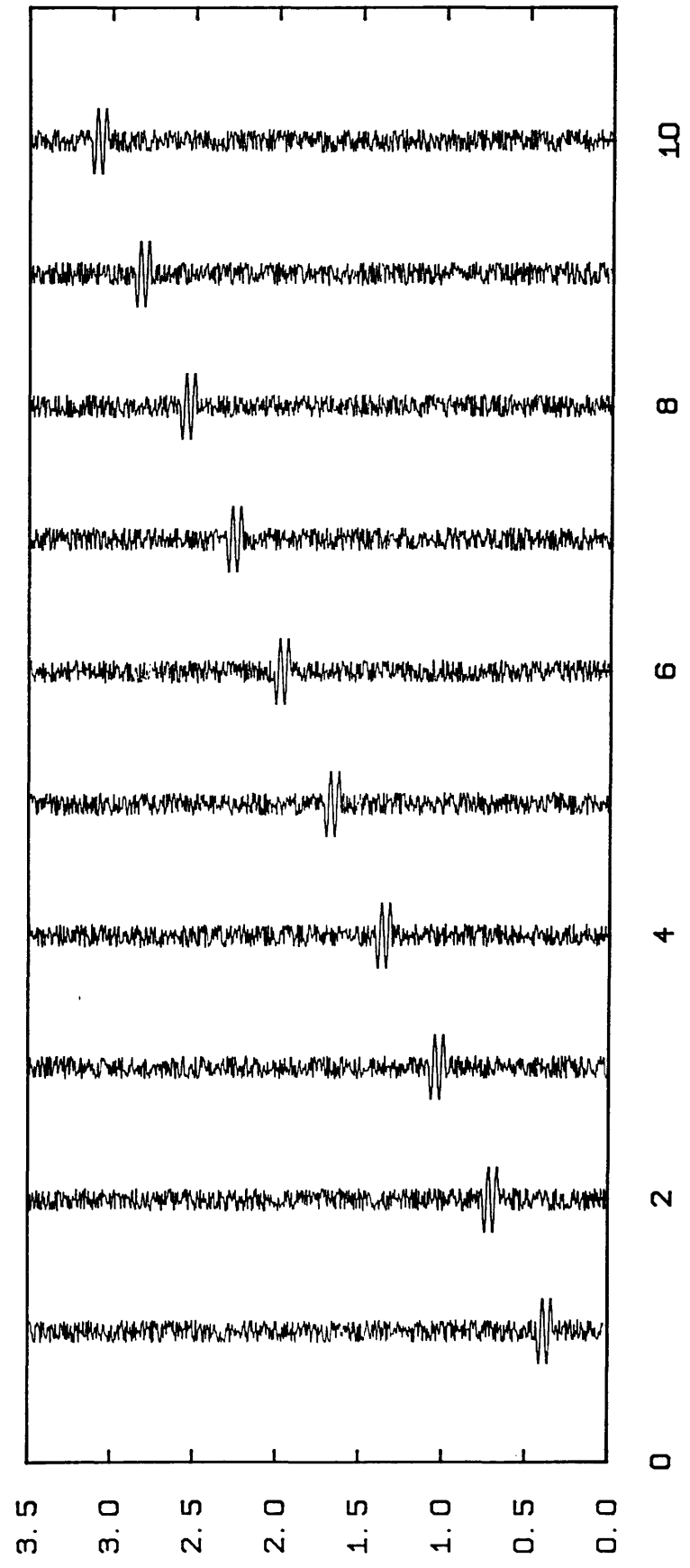


Fig.3.33a Synthetic seismic traces, set "direct", containing a direct event with: time intercept =0.0s, with surface velocity =3.0 km/s and velocity gradient =0.5 km/s/km , span =100 ms, frequency =20 Hz and peak amplitude =3.

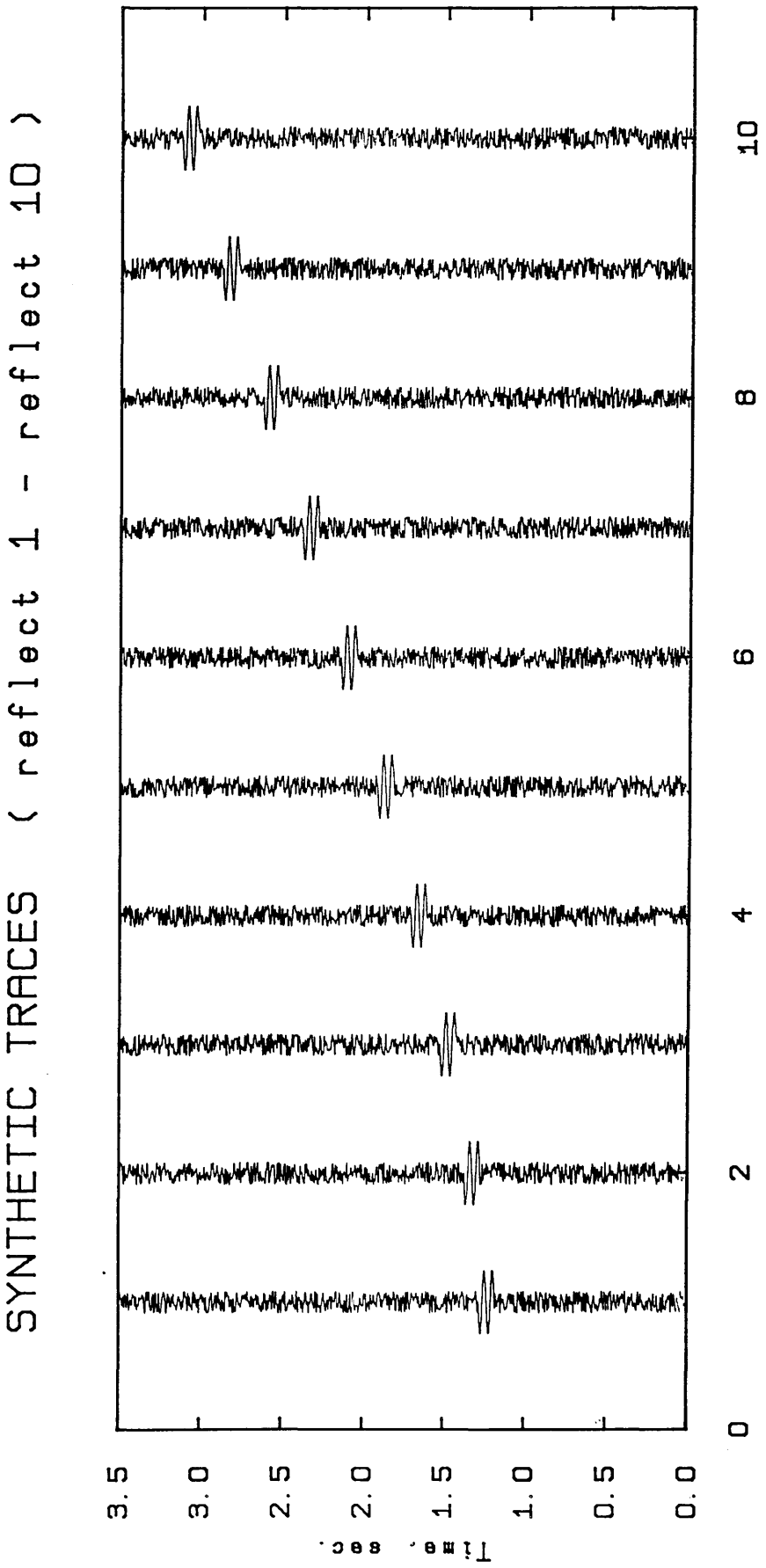


Fig.3.33b Synthetic seismic traces, set "reflect", containing a reflected event with: normal TWT =1.18s, velocity =3.5 km/s, span = 100 ms, frequency =20 Hz and peak amplitude =3.

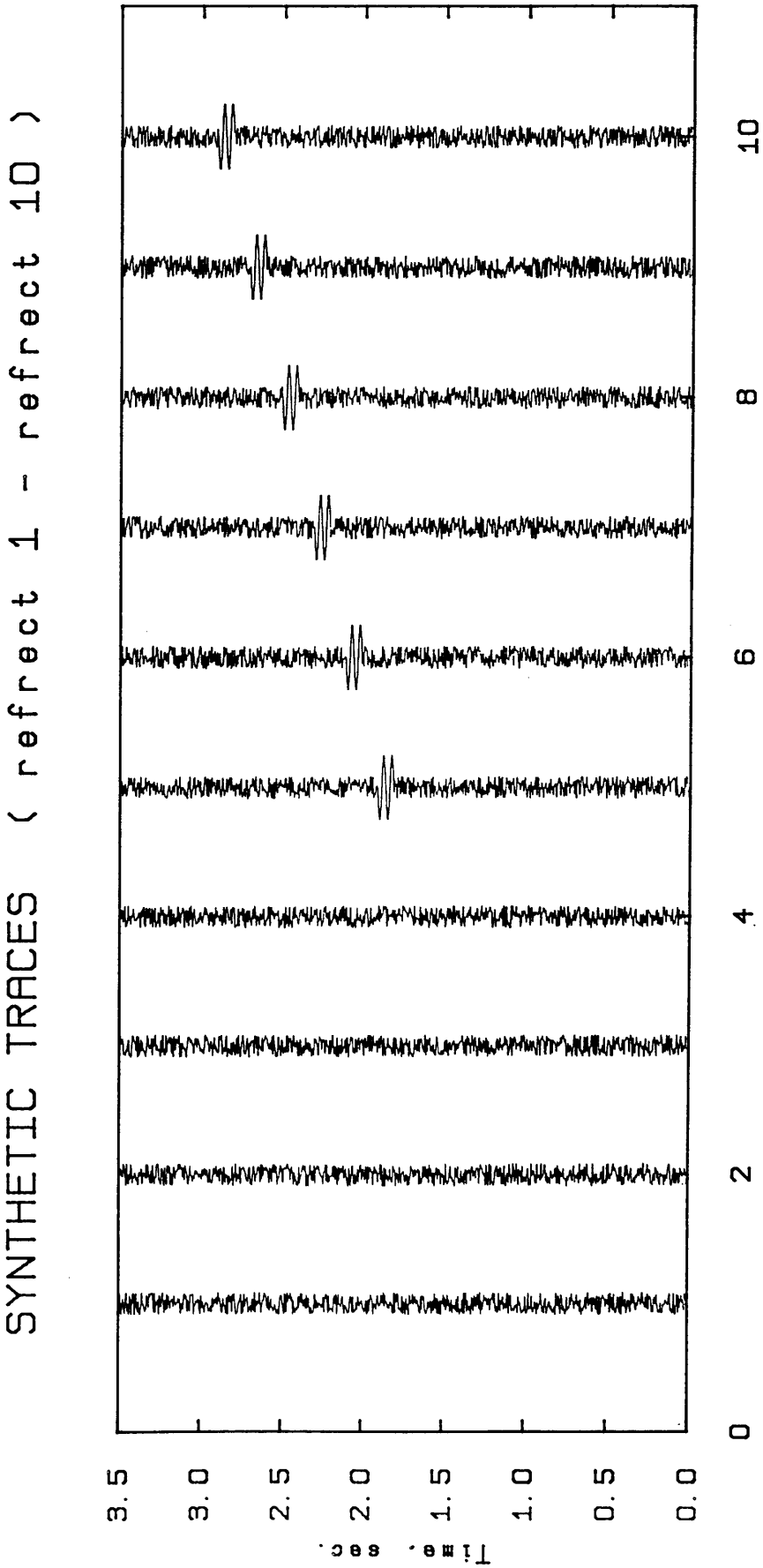


Fig.3.33c Synthetic seismic traces, set "refract", containing a refracted event with: time intercept =0.8s, velocity =5.0 km/s, span =100 ms, frequency =20 Hz and peak amplitude =3.

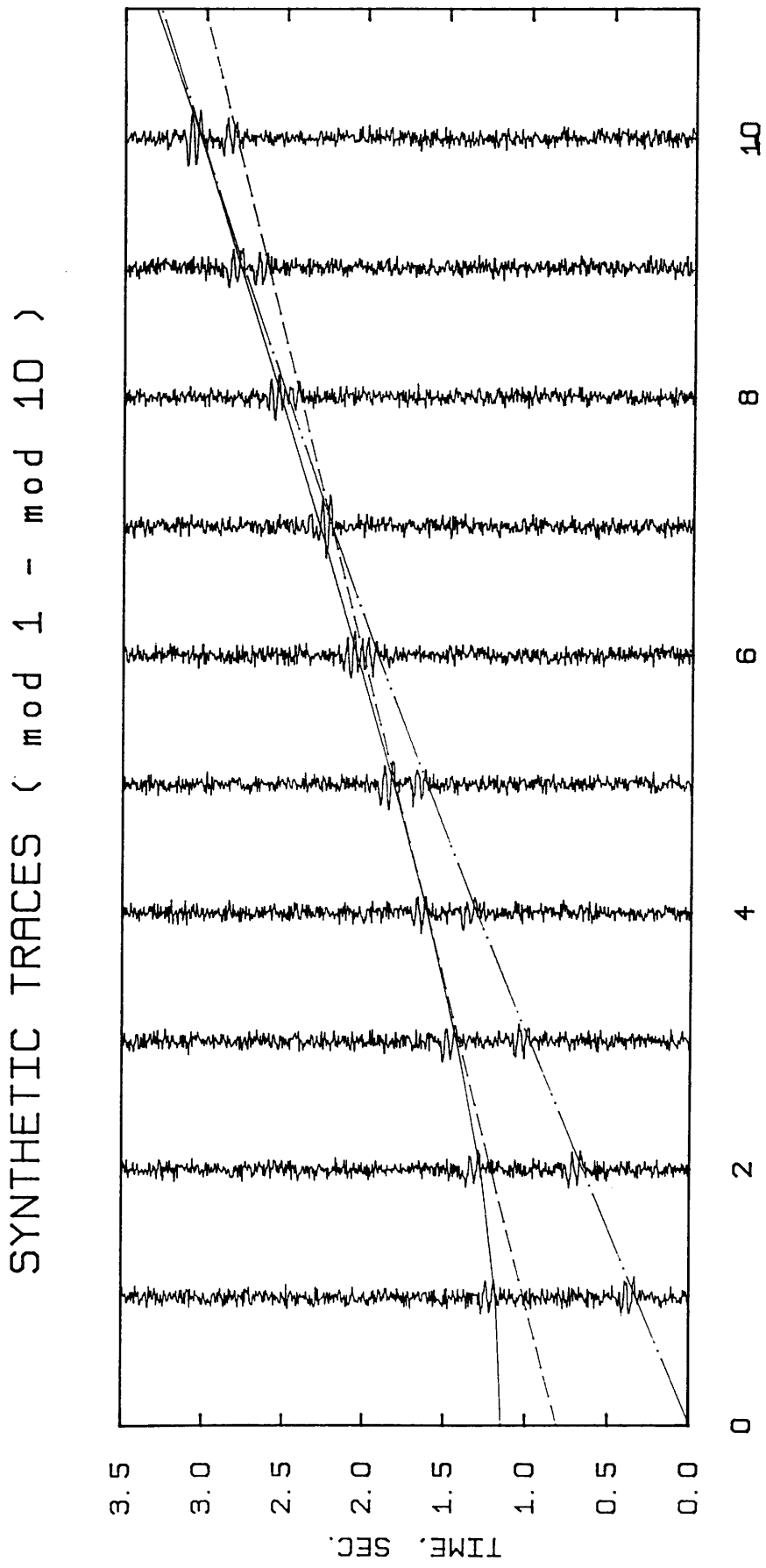


Fig.3.34 Synthetic seismic traces, set "mod", which was constructed by stacking traces of the sets: "direct", Fig. 3.33a, " reflect ", Fig. 3.33b and the set "refract", Fig. 3.33c.

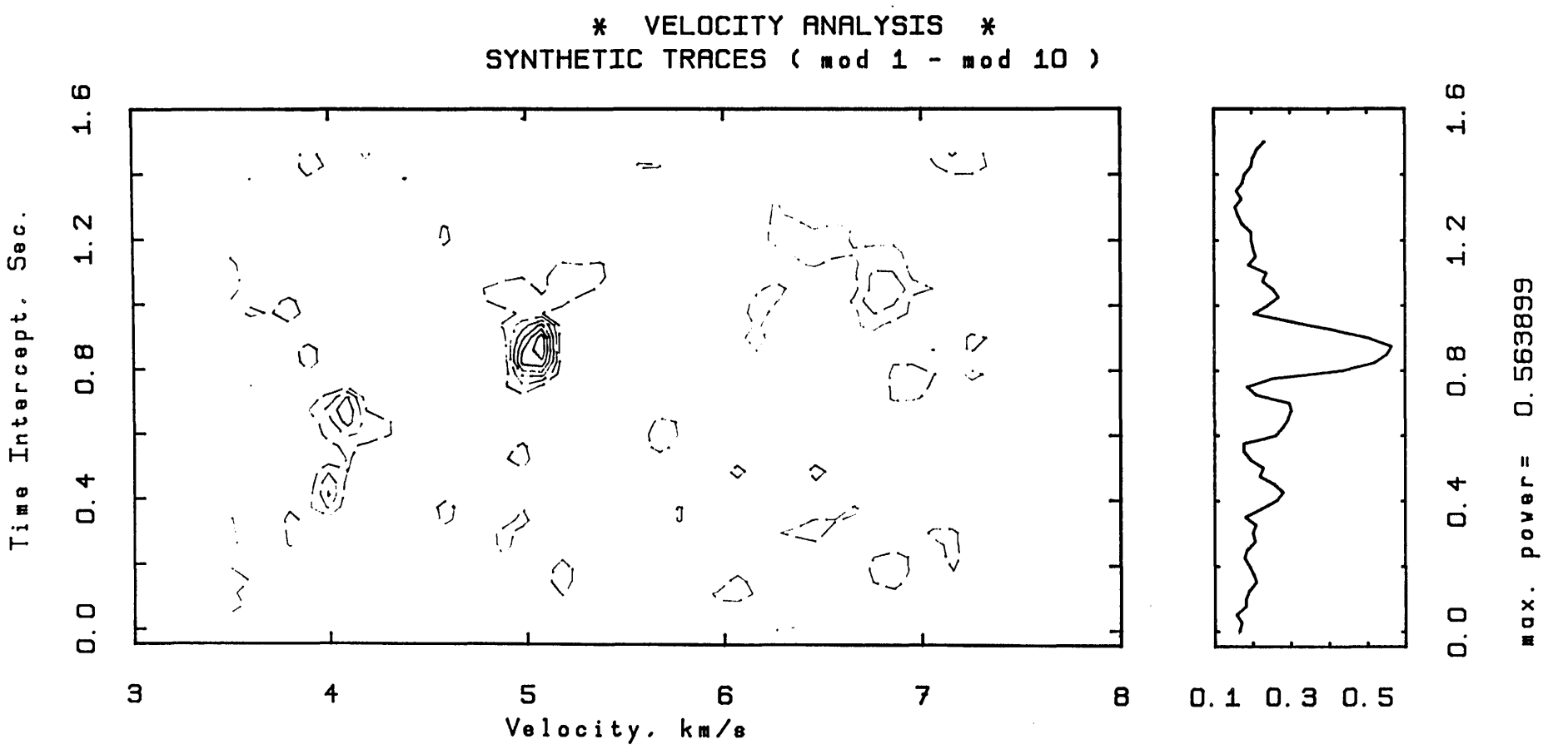


Fig.3.35a Results of applying semblance method to dataset "mod" displayed in contour format, for **refracted** events, with *large* ranges and increments of velocity and time.

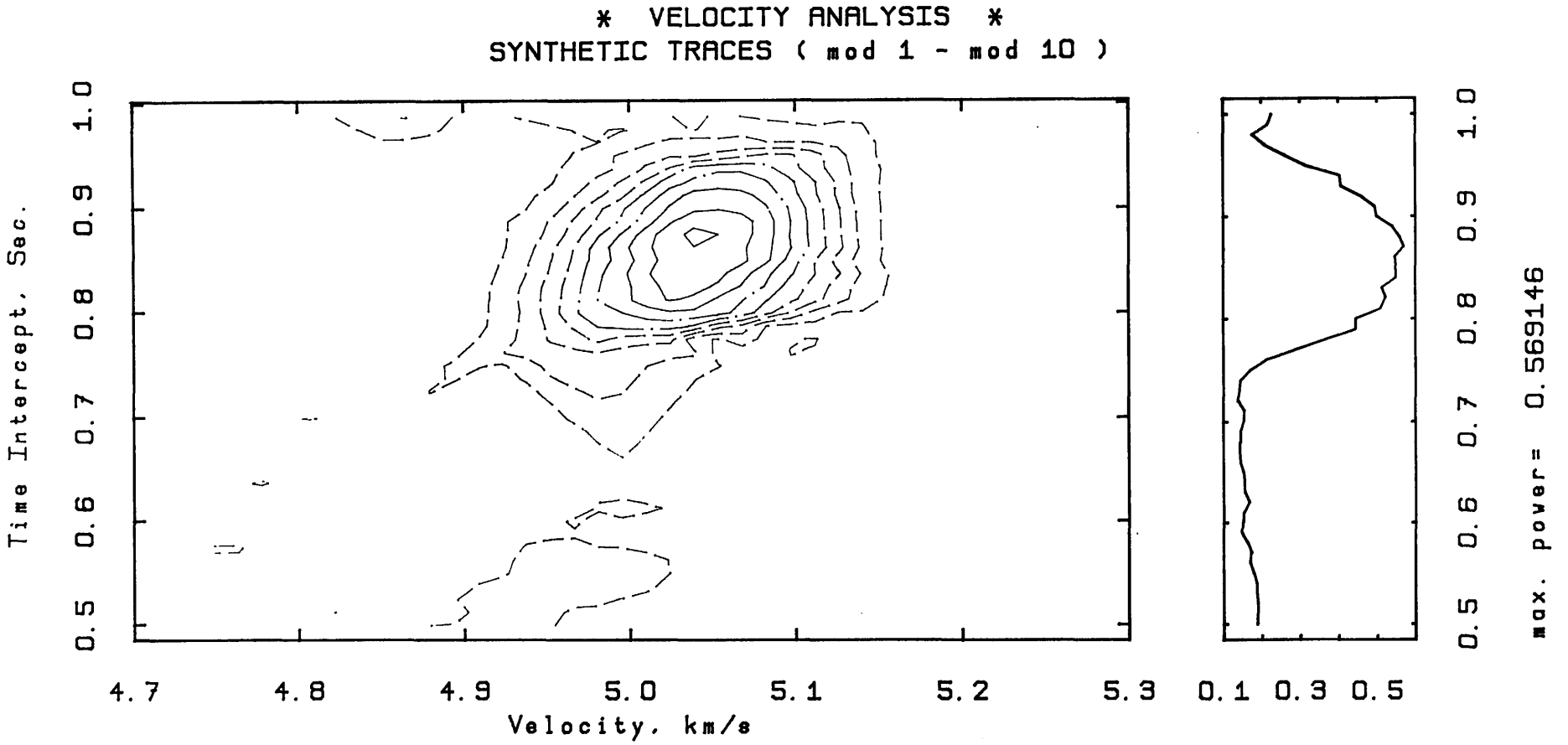


Fig.3.35b Results of applying semblance method to dataset "mod" displayed in contour format, for **refracted** events, with *small* ranges and increments of velocity and time.

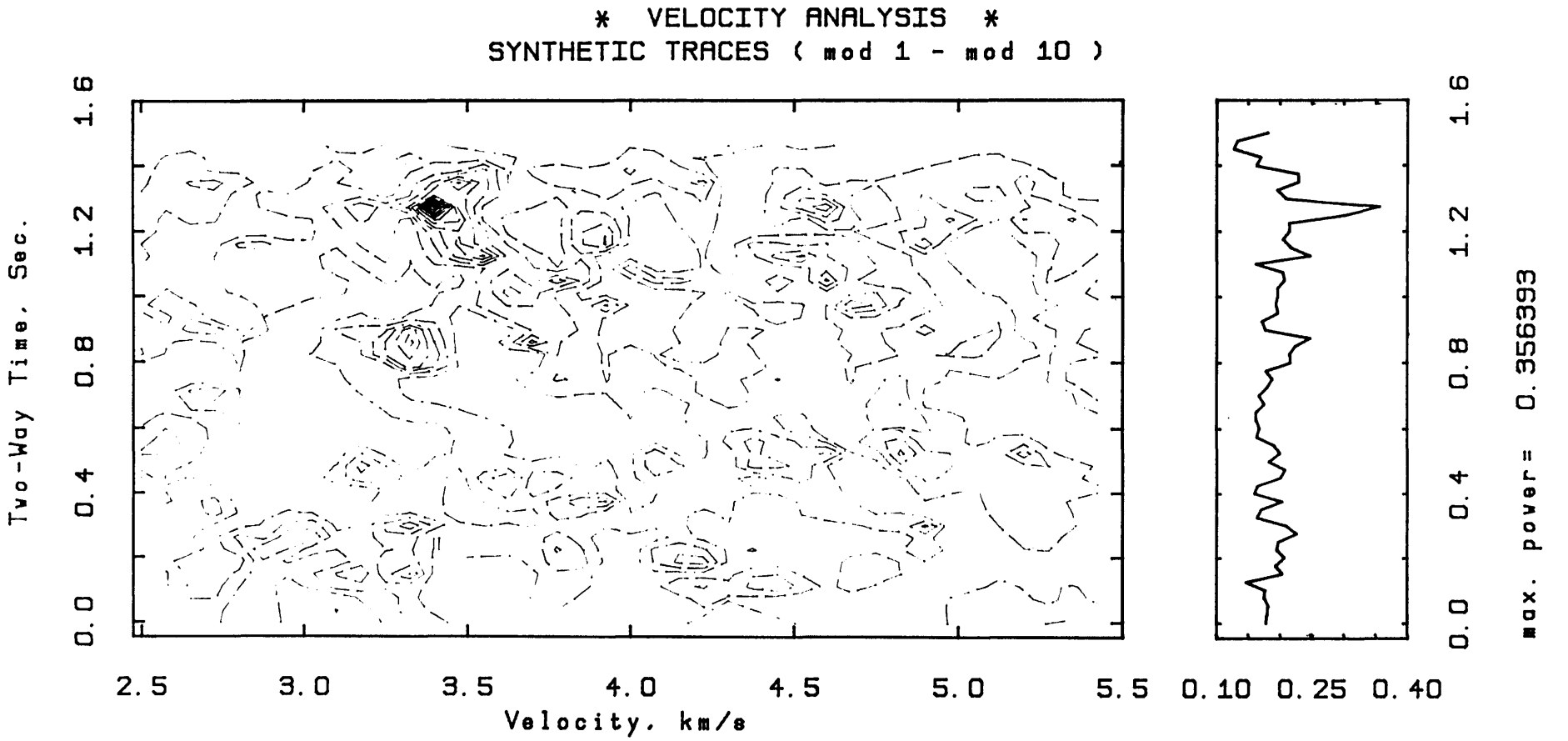


Fig.3.36a Results of applying semblance method to dataset "mod" displayed in contour format, for **reflected** events, with *large* ranges and increments of velocity and time.

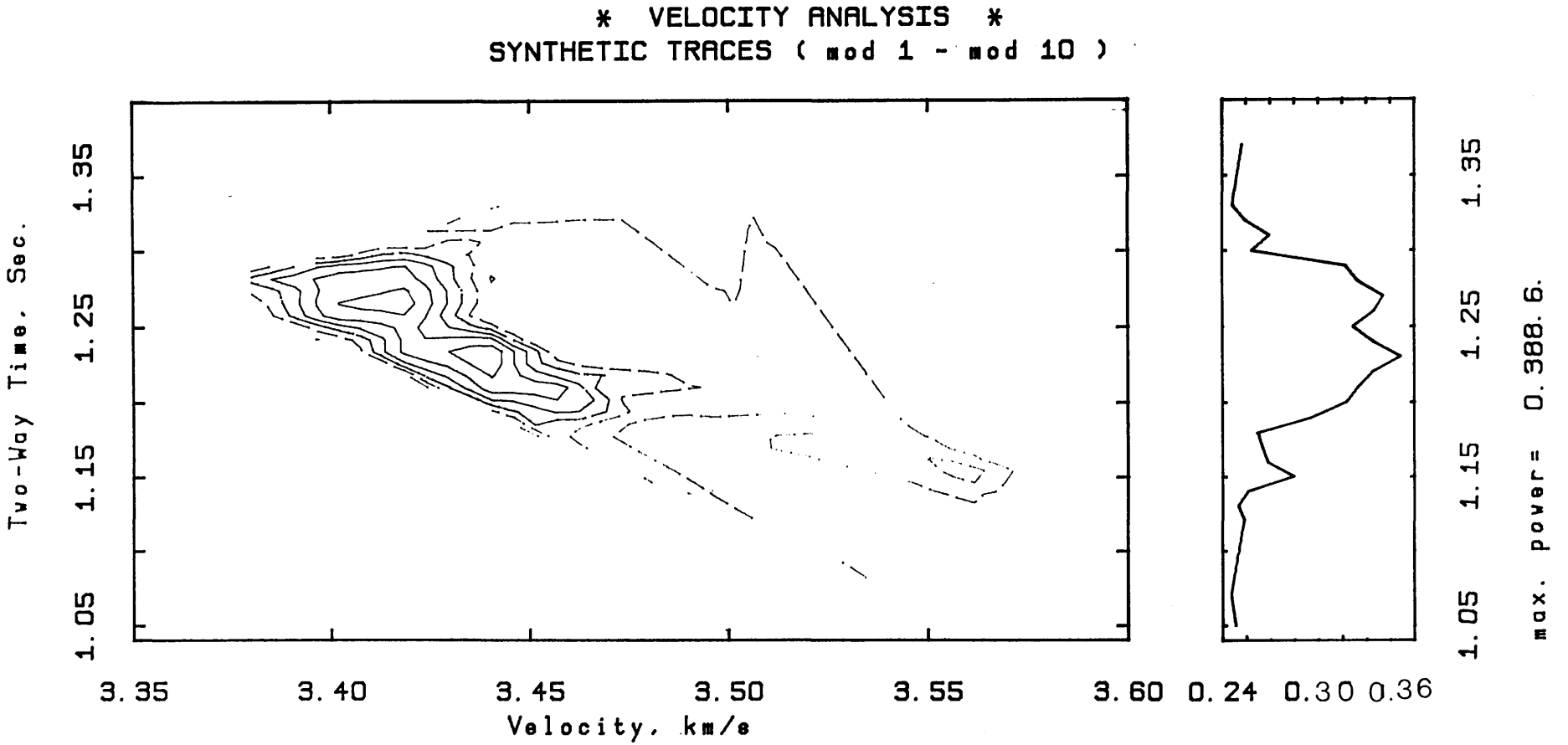


Fig.3.36b Results of applying semblance method to dataset "mod" displayed in contour format, for **reflected** events, with *small* ranges and increments of velocity and time.

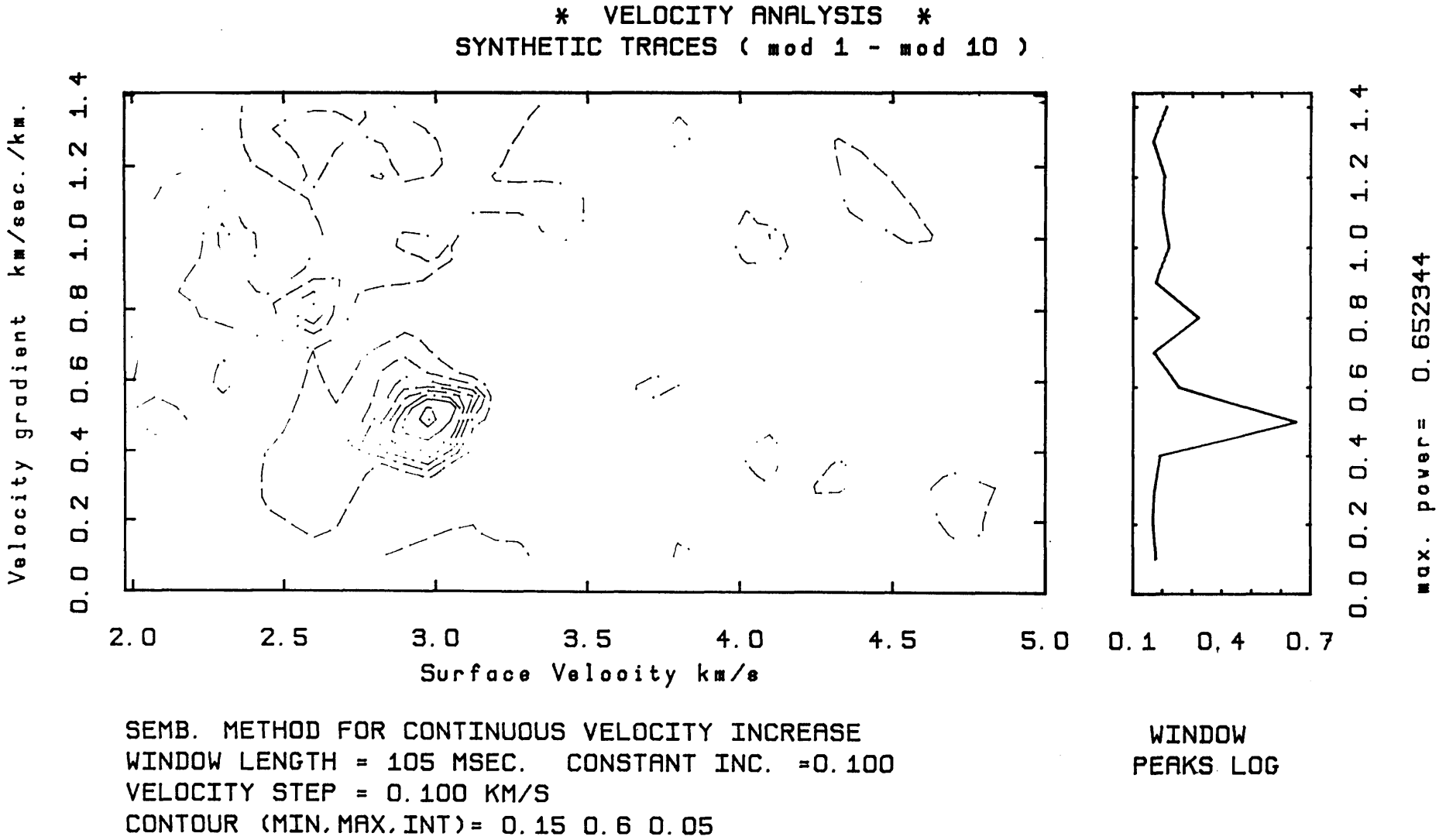


Fig.3.37a Results of applying semblance method to dataset "mod" displayed in contour format, for **continuous velocity increase with depth (direct)** events, with *large* ranges and increments of velocity and time.

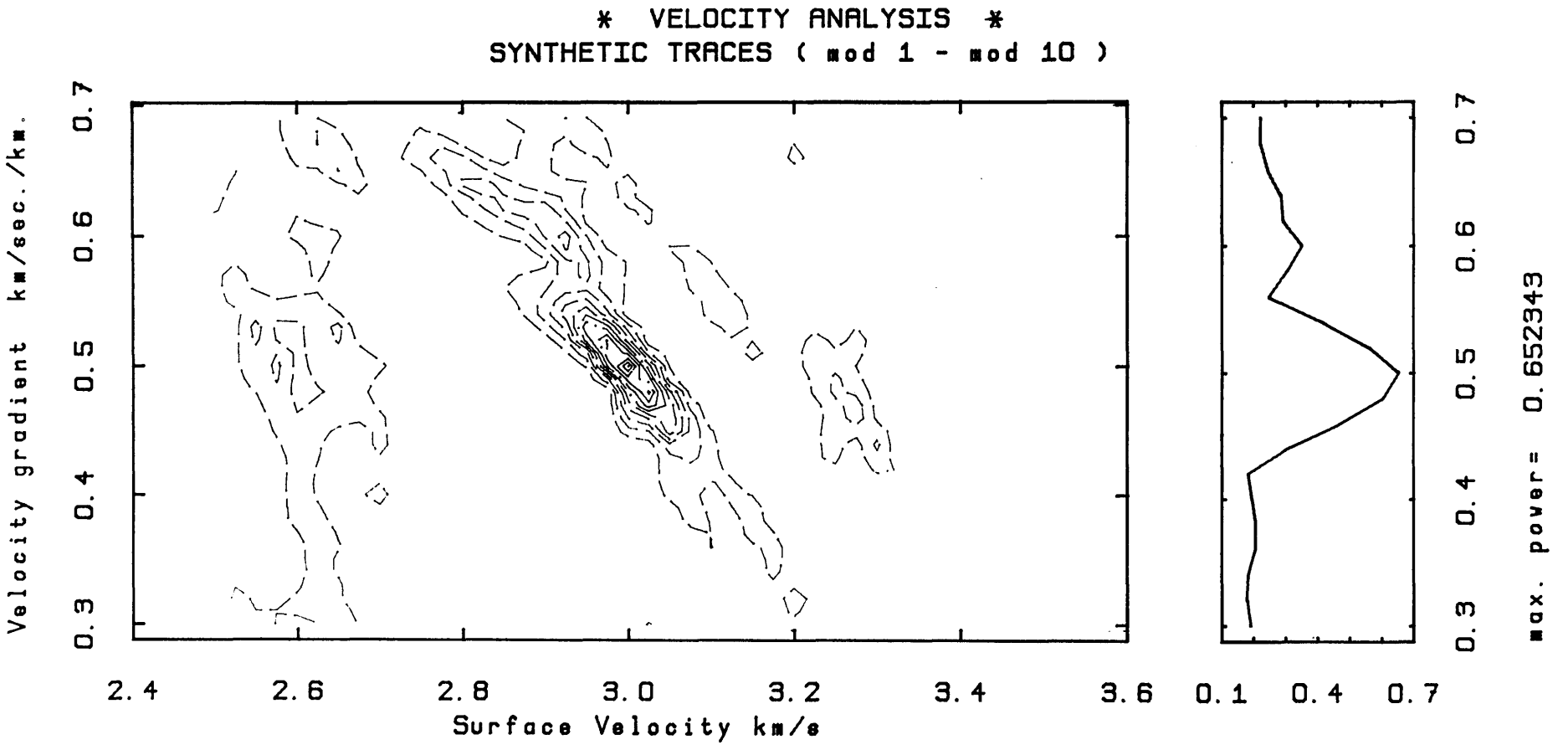


Fig.3.37b Results of applying semblance method to dataset "mod" displayed in contour format, for **continuous velocity increase with depth (direct)** events, with *small* ranges and increments of velocity and time.

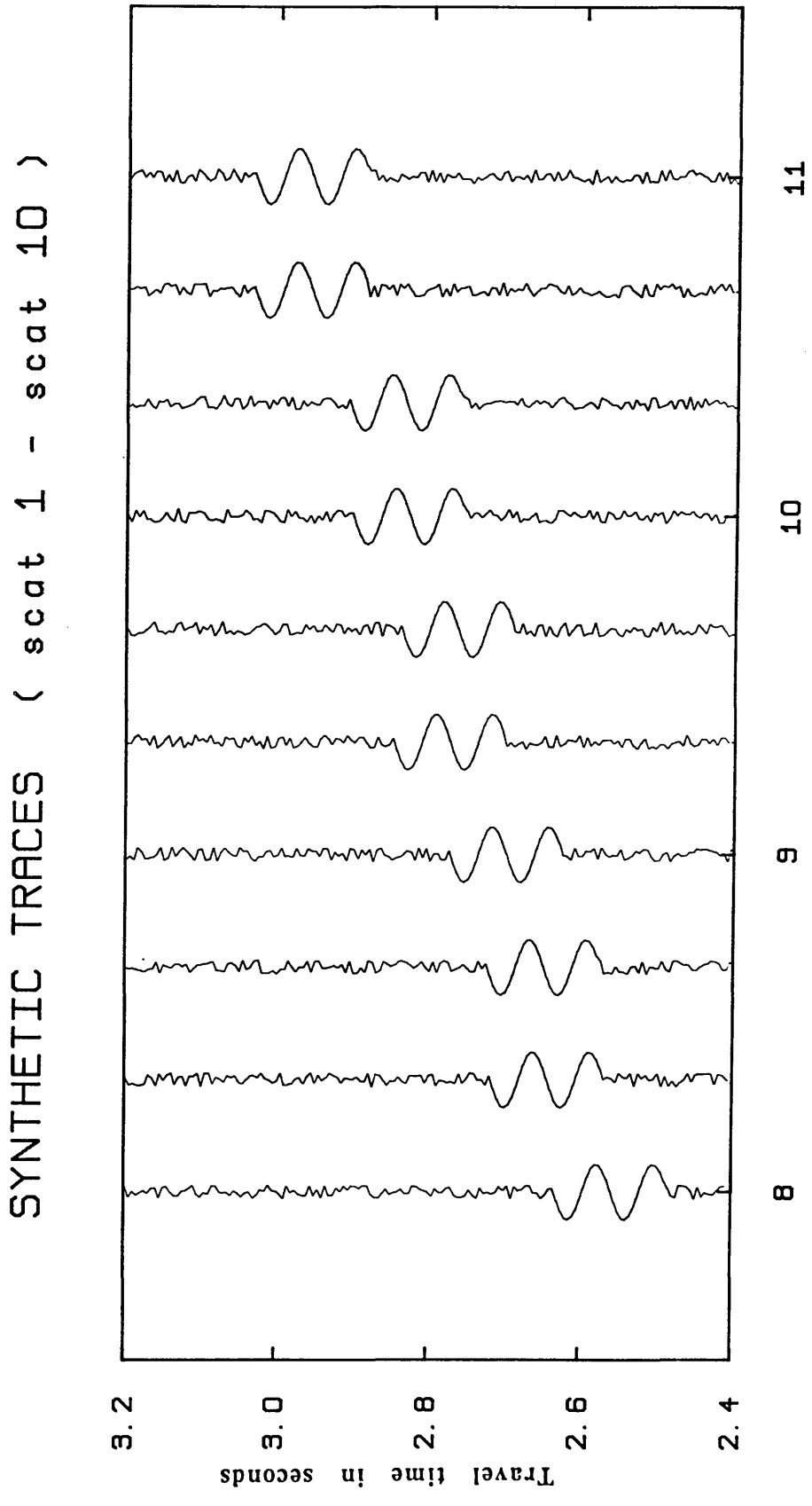


Fig.3.38 Synthetic seismic traces set "scat" formed by applying static shifts (see Table 3.13) to the set "ints", Fig. 3.24.

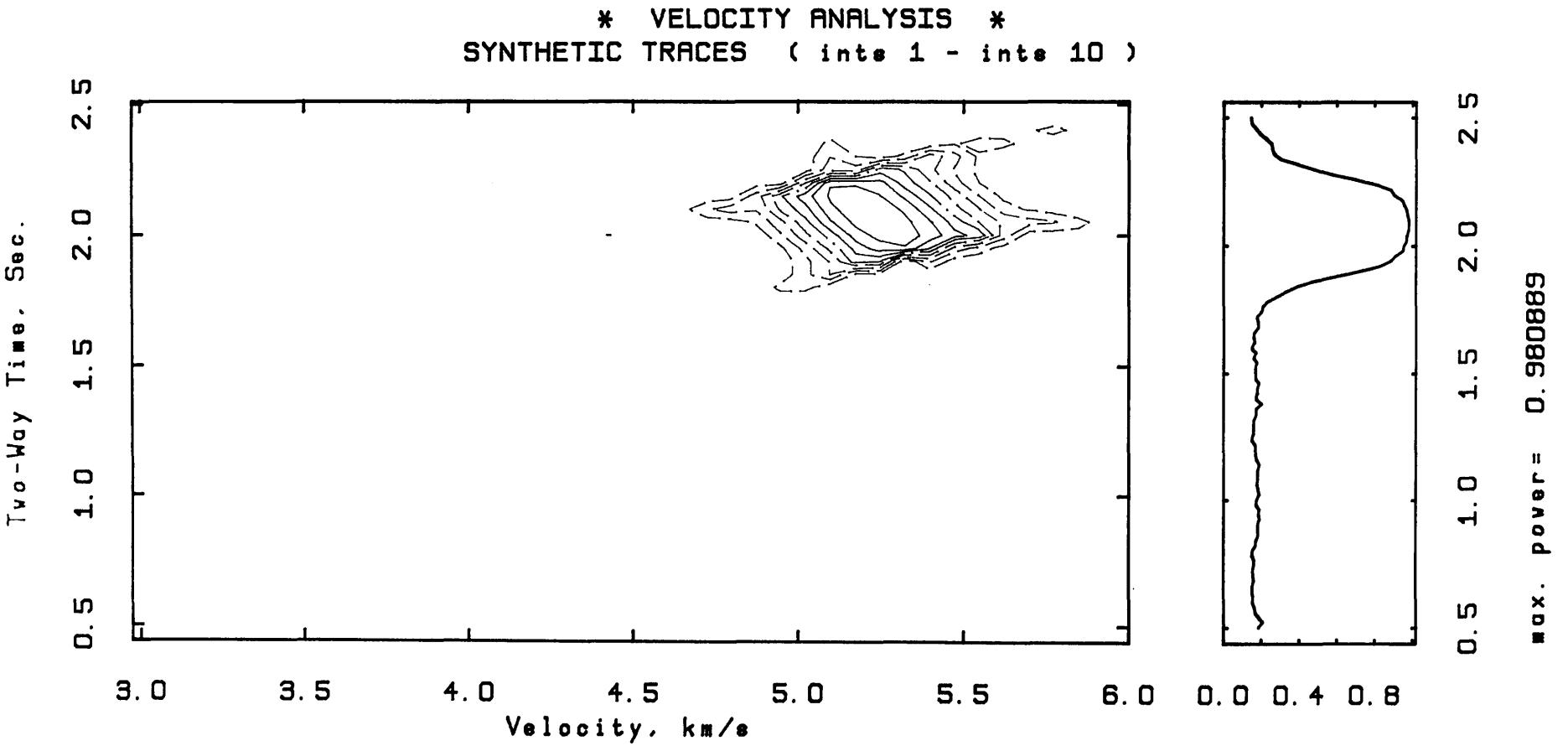


Fig.3.39 Results of applying semblance method to dataset "ints" displayed in contour format, exhibiting a good performance of the software in extracting the event at the proper time and velocity.

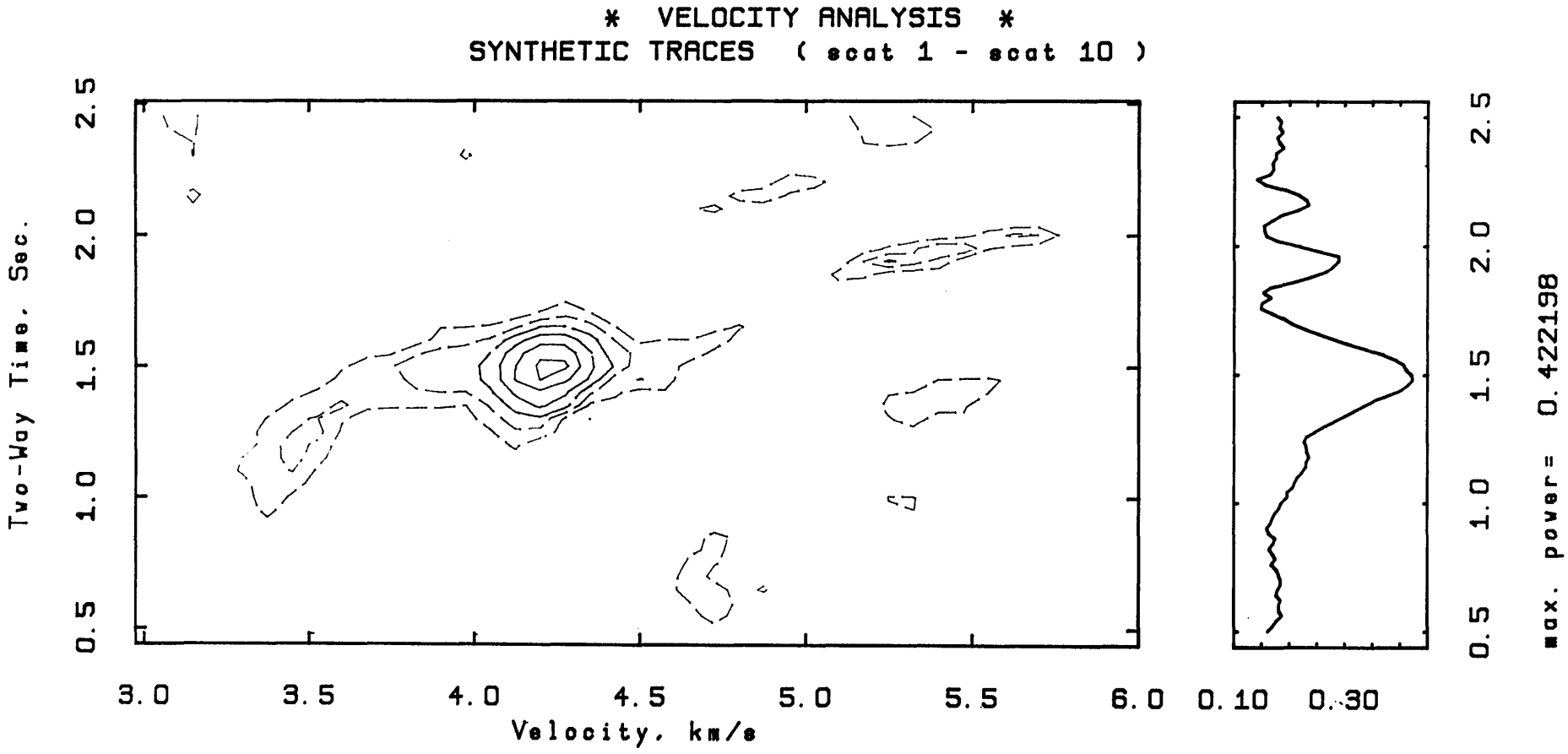


Fig.3.40 Results of applying semblance method to dataset "scat". displayed in contour format. Contrast the results with those from the equivalent unscattered data (Fig. 3.39).

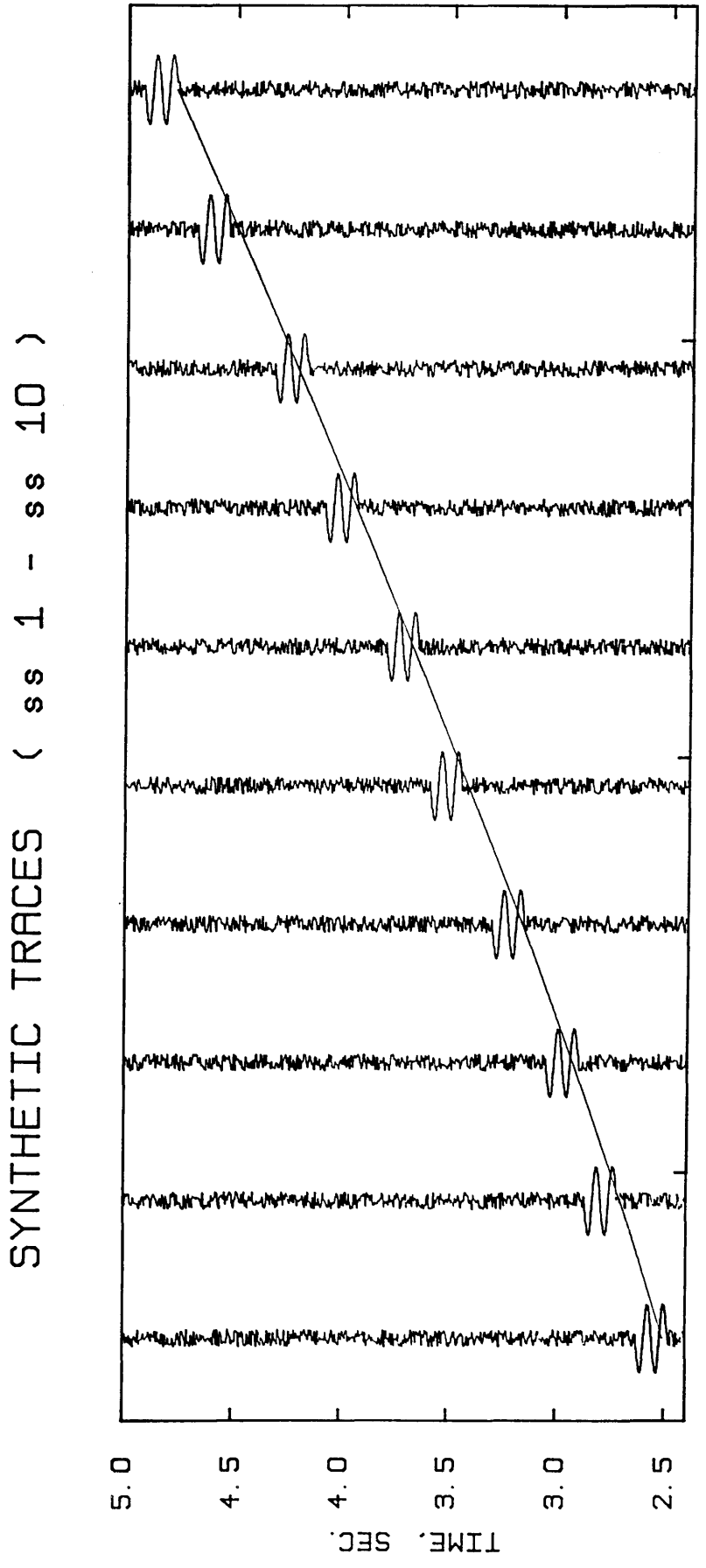


Fig.3.41 Synthetic seismic traces set "ss", containing the data of set "scat", Fig. 3.38, re-arranged over a long range of offset.

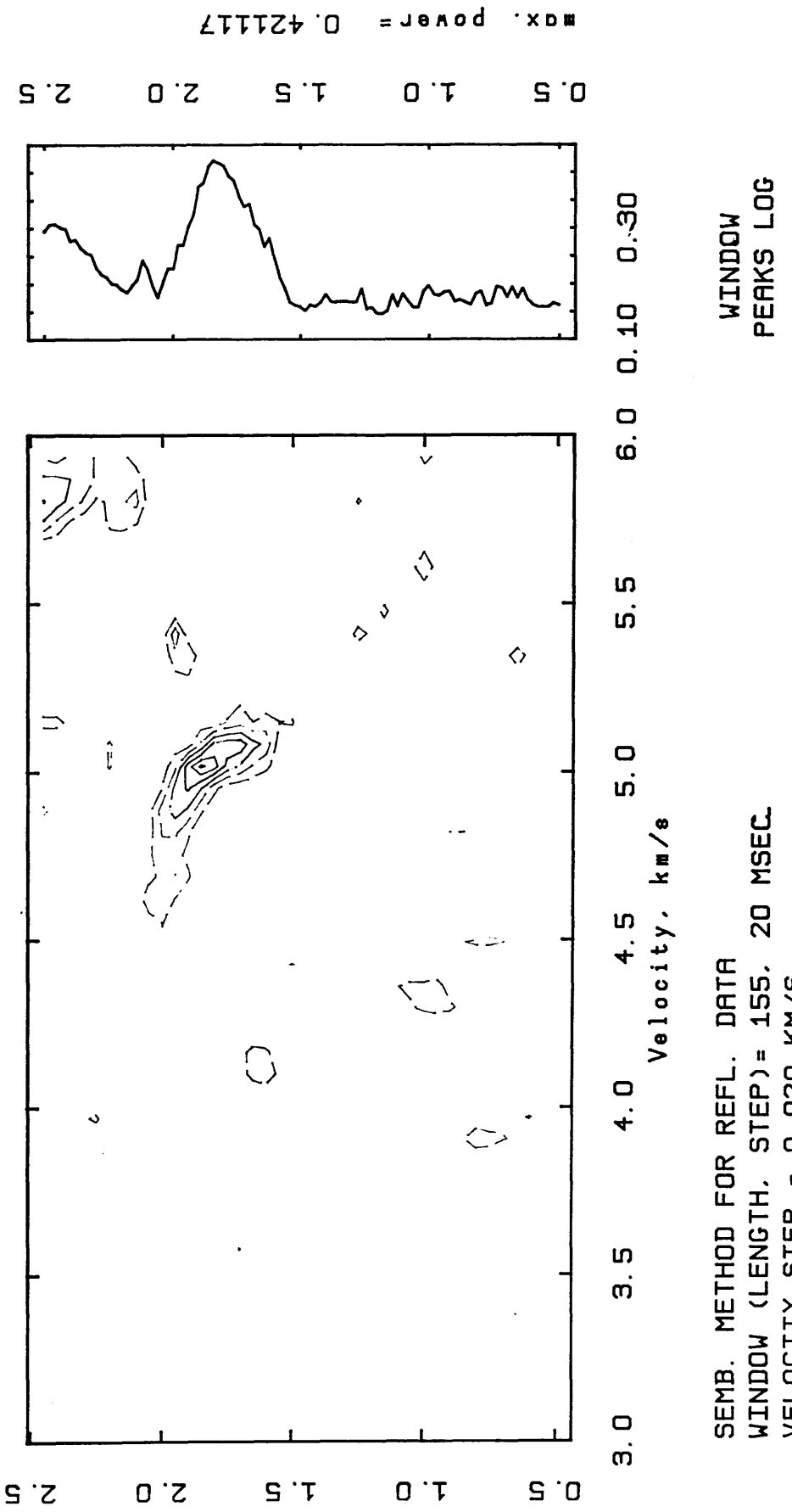


Fig.3.42 Results of applying semblance method to dataset "ss". Compare with Fig. 3.39 and 3.40.

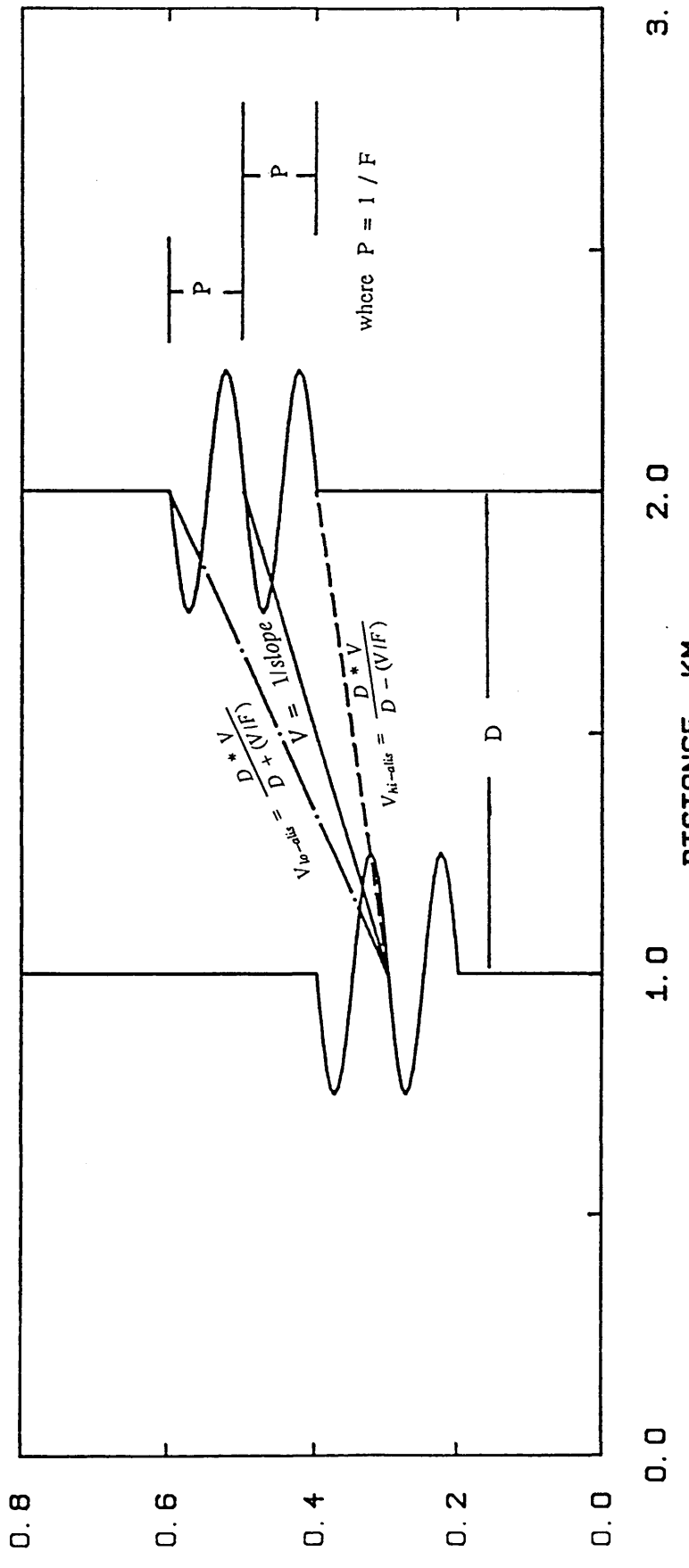


Fig.3.43 Upper and lower aliasing velocities computation, for a given velocity ( V ), inter receiver distance ( D ) and frequency ( F ).

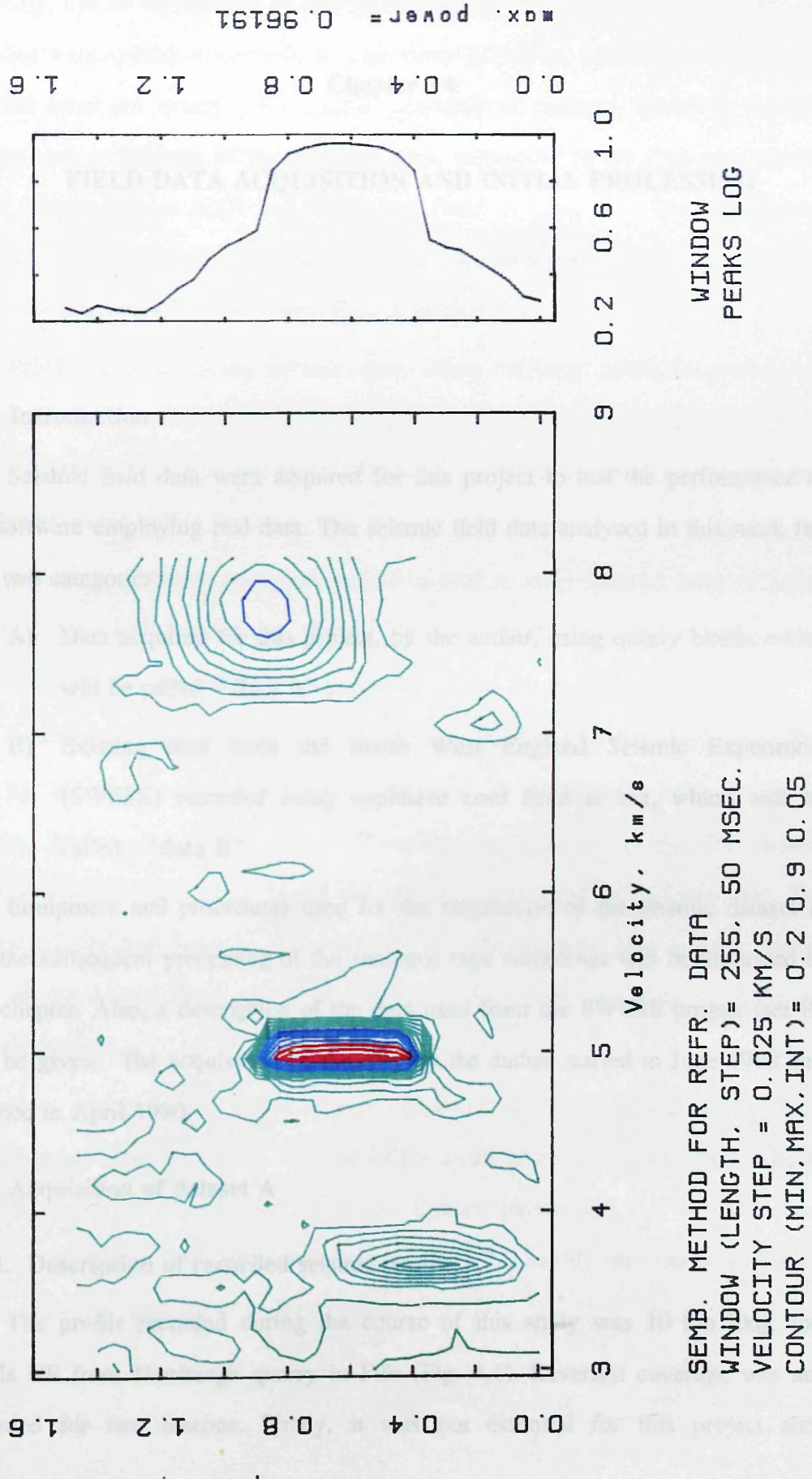


Fig.3.44 Results of applying the semblance method to dataset "frq1", Fig. 3.19a, employing a large range for the velocity to illustrate the upper and lower aliasing velocities.

# Chapter 4

# FIELD DATA ACQUISITION AND INITIAL PROCESSING

## 4.1. Introduction

Seismic field data were acquired for this project to test the performance of the software employing real data. The seismic field data analysed in this work fall into two categories:

A) Data acquired for this project, by the author, using quarry blasts, which will be called **"data A"** .

B) Existing data from the South West England Seismic Experiment (SWESE) recorded using explosive cord fired at sea, which will be called **"data B"** .

Equipment and procedures used for the acquisition of the seismic dataset A and the subsequent processing of the analogue tape recordings will be discussed in this chapter. Also, a description of the data used from the SWESE project (set B) will be given. The acquisition of the data by the author started in June 1988 and finished in April 1990.

## 4.2. Acquisition of dataset A

### 4.2.1. Description of recorded seismic profile

The profile recorded during the course of this study was 10 km long and trends NE from Newburgh quarry in Fife (Fig. 4.1). Reversed coverage was not recorded for two reasons. Firstly, it was not essential for this project and,

secondly, due to the absence of reasonable seismic sources in the area of interest. Stations were spaced at intervals of approximately 400 m, and the first station was 1.8 km from the quarry. The profile consisted of eighteen recording stations. Names and coordinates of the recorded sites, referenced to the Ordnance Survey maps (sheets number 21/31 and 22/32), are listed in Table 4.1. The seismic section for the profile is displayed in Fig. 4.2 and frequency analysis is shown in Fig. 4.3. The seismograph used is described in section 4.2.2.

Problems in acquiring seismic data, when the only available sources are quarry blasts, have been discussed in detail by many researchers (e.g. Al-Mansouri 1986, Dentith 1987, Kamaliddin 1988). Such problems are well known and will not be discussed in this thesis.

All stations, except one, were buried in drift to keep them as close as possible to their ideal location on the profile. This was preferable to using rock outcrops available only at significant distances from the profile.

In a typical blast the total amount of explosive used by the quarry was 130-260 kg, divided into 4-8 holes with a delay of 25 ms between each successive charge, fired with one delay/hole. Therefore the effective charge for seismic interest was 32.5 kg, which is the amount of charge fired in the first hole. The quarry usually drill holes to a depth of 12 m. The working face was on the far side of the quarry from the profile, reducing the energy travelling toward the seismic stations.

Gain setting was a key factor in determining the amplitude of the data. Mostly gain values were high because of the small amount of explosive fired and the orientation of the quarry face. These factors are outwith the control of the author. Moreover, two additional factors, weather (mostly the wind) and local noise, affect the gain value at each station.

Table 4.1 Names, coordinates, and offsets of recorded sites.

| Site | Name | X-coord. (km) | Y-coord. (km) | Offset (km) (km) |
|---|---|---|---|---|
| source | Newburgh quarry | 24.550 | 17.600 | 0.000 |
| st 01 | Park Hill | 25.525 | 18.487 | 1.816 |
| st 02 | Silver Hill | 25.837 | 18.743 | 2.219 |
| st 2.5 | Silver Hill | 26.077 | 18.859 | 2.482 |
| st 03 | Silver Hill | 26.244 | 18.961 | 2.678 |
| st 04 | Higham Hill | 26.650 | 19.260 | 3.112 |
| st 05 | Higham Hill | 27.088 | 19.375 | 3.544 |
| st 09 | Logie Low | 28.435 | 20.150 | 5.098 |
| st 11 | Logie Hill | 29.075 | 20.437 | 5.795 |
| st 12 | Logie East | 29.415 | 20.750 | 6.255 |
| st 13 | Fliskmillan Hill | 29.790 | 20.900 | 6.650 |
| st 14 | Fliskmillan | 30.100 | 21.050 | 6.995 |
| st 15 | Fliskmillan | 30.500 | 21.200 | 7.415 |
| st 16 | Pittachope Plantation | 30.775 | 21.412 | 7.637 |
| st 17 | Balhelvie | 31.100 | 21.775 | 8.100 |
| st 18 | Canal Plantation | 31.425 | 21.825 | 8.406 |
| st 19 | West Flisk | 31.782 | 22.100 | 8.853 |
| st 20 | East Flisk | 32.160 | 22.250 | 9.255 |
| st 21 | East Flisk | 32.535 | 22.375 | 9.770 |

### 4.2.2. The Glasgow FM Mark 2 recording system

A pool of forty single station analogue recording units were used in this work. The units were designed and constructed by Dr. J. Hall and Mr. G. Gordon in the Department of Geology and Applied Geology, University of Glasgow. A unit consists of integral amplifier, modulator, tuned radio receiver to record the 60 kHz MSF time signal from Rugby, and a vertical 4.5 Hz LI5B Mark geophone (Fig. 4.4). The recorder has a four track recording head and uses a standard stereo cassette, i.e. four tracks are recorded on a normally two-sided two-track (stereo) tape. Using a C120 tape, the recording window is one hour. The signal is pre-amplified and filtered with a 1.5 - 60 Hz analogue filter, to ensure recording only of frequencies within the plateau of the system. Then, the recorded data are passed to two separate gain amplifiers differing by 18 dB. The first amplifier, which will be recorded on the first channel, has a gain range of 82 - 118 dB in 6 dB steps. The second amplifier has a gain range of 64 - 96 dB and will be recorded on the second channel. The third channel is an auxiliary channel not used in this work. Lastly, the fourth channel was used to record the 60 kHz MSF time signal transmitted from Rugby. This signal, which can be decoded and displayed in digital form, was essential in locating the events on the tape. A remote starting mechanism and electronic clock allows the user to establish the recording units in the field up to 24 hours before the desired recording time.

The playback and digitising system used in this project consists of a cassette player, demodulater, filters and ultra-violet oscillograph (Fig. 4.5). The cassette player has a tape head similar to that of the recorders. The data are amplified and passed through a demodulater to an analogue filter, which can be chosen to fulfil the requirements of the user. The filtered data are then amplified and passed to the UV oscillograph, which has the facility to run at selected paper speeds. The fourth channel (MSF time signal) is passed directly to the amplifier, after the demodulator. A Schmidt trigger, if required, was available to give the time signal

a box shape on the playback for easy time picking. Finally the MSF signal is passed to the decoder which will display the recorded time in days, hours, minutes, and seconds to assist locating the desired arrivals on the tape.

A Programmable Data Processer (PDP 11/23) PLUS computer and software written by Mr. R. Cumberland were used to convert the data from the analogue to digital form. The playback system, described above, was used with the output passing through anti-aliasing 40 Hz analogue filter. An analogue input board (ADV11-C), accepts 1-16 signal ended bipolar input, sampling the data at 200 samples/second. Variations in the sampling rate of up to 5 % occur due to the differences in the speed of tapes as recorded in the field. All traces were digitised for a nominal 15 seconds and then resampled to ensure a correct rate.

### 4.3. Data of the SWESE project

During 1979 a network of seven long seismic wide-angle lines were recorded across the peninsula of South West England. The project was called the South West England Seismic Experiment (SWESE) and is described by Brooks *et al.* (1984), Doody (1985).

Two types of land recorders were used: MARS (Modulator-Amplifier-Receiver System) and Racal Geostore systems. Analogue data for the MARS recorders were digitised at University College, Cardiff, while those from the Geostore recorders were digitised at the British Geological Survey, Edinburgh. Methods and equipment utilised in acquiring the data for SWESE project and its initial processing are well documented by Doody (1985). In this project only the vertical component was used.

Lines 1-6 were simple land recording lines reversed by marine shots. The seventh consisted of ten marine shots fired between the Lizard and Start peninsulas and recorded at three land recording arrays on the peninsulas (Fig. 4.6a). Recording line 7 was on the Start peninsula, while lines 8 and 9 were established

on the Lizard peninsula (Fig. 4.6b). Line 8 consisted of eleven recording sites and line 9 was a shorter array of five receivers. Average station spacing was 1.5 km along line 8 and 2.3 km along line 9. Configuration of the Lizard-Start line allows the data to be viewed in two ways:

[1] One station recording all shots.

[2] One shot recorded along an array of recording.

Fig. 4.7 shows the seismic sections of shots used in the present study.

Line 5, also analysed in this work , was one of three N-S lines of the SWESE network. It was established between Polperro, in the south, and Hartland Point. The line was reversed by shots fired at locations 5 S and 5 N immediately offshore (Fig. 4.6). The profile of shot 5 S consists of 26 recording stations, while shot 5 N consists of 27. Stations were spaced at intervals of approximately 2 km, see Fig. 4.8.

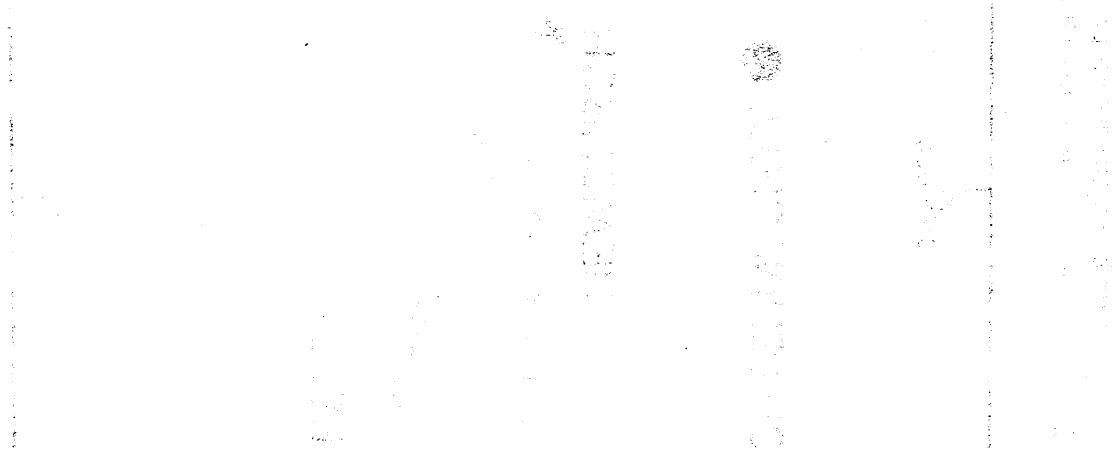

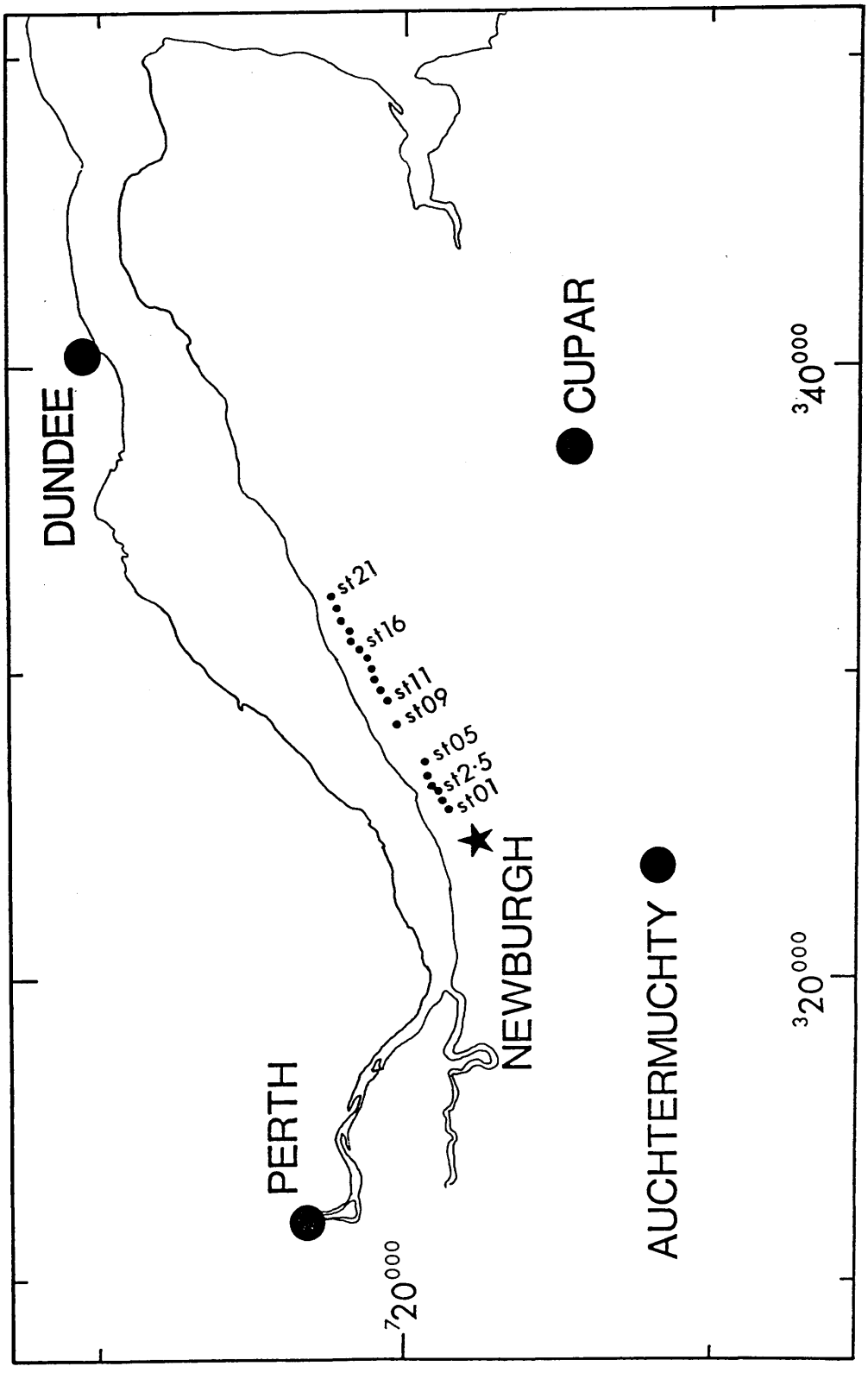


Fig.4.1 Location map of the profile recorded from Newburgh quarry during this project. Recording stations shown by small dots.

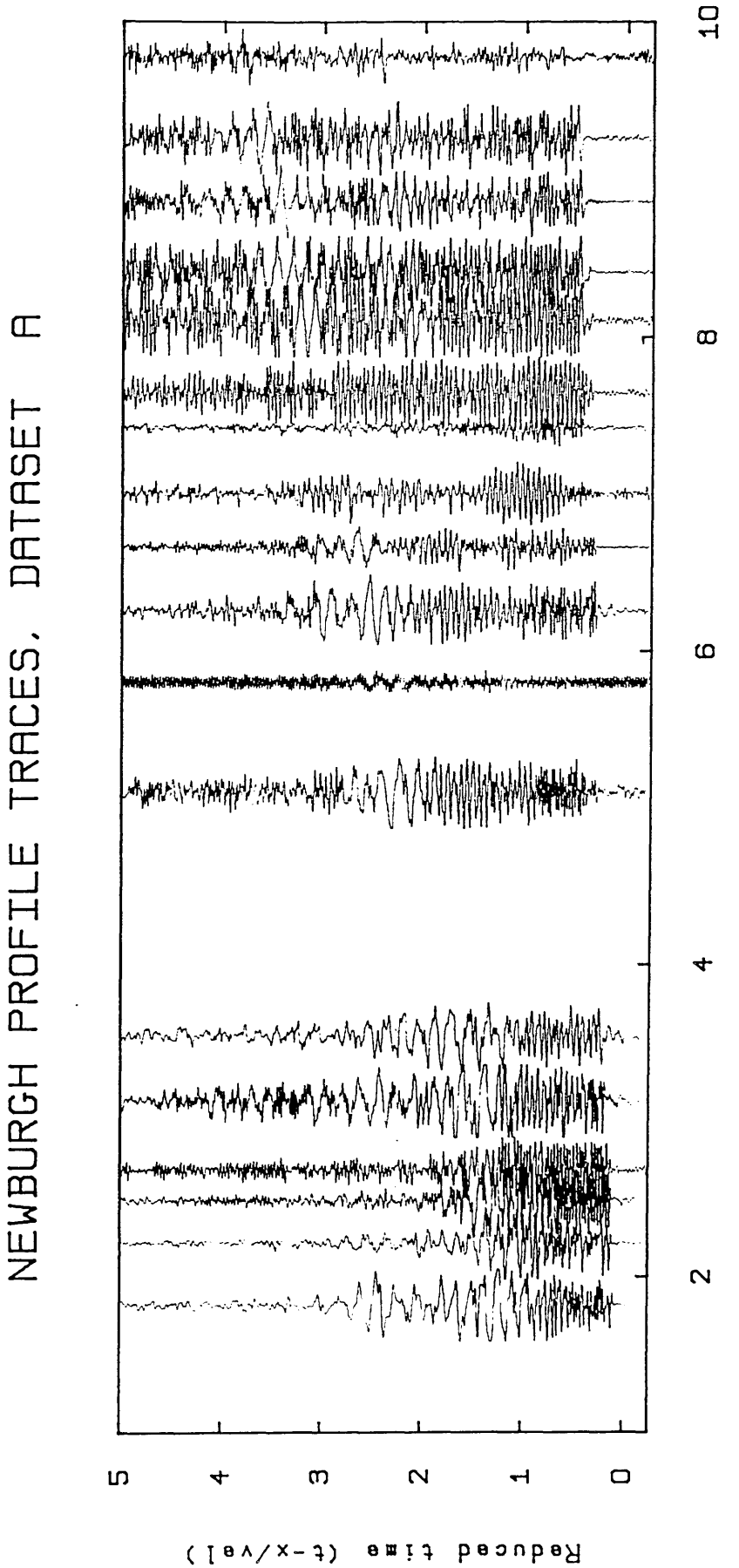


Fig.4.2 Seismic profile recorded during the course of this project, dataset A. Reduction velocity 6.0 km/s. See Fig. 4.1 for profile location.

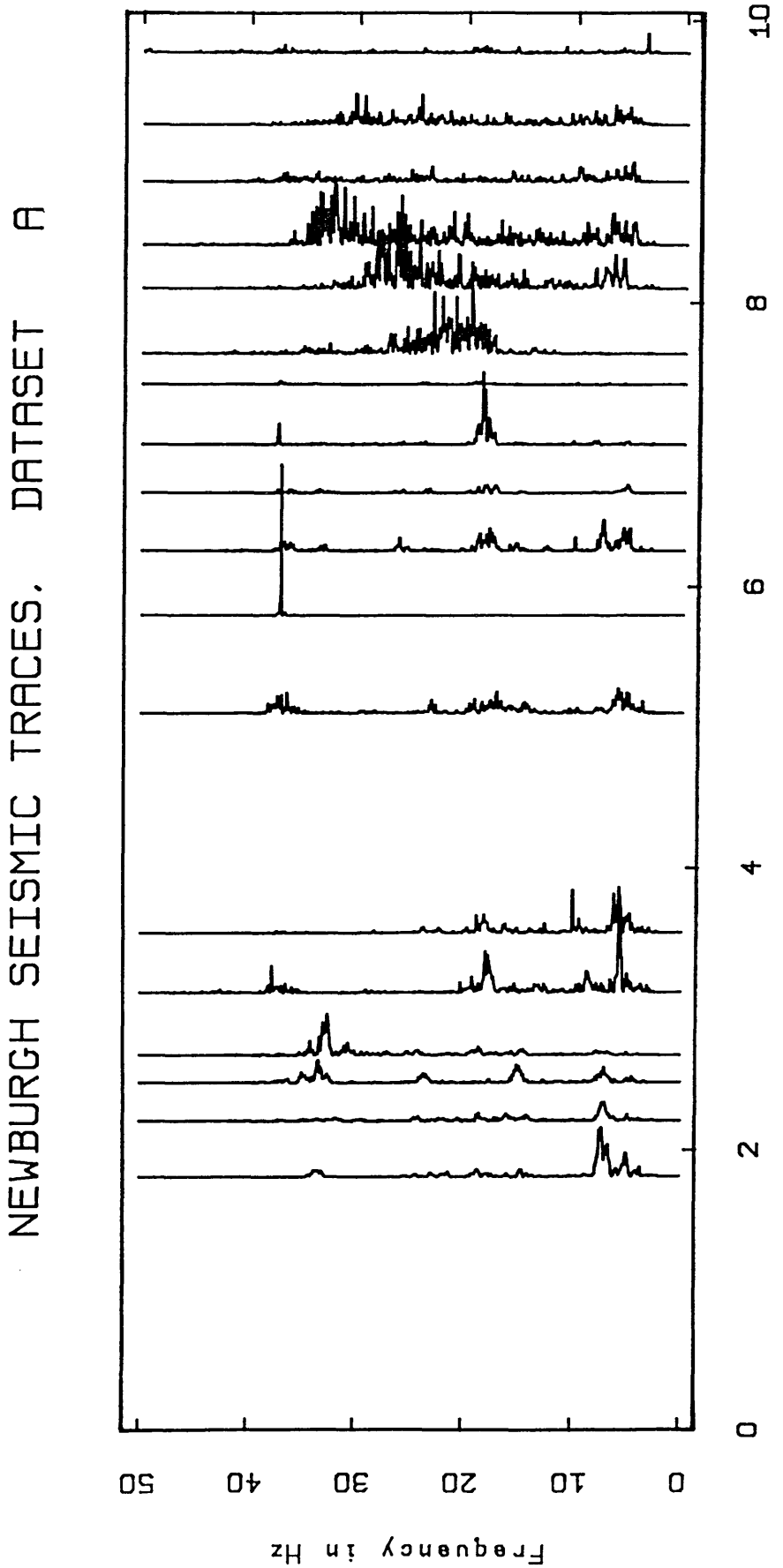


Fig.4.3 Frequency analysis of dataset A (see fig. 4.2). Frequency range 0 - 50 Hz.

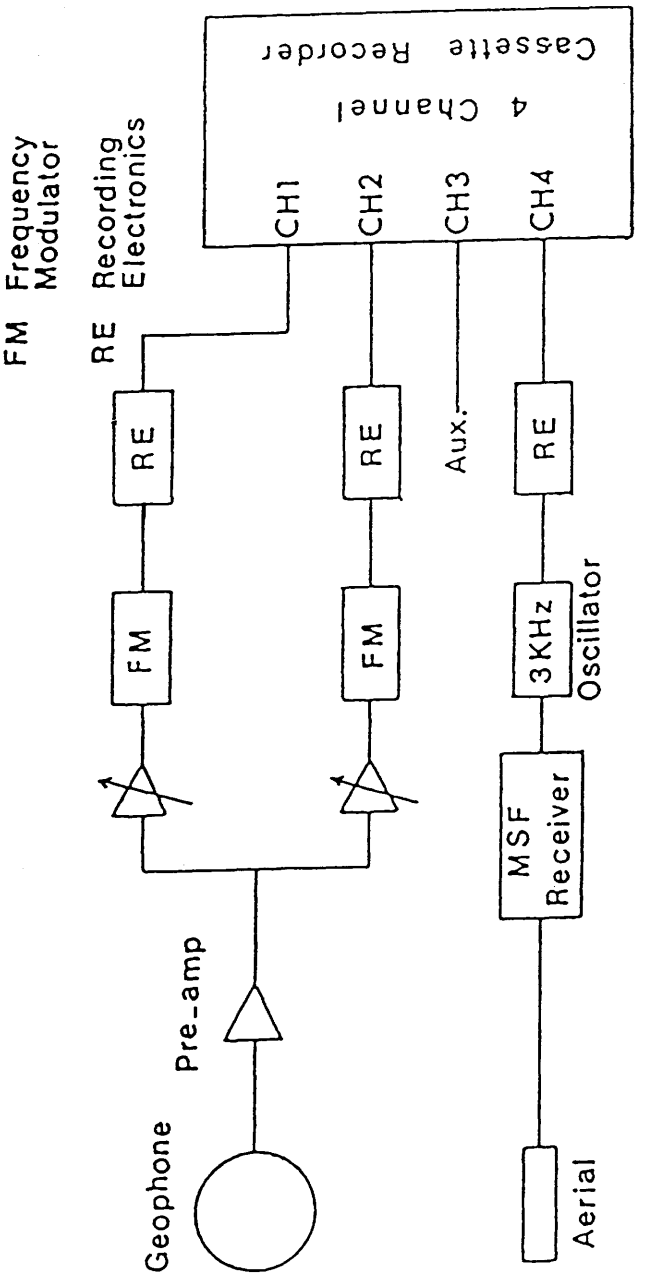


Fig.4.4 Block diagram showing the recording arrangement of the Glasgow F.M. Mark 2 unit.

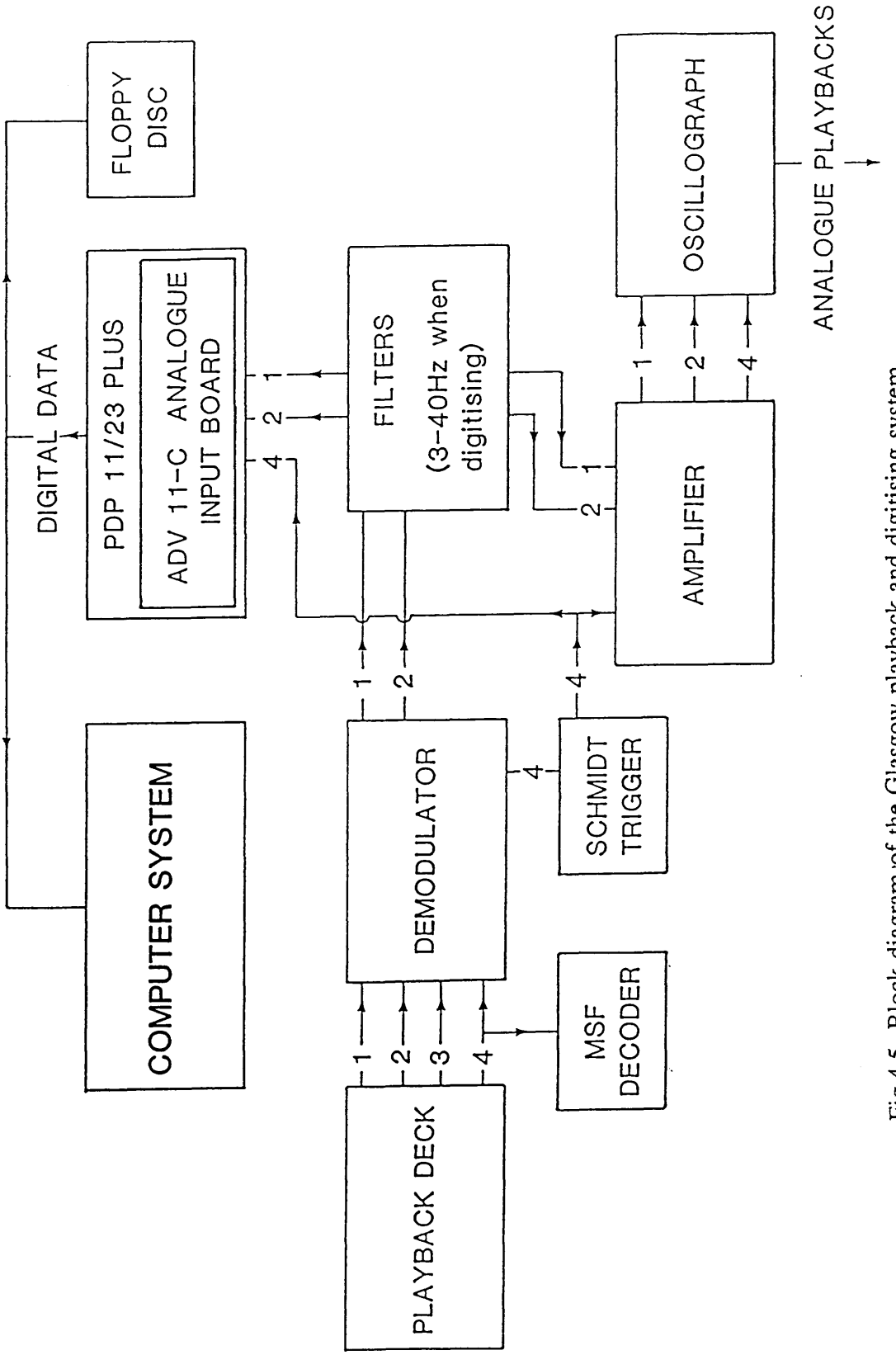


Fig.4.5 Block diagram of the Glasgow playback and digitising system.

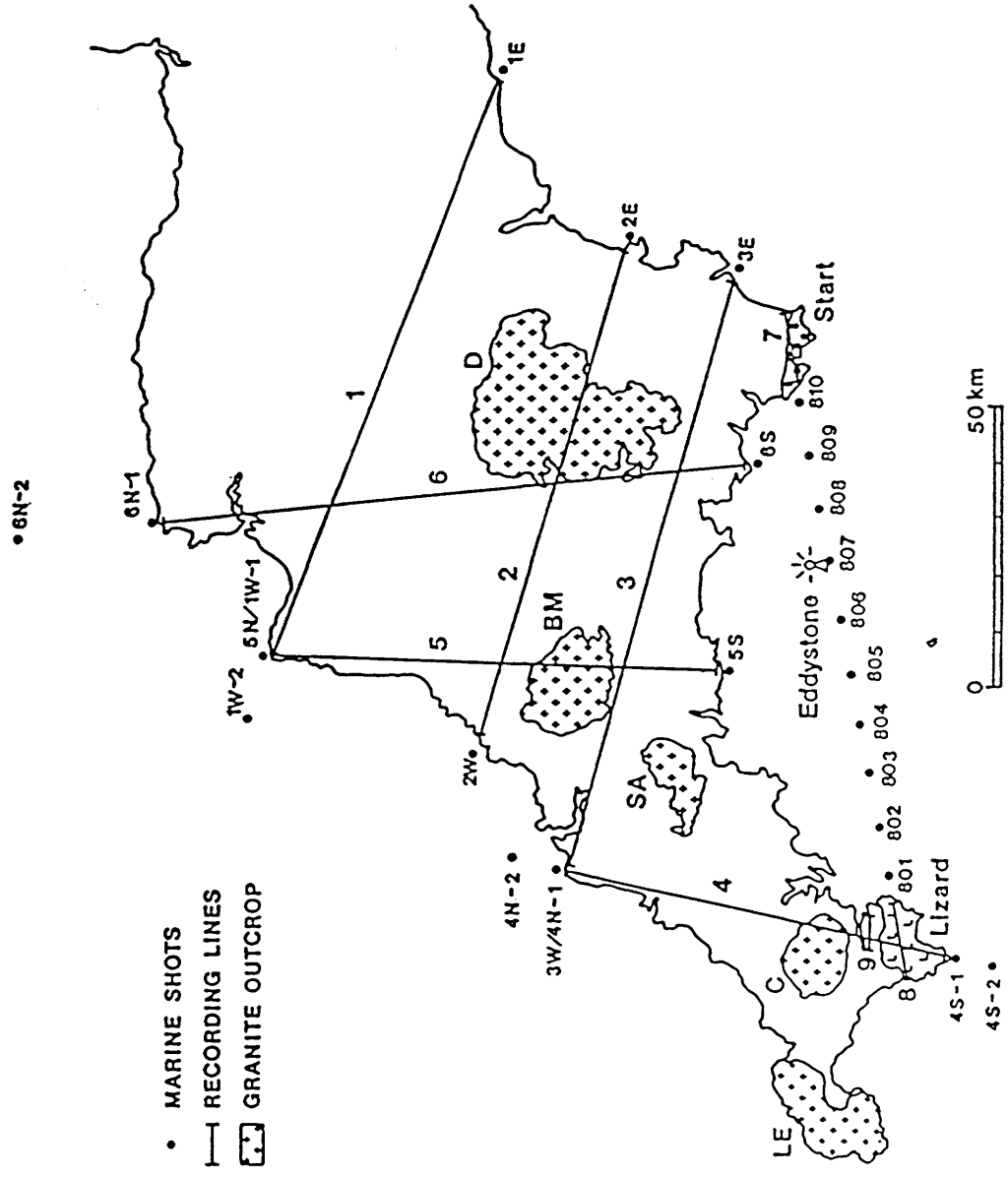


Fig.4.6a Seismic lines established during SWESE.
Granite outcrops: BM = Bodmin Moor; C = Carnmenellis; D = Dartmoor; LE = Land's End; SA = St Austell. (after Doody, 1985)

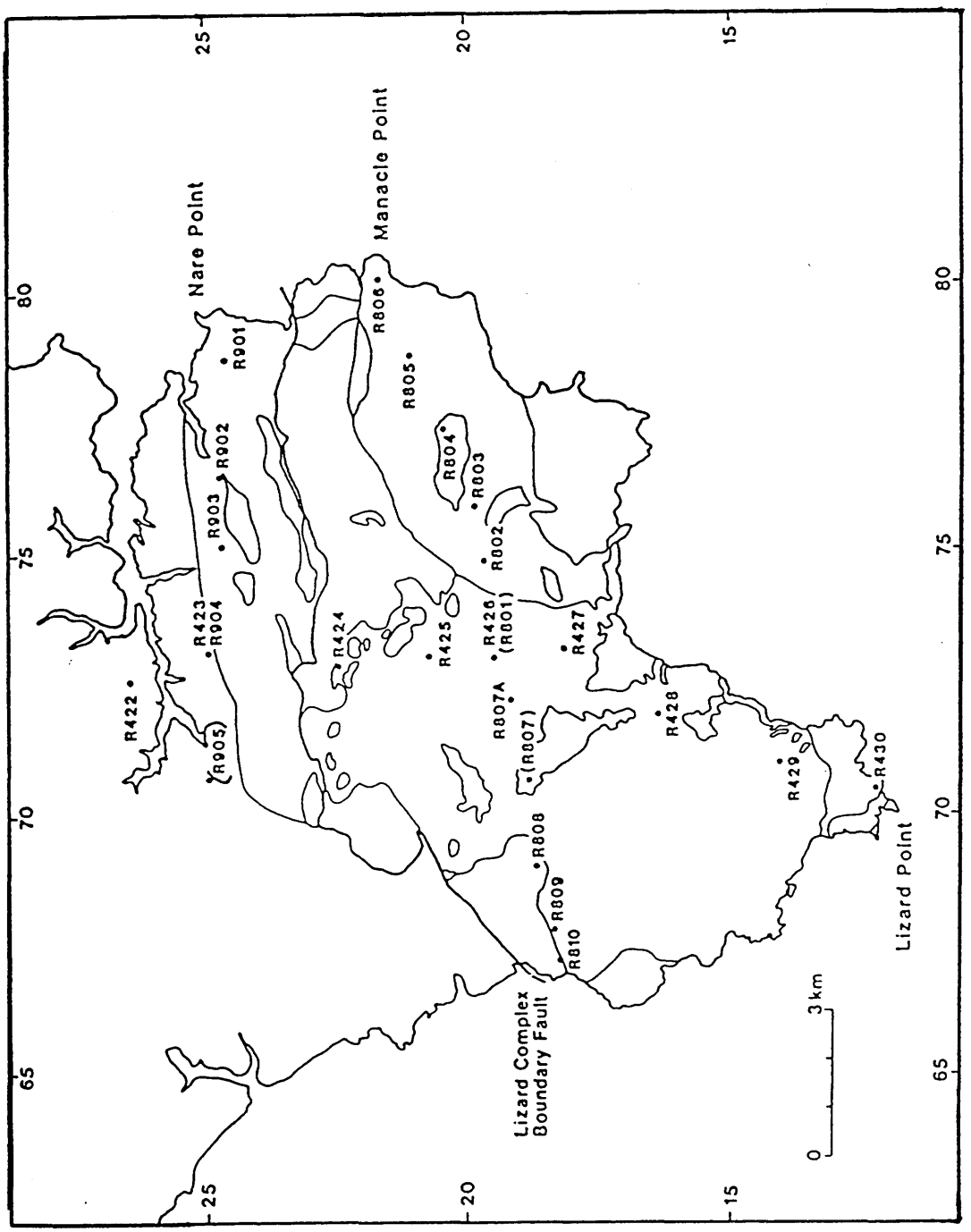


Fig.4.6b Lizard-Start line. Recording station locations of lines 8 and 9. Bracketed stations were occupied, but no data were obtained. (after Doody, 1985)

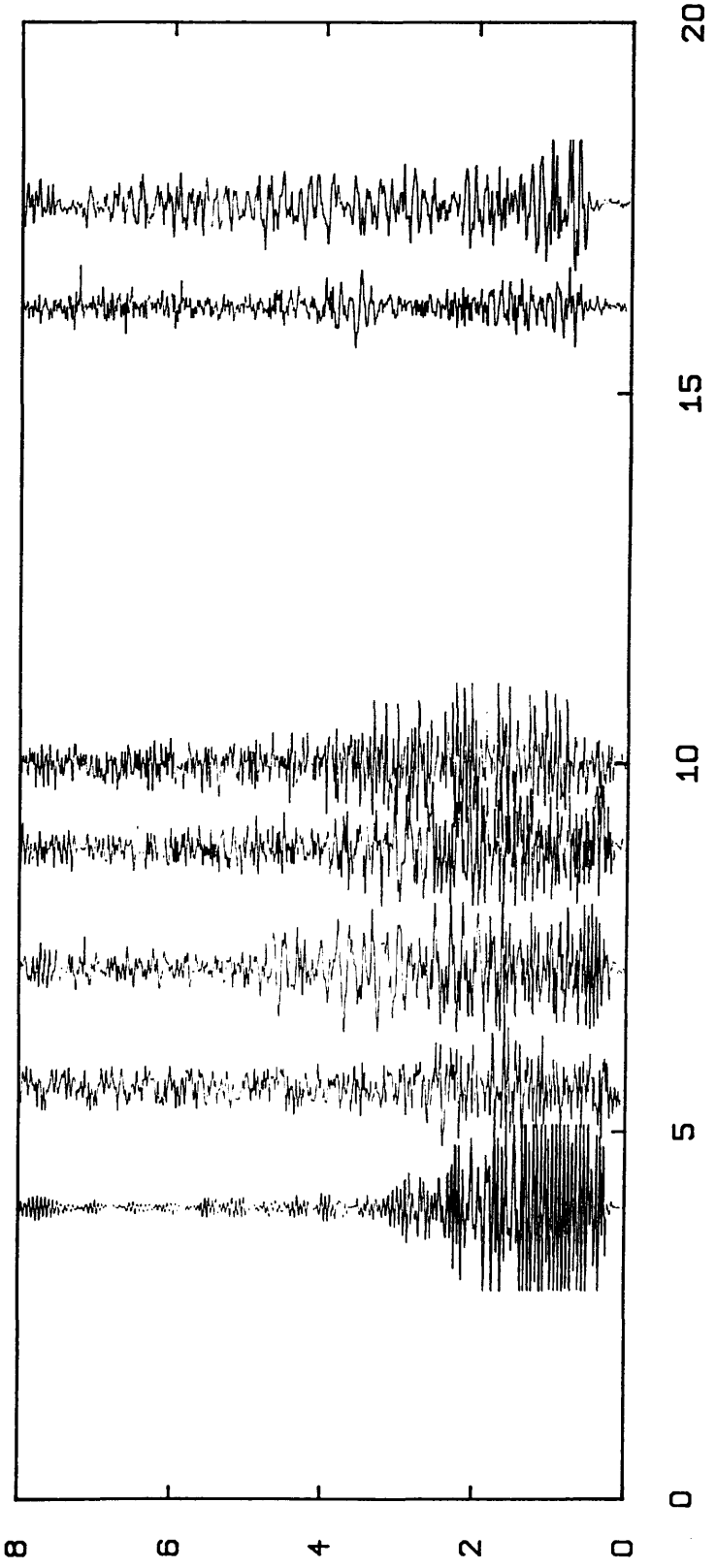


Fig.4.7a One shot seismic section, R801N.

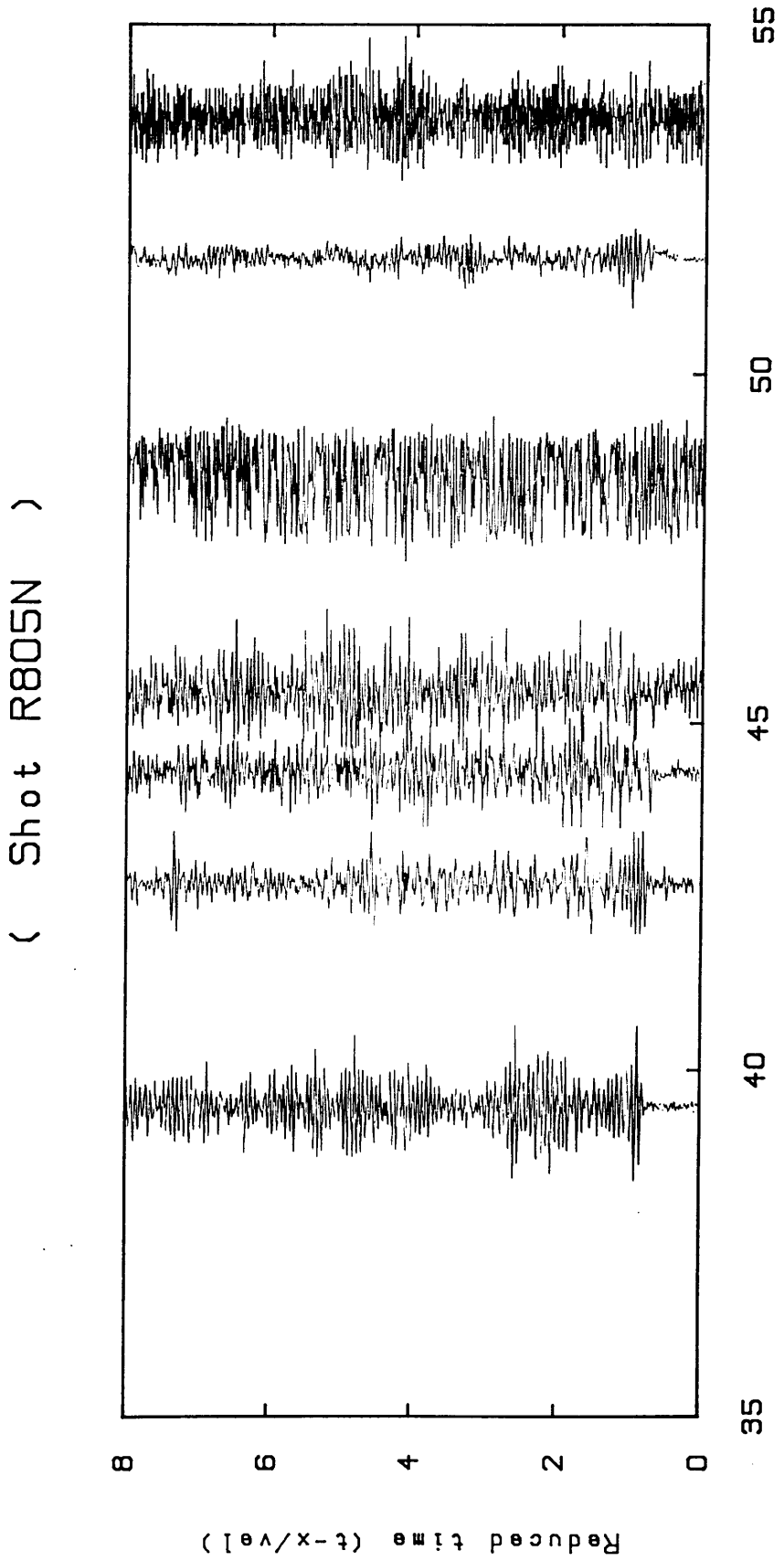


Fig.4.7b One shot seismic section, R805N.

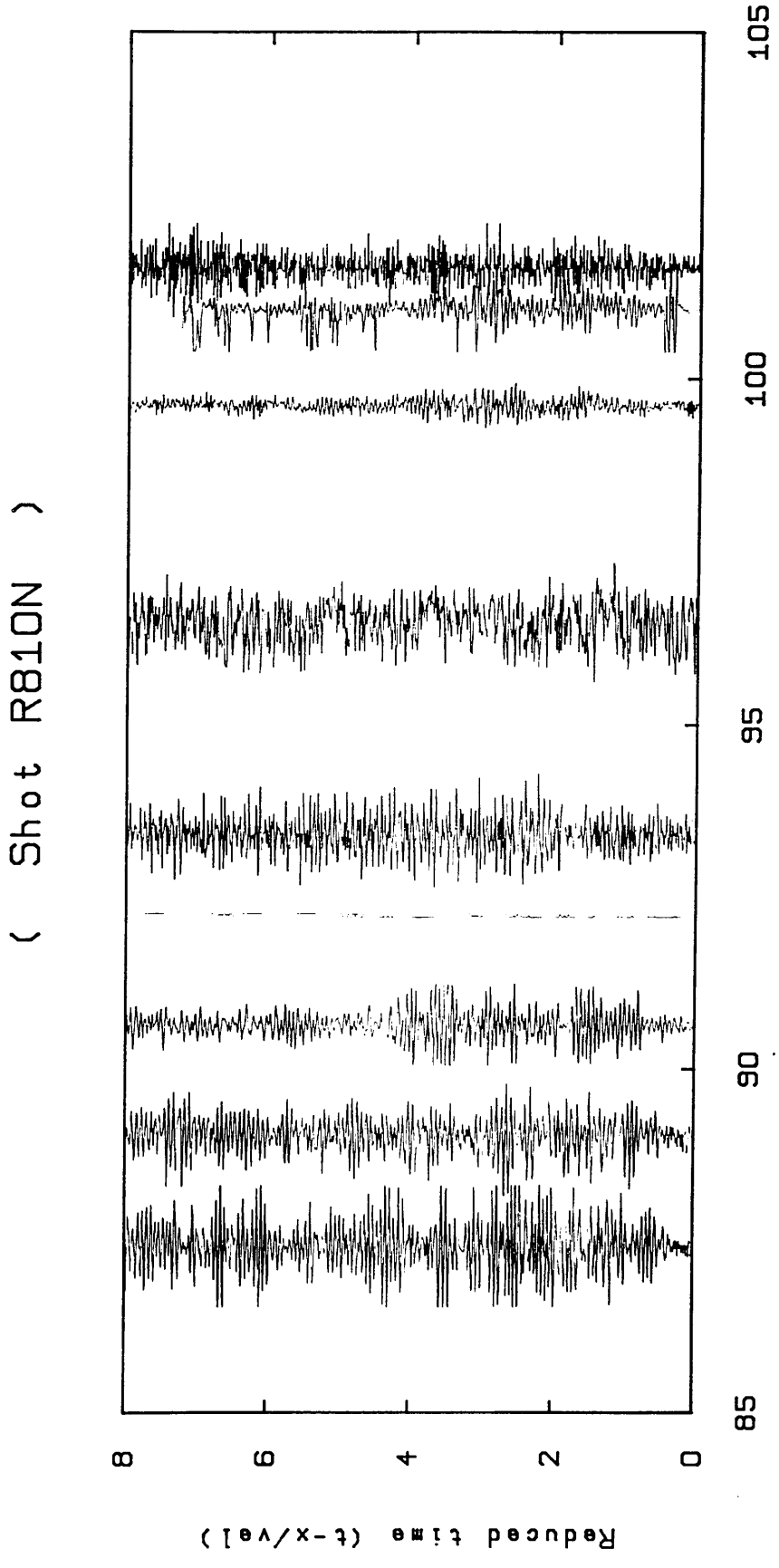


Fig.4.7c One shot seismic section, R810N.

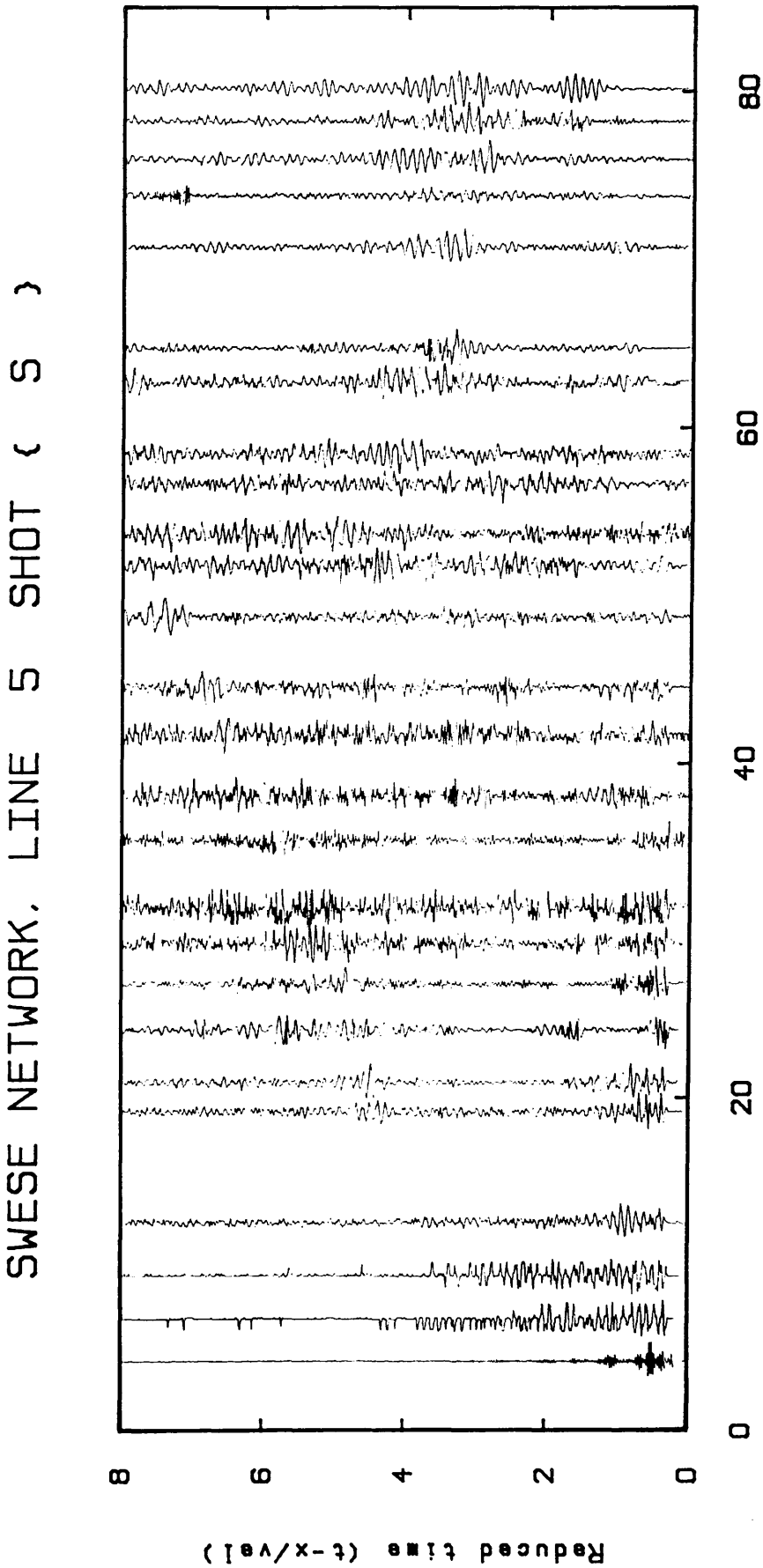


Fig.4.8a The profile of line 5, shot 5 S.

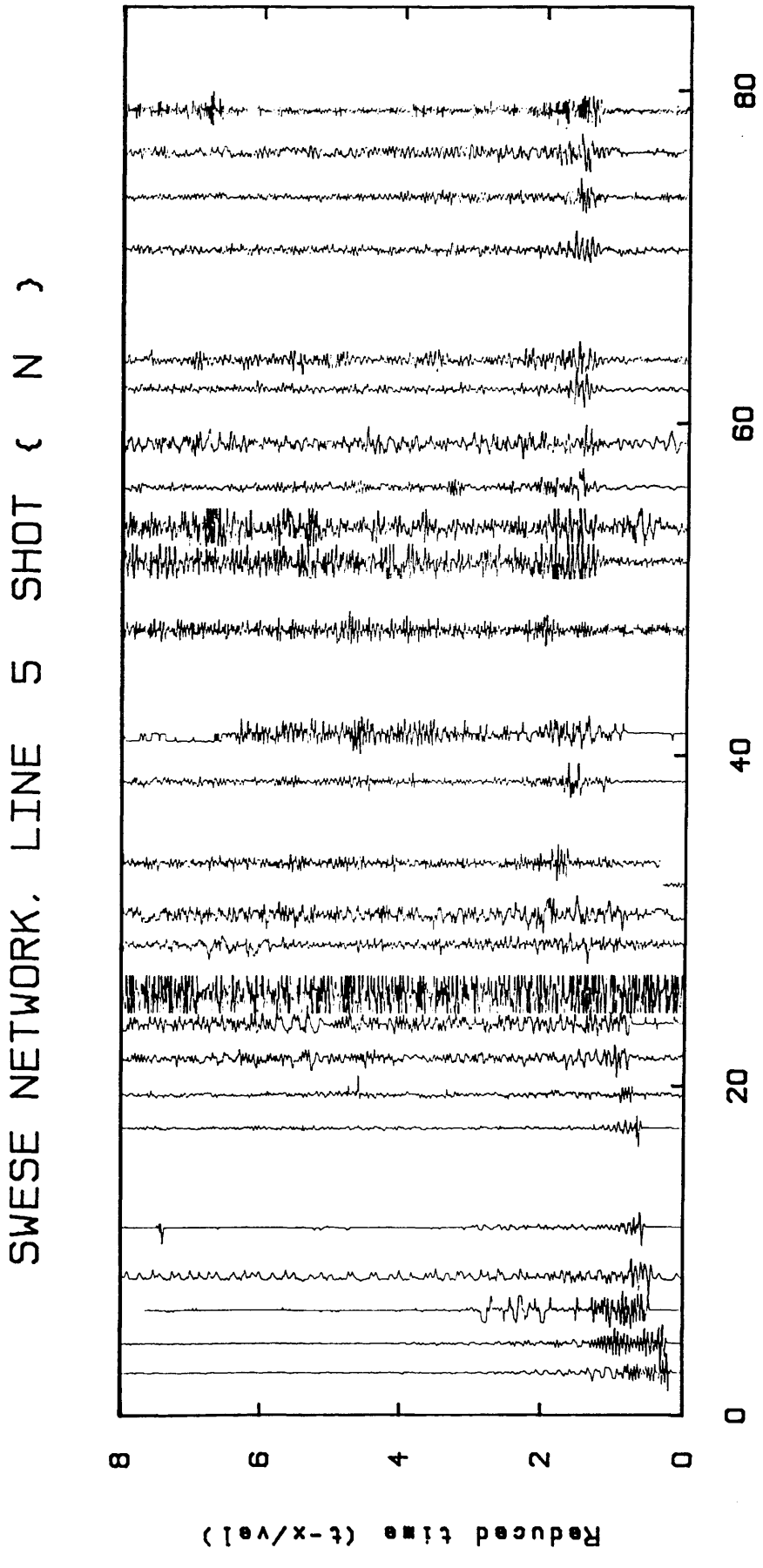


Fig.4.8b The profile of line 5, shot 5 N.

# Chapter 5

# ANALYSIS OF FIELD DATA

## 5.1. Introduction

The datasets described in the previous chapter will be analysed and interpreted in this chapter using the new software. A brief review of relevant interpretations arising from previous seismic work will be discussed.

## 5.2. Analysis of dataset A

### 5.2.1. Previous seismic analysis

Newburgh quarry is situated near to the Tay Graben, the southern boundary of which is the South Tay Fault which lies to the north of the quarry. The main exposures in the area of interest are rocks of Upper Devonian and Carboniferous age (seismic layer 1), and those of Lower Devonian and Lower Paleozoic ages which form seismic layer 2. See Davidson *et al.* (1984) and Davidson (1986). These layers are mostly sedimentary. However, there is a significant volcanic component particularly of Lower Devonian age. Trending in an E-W direction, volcanic rocks of Lower Devonian age are exposed in the area and are split by the Tay Graben into two outcrops. The southern outcrop, where these data were acquired, is called the North Fife Hills. Kamaliddin (1988) carried out a seismic survey in the region which included three profiles from Newburgh quarry in north, south and west directions, see Fig. 4.1. The quarry blasts were used as sources. Stations were spaced at intervals of approximately 1.4 km. Newburgh quarry was

recorded to the north and south by 11 stations in each direction along Kamaliddin's main profile, while a profile to the west consisted of 8 stations. Velocities obtained by this work are presented in Table 5.1. Differences between these velocities were related to the effect of anisotropy.

Kamaliddin suggested that since layer 1 is thin, or non-existent, in the region, none of his seismic data related to this layer. However he divided layer 2, locally, into upper and lower sub-layers.

Table 5.1 Velocity and thickness values obtained by Kamaliddin for regional seismic layer 2.

| Profile | Upper V 2 km/s | Lower V 2 km/s | Thickness of upper V 2 km |
|---|---|---|---|
| South | 4.81 | 5.28 | 1.62 |
| West | - | 5.38 | 0.00 |
| North | 4.70 | 5.80 | 2.20 |

### 5.2.2. Interpretation and analysis of dataset A

This dataset was collected using quarry blasts from Newburgh as sources and employing one type of recorder. The aim was to test the performance of the software in an area of simple geology. Over the distances at which this dataset was collected, it was predicted that first arrivals would be due to only the two sub-layers discussed in section 5.2.1. After examining Kamaliddin's data and considering the dominant frequency and velocities determined, it was decided that a station spacing of less than 0.5 km was needed to reduce aliasing effects. A spacing of 0.4 km was used. An initial interpretation of dataset A was carried out using the assumption of layers of uniform velocity. This simple interpretation served as a guide for comparing the results with the software results. Regression analysis was used to determine all velocity values derived from the T-X graph.

Table 5.2 Time and offsets of the first arrivals of dataset A.

| Station No. | Time sec. | Offset km/s |
|---|---|---|
| 01 | 0.365 | 1.816 |
| 02 | 0.455 | 2.220 |
| 2.5 | 0.497 | 2.482 |
| 03 | 0.535 | 2.678 |
| 04 | 0.600 | 3.112 |
| 05 | 0.685 | 3.545 |
| 09 | 1.081 | 5.098 |
| 12 | 1.315 | 6.255 |
| 13 | 1.411 | 6.650 |
| 14 | 1.500 | 6.995 |
| 15 | 1.575 | 7.415 |
| 16 | 1.585 | 7.637 |
| 17 | 1.698 | 8.100 |
| 18 | 1.773 | 8.406 |
| 19 | 1.893 | 8.853 |
| 20 | 1.990 | 9.255 |
| 21 | 2.045 | 9.770 |

Table 5.3 Time intercept and velocities derived from dataset A by regression analysis.

| Segment No. | Time intercept sec. | Velocity km/s |
|---|---|---|
| 1 | 0.01 | 5.17 |
| 2 | -0.05 | 4.58 |

Figure 5.1 shows the time-distance graph of all first arrivals extracted from this dataset (see Fig. 4.2). Two segments may be derived from the time-distance graph, corresponding to different layers, see Fig. 5.2. Table 5.2 shows the time and offset values of first arrivals and Table 5.3 shows the time intercept and velocity for each segment.

The software was executed three times each with different window length, time, and velocity ranges and steps for the first segment, recorded at stations nu01-nu09. The optimum combination of intercept time and velocity is shown in Table 5.4 and displayed in Fig. 5.3. These results were obtained employing a window length of 105 ms with small increments and ranges of time and velocity. However, other window lengths also produced results close to the best combination.

The second segment, stations nu12-nu21, was executed with different window lengths to decide the optimum for this set of stations. It was found that the best results were provided when a window length of 0.305 s employed. The highest coherency coefficient of intercept time and velocity are listed in Table 5.4 and displayed in Fig. 5.4. A second intensive area of contour lines occurred at an intercept time of 0.01 s and velocity 4.08 km/s, which does not fit well with the field data.

Table 5.4 Time intercept and velocities obtained from the software

| Segment No. | Time intercept sec. | Velocity km/s |
|---|---|---|
| 1 | 0.02 | 5.2 |
| 2 | -0.01 | 4.55 |

Velocity values obtained for both segments by regression analysis and the new software are well matched. Moreover, the first velocity segment matches with the value obtained from the Newburgh West profile of Kamaliddin (1988), see Tables 5.1, 5.3, and 5.4. It appears that the Lower Devonian volcanics (which retain higher velocities near surface) beneath the Newburgh West profile continue and thin towards the east, being too thin to resolve on the scale of this experiment from approximately 5 km east of Newburgh quarry. Beyond that distance typical upper layer 2 velocity values are seen, suggesting a dominantly sedimentary sequence. No first arrivals were obtained from the bulk of seismic layer 2, i. e. from Kamaliddin's lower sub-layer.

The results obtained by the analysis of P-wave guided the search for S-wave arrivals. This was undertaken by executing the software many times, treating each segment separately. The best results are displayed in Fig. 5.5. Second arrivals for the first segment showed that the best combination was at time 0.805 s and velocity 2.12 km/s. The best coherency coefficient for the second arrivals of the second segment was given at a time of 0.62 s and velocity 2.16 km/s. Poisson's ratio of the first segment is 0.203 and for the second segment is 0.374. Both values were out of the range of expected Possion's ratio and the time intercepts for the shear wave segments are rather later than would be expected given the corresponding P-wave segments. The above arguments suggest that the second arrivals (shear waves) could be better related to other refractors.

Results listed in Tables 5.3 and 5.4 indicate that implementation of the software, for such data, could confirm the results derived from the data using other methods in interpreting that data.

The variation of the optimum window length for the segments, 105 ms for the first and 305 ms for the second, highlighted the importance of the window length. This is because, as Fig. 4.3 shows, most traces involved in segment 2 have a wide range of frequencies, while those of segment 1 have a clear dominant frequency.

## 5.3. Analysis of dataset B

### 5.3.1. Previous analysis of line 5

Line 5 crossed, from south to north, Devonian sediments, the Bodmin Moor granite outcrop and Carboniferous sediments of the Culm Synclinorium. Interpretations of shot 5S and 5N provided by Doody (1985) are presented in Figs. 5.6a and 5.6b respectively. The final ray-tracing model produced for the line is displayed in Fig. 5.7.

Velocities used in modelling the upper crust below this line were little different to the observed values. However, velocities of 6.4 km/s and over 8.0 km/s had to be assumed for the lower crust and upper mantle respectively.

Arrivals were usually modelled to within +/- 0.05 s for headwave arrivals, and +/- 0.10 s for reflected events from deeper crust and mantle. For a velocity given distribution, refractors were probably located to a depth accuracy of a few hundred metres, and reflectors to within about a kilometre (Doody, 1985).

### 5.3.2. Interpretation and analysis of line 5

It was desired to test the software on data recorded in a complex geological area. For this reason, the SWESE dataset (see chapter 4) was chosen since it was recorded where a large granite intrudes, and so disrupts, the regional crustal layers.

This line was recorded with large spacing and offsets. All types of arrivals were used to test the software.

Many runs were made with different sets of traces and processing parameters (time and velocity ranges, increments, and window length) to extract the best results, mostly guided by the previous interpretation.

[1] Shot 5S :

Looking for direct events, the first three traces (r502-r504) were used. The best result, of intercept time 0.02 s and velocity 5.3 km/s, was obtained employing a window length of 110 ms with small time and velocity steps of 10 ms and 0.01 km/s respectively, see Fig. 5.8. Adding on trace r505 to the above set of traces changed the result entirely and the maximum coherency coefficient value dropped down significantly, indicating that that trace does not fit with the direct segment.

Using two traces (r507 & r501) to detect the interpreted headwave of time intercept 0.31 s and velocity 6.25 km/s, see Fig. 5.6, gave unrealistic results, probably because only two traces were involved in the process.

Detecting for the headwave segment of time intercept 0.01 +/- 0.14 s and velocity 5.86 +/- 0.17 km/s a set of four traces (r508A - r511) was used with range of time 0.0 - 0.4 s and velocity range 5.4 - 6.4 km/s. The best result, which was at time 0.29 s and velocity 5.94 km/s, was provided employing a window length of 310 ms, see Fig. 5.9. By adding one trace (r512) to the above set, the result was shifted dramatically and the maximum coherency coefficient dropped down significantly which indicates that trace r512 is not a part of this segment.

Employing various processing parameters and combinations of traces the software failed to detect the segment which was interpreted as a headwave for the next seven traces (r512 - r519) with a time intercept 0.17 s and velocity 6.00 km/s. Two reasons could be considered for this failure. Either the event was scattered, or there was a reverse polarity trace (or traces) within that set.

A set of five traces (r527 - r531) was used in detecting reflected events. The best results, which displayed a high coherency coefficient and fit the data, are shown in Fig. 5.10 and 5.11. The first event was at an intercept time of 5.93 s and velocity 6.03 km/s, giving a depth of 17.88 km assuming a horizontal reflector and uniform overburden. The ranges of time and velocity used were 5.0 - 7.0 s and 6.0 - 7.0 km/s respectively. Combination of time and velocity for the second event was 9.85 s and 6.42 km/s, which gives a depth of 31.62 km.

Executing the software to analyse shear waves showed that the best result was at time 0.88 s and velocity 3.12 km/s for the set of four traces r508A-r511, see Fig. 5.12. Moreover, adding trace r512 to the set the result did not fit the data and the value of the maximum coherency coefficient was degraded.

[2] Shot 5N :

To start with the tests for this shot the first three traces (r531 - r529) were used to detect the direct arrival, guided by the available interpretation. The result was enhanced by adding a fourth trace, r528, to the set and the highest coherency coefficient was at an intercept time 0.11 s and velocity 5.07 km/s, employing a window length of 210 ms (Fig. 5.13). Detecting for the second segment a set of four traces (r528 - r524) was used. The results, displayed in Fig. 5.14, showed that the maximum coherency coefficient was at time 0.21 s and velocity 5.44 km/s, employing a window length of 210 ms. This is earlier than the first arrivals but the arrivals are within the limits of the window length. A second area of high coherency coefficient contour lines was displayed at time 0.36 s and velocity 5.71 km/s, which did not fit the data. The software failed to detect the third segment (r523 - r518) which was interpreted as a headwave of time intercept 0.39 s and velocity 5.61 km/s, see previous section for reasons for that failure.

Detecting for reflected events the software was executed, as in all other cases, with different sets of traces, time velocities, and ranges. Results for the set of four traces (r518 - r514) showed a high density of contour lines at two

combinations of time and velocity, Fig. 5.15. The first at an intercept time of 4.15 s and velocity 5.3 km/s and the second at an intercept time of 4.36 s and velocity 5.97 km/s. The second combination of time and velocity fits the data better, and so is considered to be more likely than the first.

The final dataset consisted of five traces (r507-r502). It was tested for refraction, which did not give reasonable results, and reflection. The results of reflection tests are displayed in Fig. 5.16. The maximum coherency coefficient was at an intercept time of 4.09 s and velocity 5.72 km/s. Adding trace r501 to the above set the coherency coefficient value was increased and gave a similar combination of intercept time 3.95 s and velocity 5.70 km/s, see Fig. 5.17.

Results of both shots, 5S and 5N, and previous interpretation were combined together and displayed in Fig. 5.18. Although the software failed to detect one of the main headwave events, at intercept time 0.17 s and velocity 6.00 km/s, when comparing the results, old and new, it is obvious that there is some consistency between them.

Direct arrivals of shots 5S and 5N, in the new interpretation, have a good resemblance with the previous model. The match is also acceptable for the headwaves. Reflectors 5 and 8 of Fig. 5.18 occur at depths similar to reflector R2 of the original SWESE interpretation. These reflectors may simply be new estimates of interface R2, or they may indicate that R2 is better described as a reflective zone, rather than a single interface.

### 5.3.3. Previous analysis of lines 8 and 9

The interpretation of the Lizard-Start line produced by Doody (1985) made good use of the huge amount of seismic data provided by SWESE project. In the present work only three (typical) shots (801N, 805N, and 810N), which were described in chapter 4, will be analysed to compare the observed (interpreted) velocity values with the values extracted by the software. Interpretations of the

three shots mentioned above, for lines 8 and 9, are shown in Fig. 5.19 and 5.20, respectively. A model for the Lizard-Start line derived by ray-tracing is displayed in Fig. 5.21.

### 5.3.4. Interpretation and analysis of line 8 and 9

Along Line 8 and 9 several velocity segments were interpreted although each segment was represented by only a small number of traces.

[1] Shot 801N :

Using the closest two stations only (r806 & r805) the maximum coherency coefficient was at time 0.26 s and velocity 5.65 km/s. Increasing the number of traces to three, adding trace r804, the maximum coefficient was at time 0.27 s and velocity 5.72 km/s, see Fig. 5.22. A set of three traces (r804, r803 and r802) was executed to detect for headwave events. Results are displayed in Fig. 5.23 which shows a high coherency coefficient at time 0.21 s and velocity 6.35 km/s. The first arrivals of four traces (r806, r805, r808, and r809) were interpreted as a direct-wave with time intercept 0.05 s and velocity 5.44 km/s, but the results did not fit the data.

Results for line 9 analysis using three traces (r902, 904, and 905), displayed in Fig. 5.24, showed that the maximum coherency coefficient was at time intercept of -0.09 s and velocity 4.95 km/s, which fits the first arrivals of the direct waves in the previous work. This segment was interpreted as a direct wave the velocity being similar to the 5.14 km/s determined, in the previous work, Fig. 5.20a.

[2] Shot 805N :

The first two traces (r806-r805) were used in an attempt to extract the the event interpreted as a headwave with velocity of 6.2 km/s, see Fig 5.19b. The result shows that an area of intensive contour lines was at intercept time of 0.28 s and velocity 5.43 km/s, Fig. 5.25. By adding trace r804 to the set the highest coherency coefficient was at time intercept 0.28 s and velocity 5.43 km/s. When a

fourth trace was added to the set of traces the maximum coherency coefficient was at time intercept of 0.21 and velocity 5.43 km/s, Fig. 5.26. In all tests mentioned above a window length of 210 ms was employed. The trajectory passes obliquely through the maximum amplitude trend of the first arrivals. A fifth trace was included in a further test employing the same processing parameters, this resulted in different combination of time and velocity for the maximum coherency coefficient. This did not fit the data and, moreover, the coherency coefficient value dropped significantly. These tests may suggest that the first four traces(r806-r803) are one segment, not two segments as they were interpreted in the previous interpretation, and traces r802 onwards are not a part of that segment. No high coefficients were found at intercept times and velocities consistent with the original interpretation of these data.

Previous interpretation of line 9 suggested that a headwave event with time intercept and velocity 6.16 km/s occurs across the two traces (Fig. 5.20b). The software could not detect any significant results.

[3] Shot 810N

The first headwave event was interpreted with velocity of 6.27 km/s, on the first two traces only, Fig. 5.19c. Results of executing the software for these two traces, and also by adding another trace (r804), gave an unrealistic combination of time and velocity. In the previous interpretation of the data of this shot a Moho reflector (R3) was highlighted across all the traces. The software extracted a strong reflector at time intercept of 5.36 s and velocity 6.02 km/s, giving a depth of only 16.13 km, Fig. 5.27. A second coherent energy was detected at a time intercept of 8.01 s, a velocity of 5.30, and depth of 21.23 km. This energy could be interpreted as representing a low-velocity layer although it is most unlikely that such a layer could be found at such depth, Fig. 5.28. All traces, except r803, Fig. 5.19c. were used in looking for reflectors.

Only two traces were available on line 9 for this shot, for which the software failed to display reliable results.

Applying the software to SWESE lines 8 and 9 gave good matches, mostly, on velocity segments with 3 traces and more when applied to segments. With three or less traces the results were not matched because of the possibility of the presence of coherent noise which produce a higher coherency coefficient. Moreover, applying the software on such few traces cannot be undertaken with a great deal of confidence or reliability in the results.

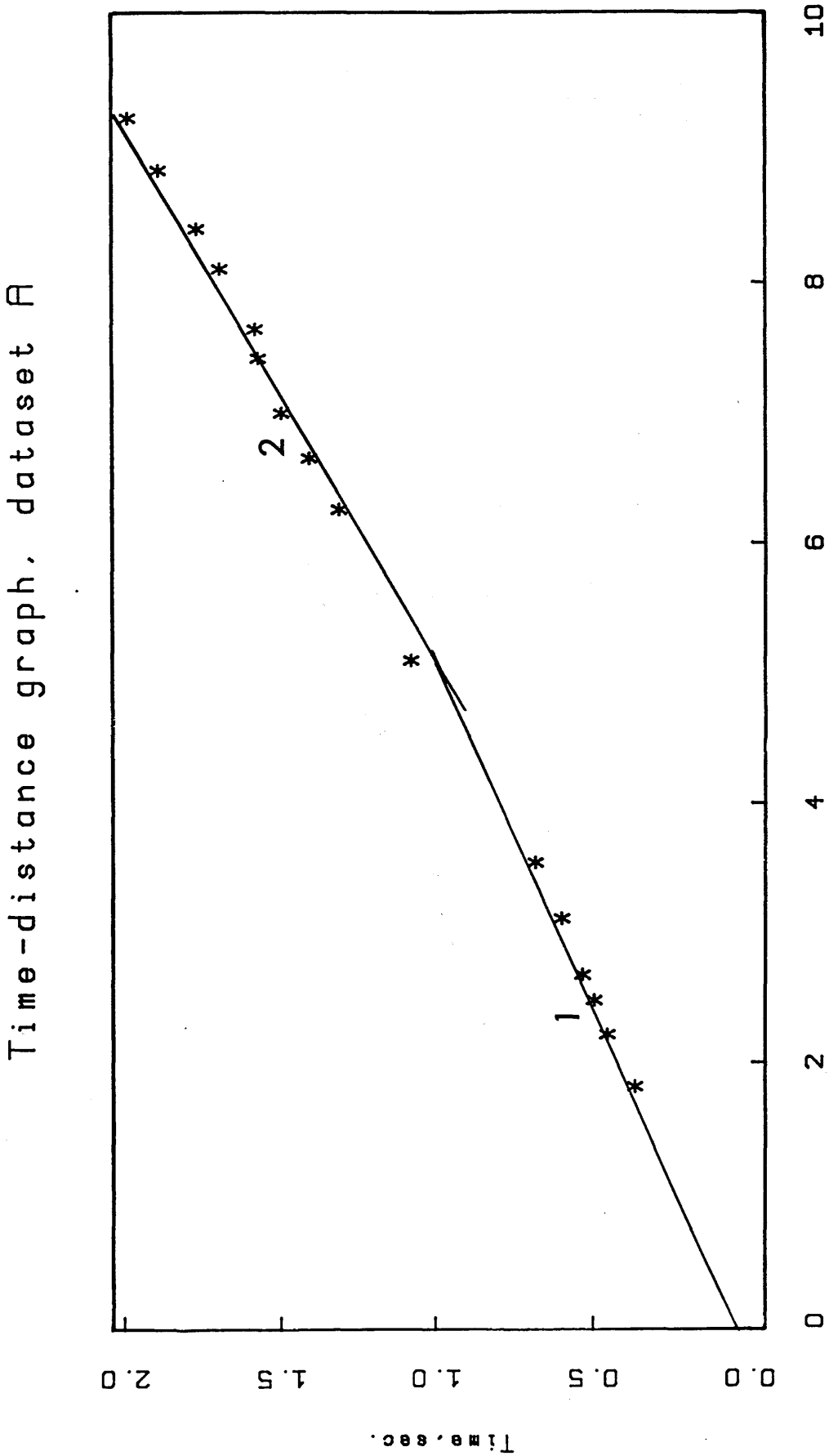


Fig.5.1 Time-distance graph for first arrivals of dataset A.

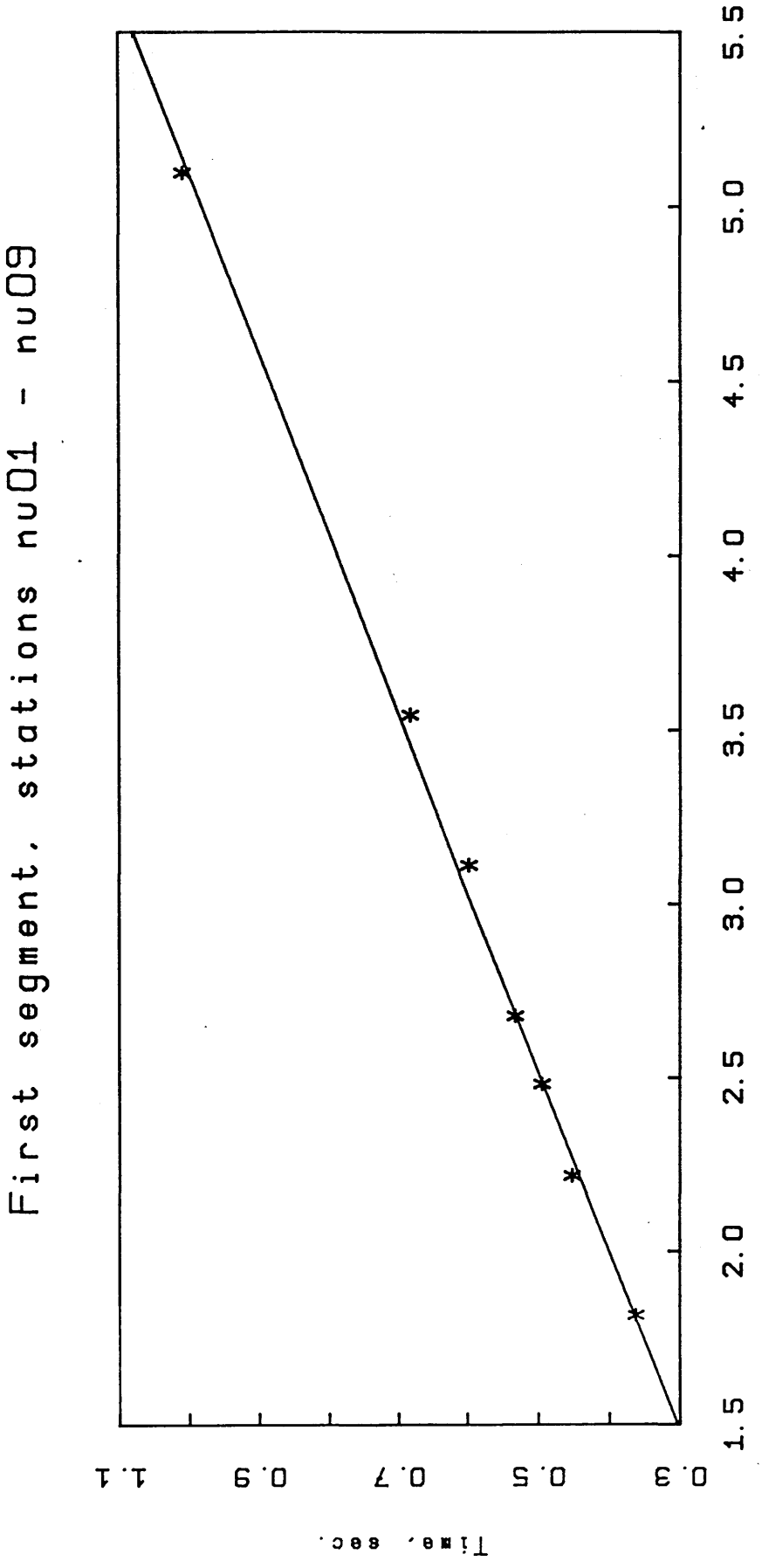


Fig.5.2a. Regression analysis for segment 1 of dataset A.

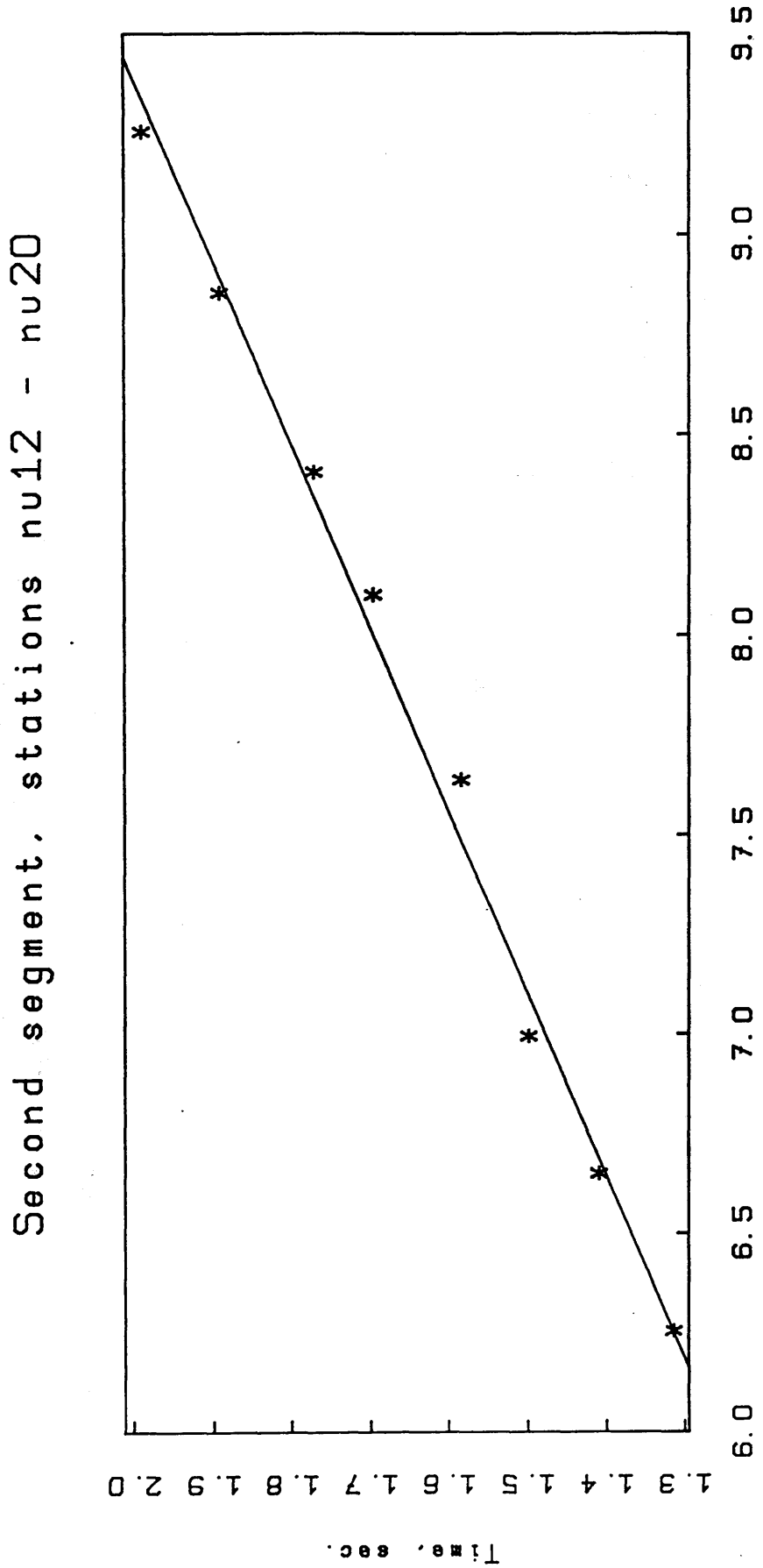


Fig.5.2b. Regression analysis for segment 2 of dataset A.

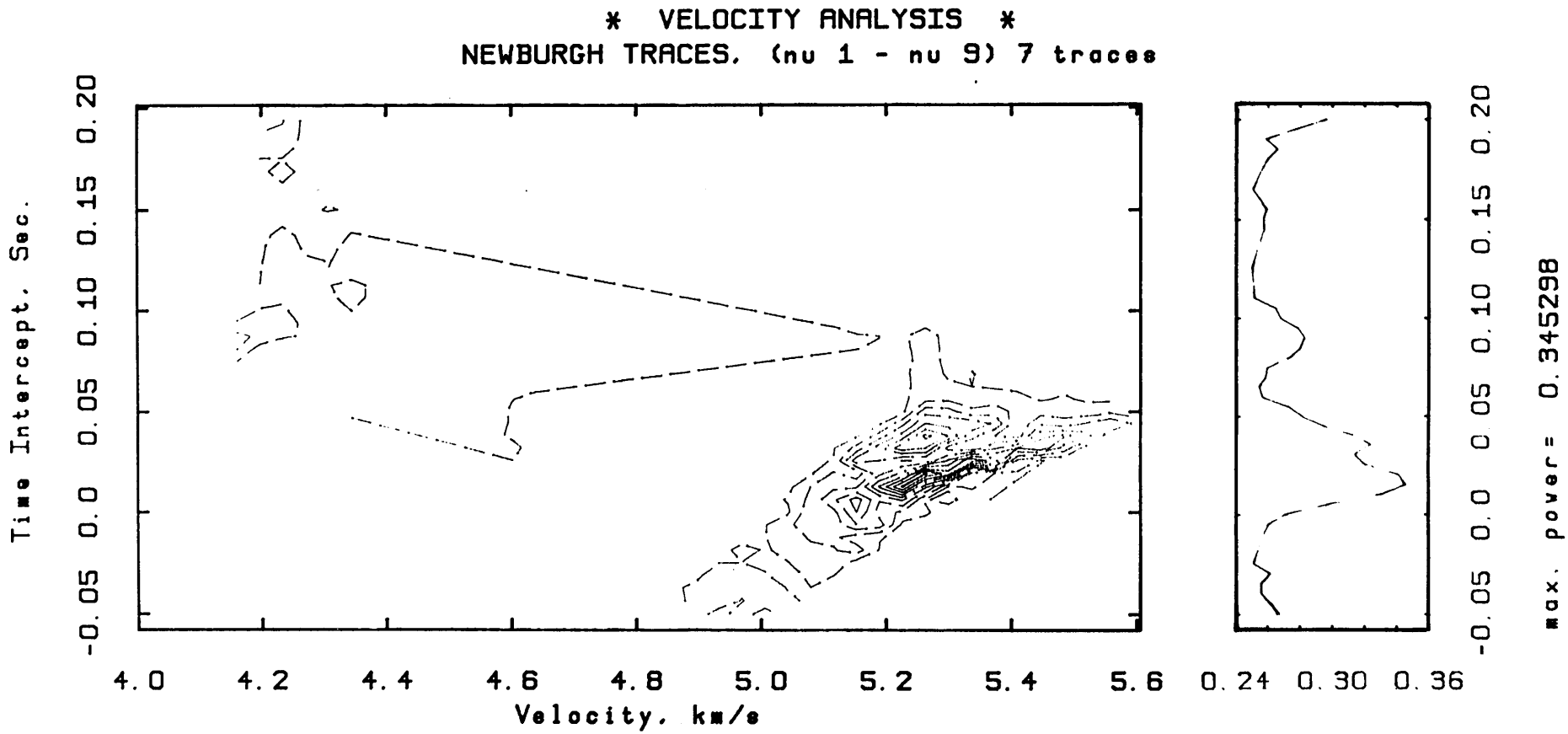


SEMB. METHOD FOR REFR. DATA
WINDOW (LENGTH. STEP)= 105. 5 MSEC.
VELOCITY STEP = 0.010 KM/S
CONTOUR (MIN.MAX.INT)= 0.25 0.33 0.01

WINDOW
PEAKS LOG

Fig.5.3 Results of applying the software to stations nu1-nu9 (segment 1) of dataset A showing the maximum coherency coefficient at a time intercept of 0.02 s and velocity 5.24 km/s.

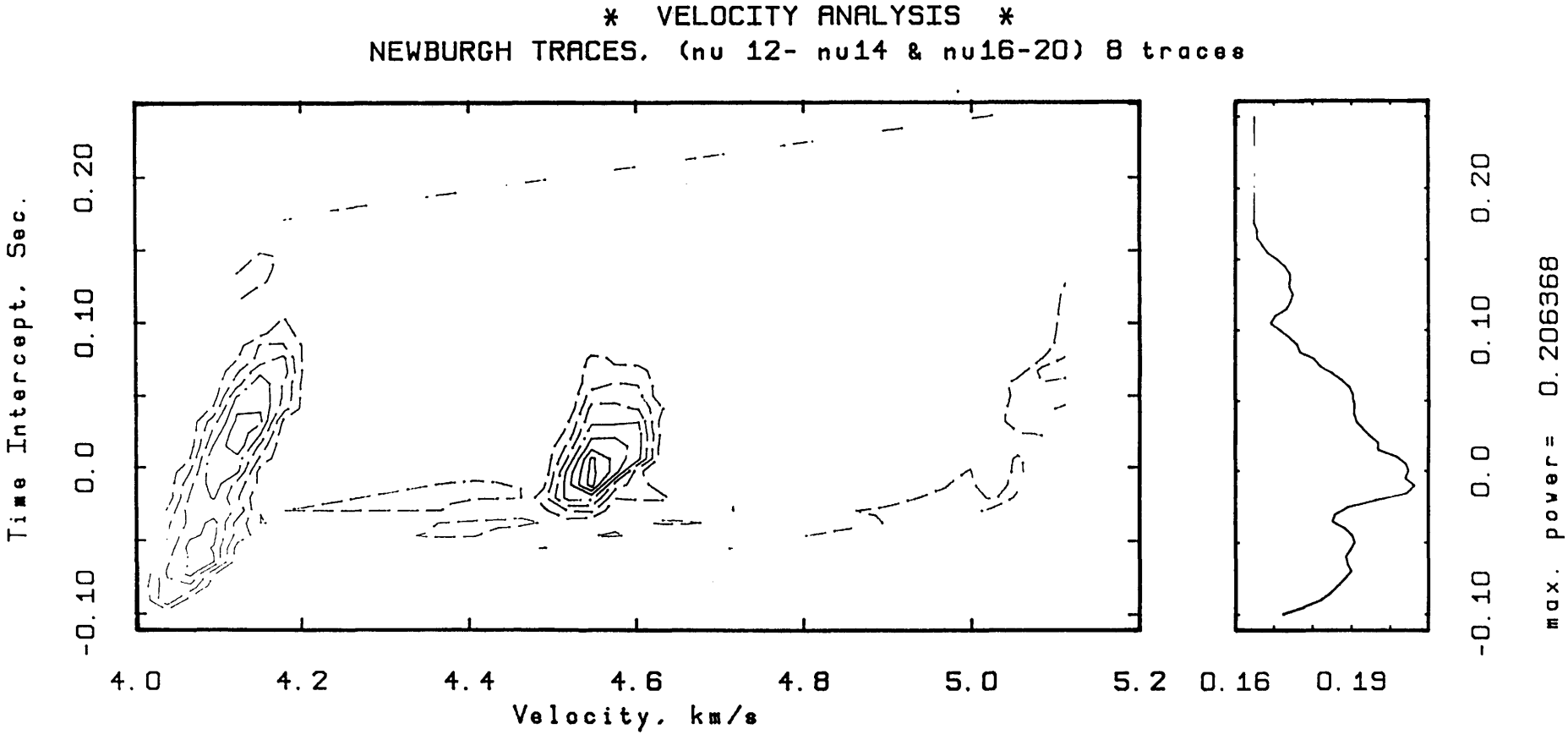


Fig.5.4 Results of applying the software to stations nu12-nu20 (segment 2), except nu15, of dataset A showing the maximum coherency coefficient at a time intercept of -0.01 s and velocity 4.55 km/s.

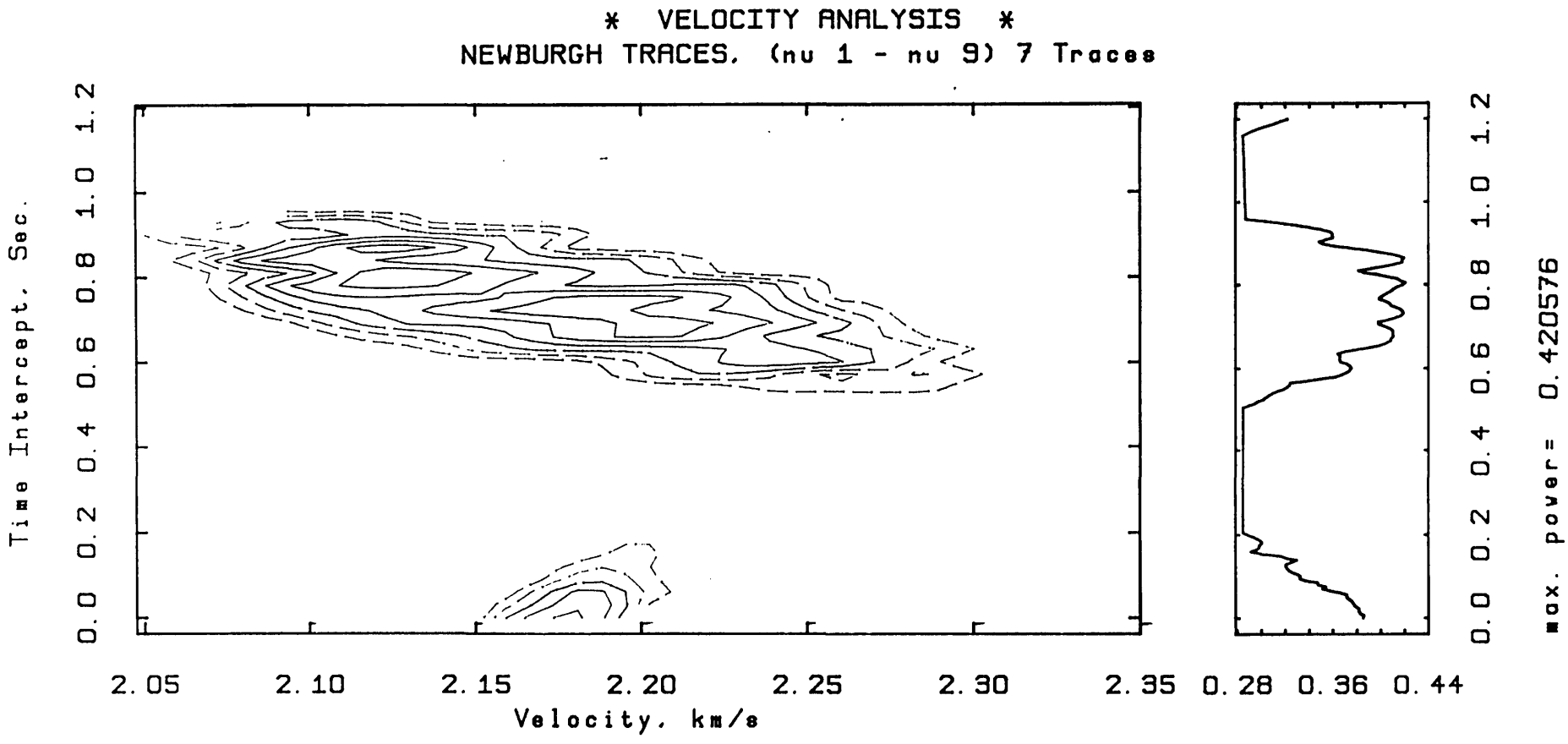


Fig.5.5a Results of applying the software to stations nu1-nu9 (segment 1) of dataset A, searching for S-wave arrivals, showing the maximum coherency coefficient at time intercept of 0.81 s and velocity 2.12 km/s.

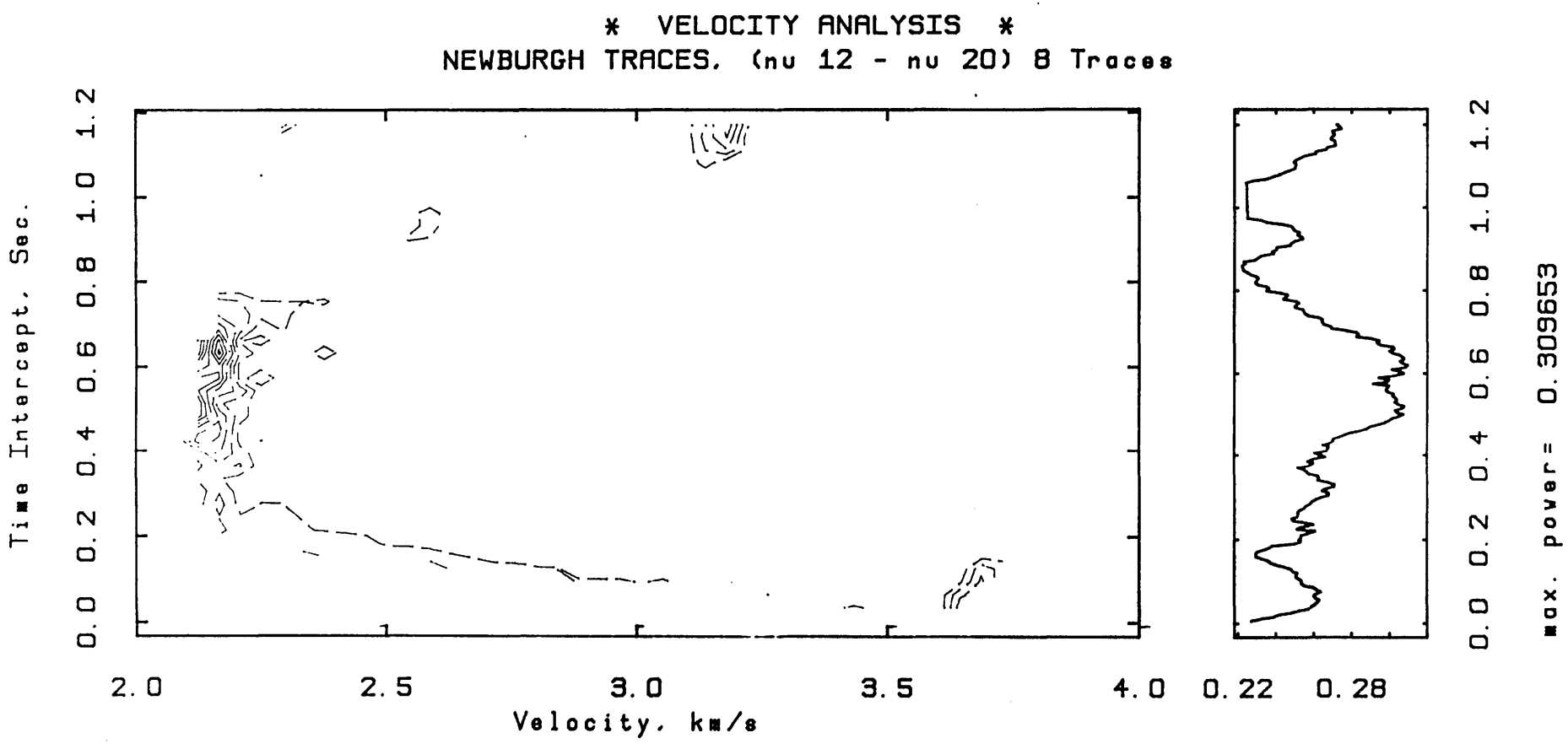


Fig.5.5b Results of applying the software to stations nu12-nu20 (segment 2) of dataset A, except nu15 searching for S-waves arrivals, showing the maximum coherency coefficient at time intercept of 0.62 s and velocity 2.16 km/s.

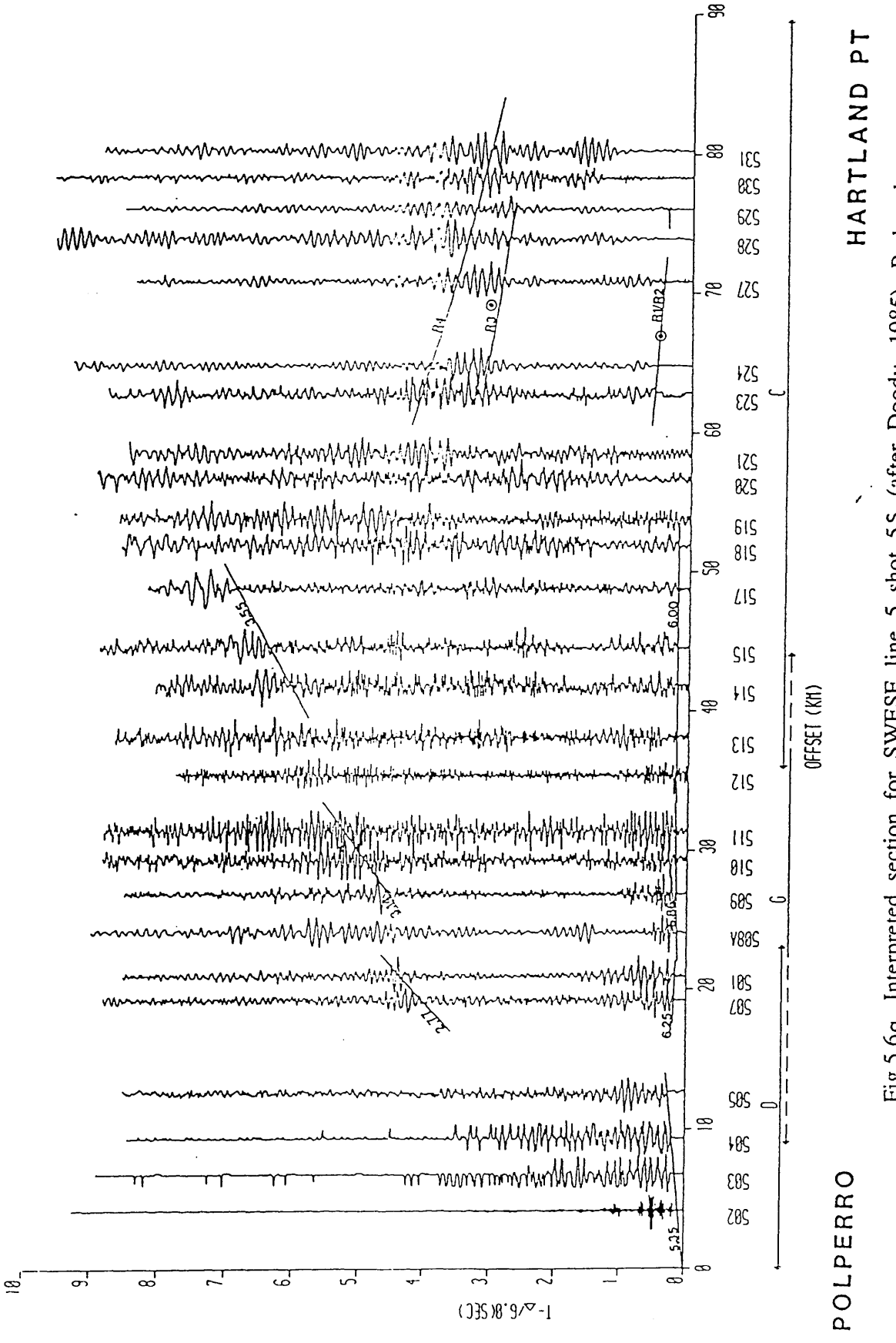


Fig.5.6a Interpreted section for SWESE line 5 shot 5S (after Doody, 1985). Reduced velocity = 6.0 km/s.

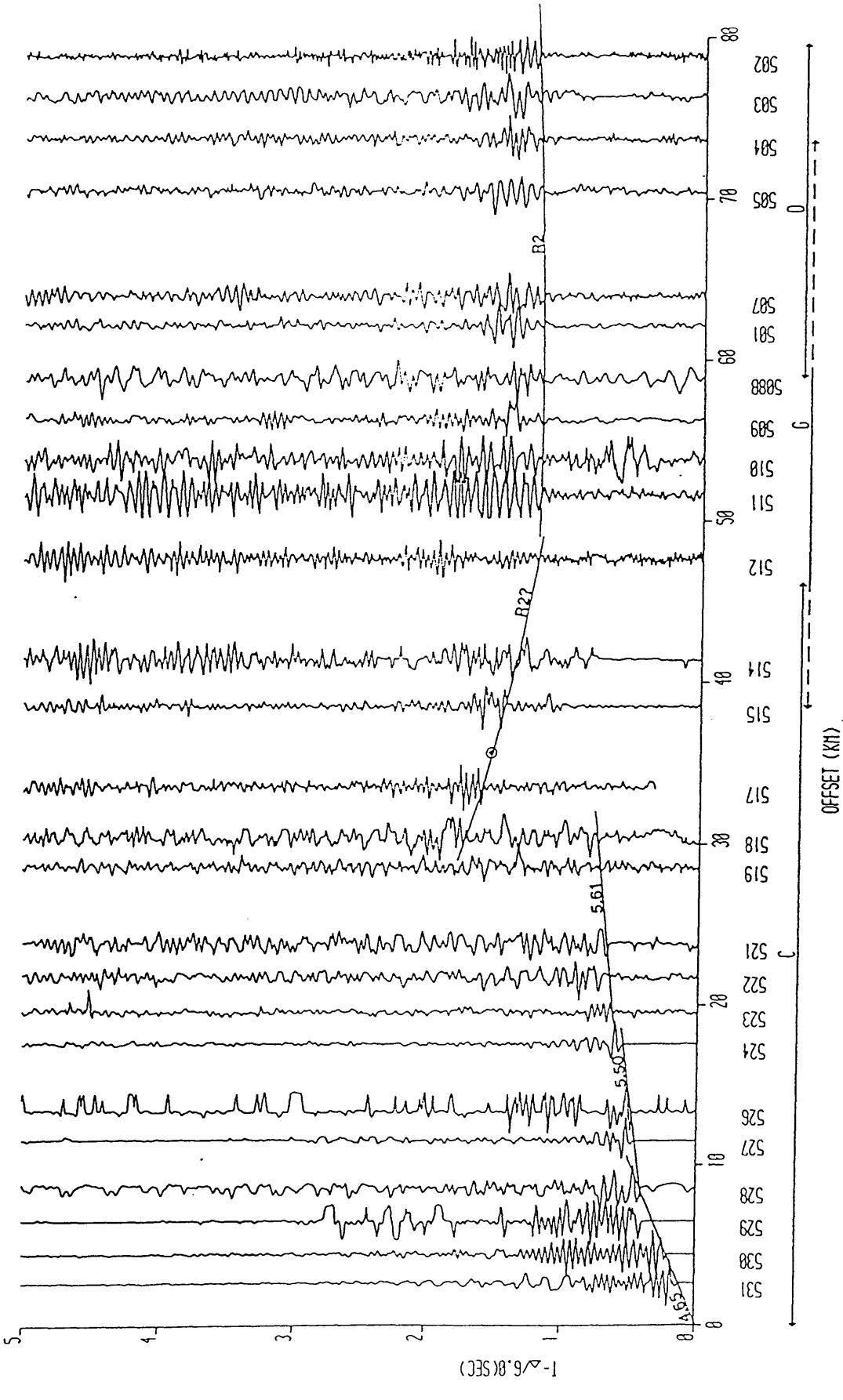


Fig.5.6b Interpreted section for SWESE line 5 shot 5N (after Doody, 1985). Reduced velocity = 6.0 km/s.

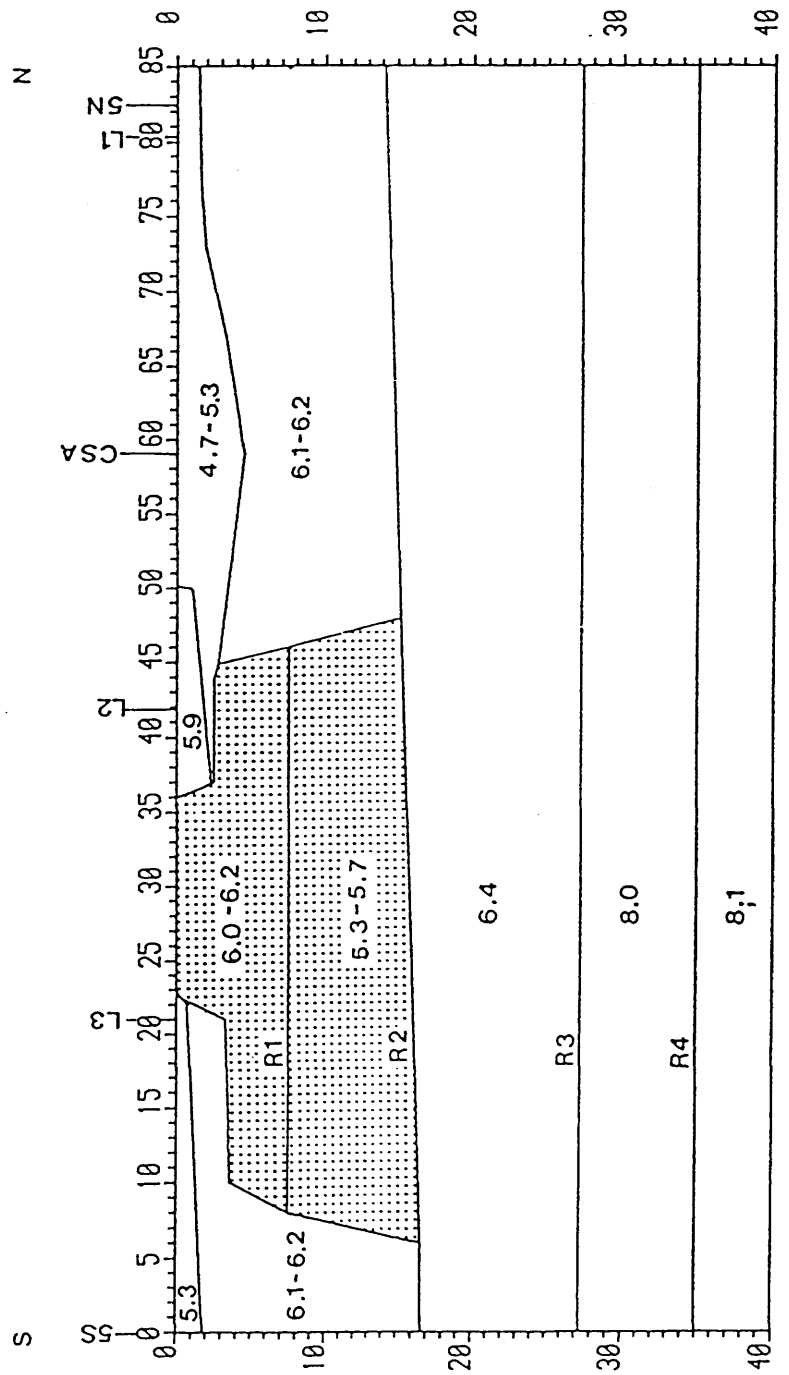


Fig.5.7 Final model of SWESE derived from raytracing (after Doody, 1985).

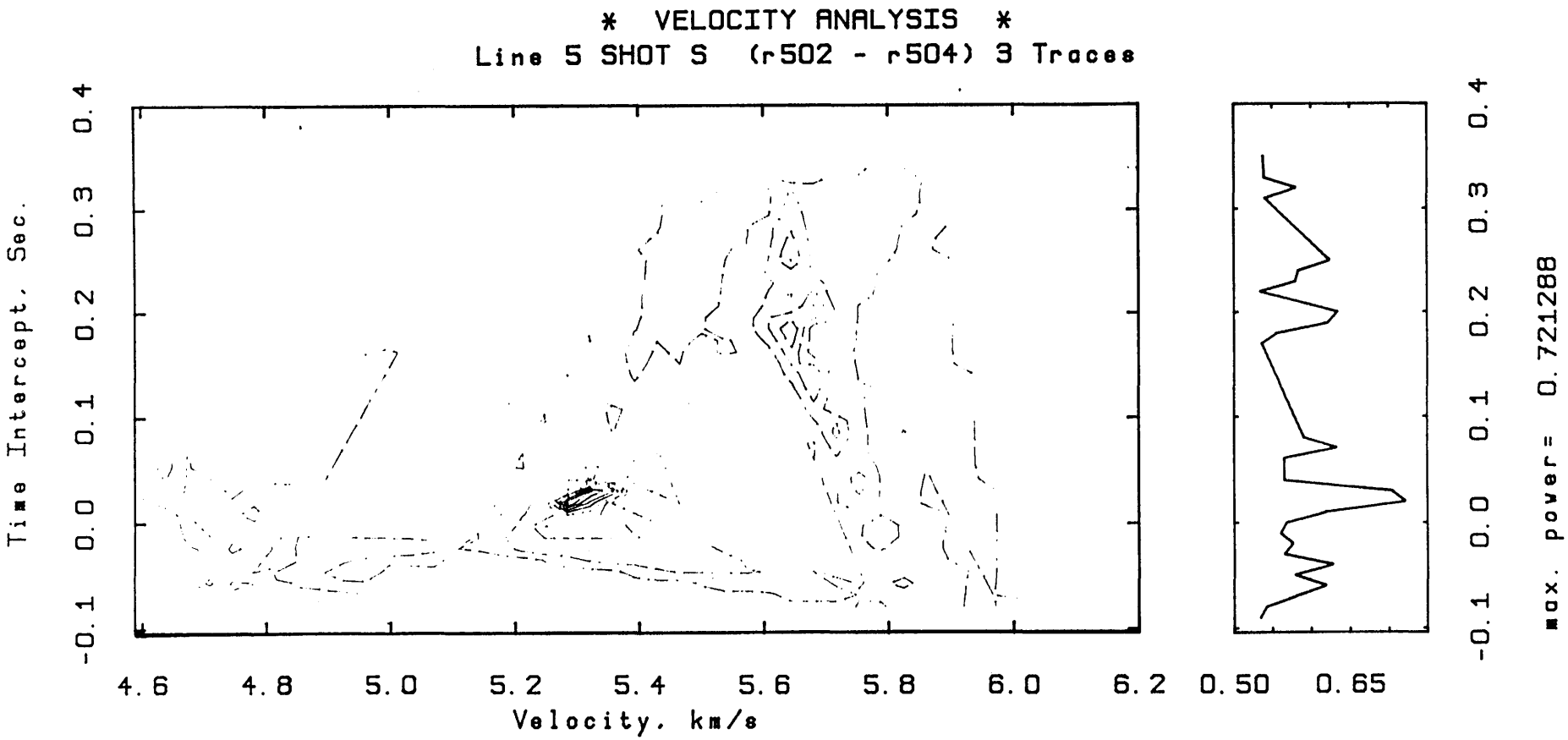


Fig.5.8 Results of applying the software to stations r502-r504 of Fig. 5.6a showing the maximum coherency coefficient at time intercept of 0.02 s and velocity 5.30 km/s.

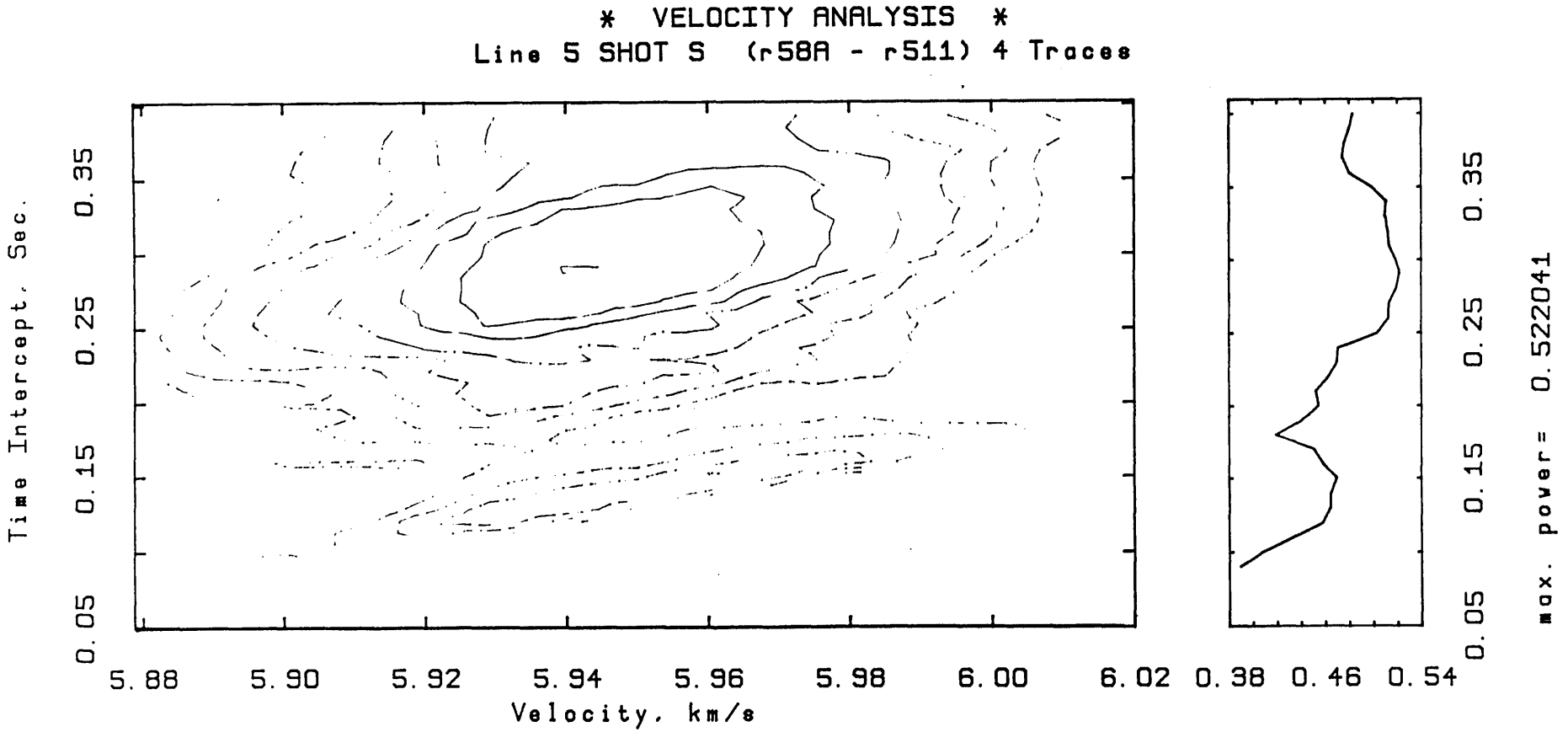


Fig.5.9 Results of applying the software to stations r508A-r511, of Fig 5.6a showing the maximum coherency coefficient at time intercept of 0.29 s and velocity 5.94 km/s. Time range 0.0-0.4 s and velocity range employed 5.4-6.4 km/s.

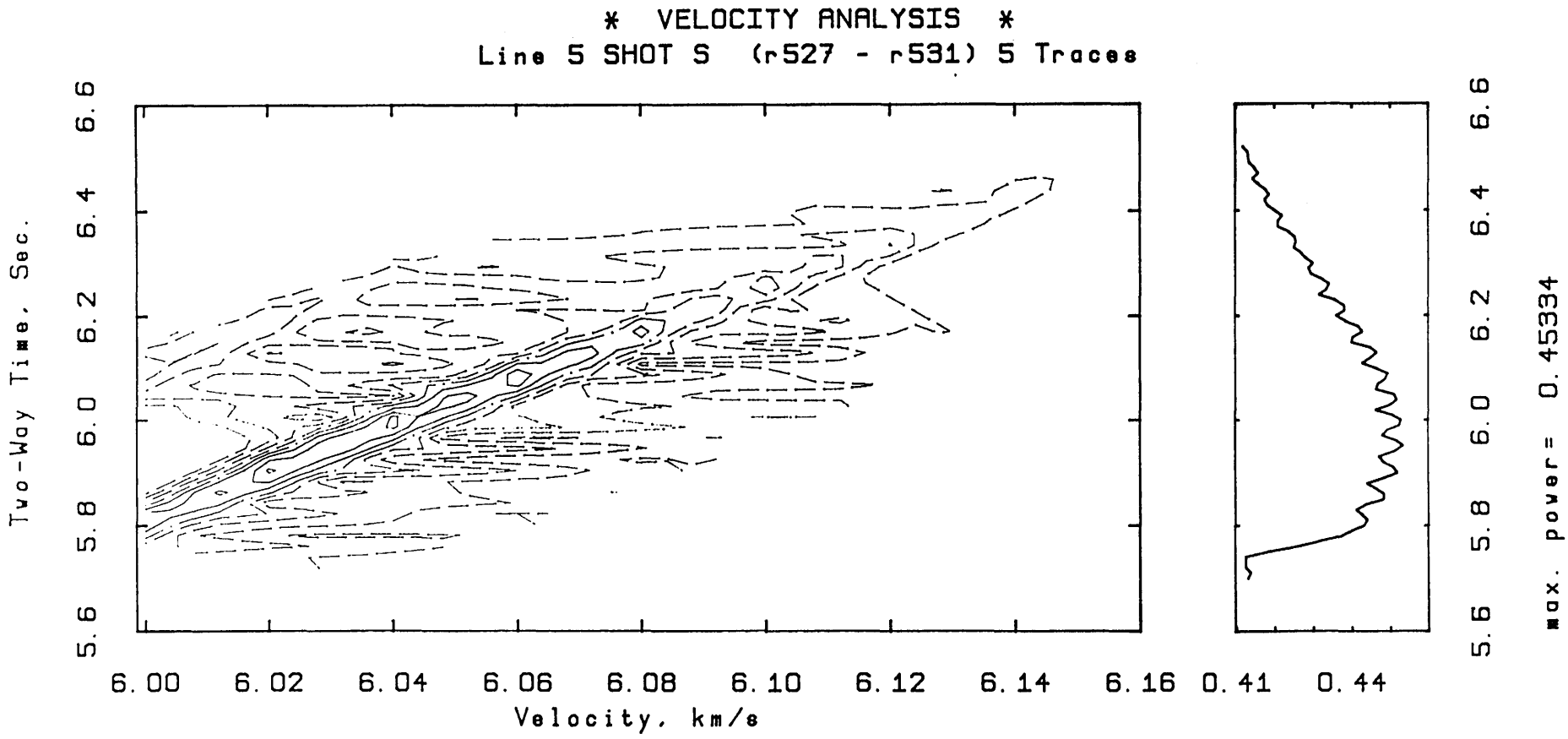


Fig.5.10 Results of applying the software to stations r527-r531, of Fig 5.6a showing the maximum coherency coefficient at time intercept of 5.95 s and velocity 6.03 km/s. Time range executed 5.0-7.0 s and velocity range employed 5.4-6.4 km/s.

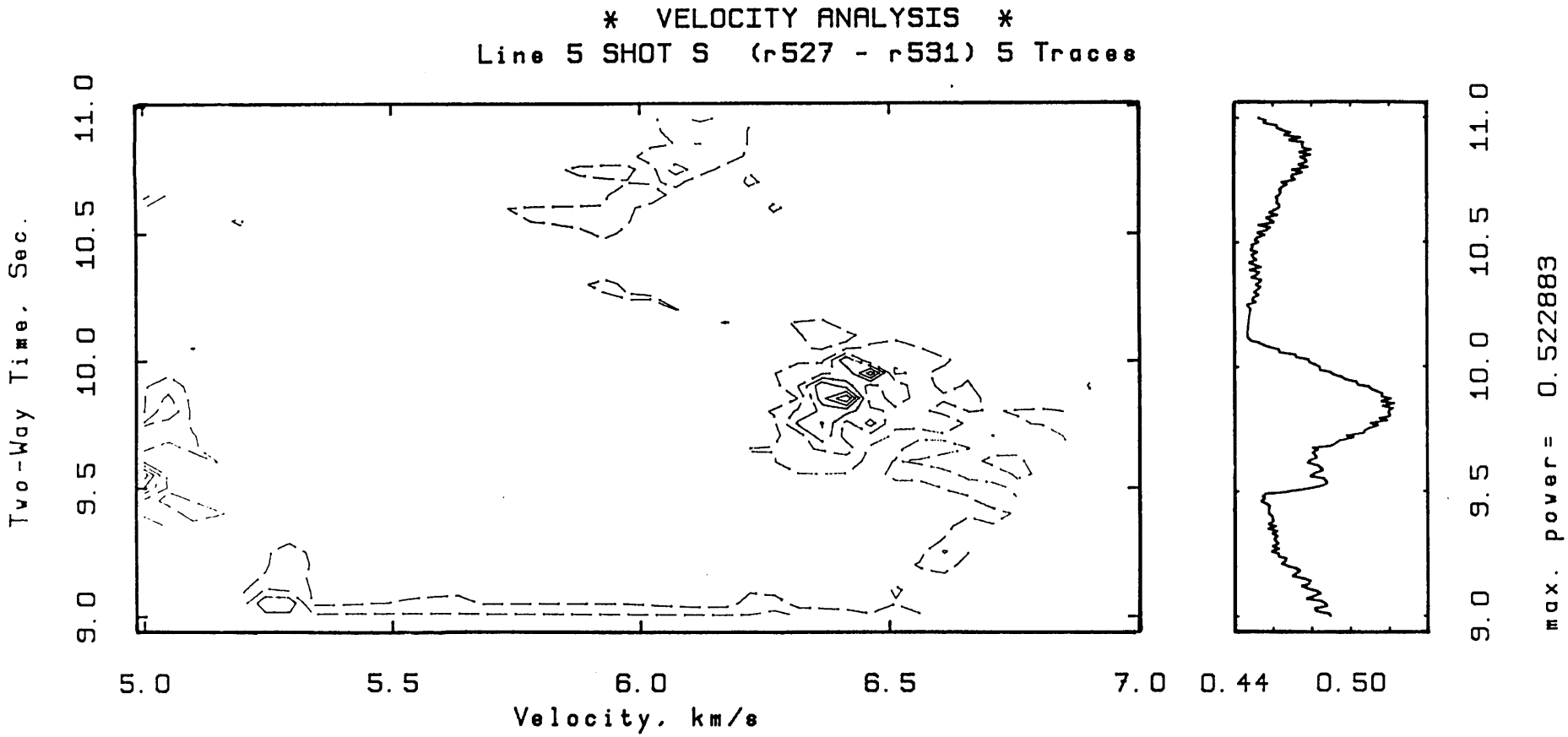


Fig.5.11 Results of applying the software to stations r527-r531 of Fig 5.6a showing the maximum coherency coefficient at time intercept of 9.85 s and velocity 6.42 km/s. Time range executed 9.0-11.0 s and velocity range employed 5.4-6.4 km/s.

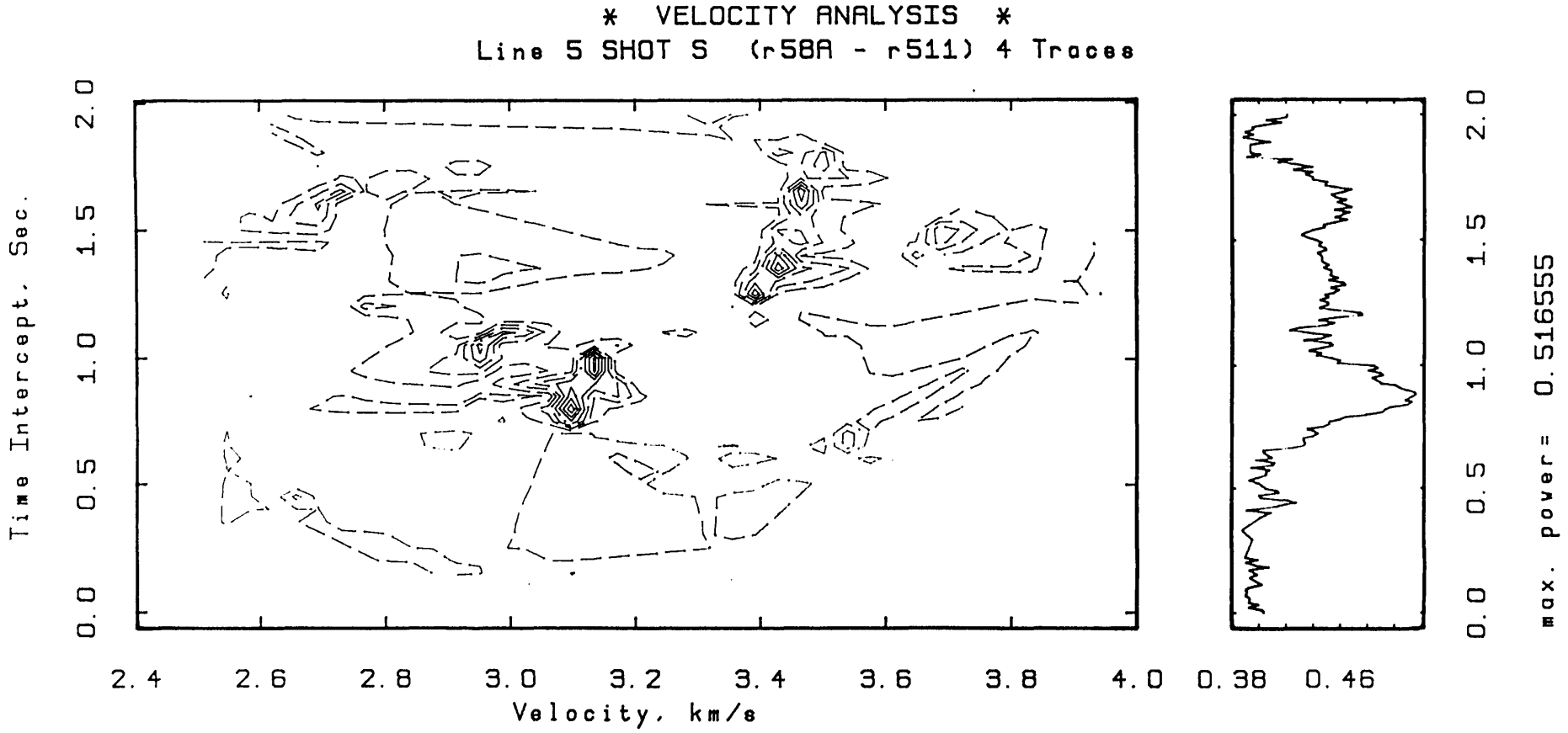


Fig.5.12 Results of applying the software to stations r508A-r511 of Fig 5.6a showing the maximum coherency coefficient at time intercept of 0.90 s and velocity 3.12 km/s.

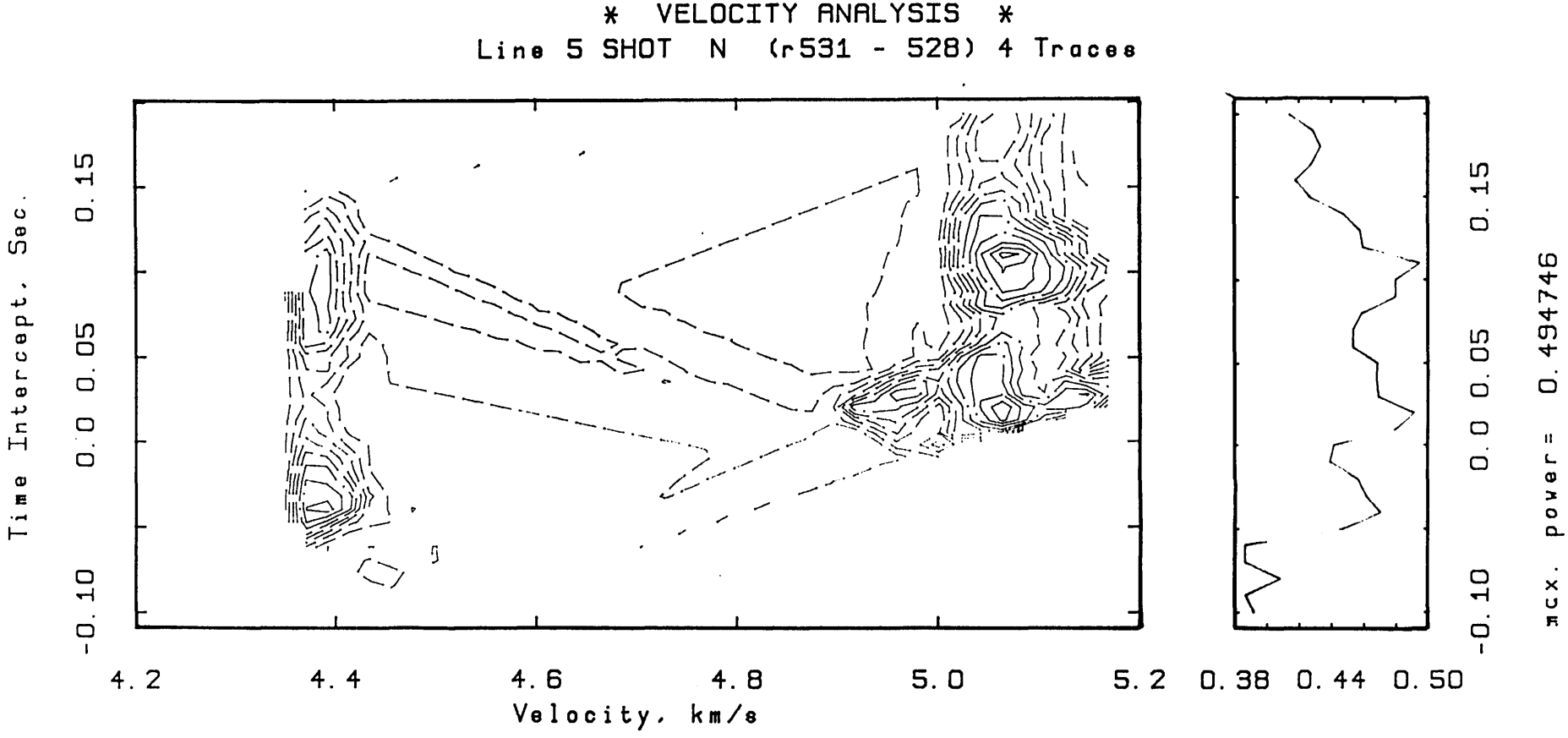


Fig.5.13 Results of applying the software to stations r531-r528 of Fig 5.6b showing the maximum coherency coefficient at time intercept of 0.11 s and velocity 5.07 km/s.

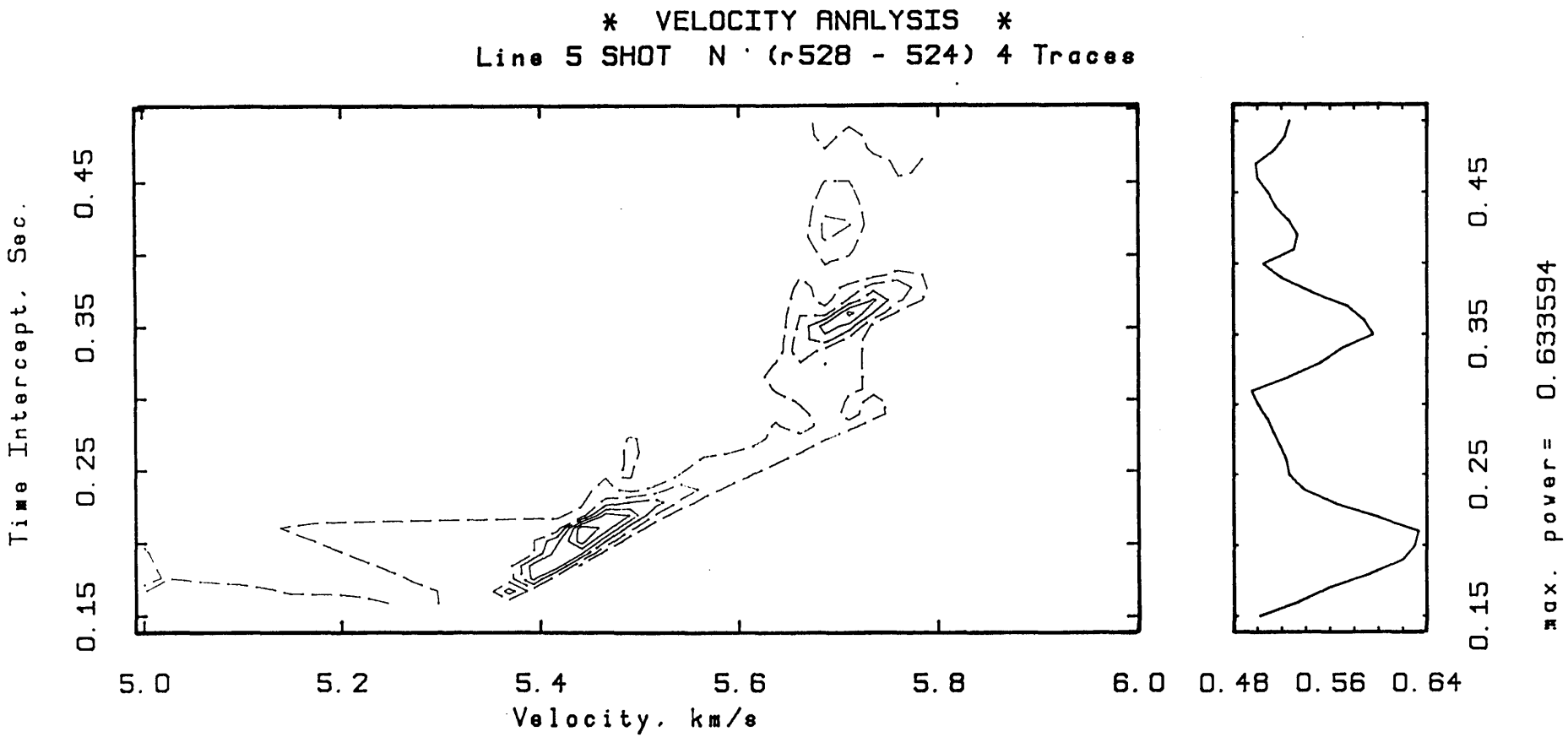


Fig.5.14 Results of applying the software to stations r528-r524 of Fig 5.6b showing the maximum coherency coefficient at time intercept of 0.21 s and velocity 5.44 km/s.

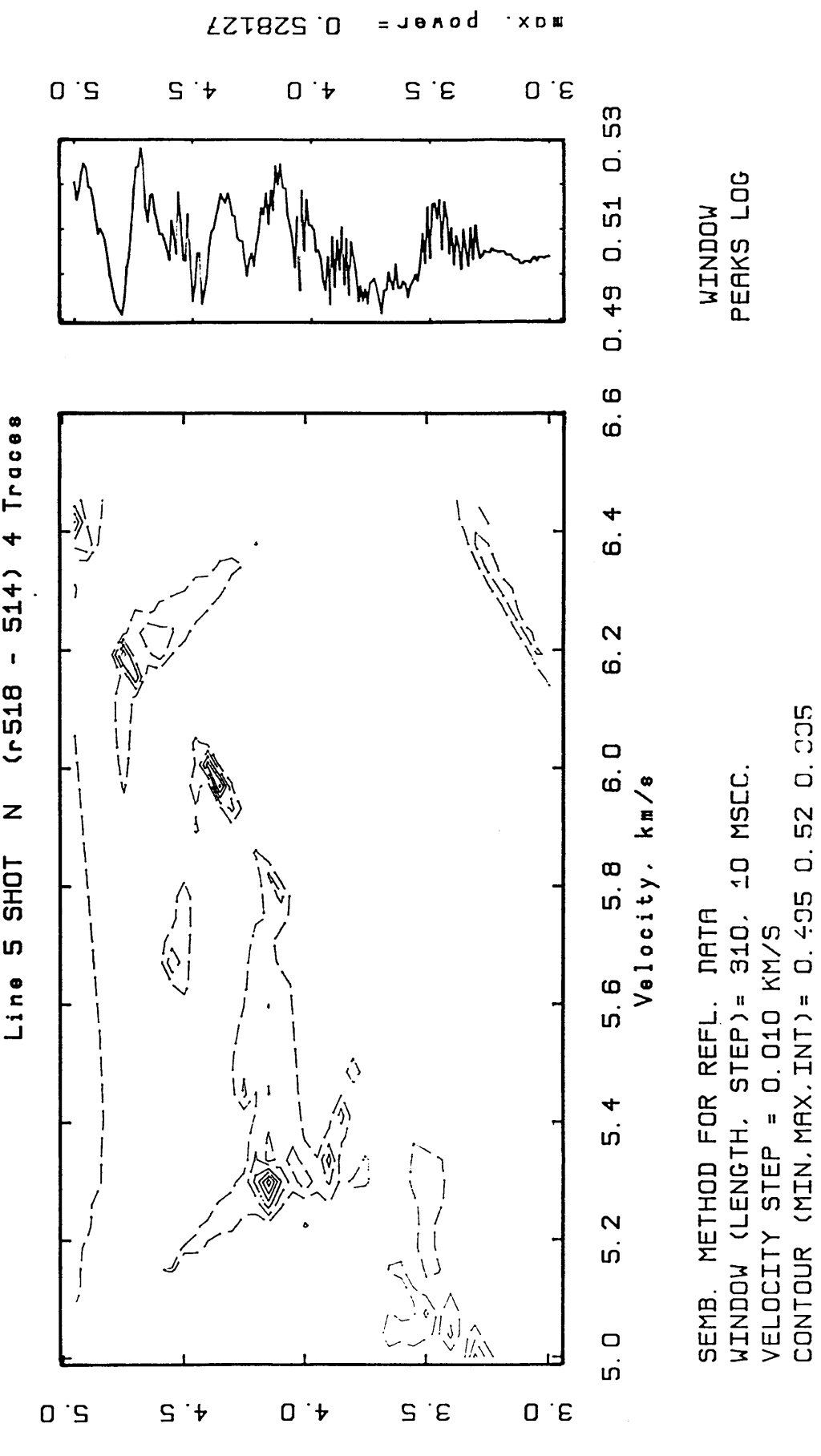


Fig.5.15 Results of applying the software to stations r518-r514 of Fig 5.6b showing high density contour lines at two combination of time and velocity.

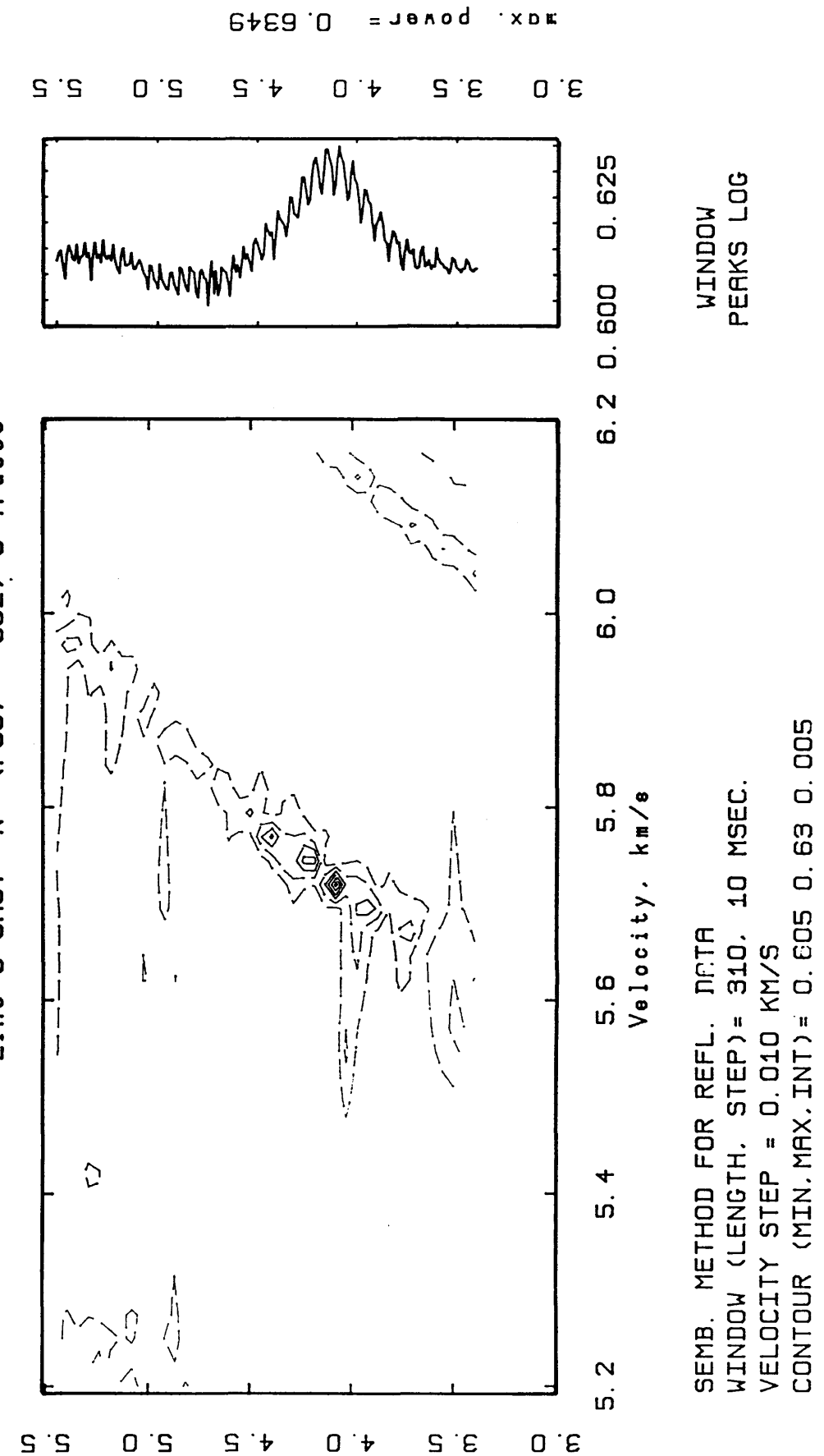


Fig.5.16 Results of applying the software to stations r507-r502 of Fig 5.6b showing the maximum coherency coefficient at time intercept of 4.09 s and velocity 5.72 km/s.

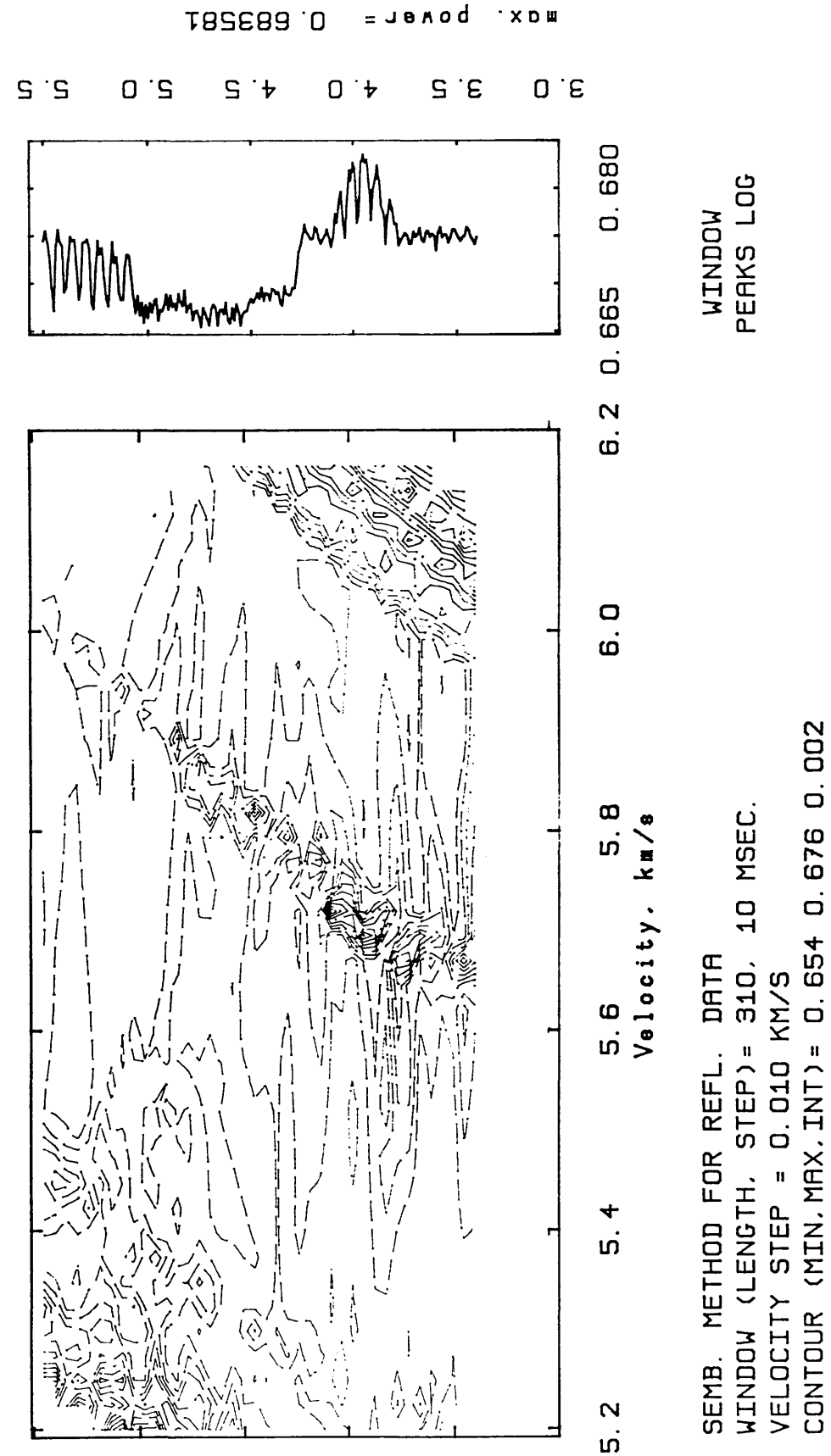


Fig.5.17 Results of applying the software to stations r501-r502 of Fig 5.6b showing the maximum coherency coefficient at time intercept of 3.95 s and velocity 5.70 km/s.

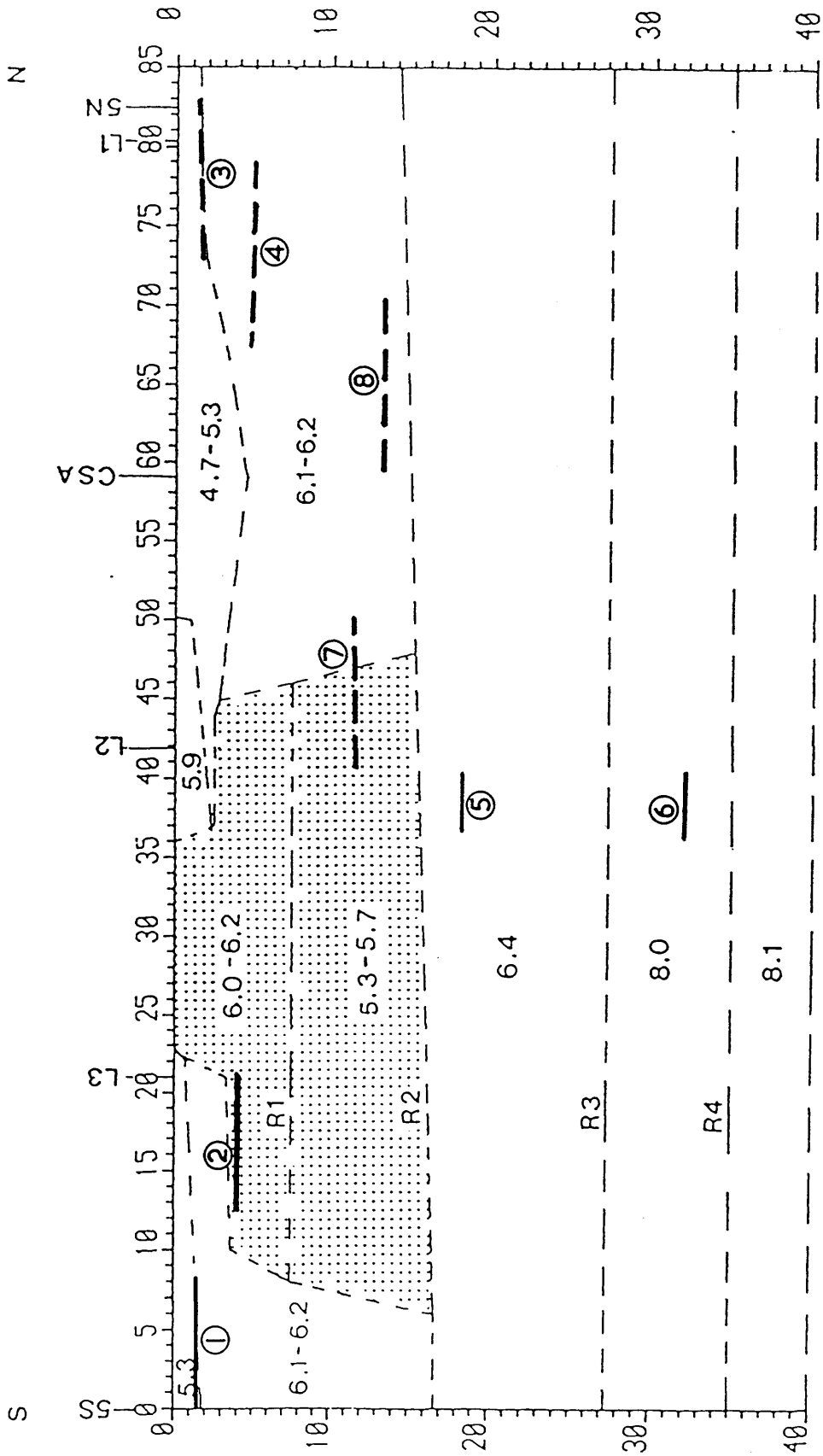


Fig.5.18 Results of both shots and previous interpretation combined together. Solid lines represent results obtained from shot 5S and dashed lines for shot 5N. Refractors are numbered 1 to 4 and reflectors from 5 to 8

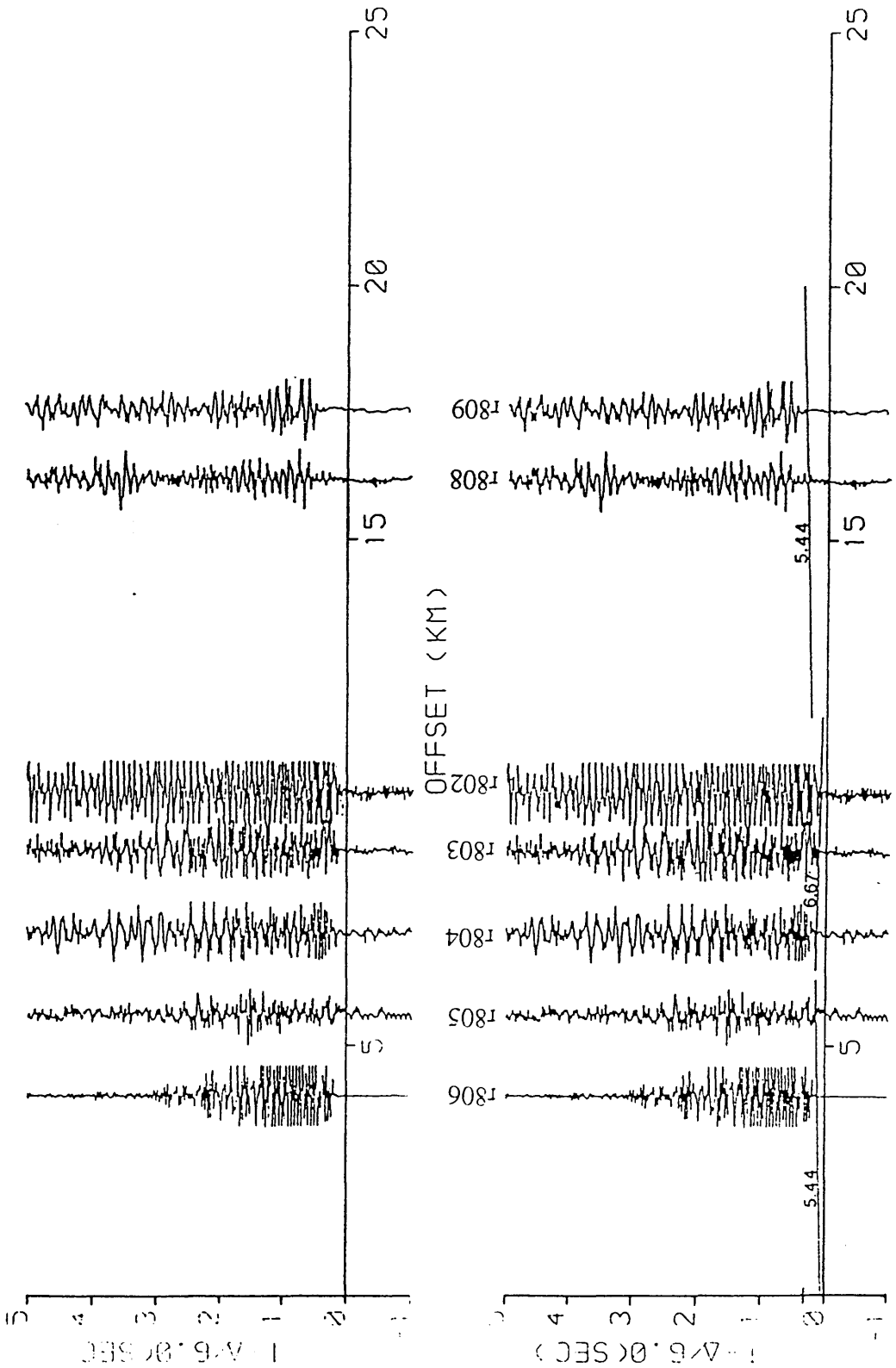


Fig.5.19a Shot 801N recorded along line 8 (after Doody 1985). Velocities given in km/s.

Reduction velocity = 6.0 km/s.

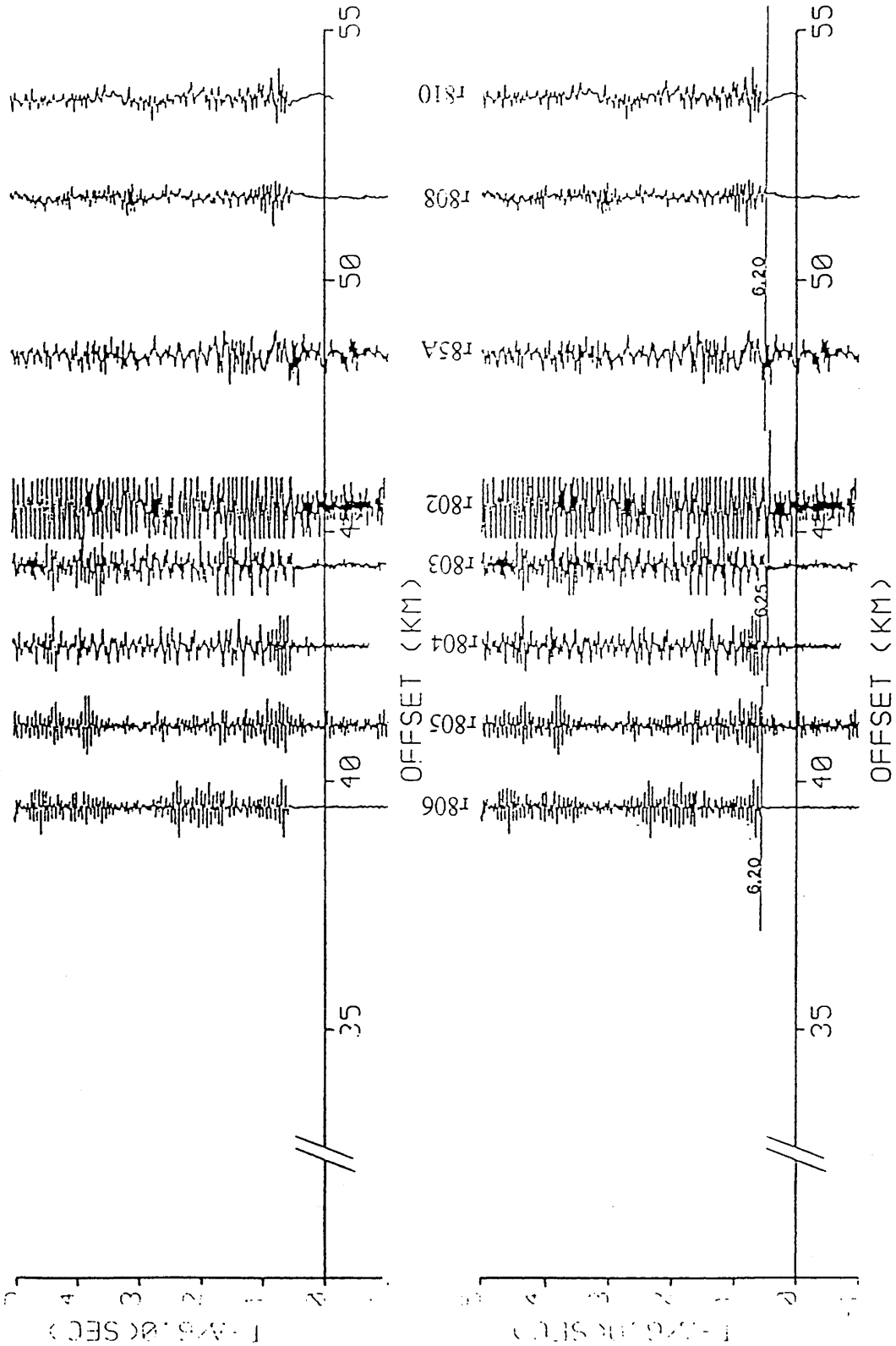


Fig.5.19b Shot 805N recorded along line 8 (after Doody 1985). Velocities given in km/s.

Reduction velocity = 6.0 km/s.

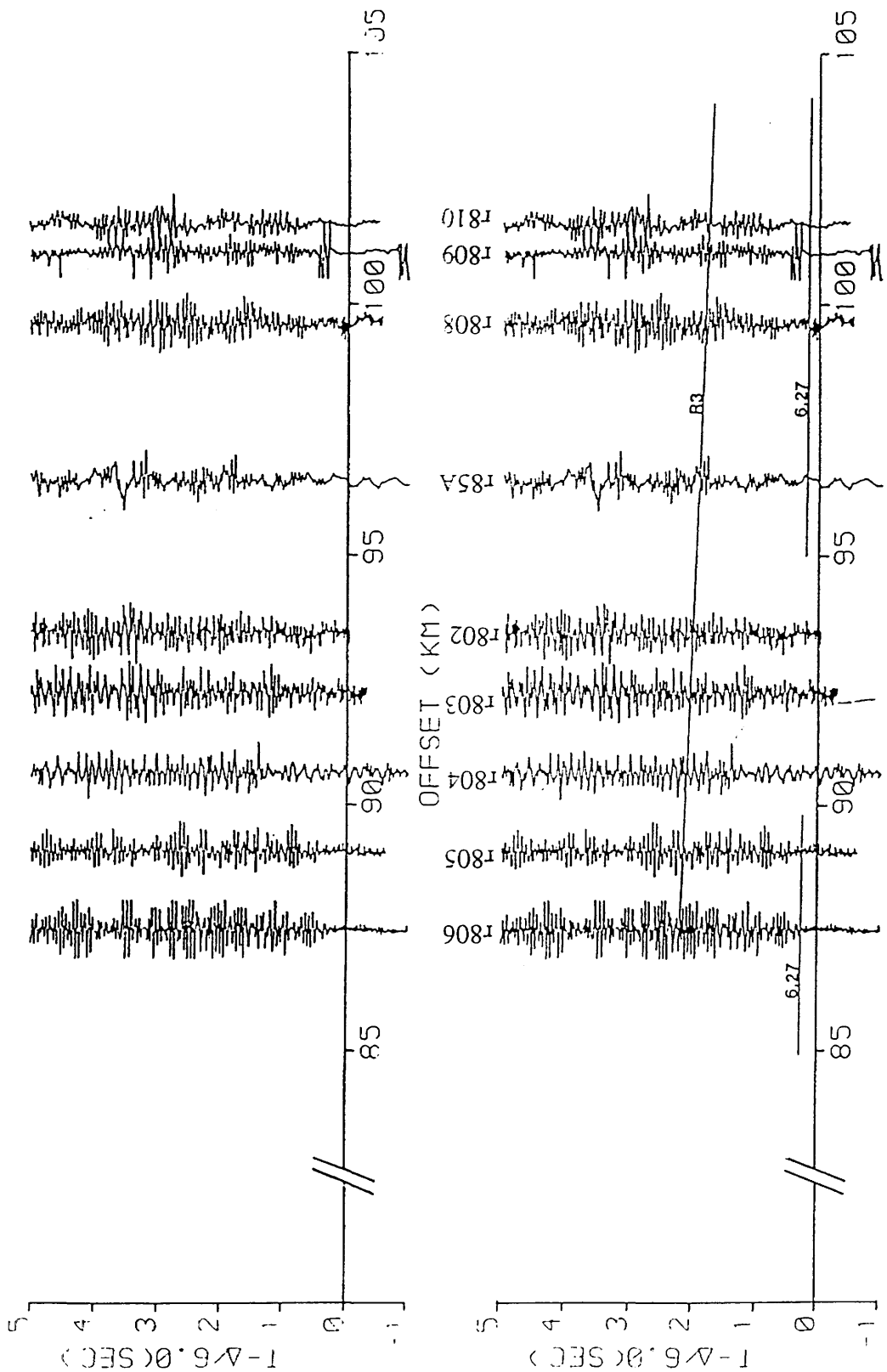


Fig.5.19c Shot 810N recorded along line 8 (after Doody 1985). Velocities given in km/s.

Reduction velocity = 6.0 km/s.

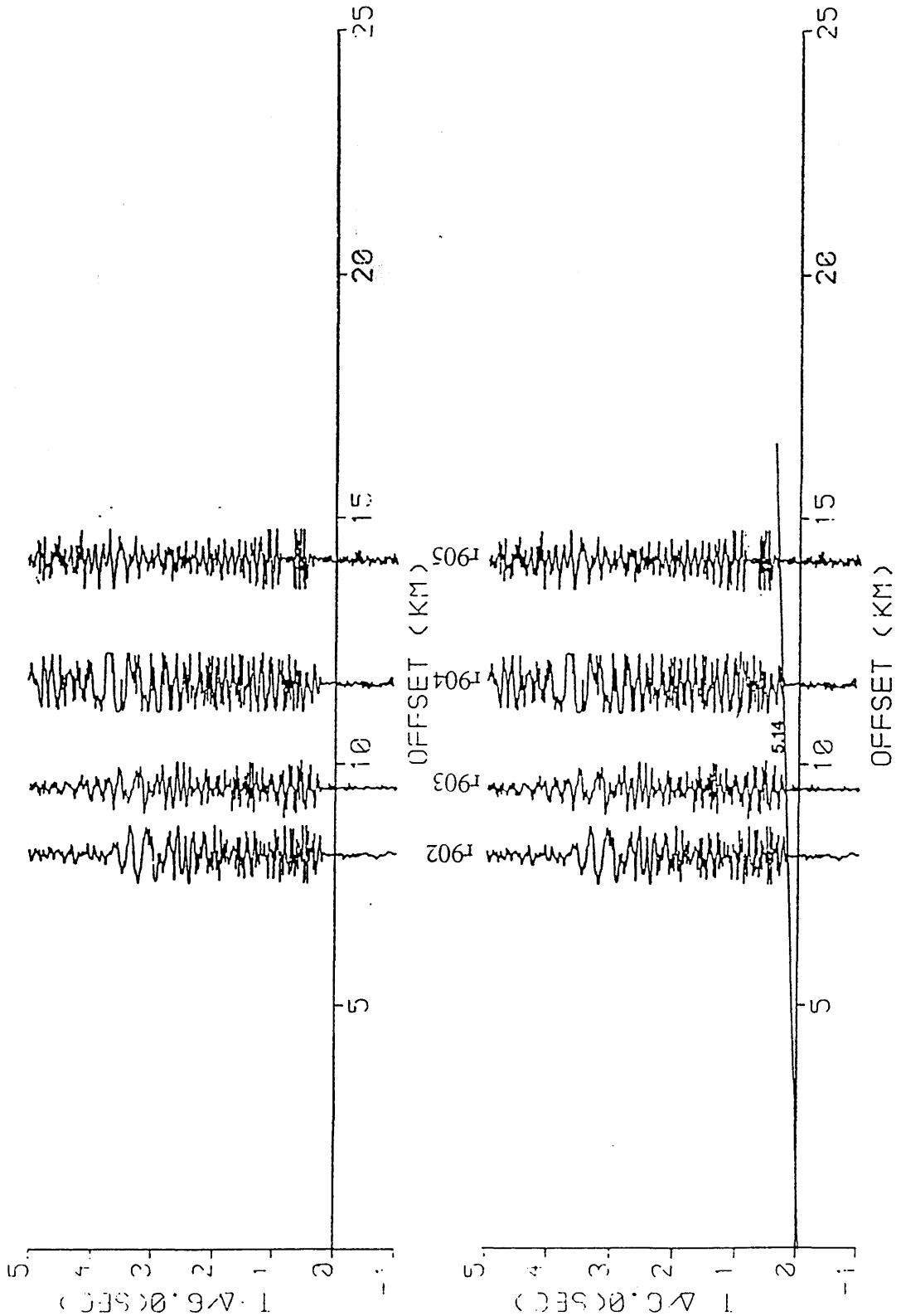


Fig.5.20a Shot 801N recorded along line 9 (after Doody 1985). Velocities given in km/s.

Reduction velocity = 6.0 km/s.

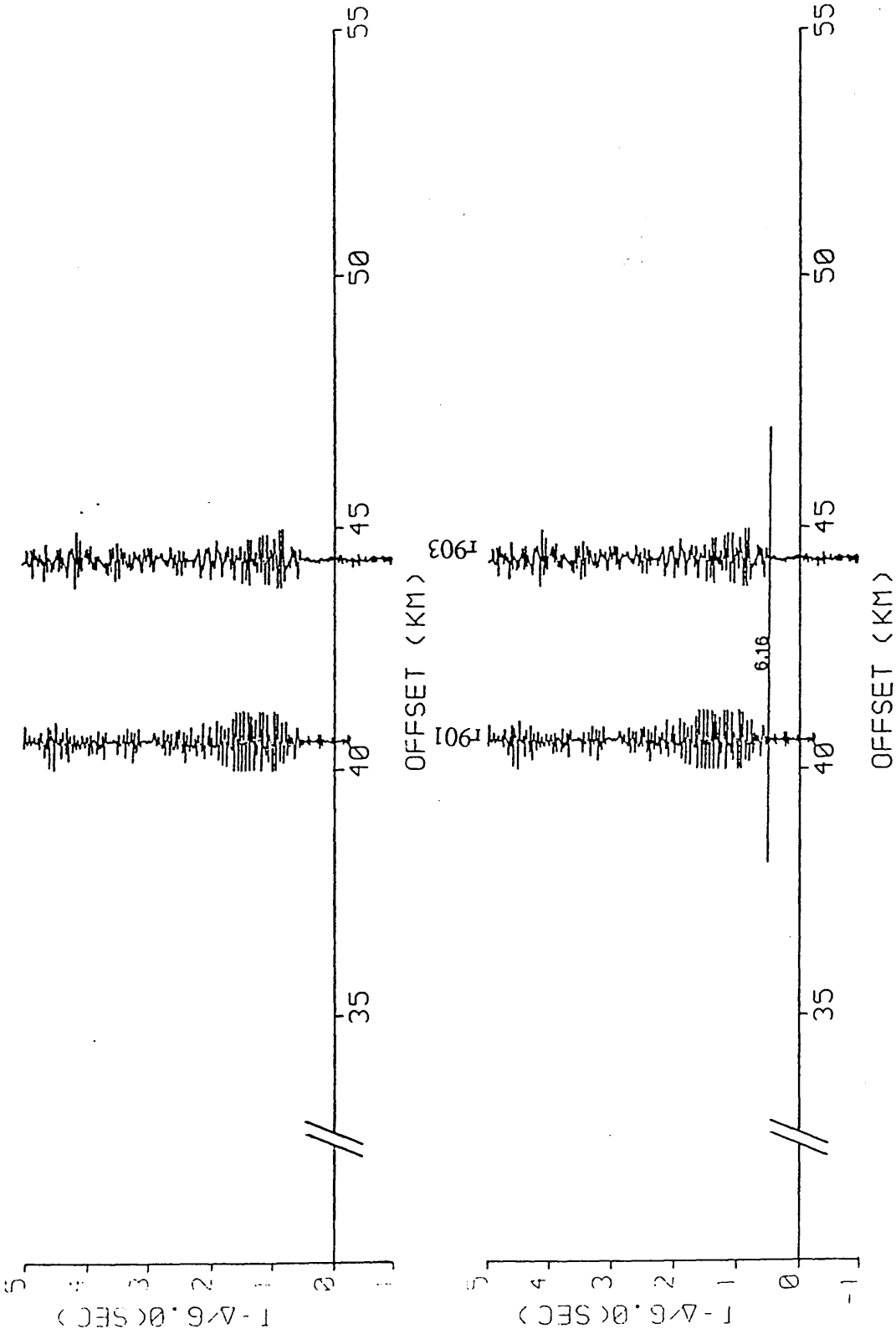


Fig.5.20b Shot 805N recorded along line 9 (after Doody 1985). Velocities given in km/s.

Reduction velocity = 6.0 km/s.

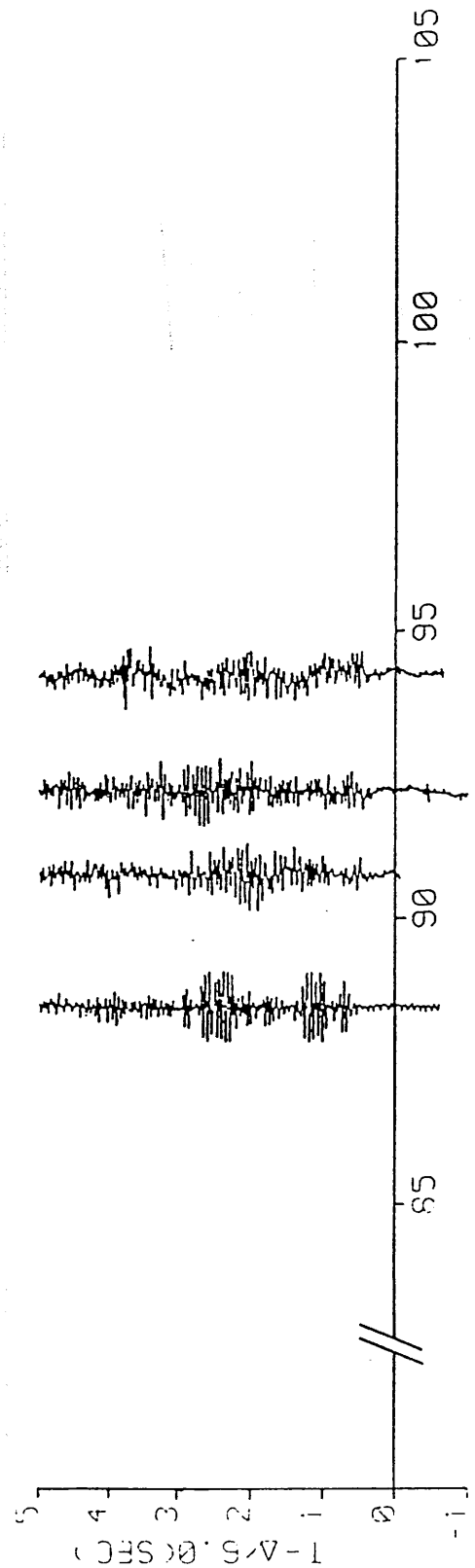


Fig.5.20c Shot 810N recorded along line 9. No first arrival determined (after Velocities given in km/s. Reduction velocity = 6.0 km/s. Doody 1985).

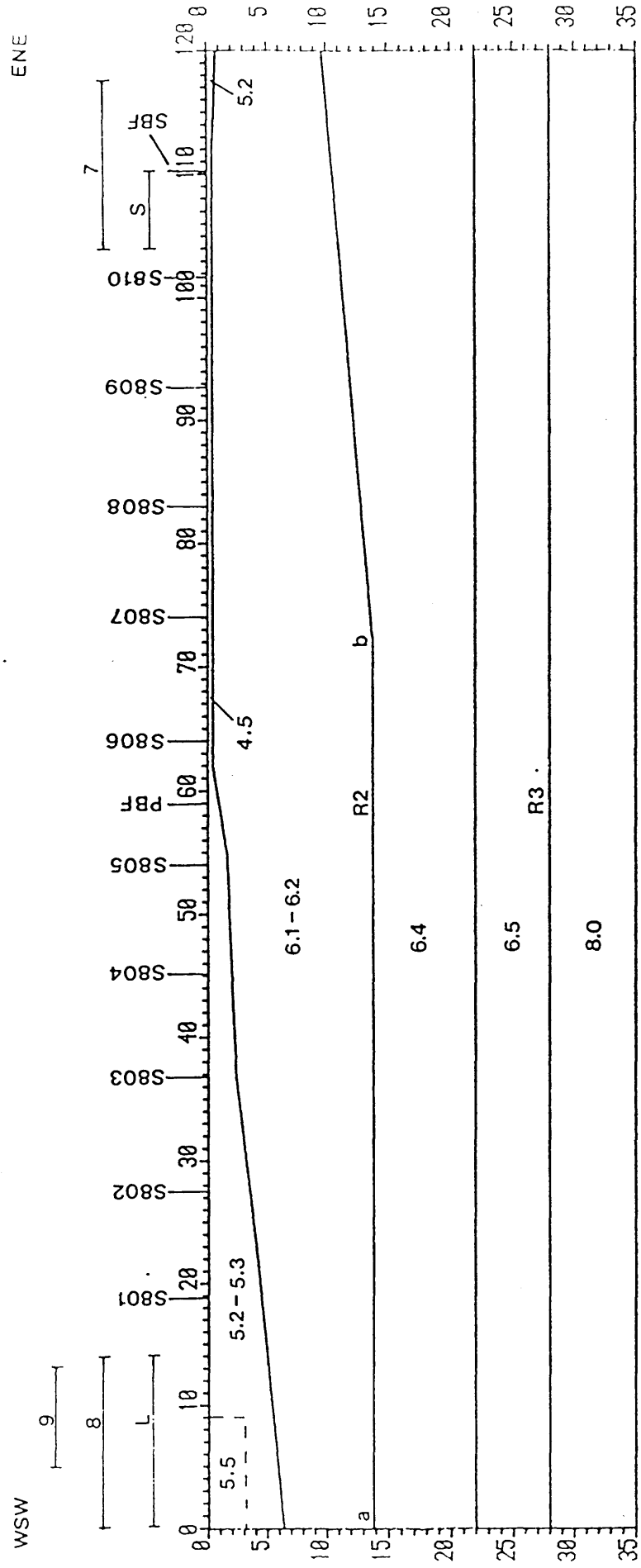


Fig.5.21 Lizard-Start line. Model derived by raytracing (after Doody 1985).

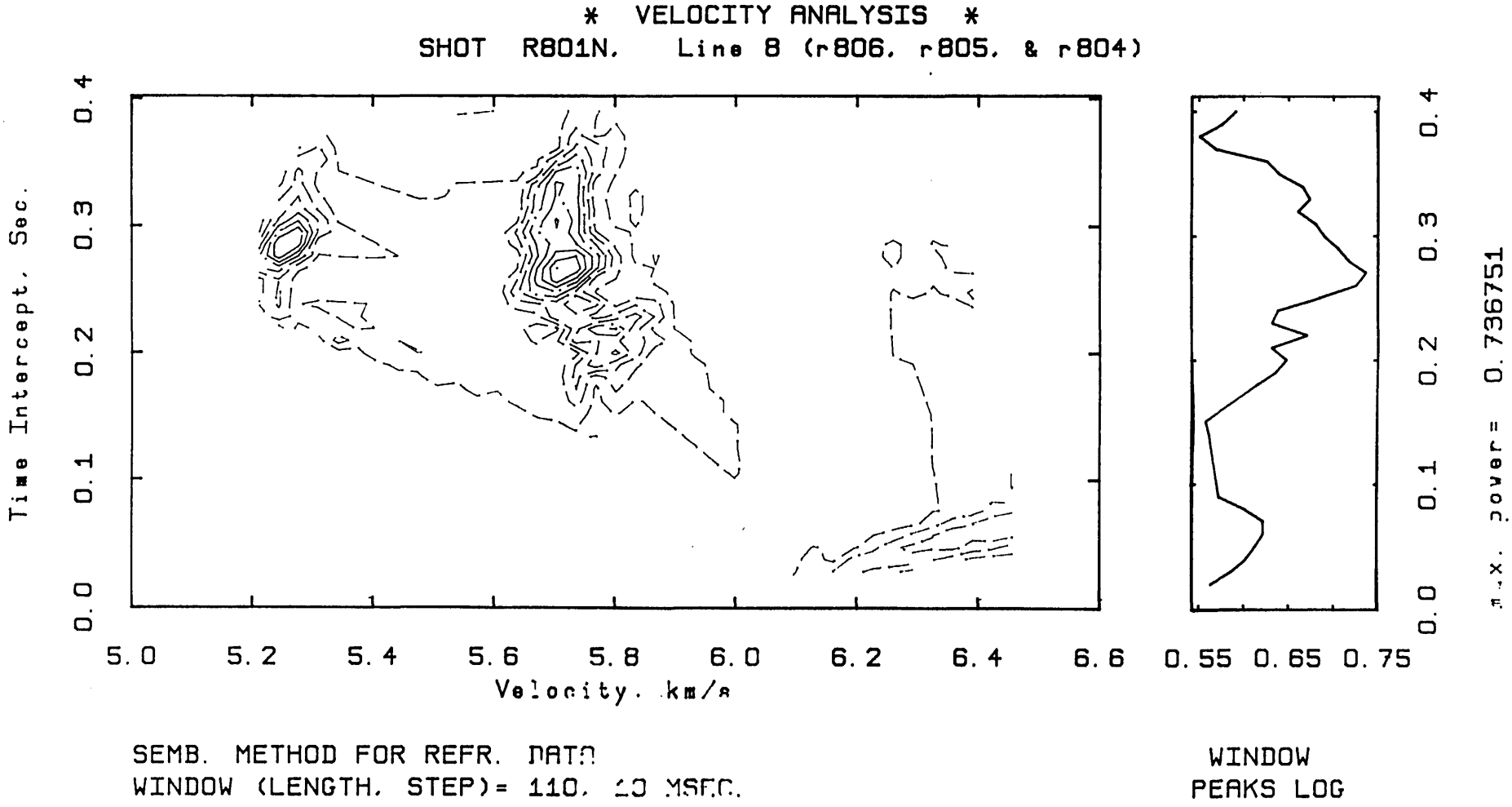


Fig.5.22 Results of applying the software to stations r806-r804 of Fig 5.19a showing the maximum coherency coefficient at time intercept of 0.27 s and velocity 5.72km/s.

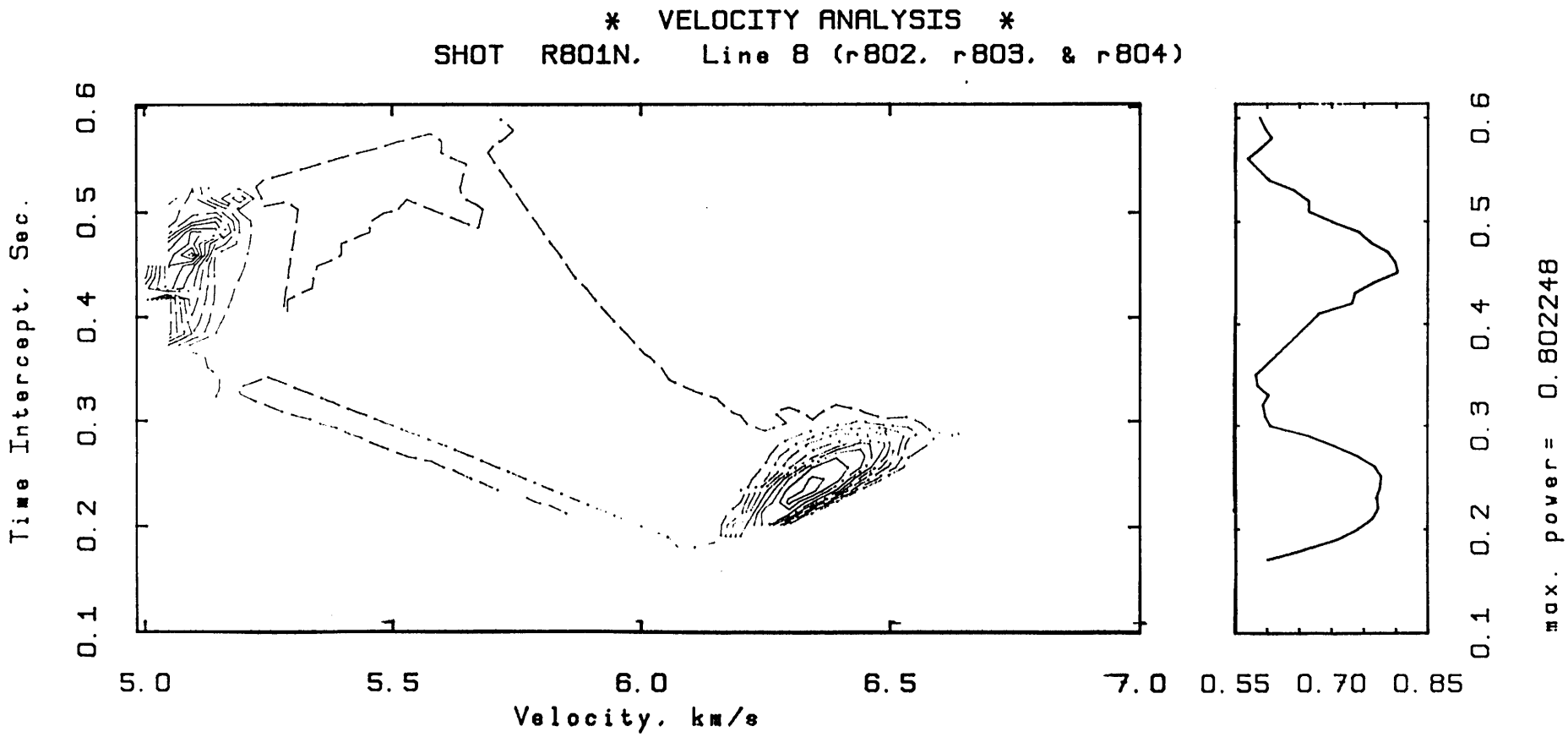


Fig.5.23 Results of applying the software to stations r804-r802 of Fig 5.19a showing the maximum coherency coefficient at time intercept of 0.56 s and velocity 6.30km/s.

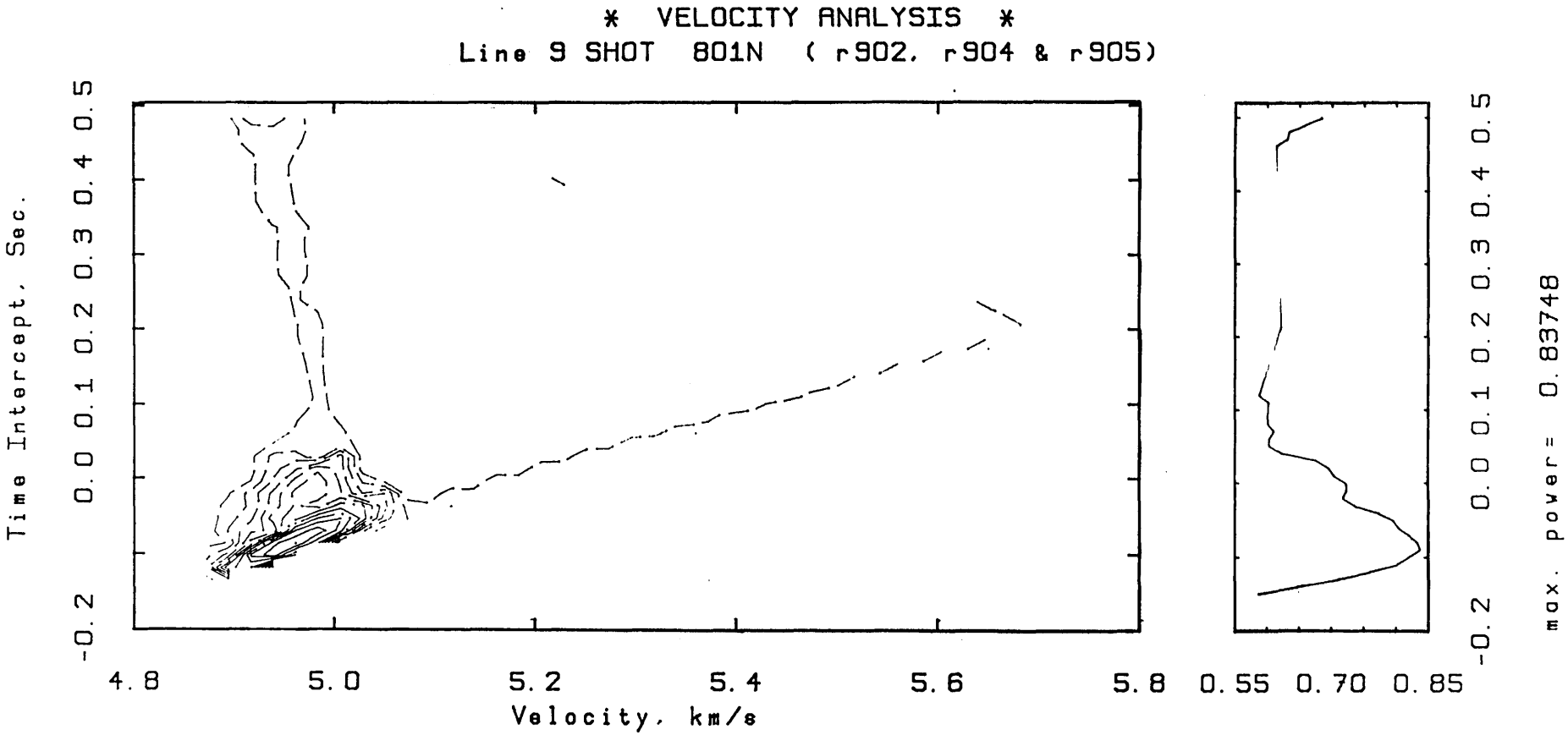


Fig.5.24 Results of applying the software to stations r904-r202 of Fig 5.20a showing the maximum coherency coefficient at time intercept of 0.09 s and velocity 4.95km/s.

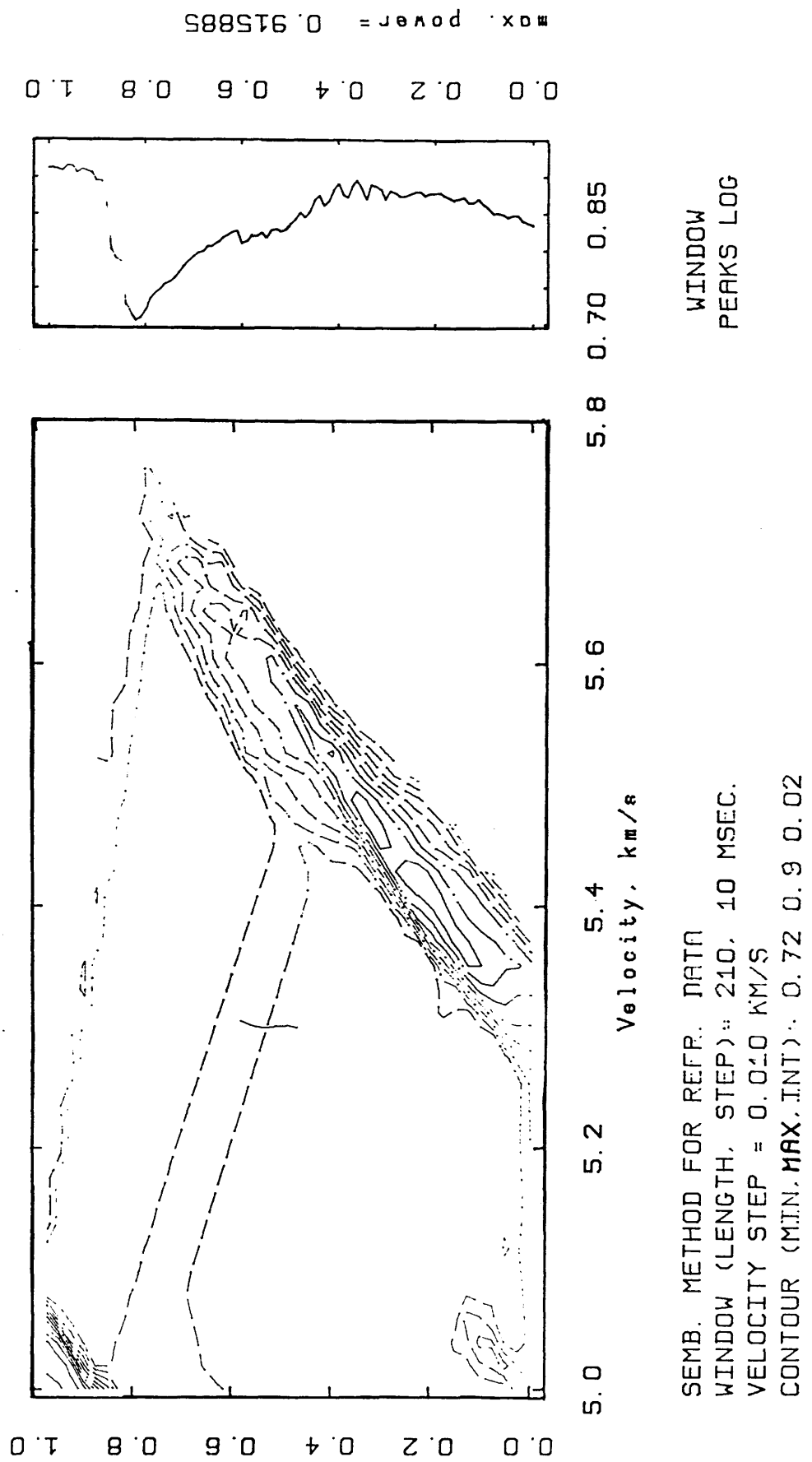


Fig.5.25 Results of applying the software to stations r806-r805 of Fig 5.19b showing the maximum coherency coefficient at time intercept of 0.28 s and velocity 5.43km/s.

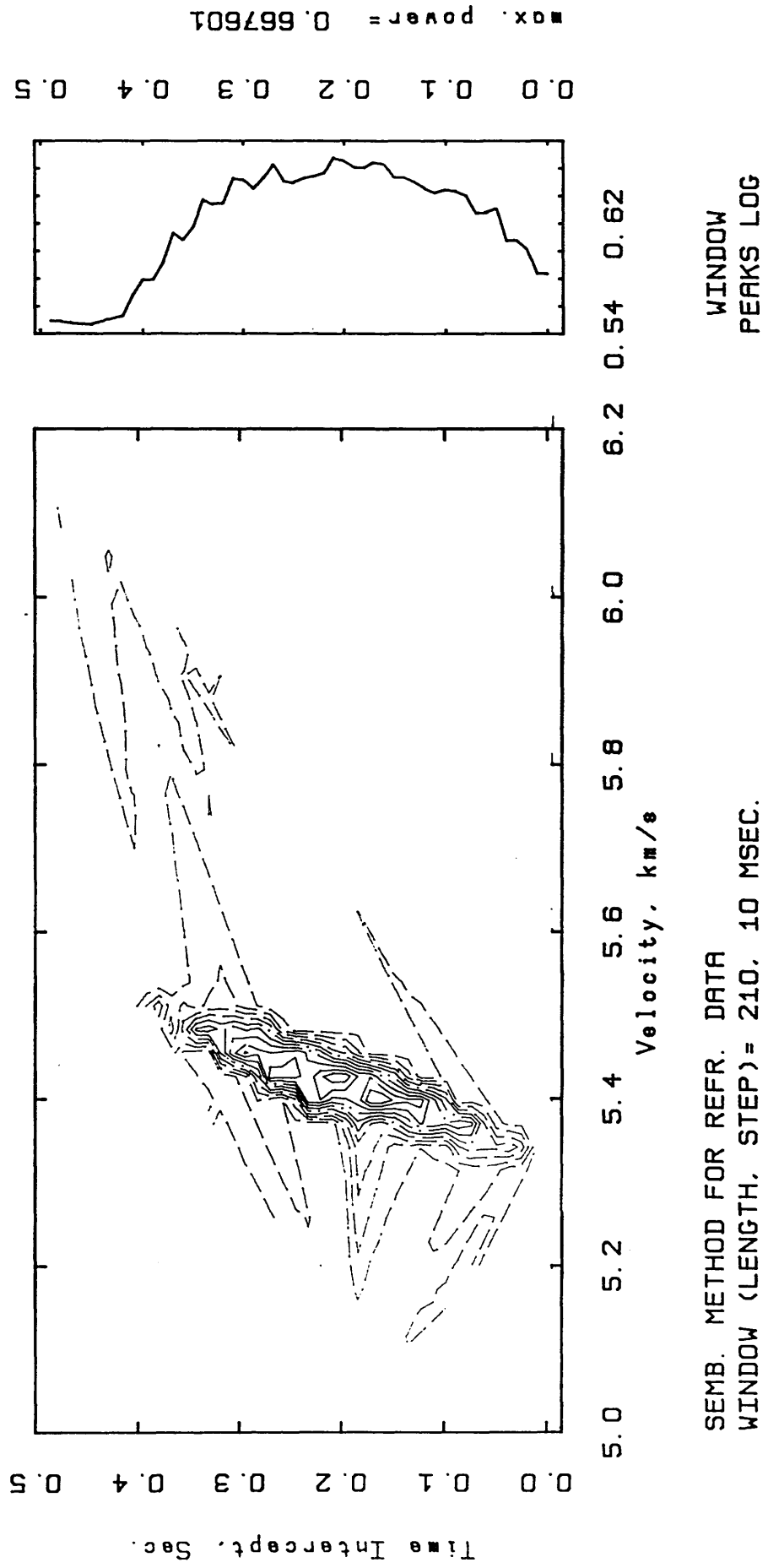


Fig.5.26 Results of applying the software to stations r806-r803 of Fig 5.19b showing the maximum coherency coefficient at time intercept of 0.21 s and velocity 5.43km/s.

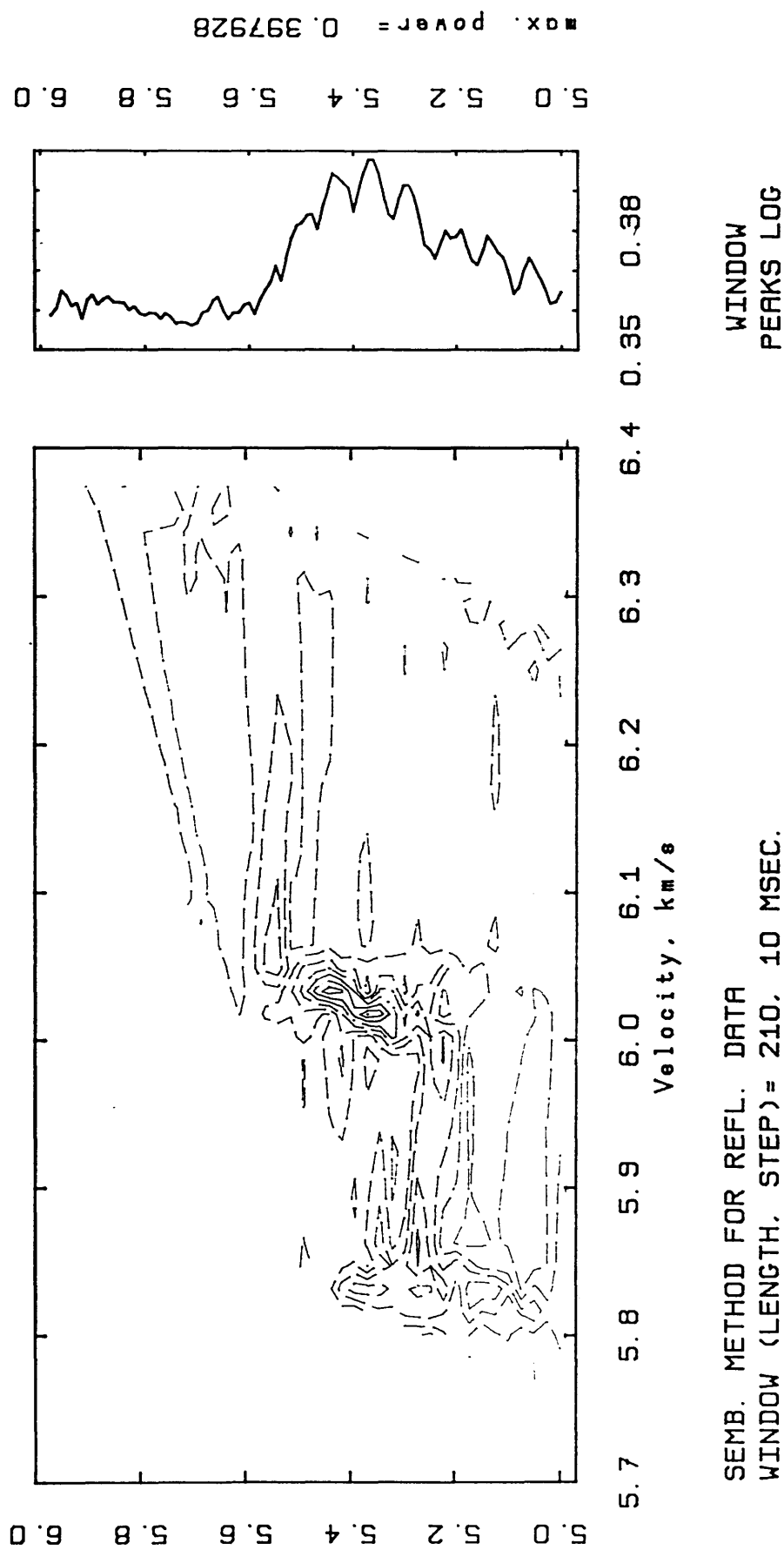


Fig.5.27 Results of applying the software to stations r806-r810 of Fig 5.19c showing the maximum coherency coefficient at time intercept of 5.36 s and velocity 6.02km/s.

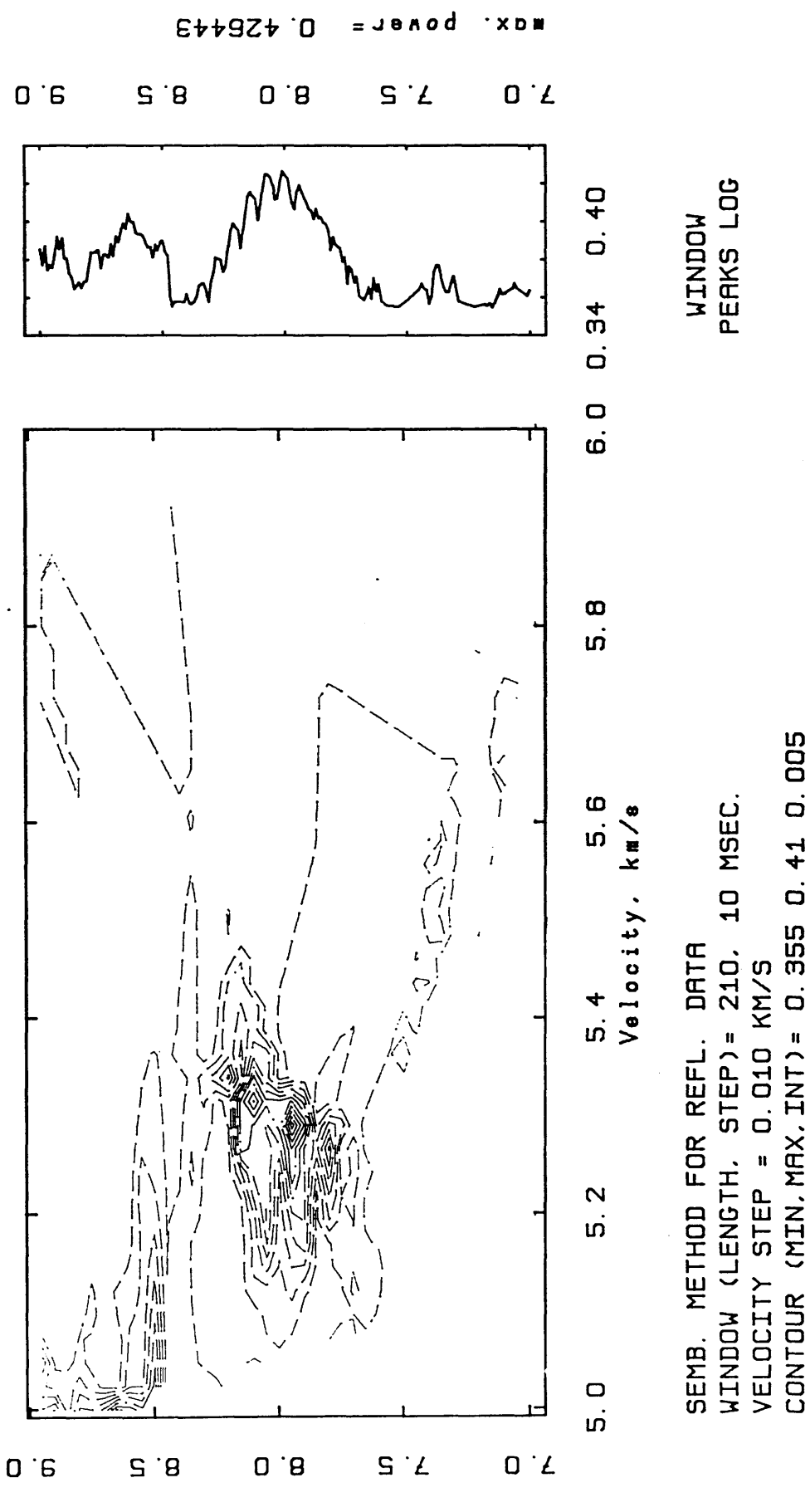


Fig.5.28 Results of applying the software to stations r806-r810 of Fig 5.19c showing the maximum coherency coefficient at time intercept of 8.01 s and velocity 5.30km/s.

# Chapter 6

# Conclusions and Recommendations

## 6.1. Introduction

The end product of any seismic project is to obtain a geophysical model for the particular area of interest. Seismic velocity determination is an important and probably most crucial factor in achieving this. In this chapter conclusions are drawn about the seismic velocity analysis software developed here and the recommendations for further work are outlined.

## 6.2. Conclusions

The following points summarise the main conclusions which were derived from the work carried out in this project. Firstly conclusions relating to the software itself:

[1] The unnormalised methods (unnormalised crosscorrelation and the mean amplitude summation) did not detect weak events in the presence of a strong event, unlike the normalised methods. The statistical normalised crosscorrelation method required longer computer time than other methods. Semblance and energy normalised crosscorrelation methods gave similar results, although the semblance method showed small improvement in the coherency coefficient value.

[2] Events with poor S/N ratio (<1) will display reliable results, when other factors are ideal or reasonable.

[3] An event suffering interference from other events can be related to its proper combination of time and velocity. However, it is possible that a weak event may not be extracted in the presence of a much stronger one.

[4] Velocity aliasing, when correcting for refraction with a long train of energy, sometimes will produce erroneous results, in the presence of a dominant frequency.

[5] Time correction in search of a certain type of event may give misleading results, whenever a strong event of different type occurs with a similar path. For example, low curvature reflection may be picked when scanning for refraction trajectories.

[6] Arrival time scattering, due to any factor, will reduce the efficiency of the software, especially when the shift is half the period of the dominant frequency.

[7] The polarity of the traces must be ensured before executing the program.

[8] Since the window length used proved to be of crucial importance, tests to determine the appropriate window length should be made prior to working on any data.

[9] The possibility of the program to misinterpret coherent noise as a consistent energy is higher in the case of a small number (<4) of traces.

Overall, it is anticipated that the application of this software could be used as a preliminary analysis tool or to confirm other seismic interpretation methods.

Conclusions concerning the field areas are:

[10] Along the Newburgh profile results obtained by the program were very similar to those obtained by the regression analysis. A geophysical model of two layers was produced . The first layer with a velocity 5.2 km/s and time intercept of 0.02 s and the second of 4.55 km/s and time intercept -0.01.

[11] Use of the software has broadly confirmed the presence and parameters of regional refractors and reflectors beneath SW Britain, as interpreted by Doody (1985) from the SWESE experiment.

## 6.3. Recommendations for further work

Ideas for work beyond that of this project are:

[1] To save computing time, the time and velocity ranges used in the program could be altered so that the program will accept variant ranges. For example, where the range of velocity moves upwards with increasing time.

[2] Static corrections applied to the data could improve the results.

[3] For easier use it is suggested that the main program be adapted to call the S-Macros automatically, based on parameters within the control file.

## References

AL-CHALABI, M., 1973. Series approximation in velocity and travel time computations. *Geophysical Prospecting,* v. 21, p. 783-95.

AL-MANSOURI, D., 1986. Seismological Studies if Upper-Crustal Structure in the Vicinity of the Girvan-Ballantrae Area, SW Scotland. Ph.D. thesis (Unpubl), *University of Glasgow.*

AL-SADI, H. N., 1980. Seismic Exploration Technique and Processing. *Birkhauser,* Basel.

ANDERSON, R. G., and McMECHAN, G. A., 1989. Automatic editing of noisy seismic data. *Geophysical Prospecting,* v. 37, p. 875-92.

ANSTEY, N. A., 1970. Signal Characteristics and Instrument Specifications. v1 of seismic prospecting instruments, *Borntraegen.*

BECKER, R. A., and CHAMBERS, J. M., 1984. S : an Interactive Environment for Data Analysis and Graphics. *Bell Telephone Laboratories, Inc.* Murray Hill, New Jersey.

BRACEWELL, R. N., 1965. The Fourier Transform and its Applications,. *McGraw-Hill Book Co.*

BROOKS, M., DOODY, J, J., and AL-RAWI, F. R. J., 1984, Major crustal reflectors beneath SW England. *J. Geol. Soc. London,* v. 141, p. 97-103.

DAVIDSON, K. A. S., SOLA, M. A., POWELL, D. W., and HALL, J., 1984. A geophysical model for the Midland valley of Scotland. *Trans. R. Soc. Edin. Earth Sci.* v. 75, p. 175-81.

DAVIDSON, K. A. S., 1986. Seismology Studies of Upper Crustal Structure of the Southern Midland Valley of Scotland. Ph.D. thesis (Unpubl). *University of Glasgow.*

DENTITH, M. C., 1987. Geophysical Constraints on Upper Crustal Structure in the Midland Valley of Scotland. Ph.D. thesis (Unpubl), *University of Glasgow.*

DIX, C. H., 1955. Seismic velocities from surface measurements. *Geophysics,* v. 20, p. 68-86.

DOBRIN, M. B., 1976. Introduction to Geophysical Prospecting. (3rd Edition) *McGraw Hill,* New York.

DOODY, J. J., 1985. Deep Crustal Seismic Studies of Southwest Britain. Ph.D thesis (Unpubl), *University College,* Cardiff.

DOUZE, E. J., and LASTER, S. J., 1979. Statistics of Semblance. *Geophysics* v. 44, p. 1999-2003.

EMBREE, P., BURG, J. P., and ABACKUS M. M., 1963. Wide band velocity filtering-The pie-slice process. *Geophysics,* v. 28, p. 948-74.

GAROTTA, R., and MICHON, D., 1967. Continuous analysis function and of the move out corrections. *Geophysical Prospecting,* v. 15, p 584-97.

HATTON, L., WORTHINGTON, M. H., and MAKIN, J., 1986. Seismic Data Processing: Theory and practice, *Blackwell,* London.

KAMALIDDIN, Z. A. R., 1988. Seismic Interpretation of Basin-Basement Relation in the Eastern Midland Valley of Scotland Using Quarry Blasts. MS.c. thesis (Unpubl). *University of Glasgow.*

KANASEWICH, E.R., 1981. Time Sequence Analysis in Geophysics. U. O. *Alberta Press,* Edmonton, 3rd ED..

KANASEWICH, E.R., HEMMINGS, C.D., and ALPASLAN, T., 1973. Nth root stack non-linear filter. *Geophysics,* v. 38, p. 327-38.

KEAREY, P., and BROOKS, M., 1984. An Introduction to Geophysical Exploration. *Blackwell,* London.

KULHANEK, O., 1976. Introduction to Digital Filtering in Geophysics. *Elsevier Scientific Publishing Company.* Amsterdam.

LEVIN, F.K., 1971. Apparent velocity from dipping interface reflections

MAY, B, T., and STRALEY, D, K., 1979. Higher-order moveout spectra. *Geophysics,* v. 44, p. 1193-1207.

MONTALBETTI, J, F., 1971. Computer determination of seismic velocities -a review. *Journal of the Canadian Society of Exploration Geophysics,* v. 7, p. 32-45.

NEIDELL, N. S., and TANER, M. T., 1971. Semblance and other coherency measures for multichannel data. *Geophysics,* v. 36, p. 482-97.

PARASNIS, D.S., 1979. Principles of Applied Geophysics. *Chapman and Hall,* London.

RICE, R. B., 1962. Inverse convolution filters. *Geophysics,* v. 27, p. 4-18.

ROBINSON, E.A., 1967. Predictive decomposition of time series with application to seismic exploration. *Geophysics,* v. 32, p. 418-84.

ROBINSON, E.A., and TREITEL, S., 1964. Principles of digital filtering. *Geophysics,* v. 29, p. 395-404.

ROBINSON, E.A., and TREITEL, S., 1980. Geophysical Signal Analysis. *Prentice-Hall,* Englewood Cliffs.

SCHNEIDER, W.A., and BACKUS, M. M., 1968. Dynamic correction analysis. *Geophysics,* v. 33, p. 105-26.

SCHNEIDER, W.A., PRINCE, E.R., JR. and GILES B.F., 1965. A New data-processing technique for multiple attenuation exploiting differential normal moveout. *Geophysics,* v. 30, p. 348-62.

SHANKS, J. L., 1967. Recursion filters for digital processing. *Geophysics,* v. 32, p. 33-51.

SHERIFF, R. E., 1968. Glossary of terms used in geophysical exploration. *Geophysics,* v. 33, p. 183-228.

SHERIFF, R. E., and L. P. GELDART, 1982. Exploration Seismology. v. 1: History, theory, and data acquisition. *Cambridge Univ. Press,* Cambridge.

SHERIFF, R. E., and L. P. GELDART, 1983. Exploration Seismology. v. 2: Data Processing and Interpretation. *Cambridge Univ. Press,* Cambridge.

SILVERMAN, D., 1967. The digital processing of seismic data. *Geophysics* , v. 32, p. 988-1002.

SLOTNIC, M.M., 1959. Lessons in Seismic Computing. *Society of Exploration Geophysics,* Tulsa.

TANER. M. T., and KOEHLER. F., 1969. Velocity spectra - digital computer derivation and application of velocity functions. *Geophysics* , v. 34, p. 859-81.

TANER, M. T., COOK. E. E., and NEIDELL, N., 1970. Limitations of the reflection seismic method; lessons from computer simulations. *Geophysics* , v. 35, p. 551-73.

TERREL, T. J., 1980. Introduction to Digital Filters. *Macmillan,* London.

TREITEL, S., SHANKS, J. L. and FRASIER, C. W., 1967. Some aspect of fan filtering. *Geophysics,* v. 32, p. 789-800.

YILMAZ, O., 1987. Seismic Data Processing. *Society of Exploration Geophysicists,* Tulsa.

# APPENDIX 1. PROGRAMS

```
C       PROGRAM coh.f
C
C    TO COMPUTE COHERENCY COEFFICIENTS FOR ARRIVALS
C     ACROSS A SEISMIC RECEIVER ARRAY EMPLOYING ONE OF THE
C     FOLLOWING METHODS : SEMBLANCE, UNNORMALISED CROSS-
C     CORRELATION SUM, ENERGY NORMALISED CROSSCORRELATION
C     STATISTICAL NORMALISED CROSSCORRELATION OR MEAN
C     AMPLITUDE SUMMATION. COEFFICIENT CALCULATION IS
C     CARRIED OUT AFTER A TIME CORRECTION IS MADE TO A
C     REFERENCE POINT.
C
C    COEFFICIENTS ARE CALCULATED FOR A RANGE OF PARAMETERS
C     FOR A GIVEN ARRIVAL TIME. REFRACTION AND REFLECTION
C     ARRIVALS MAY BE TESTED AS WAVE AS DIRECT ARRIVALS
C     THROUGH A LAYER OR VELOCITY INCREASING WITH DEPTH.
C
C    THIS PROGRAM WAS WRITTEN BY  EMIL K. SAID,
C                                 DEP. OF GEOLOGY,
C                                 UNIV. OF GLASGOW,
C                                 DECEMBER 1989
C
C PARAMETER         FORMAT           EXPLANATION
C=============================================================
C
C OPT1    ..MUST BE CAPITAL  KIND OF PROCESSING REQUIRED,
C              LETTERS       'REFR'   REFRACTION
C                            'REFL'   REFLECTION
C                            'SPEED'  VELOCITY GRADIENT
C
C OPT2    .......  "         TYPE OF DESIRED COHERENCY:
C                            1 'SEMB' SEMBLANCE
C                            2 'UNCR' UNNORMALIZED
C                               CROSSCORRELATION
C                            3 'SUMS' MEAN AMPLITUDE
C                               SUMMATION
C                            4 'CROS' ENERGY NORMALIZED
C                               CROSSCORRELATION SUM
C                            5 'STCR' STATISTICAL NORMALIZED
C                               CROSSCORRELATION SUM
C
C  OPT3    ...."             TO APPLY A FREQUENCY FILTER
C                            TO THE DATA BEFORE DOING THE
C                            TASK
C                                 'FILTER' USE A FILTER
C                                 'NOFILT' NO FILTERING
C
C  OPT4    ...."             NUMBER OF CHANNEL TO BE PROCESSED
C
C  TIT     ... "             TITLE FOR THE PLOT  NOT MORE THAN
C                            50 CHARACTER
C  M       ..  "             MAX. NUMBER OF TRACES
C  NS      ..  "             MAX. TRACE LENGTH
C  NSA     .   "             ACTUAL  SEISMIC TRACE LENGTH
C
C  NTRACE  ..  "             ACTUAL NUMBER OF TRACES
C  SAMPL   ...."             NUMBER OF SAMPLES / SEC.
```

```
C  N+1     ...."            TIME WINDOW LENGTH ( IN MSEC.)
C
C  TSTART ... "            TIME TO START PROCESSING (IN SEC.)
C  TSTOP   ... "            TIME TO STOP PROCESSING  (IN SEC.)
C  TINC    ...."            TIME INCREMENT  ( IN MSEC. )
C
C                          (VELOCITY GRADIENT PARAMETERS)
C  DV1     ..   "           FIRST CONSTANT
C  DV2     ..               SECOND CONSTANT
C  DVIN    ..   "           CONSTANT'S INCREMENT
C
C  VI      ...."            INITIAL VELOCITY
C  VF      ...."            FINAL VELOCITY
C  VINC    ...."            VELOCITY INCREMENT
C
C
C=========================================================
C                    {  INPUT CONTROL SYSTEM FILE  }
C
C LINE   1 :
C---------     OPT1  OPT2   OPT3
C
C LINE   2 :   TIT
C-----------
C
C LINE   3 :
C---------    NTRACE   SAMPL   OPT4      ( UNFORMATTED )
C
C LINE   4 :
C---------      N                                  "
C
C LINE   5 :
C---------
C              IF  ( OPT1 )  WAS FOR 'REFL' OR 'REFR'
C
C                   THEN WRITE   TSTART   TSTOP     TINC
C
C
C             IF  ( OPT1 )  WAS FOR 'SPEED'
C
C                   THEN  WRITE   DV1   DV2   DVIN
C
C
C LINE   6 :
C_________          VI     VF     VINC        ( UNFORMATTED )
C
C LINE   7 :
C---------       FIRST TRACE FILE NAME, NOT MORE THAN
C                ( 50 CHARACTERS )
C
C LINE   8 :
C---------      SECOND TRACE FILE NAME
C                    .
C                    .
C                    .
C LINE   N :
```

```
C---------        LAST TRACE FILE NAME
C
C=======================================================
C
C       PROGRAM COHERENCY
        PARAMETER (NS=4500,M=48,ICH=11)
        PARAMETER (NTF=2050, NT2=4098)
        DIMENSION XT(M,-NS:NS),ABC(NS)
        DIMENSION IXT(ICH),XX(ICH),II(M),IK(M)
        DIMENSION POS(M,ICH),IGAN(M,ICH),IPOL(M,ICH),
     * ISAMP(M,ICH),AMPT(M,ICH)
C
        COMMON XTC(M,-NS:NS),SEMB,SUMS
        COMMON/C2/ F(NT2), R(NT2),S(NTF)
        COMMON/CON/ PII,P7,P7TWO,C22,S22,PI2
C
        CHARACTER  TIT(50)*1, INFILE * 50
        CHARACTER *8 RSN,SSN,AUT,DAT,INST
        CHARACTER  OPT1 * 5,OPT2 * 4,OPT3 * 6
C
        CALL SYSTEM('date>startfile')
C
C-------------------------------------------------
C             (((     READING  SECTION    )))
C-------------------------------------------------
C
        READ(5,*) OPT1,OPT2,OPT3
C
C       Checking options (1, 2 and 3) for any incorrect input
C       If so, then print warning message and stop
C       the program
C*************************************************************
C              checking option 1
C                -----------------
        WRITE(6,5680)
             IF (OPT1.EQ.'REFL') THEN
        WRITE(6,1900)
1900    FORMAT(/,'TIME CORRECTION (NMO) WILL BE FOR
     * REFLECTION DATA')
             ELSE IF (OPT1.EQ.'REFR') THEN
        WRITE(6,1901)
1901    FORMAT(/,'TIME CORRECTION WILL BE FOR  REFRACTION
     * DATA')
             ELSE IF (OPT1.EQ.'SPEED')  THEN
        WRITE(6,1022)
1022    FORMAT(/,'TIME CORRECTION WILL BE COMPUTED FOR
     * CONTINUOUS VELOCITY INCREASE WITH DEPTH')
             ELSE
          WRITE(6,5680)
                WRITE(6,1903)
1903    FORMAT(//3x,'ERROR IN KIND OF PROCESSING'
     *//17x,'ONLY THREE CHOICES  EXIST and must be in
     * CAPITAL letters:-',
     *//30X,'  *  REFL  *    FOR REFLECTION'
     *//30X,' **  REFR  **   FOR REFRACTION'
     *//30X,' **  SPEED  **  FOR  CONTINUOUS VELOCITY
```

```
     * INCREASE')

C
       GO TO 733
            END IF
C
C*************************************************************
C              checking option 2
C                -----------------
            IF (OPT2.EQ.'SEMB') THEN
          WRITE(6,1910)
1910     FORMAT(/,'COHERENCY WILL BE COMPUTED EMPLOYING
     * SEMBLANCE METHOD'/)
             ELSE IF (OPT2.EQ.'UNCR') THEN
          WRITE(6,1911)
1911     FORMAT(/,'COHERENCY WILL BE COMPUTED EMPLOYING
     * UNNORMALIZED CROSSCORRELATION METHOD'/)
             ELSE IF (OPT2.EQ.'CROS')THEN
          WRITE(6,1912)
1912     FORMAT(/,'COHERENCY WILL BE COMPUTED EMPLOYING
     * ENERGY NORMALIZED CROSSCORRELATION METHOD'/)
             ELSE IF (OPT2.EQ.'SUMS')THEN
          WRITE(6,1913)
1913     FORMAT(/,'COHERENCY WILL BE COMPUTED EMPLOYING MEAN
     * AMPLITUDE SUMMATION METHOD'/)
          ELSE IF (OPT2.EQ.'STCR') THEN
          WRITE(6,5019)
5019     FORMAT(/,'COHERENCY WILL BE COMPUTED EMPLOYING
     * STATISTICAL CROSSCORRELATION SUM METHOD'/)
C
            ELSE
          WRITE(6,5680)
                WRITE(6,1914)
1914     FORMAT(//,'? ? ? ? ? ? '
     *///5X,'ERROR IN THE CHOICE OF COHERENCY METHOD'
     *//5X,'YOU CAN CHOOSE ONE OF THESE FIVE, IN THE CONTROL
     *  FILE'
     *//15X,'( SEMB ) FOR SEMBLANCE METHOD'
     *//15X,'( UNCR ) FOR UNNORMALIZED CROSSCORRELATION'
     *//15X,'( CROS ) FOR ENERGY NORMALIZED
     *  CROSSCORRELATION'
     *//15X,'( STCR ) FOR STATISTICAL NORMALIZED X-
     *  CORRELATION SUM'
     *//15X,'( SUMS ) FOR MEAN AMPLITUDE SUMMATION')
C
            GO TO 733
          END IF
C
C*************************************************************
C                    checking option 3
C                  -----------------
         IF (OPT3.EQ.'NOFILT')       THEN
               FIL=0
         ELSEIF (OPT3.EQ.'FILTER')   THEN
               FIL=1
          ELSE
```

```
                WRITE(6,5680)
                WRITE(6,5690)
5690    FORMAT(///10X,'ERROR IN * FILTER *
     * OPTION',//////////)
                GO TO 733
          END IF
C
C*********************************************************
C
        OPEN(UNIT=10,FILE='outcoh1')
        OPEN(UNIT=9,FILE='outcoh2')
C
C       write TITLE and SUBTITLES to a separate file,
C       'outcoh2',for later input to ' S ' package
C
       WRITE(9,5218)
5218   FORMAT('"*  VELOCITY ANALYSIS  *"')
C
       READ(5,1092)  TIT
1092   FORMAT (50A)
C
       DO 8741 I=50,1,-1
              IF (TIT(I).NE." ") GO TO 8801
8741   CONTINUE
8801   NTIT=I+1
C
       TIT(NTIT)=('"')
C
       WRITE(9,1099) (TIT(I), I=1,NTIT)
1099   FORMAT ('"',50A)
C
               IF (FIL.EQ.0) WRITE (9,8191)
               IF (FIL.EQ.1) WRITE (9,8192)
C
8191   FORMAT('"0"')
8192   FORMAT('"1"')
C
               IF (OPT1.EQ.'REFR') WRITE (9,9117)
               IF (OPT1.EQ.'REFL') WRITE (9,9118)
               IF (OPT1.EQ.'SPEED') WRITE (9,9119)
C
9117    FORMAT('"REFR. DATA"')
9118    FORMAT('"REFL. DATA"')
9119    FORMAT('"CONTINUOUS VELOCITY INCREASE"')
C
             IF (OPT2.EQ.'SEMB') WRITE (9,1105)
             IF (OPT2.EQ.'UNCR') WRITE (9,1106)
             IF (OPT2.EQ.'SUMS') WRITE (9,1107)
             IF (OPT2.EQ.'STCR') WRITE (9,1108)
             IF (OPT2.EQ.'CROS') WRITE (9,1109)
C
1105   FORMAT ('"SEMB. METHOD FOR"')
1106   FORMAT ('"UNNORMALIZED X-CORR. METHOD  FOR"')
1107   FORMAT ('"MEAN AMPLITUDE SUMMATION  FOR"')
1108   FORMAT ('"STAT. NORM. X-CORR. METHOD FOR"')
1109   FORMAT ('"ENERGY NORM. X-CORR. METHOD FOR"')
```

```
C
        IF (OPT1.EQ.'REFR'.OR.OPT1.EQ.'REFL') NAB=1
        IF (OPT1.EQ.'SPEED')                  NAB=0
C
       READ(5,*) NTRACE,SAMPL,OPT4
C
        IF (NTRACE.EQ.1) THEN
        WRITE(6,5680)
        WRITE(6,1612)
1612   FORMAT(8X,'ERROR WAS FOUND, NUMBER OF TRACES = 1
     * !!??',//)
         GO TO 733
        END IF
C
       READ(5,*) N
C
        IF (NAB.EQ.1)  READ(5,*) TSTART,TSTOP,TINC
C
        IF (NAB.EQ.0)  THEN
           READ(5,*) DV1,DV2,DVIN
              IF (DV1.EQ.0.0) THEN   DV1=0.0001
C
       END IF
C
       READ(5,*) VI,VF,VINC
       IXXI=SAMPL
       NCHJ=OPT4
C
       XIX=(TSTART*IXXI)
C
       WRITE(6,1988) NTRACE,IXXI,NCHJ
1988   FORMAT(/10X,'   NUMBER OF TRACES = ',I2,
     */5X,' NUMBER OF SAMPLES / SEC.= ',I4,
     */1X,'CHANNEL NUMBER TO BE PROCESS = ',I2)
C
       ITINC=TINC
       IF (NAB.EQ.1) WRITE (6,1156) ITINC,N,TSTART
1156    FORMAT(/15X,'TIME INCREMENT = ',I4,' MSEC.'
     */5X,'           WINDOW LENGTH = ',I4,' MSEC.'
     */5X,'TIME TO START PROCESSING = ',F6.3,' SEC.')
C
         IF (NAB.EQ.0) WRITE (6,1157) DV1,DV2,DVIN
1157   FORMAT(//15X,'  INITIAL CONSTANT =',F7.4,
     */15X,'    FINAL CONSTANT =',F7.4,
     */15X,'CONSTANT INCREMENT =',F7.4)
C
       WRITE(6,9990) VI,VF,VINC
9990    FORMAT(//5X,'     INITIAL VELOCITY =',F6.3,' K/SEC.'
     */5X,'       FINAL VELOCITY =',F6.3  ,' K/SEC.'
     */5X,'INCREMENT OF VELOCITY =',F6.3,' K/SEC.')
C
C  Write to file 'outcoh2' processing control parameters.
C
       IF (NAB.EQ.1) WRITE (9,1989) N,ITINC
       IF (NAB.EQ.0) WRITE (9,1563) N,DVIN
C
```

```
1989    FORMAT('"WINDOW (LENGTH, STEP)=',I4,',',I3,' MSEC."')
1563    FORMAT('"WINDOW LENGTH =',I4,'MSEC. CONSTANT INC.
     * =',F5.3,'"')
C
        WRITE(9,4117) VINC
4117    FORMAT('"VELOCITY STEP =',F6.3,' KM/S"')
C
         IF (OPT1.EQ.'REFR') WRITE(9,*)  '"0"'
         IF (OPT1.EQ.'REFL') WRITE(9,*)  '"1"'
         IF (OPT1.EQ.'SPEED') WRITE(9,*) '"2"'
C
        WRITE(9,1315)
1315    FORMAT(/10X,' ---------------------------------  '
     *//10X,' STARTING & ENDING TIMES FOR THE JOB '/)
C
                  CLOSE(9)
C
          DO 11 I=1,NTRACE
C
            READ(5,101) INFILE
        OPEN(UNIT=1,FILE=INFILE)
            READ(1,1) RSN, SSN, AUT,DAT, NCHAN, INST
C
C*********************************************************
C                     checking option 4
C                  -----------------
C       Checking option ( 4 ) for any incorrect input
C        If so, then print warning message and stop
C       the program
C
             IF(OPT4.LT.0.OR.OPT4.GT.NCHAN) THEN
        WRITE (6,5680)
        WRITE (6,1502) NCHAN
1502    FORMAT(5X,' !!!!   ERROR IN CHANNEL NUMBER TO BE'
     */5X,' PROCESSED. THERE IS ONLY (',I3,'  ) CHANNELS'
     */5X,'  IN THE INPUT FILES.'////)
          GO TO 733
             END IF
C
          DO 41 L=1,NCHAN
        READ(1,2) POS(I,L),IGAN(I,L),IPOL(I,L),
     *  ISAMP(I,L),AMPT(I,L)
  41       CONTINUE
C
C   checking the polarity of trace (I) for any error
C   or reverse polarity.
C
        IF (IPOL(I,1).EQ.1)     PC=-1.0
        IF (IPOL(I,1).EQ.0)     PC=1.0
C
        IF (IPOL(I,1).LT.0.OR.IPOL(I,1).GT.1) THEN
        PRINT*,'ERROR IN POLARITY CODE OF TRACE !',INFILE
            GO TO 733
        END IF
C
         II(I)=0
```

```
C
         DO  88 J=1-(ISAMP(I,1)),4500
C
             IF (INST.EQ.'GLAMK2') THEN
       READ(1,7333,END=1000)  (IXT(NJ), NJ=1,NCHAN )
       XT(I,J)=IXT(NCHJ)*PC
C
          ELSE IF (INST.EQ.'GEOSTR'.OR.INST.EQ.'MARS') THEN
       READ(1,7334,END=1000) (IXT(NJ), NJ=1,NCHAN)
       XT(I,J)=IXT(NCHJ)*PC
C
          ELSE
       READ(1,*,END=1000) ( XX(NJ), NJ=1,NCHAN )
        XT(I,J)=XX(NCHJ)*PC
C
          END IF
C
       II(I)=II(I)+1
C
88     CONTINUE
1000   CONTINUE
C
C=============================================================
C          ZERO-CENTER THE DATA & FILTER SECTION
C
C Removing any DC bias on the trace and If 'FILTER' has
C been called , then filter each trace with the filter
C operator generated by program 'fwfir'
C
       KK=IK(I)
C
             DO 83 J=1,KK
          ABC(J)=XT(I,J)
83           CONTINUE
C
       CALL REMAV (KK,ABC)
C
           IF (FIL.EQ.1)  THEN
       CALL PWR2 (KK,ABC,JIL)
       CALL FASTFILT (ABC,JIL,I,ICORR)
          END IF

C
             DO 91 J=1,KK
          XT(I,J)=ABC(J)
91           CONTINUE
C
C=============================================================
C
        CLOSE (UNIT=1)
C
11      CONTINUE
C
C-------------------------------------------------
C   (((   END OF READING AND FILTERING SECTION  )))
C-------------------------------------------------
```

```
C
C
C  XT(I,J) the J-th sample in the I-th channel
C
C   SSK    is  centre of the window, if OPT1 is 'REFR' or
C          'REFL', or  velocity gradient's increment,
C           if OPT1 is 'SPEED'.
C
        NNEW=(N*SAMPL)/1000
C
C  NNEW     window length in samples
C
          DO 900 I=1,NTRACE
               IK(I)=II(I)-ISAMP(I,1)
900        CONTINUE
C
        LESS=IK(1)
C
         DO 808 I=2,NTRACE
           IF( LESS.GT.IK(I) ) THEN
            LESS=IK(I)
           END IF
808       CONTINUE
C
C    TOPI   sample number to stop processing
C    EN1    related time  to stop processing
C    STEP   time increment related to samples
C    XIX    sample number to start processing
C    CONS   sample interval
C
        TOPI=TSTOP*SAMPL
C
        IF (TOPI.GT.(LESS-(NNEW/2))) THEN
          TOPI=LESS-(NNEW/2)
        END IF
C
        EN1=TOPI/SAMPL
C
         IF (NAB.EQ.1) WRITE(6,1920) EN1
1920    FORMAT(/,'PROCESSING ENDS AT TIME =',F6.3,' SEC.')
C
        STEP=(TINC*IXXI)/1000.00
C
        CONS=1000.00/SAMPL
C
              IF (NAB.EQ.0) THEN
         XIX=DV1
         TOPI=DV2
         STEP=DVIN
              END IF
C
C^^^^^^^^^^^^^^^^^^^^^^^^^^^^^^^^^^^^^^^^^^^^^^^^^^^^^^^^^^^^^^^^^^^^^^^^
C                    Computing section
C
C^^^^^^^^^^^^^^^^^^^^^^^^^^^^^^^^^^^^^^^^^^^^^^^^^^^^^^^^^^^^^^^^^^^^^^^^
C
```

```
      DO  2000 SSK=XIX,TOPI,STEP
C
       TK=0.0
C
          IF (NAB.EQ.1)  THEN
                      TK=SSK/SAMPL
                      K=SSK
         END IF
C
          IF (NAB.EQ.0) THEN
                      TK=0.00
                       K=0
         END IF
C
         DO  2001  VEL=VI,VF,VINC
C
            DO  2002  I=1,NTRACE
C
         DTK=0.00
C
            IF (OPT1.EQ.'REFL') THEN
              DTK=(SQRT((TK**2)+(POS(I,1)**2/VEL**2)))-TK
            ELSE IF (OPT1.EQ.'REFR') THEN
              DTK=( POS(I,1) )/ ( VEL )
            ELSE
              PTL=0.00
              SIL=0.00
              ZAK=0.00
              PTL=(SSK*POS(I,1))/(2.0*VEL)
              SIL=LOG(PTL+(SQRT((PTL**2)+1.00)))
              DTK=(2.00/SSK)*SIL
            END IF
C
                MCR=INT(DTK*SAMPL)
C
C   TK   K-th sample equivlant time
C   DTK  delta ( TK )
C   MCR  number of samples relative to ( DTK )
C
       FF1=DTK+TK
       FF2=REAL((K+MCR)/SAMPL)
       FF=((FF1-FF2)*1000.00)/CONS
C
                  DO  2003   J=K-(NNEW/2),K+(NNEW/2)
                             JC=J+MCR
C
C  Checking that the new location of the sample (JC)
C  is within the trace length. If not, write message
C  (4367) and terminate this  (VEL)  loop.
C
       IF (JC.LT.(ISAMP(I,NCHJ)*(-1)).OR.JC.GT.IK(I)) THEN
C
            WRITE (6,4367) TK,VEL,I
4367   FORMAT (/X,'AT TIME =',F7.3,'S. EMPLOYING VELOCITY
     * =',F7.3,'KM/S FOR TRACE No.(',I2,'),  NO DATA'/)
C
```

```
          GO TO 2222
        END IF
C
C    computing the amplitude for (XTC), by linear
C    interpolation.
C
       XTC(I,J)=XT(I,JC)+((XT(I,JC+1)-XT(I,JC))*FF)
C
C  XTC(I,J)  (Jth) sample in the (Ith) trace
C            after correction
2003            CONTINUE
C
2002     CONTINUE
C
C
       SUMS=0.00
       SEMB=0.00
C-------------------------------------------------
C
       IF (OPT2.EQ.'SEMB')  CALL SEMBLANCE1(K,NNEW,NTRACE)
C
C       computing coherency coeff. using
C  *    semblance method    *
C-------------------------------------------------
C
       IF (OPT2.EQ.'UNCR')  CALL SEMBLANCE2(K,NNEW,NTRACE)
C
C       computing coherency coeff. using
C  **   unnormalized crosscorrelation   **
C-------------------------------------------------
C
        IF (OPT2.EQ.'CROS')  CALL SEMBLANCE3(K,NNEW,NTRACE)
C
C       computing coherency coeff. using
C  ***  energy normalized crosscorrelation method   ***
C-------------------------------------------------
C
       IF (OPT2.EQ.'SUMS')   CALL SEMBLANCE4(K,NNEW,NTRACE)
C
C       calculation for coherency coeff. using
C  ****  mean amplitude summation method    *****
C-------------------------------------------------
C
       IF (OPT2.EQ.'STCR')   CALL SEMBLANCE5(K,NNEW,NTRACE)
C
C       computing coherency coeff. using
C ***** statistical normalized crosscorrelation method *****
C-------------------------------------------------
C
       IF (SUMS.EQ.0.00) GO TO 6556
C
           IF (NAB.EQ.1) WRITE(10,99)  TK,VEL,SEMB
           IF (NAB.EQ.0) WRITE(10,99) SSK,VEL,SEMB
C
C
2222    CONTINUE
```

```
C
2001     CONTINUE
C
       WRITE(10,777)
2000    CONTINUE
C
       WRITE(6,5680)
C
       IF (SUMS.NE.0.00) THEN
          WRITE (6,4516)
           GO TO 7189
       END IF
C
4516    FORMAT (/////15X,'*************************')
C
6556   WRITE(6,5551) TK,VEL
5551    FORMAT(//5X,'PROCESSING STOPPED AT',F6.3,' SEC.'
     */,'NO DATA AFTER THIS TIME ',/'VELOCITY USED',F6.3,'
     * KM/SEC. FOR NMO CORRECTION')
C
7189   CONTINUE
C
       CLOSE(UNIT=10)
C*************************************************************
C
       WRITE(6,3971)
C
3971   FORMAT (/3X,'To plot the results',
     */6x,'type  " S "  then  <RETURN>  then  "device"',
     */16x,'eg   tek14,  tek4107,  gould  or  unixplot',
     *//10x,'followed by one of these interactive MACROS',
     *//15X,'?plocon  Display contour map of the results',
     */15X,'?plomax   Display max. coefficient values',
     */15X,'?plospc   Display typical velocity spectra',
     */15X,'?plopek   Display peaks log',
     *///10X,'"device"  refer to the graphical device',
     *//15X,'when plotting to "gould"  or "unixplot"',
     */16X,'use the following forms',
     *//16X,'eg   ?plocon;?gould     ?plospc;?unixplot')
C
C
1      FORMAT (2(A6,2X),A3,2X,A8,I3,2X,A6)
2      FORMAT (F7.3,I3,I2,I6,F7.3)
99     FORMAT ( 3X,F6.3,3X,F8.3,3X,F19.6)
101    FORMAT (A)
5680   FORMAT(20(/))
7333   FORMAT (3I5)
7334   FORMAT (4I5)
777    FORMAT ( 4X,'NA',9X,'NA',17X,'NA')
C
       CALL SYSTEM('date>endfile;cat startfile endfile>tt1')
       CALL SYSTEM('cat outcoh2 tt1>time ; rm outcoh2 ')
       CALL SYSTEM('mv time outcoh2 ;
       rm startfile endfile tt1')
C
       WRITE(6,1314)
```

```
1314    FORMAT(/9X,'NOTE : Processing parameters and timing
     * for the '
     */17X,'job can be found in a file called (outcoh2)')
C
733     STOP
        END
C
C
C-------------------------------------------------
C                 SEMBLANCE METHOD
C-------------------------------------------------
C
C
        SUBROUTINE SEMBLANCE1 (K,NNEW,NTRACE)
        PARAMETER (NS=4500,M=48,ICH=11)
        COMMON XTC(M,-NS:NS),SEMB,SUMS
C
         DO 3 J=K-(NNEW/2),K+(NNEW/2)
           FSUM=0.0
C
               DO 4 I=1,NTRACE
                     FSUM=FSUM+XTC(I,J)
  4            CONTINUE
C
        FSUM=FSUM**2
        SUMS=SUMS+FSUM
C
  3      CONTINUE
C
        IF(SUMS.EQ.0.0) RETURN
C
          SUMB=0.0
C
         DO 5 J=K-(NNEW/2),K+(NNEW/2)
C
             SUMD=0.0
C
               DO 6 I=1,NTRACE
                     SUMD=SUMD+XTC(I,J)**2
  6            CONTINUE
C
         SUMB=SUMB+SUMD
C
  5      CONTINUE
C
           SUMT=NTRACE*SUMB
C
         SEMB=SUMS/SUMT
C
888       CONTINUE
C
        RETURN
              END
C-------------------------------------------------------
C            UNNORMALIZED CROSS-CORRELATION METHOD
C-------------------------------------------------------
```

```
C
      SUBROUTINE SEMBLANCE2(K,NNEW,NTRACE)
      PARAMETER (NS=4500,M=48,ICH=11)
      COMMON XTC(M,-NS:NS),SEMB,SUMS
      DIMENSION SUM(NS)
C
        DO  103  J=K-(NNEW/2),K+(NNEW/2)
C
            SUM1=0.0
                SUM2=0.0
C
             DO 14 I=1,NTRACE
                   SUM1=SUM1+XTC(I,J)
                   SUM2=SUM2+(XTC(I,J)**2)
14          CONTINUE
        SUM1=SUM1**2
                  SUM(J)=SUM1-SUM2
C
103     CONTINUE
              SUMS=0.0
C
            DO 106 J=K-(NNEW/2),K+(NNEW/2)
         SUMS=SUMS+SUM(J)
106         CONTINUE
C
      IF (SUMS.EQ.0.00) RETURN
        SEMB=SUMS*0.5
C
      RETURN
            END
C
C-------------------------------------------------
C             NORMALIZED CROSS-CORRELATION METHOD
C-------------------------------------------------
C
C
      SUBROUTINE SEMBLANCE3(K,NNEW,NTRACE)
      PARAMETER (NS=4500,M=48,ICH=11)
      COMMON XTC(M,-NS:NS),SEMB,SUMS
C
        SUM3=0.0
             SUMS=0.0
C
        DO  108  J=K-(NNEW/2),K+(NNEW/2)
C
            SUM1=0.0
            SUM2=0.0
C
             DO 13 I=1,NTRACE
        SUM1=SUM1+XTC(I,J)
        SUM2=SUM2+(XTC(I,J)**2)
 13            CONTINUE
C
        SUM1=SUM1**2
                  SUMS=SUMS+SUM2
                                SUM3=SUM3+(SUM1-SUM2)
```

```
C
  108     CONTINUE
C
          IF   (SUMS.EQ.0.000) RETURN
               SUMS=SUMS*(NTRACE-1)
C
         SEMB=SUM3/SUMS
C
        RETURN
               END
C
C-------------------------------------------------------------
C                MEAN AMPLITUDE SUMMATION METHOD
C-------------------------------------------------------------
C
        SUBROUTINE SEMBLANCE4(K,NNEW,NTRACE)
        PARAMETER (NS=4500,M=48,ICH=11)
        COMMON XTC(M,-NS:NS),SEMB,SUMS
C
               DO 65234 I=1,NTRACE
                   SUML=0.00
C
          DO 1923 J=K-(NNEW/2),K+(NNEW/2)
                  SUML=SUML+XTC(I,J)
1923      CONTINUE
C
                   SUML=SUML/(NNEW*1.00)
            SUMS=SUMS+SUML
C
65234          CONTINUE
C
          IF (SUMS.EQ.0.000) RETURN
C
               SEMB=SUMS
         RETURN
C
        END
C
C-------------------------------------------------------------
C
C     STATISTICAL NORMALIZED CROSSCORRELATION SUM
C
C-------------------------------------------------------------
C
        SUBROUTINE SEMBLANCE5(K,NNEW,NTRACE)
        PARAMETER (NS=4500,M=48,ICH=11)
        COMMON XTC(M,-NS:NS),SEMB,SUMS
        DIMENSION AK(M)
C
         AKH=2.00/((NTRACE-1)*NTRACE)
C
          DO 391 I=1,NTRACE
        SUNN=0.0
          DO 392 J=K-(NNEW/2),K+(NNEW/2)
           SUNN=SUNN+(XTC(I,J)**2)
392     CONTINUE
```

```
      AK(I)=SUNN
391   CONTINUE
       SUMJ=0.00
C
      DO 1101 J=K-(NNEW/2),K+(NNEW/2)
C
          SUMP=0.00
                DO 2201 IP=1,(NTRACE-1)
                    SUMI=0.00
                         DO 3301 I=1,NTRACE-IP
        AMAG=XTC(I,J)*XTC((I+IP),J)
        SUMS=SQRT(AK(I)*AK(I+IP))
C
      IF (SUMS.EQ.0.0) RETURN
C
              SUMI=SUMI+(AMAG/SUMS)
C
3301                  CONTINUE
           SUMP=SUMP+SUMI
2201            CONTINUE
         SUMJ=SUMJ+SUMP
1101          CONTINUE
C
       SEMB=SUMJ*AKH
C
      RETURN
              END
```

```
C       PROGRM  stk.f
C
C     THIS PROGRAM WILL STACK ALL THE INPUT TRACES
C     AND THE OUTPUT WILL BE ONE TRACE ONLY
C
C
C NOTES :
C-------
C    (1) TRACES MUST NOT BE MORE THAN (( 48 ))
C
C
C    (2) NUMBER OF SAMPLES PER TRACE MUST NOT BE MORE THAN
C        (( 4500 ))
C
C
C  PARAMETER     FORMAT      EXPLANATION
C  ---------     ------      -----------
C   OUTFILE ...    **   .... NAME OF THE OUTPUT FILE
C     NF   ......  **   .... ACTUAL NUMBER OF TRACES
C
C
C_____________________________________________________
C
C              CONTROL FILE
C_____________________________________________________
C
C  LINE 1 :
C----------     THE OUTPUT FILE NAME
C
C  LINE 2 :
C----------     NF   ( NUMBER OF TRACES )
C
C  LINE 3 :
C----------    1st TRACE FILE NAME
C                    .
C                    .
C                    .
C                    .
C  LINE N :
C----------  Nth TRACE FILE NAME
C
C
C
C_____________________________________________________
C
C         READING SECTION
C_____________________________________________________
C
        PARAMETER (ns=8500,m=48)
        DIMENSION xt(m,-ns:ns),II(ns),EK(m)
        DIMENSION pos(m,3),igan(m,3),ipol(m,3),
     * isamp(m,3),ampt(m,3)
        CHARACTER*15 OUTFILE,INFILE
        CHARACTER *8 rsn,ssn,aut,dat,nchan,inst
C
```

```
      READ(5,*) OUTFILE
       OPEN(UNIT=10,FILE=OUTFILE)
C
      READ(5,*) nf
      PRINT*, OUTFILE
      PRINt*, 'NUMBER OF TRACES=',nf
C
        DO 11 i=1,nf
          READ(5,101) infile
C
      OPEN(unit=1,file=infile)
        READ(1,1) rsn, ssn, aut,dat, nchan, inst
C
           DO 41 l=1,3
      READ(1,2) pos(i,l),igan(i,l),ipol(i,l),
     * isamp(i,l),ampt(i,l)
41         CONTINUE
C
      is=isamp(i,1)
      PRINT*,'ISAMP OF TRACE No.',i,'=',is
C
       II(I)=0
            DO  88 j=1-is,8500
      READ(1,*,end=1000) xtrace
C
         IF  ( ipol(i,1).EQ.1 ) THEN
      xt(i,j)=xtrace*(-1)
         ELSE
      xt(i,j)=xtrace
         END IF
C
      II(I)=II(I)+1
C
88         CONTINUE
1000  PRINT*,'No. OF SAMPLES OF TR.',i,'=',II(I)
C
       CLOSE (unit=1)
C
11     CONTINUE
C
      WRITE(10,3)
      WRITE(10,4) pos(1,1)
C
           DO 48 I=1,2
      WRITE(10,5)
 48        CONTINUE
C_____________________________________________________________
C             (( CALCULATION SECTION ))
C
C    xt(i,j) : THE Jth SAMPLE IN THE Ith CHENNAL
C
             DO 953 I=1,NF
                 EK(I)=II(I)-ISAMP(I,1)
 953           CONTINUE
C
        LESS=EK(1)
```

```
C
              DO 956 I=2,NF
C
                IF (LESS.GT.EK(I) )THEN
                LESS=EK(I)
                END IF
C
 956           CONTINUE
       PRINT*,'END OF PROCESSING; AT SAMPLE NUMBER:',LESS
c
         DO  20  L=1,LESS
C
       ISUM=0.0
              SUM=0.0
C
            DO  30  N=1,nf
        SUM=SUM+xt(N,L)
 30     CONTINUE
       ISUM=SUM/NF
       WRITE(10,1988) ISUM,0,0
 20         CONTINUE
C
        print*,'*  OUTPUT FILE NAME IS (( ',OUTFILE,'))  *'
           CLOSE(UNIT=10)
C
1       FORMAT (2(a6,2x),a3,2x,a8,i3,2x,a6)
2       FORMAT (f7.3,i3,i2,i6,f7.3)
3       FORMAT ('SUM ',4X,'WAVE',4X,'EKS',2X,'20-04-88',2X
     *,'3',2X,'GLAMK2')
4       FORMAT ( f7.3,2X,'1',X,'0',3X,'000',2X,'0.000')
5       FORMAT (X,'00.000',2X,'1',X,'0',3X,'000',2X,'0.000')
101     FORMAT (a)
1988    FORMAT (3I5)
C
          STOP
              END
```

```
C       PROGRAM SYNTH.f
C
C  THIS PROGRAM WILL GENERATE RANDOM NOISE BY CALLING
C  MACRO ?noise, IN THE  "S"   PACKAGE AND SIGNAL
C  FOR DIFFERENT: ARRIVAL TIME, FREQUENCY, SPAN,
C  S/N AND SAMPLING RATE.
C
C

        PARAMETER (KN=4000)
        REAL X1(KN),Y(KN)
        INTEGER IX1(KN),IY(KN)
        CHARACTER * 18 A
        CHARACTER * 1 N
C
        WRITE(6,5151)
515     FORMAT(////,' CREATE RANDOM NOISE IN THE " S "'
     *//9X,'BY TYPING   ?noise (time)   THEN   < RETURN >'
     *//9x,'AFTER THE PROMPT >  APPEARS ON THE SCREEN.'
     *//9X,' WHERE  time  IS THE LENGTH OF NOISE IN SECONDS'
     *//9X,' AND   200   IS THE SAMPLING RATE')
C
        CALL SYSTEM ('S ')
C
C
        PRINT*,'NAME THE OUTPUT FILE PLEASE'
        READ*, A
C
      OPEN (UNIT=1,FILE=A)
C
      PRINT*,'IF YOU NEED TITLE AT THE BEGINNING OF THE
     * OUTPUT FILE, THEN TYPE ( yes ).
     * IF NOT THEN TYPE ( no)'
C
      READ*,N
C
        IF (N.EQ.'y') THEN
C
      PRINT*,'TYPE THE DISTANCE FOR THIS TRACE, THE NUMBER
     * MUST BE REAL'
      READ(*,108)DIS
C
      PRINT*,DIS
C
        END IF
C
      SAMP=200.0
      PRINT*,'  '
      PRINT*,'TYPE EVENT S TIME (in sec.) FREQUENCY, LENGTH
     * (in msec.)* & S/N RATIO'
      READ*,T1,F1,L1,Z1
C
      IF (N.EQ.'n') WRITE (1,*) F1
C
      T1=T1*1000
```

```
        PRINT*,'TYPE THE LAST NOISE LENGTH (in sec.)'
        READ*, XL5
C
        XL5=XL5*1000
        PRINT*,'********************************'
C
        OPEN (UNIT=2,FILE="nn1")
C
        JJ=0
           DO 2020 I=1,7000
        READ(2,*,end=91) X1(I)
        X1(I)=X1(I)*2
        JJ=JJ+1
2020        CONTINUE
        print*,'END OF NOISE AT  ',JJ,'LAST SAMPLE VALUE'
     *,'=',X1(JJ)
91      CONTINUE
C
        CLOSE (UNIT=2)
C
            IF (N.EQ.'y') THEN
        DO 6563  I=1,JJ
        IX1(I)=X1(I)*1000
6563    CONTINUE
        print*,'END =',JJ,' VALUE= ',IX1(JJ)
            END IF
C-------------------------------------------------------
C      THIS SECTION TO WRITE THE TITLE ONLY
C-------------------------------------------------------
        IF (N.EQ.'y') THEN
C
        WRITE(1,1)
C
        WRITE(1,2) DIS
C
         DO 10 I=1,2
             WRITE (1,3)
10       CONTINUE
C
        END IF
C
C-------------------------------------------------------
C                CALCULATION SECTION
C-------------------------------------------------------
C
        IFIN1=T1/5
        print*,'END OF FIRST NOISE SEGMENT =',IFIN1
          DO  3030  I=1,IFIN1
            IF (N.EQ.'y') THEN
        WRITE(1,1755) IX1(I),0,0
            ELSE
        WRITE(1,*) X1(I)
            END IF
3030    CONTINUE
C
        SF2=1/F1
```

```
        ASF2=SF2*SAMP
C
        XL2=1000.0/L1
        SR2=F1/XL2
C
          DO 300 I=1,SR2*ASF2
        Y(I)=SIN((I/ASF2)*6.2832)*2*Z1
          IF (N.EQ.'y') THEN
        IY(I)=Y(I)*1000
        WRITE(1,1755) IY(I),0,0
          ELSE
        WRITE(1,*) Y(I)
          END IF
C
 300      CONTINUE
C
        K=T1+L1
        KK=K/5
        NP=XL5/5
        IFIN3=KK+NP
C
             DO 5050 I=KK,IFIN3
          IF (N.EQ.'y') THEN
        WRITE(1,1755) IX1(I),0,0
           ELSE
        WRITE(1,*) X1(I)
           END IF
5050        CONTINUE
C
        CLOSE(UNIT=1)
C
1       FORMAT ('TEST',4X,'WAVE',4X,'EKS',2X,'20-04-88',2x
     *,'3',2X,'GLAMK2')
2       FORMAT( F7.3,2X,'1',X,'0',3X,'000',2X,'0.000')
3       FORMAT (2X,'0.000',2X,'1',X,'0',3X,'000',2X,'0.000')
108     FORMAT (f7.3)
1755    FORMAT (3I5)
C
        PRINT*,'THE OUTPUT FILE NAME IS ',A
            STOP
C
                END
```

# APPENDIX 2. MACROS

```
MACRO  plopek
#
#
print("THIS  MACRO  WILL    PLOT  THE  MAX.  COEFFICIENTS
#         OF  THE  COHERENCY  COEFFICIENT  ",quote=F)
#
#
print("  ",quote=F)
tit<-read("outcoh2")
#
if(tit[3]=="1"){                #      if filter was used
    xman<-read("fwk3")          #      then to read file
#                                       "fwk3",which
    if(len(xman)==6){           #      contains filter
#                                       parameters
#
crh<-(encode(xman[2],xman[3],"Hz"))}
#
          if(len(xman)==8){
crh<-(encode("B.P.   FILTER",xman[3],xman[4],xman[5],"Hz"))}}
#
#
seisn<-matrix(read("outcoh1"),ncol=3,byrow=T)
timf<-seisn[,1]
#
j<-?missing(timf)
seis<-seisn[!j,]
#
tim<-seis[,1]
sc3<-seis[,3]
#
em<-max(sc3)
jj<-c(sc3<em)
mah<-seis[!jj,]   #   mah is the row of the max. coeff.
#
print(encode("MAX.COEFF.=",mah[3],"AT    TIME=",mah[1],"
SEC."),quote=F)
print(encode("  AND  VEL.  =",mah[2],"  KM/SEC."),
quote=F)
#
#
tt<-NULL
vv<-NULL
#
for(i  in  unique(tim))  {
     scmax<-max(sc3[tim==i])
           v<-sc3[tim==i  &  sc3==scmax]
          vv<-c(vv,v)
     tt<-c(tt,rep(i,len(v)))}
#
par(mar=c(9,4.1,4.1,3.1))
par(col=2,lty=1)
#
naj<-tit[8]
if(naj=="0"){
               yyl<-("Time Intercept, Sec.")
                xl<-("Velocity km/s")}
if(naj=="1"){
```

```
       yyl<-("Two-Way Time, Sec.")        #   (lables for
        xl<-("Velocity, km/s")}           #     X-Y axes)
if(naj=="2"){
        yyl<-("Velocity gradient, km/sec./km.")
         xl<-(" Surface Velocity, km/s")}
#
maxco<-max(vv)
yll<-(encode("MAX.  POWER=  ",maxco))
#
#
plot(vv,tt,axes=F,type="l",xlab="  ",ylab="  ")
#
#
par(col=1)
title(ylab=yyl)
mtext(xl,1,2)
axis(1,label=T)
axis(2,label=T)
axis(3,label=F)
axis(4,label=F)
box(2)
#
tit[1]<-("WINDOW  PEAKS  LOG")
ftit<-(encode(tit[5],tit[4]))
#
mtext(tit[1],3,2)
mtext(tit[2],3,1)
#
par(adj=0)
mtext(ftit,1,4)
mtext(tit[6],1,5)
mtext(tit[7],1,6)
mtext(yll,1,7)
#
if(tit[3]=="1"){
                  mtext(crh,1,8)}
#
END
```

```
MACRO  plocon
#
#    THIS  MACRO  WILL  DISPLAY  THE  COHERENCY  COIFFICIENT
#    IN  ONE  FIGURE  BY  TWO  PLOTS  :
#                                        1)   CONTOUR LINES
#                                        2)   WINDOW PEAKS LOG
#
print("       ",quote=F)
print("THIS  MACRO    HAS  THE  OPTION  TO  PLOT  COLOURED
CONTOUR",quote=F)
print("LINES  OR  TO  PLOT  IT  USING  SOLID  DOTTED  &  DASHED
LINES.",quote=F)
#
#
print("       ",quote=F)
print("       ",quote=F)
#                                              * first option *
print("     ENTER:      ",quote=F)
print("                 0    TO  CONTOUR  ALL  COHERENCY  COEFFICIENT
VALUES",quote=F)
#
print("                1    TO  CONTOUR  COEFFICIENTS    >    MEAN
VALUE",quote=F)
#
print("                2    TO  CONTOUR  COEFFICIENTS    >    ( MEAN+MAX.
VALUE)   /   2",quote=F)
#
val<-read(length=1,print=F)
#
#                                              * second option *
print("     ENTER:     ",quote=F)
print("                   THE  APPROXIMATE  NUMBER  OF  CONTOUR
LINES",quote=F)
#
user<-read(length=1,print=F)
#
#                                              * third option *
print("     ENTER:      ",quote=F)
print("                1    TO  PRINT  LABELS  ON  CONTOUR
LINES",quote=F)
print("                0    NO  LABELS",quote=F)
lbs<-read(length=1,print=F)
#
#                                              * fourth option *
print("     ENTER:      ",quote=F)
print("                1    TO  COLOUR  THE  CONTOUR  LINES",
quote=F)
print("                0    TO  USE  SOLID,  DOTTED  AND  DASHED  CONTOUR
LINES",quote=F)
```

```
#
lon<-read(length=1,print=F)
print("       ",quote=F)
print("      PROCESSING STARTS AT      ")
sys("date")
print("       ",quote=F)
#

if(lon==1){
print("ON  THE  PLOTTER  (gould)  USE  :",quote=F)
print("                          HOLE NO. 1   TO PRINT
TITLES",quote=F)
print("                          HOLE NO. 2, 3 & 4   TO PLOT
DIFFERENT  COLOURS",quote=F)
}
#
if(lon==0){
print("  ON  THE  PLOTTER  (gould)  USE  :",quote=F)
print("                 HOLE NO. 1    TO PRINT TITLES",quote=F)
print("                 HOLE NO. 2    TO PLOT DIFFERENT TYPES OF
CONTOUR LINES           ",quote=F)}
#
tit<-read("outcoh2")
#
if(tit[3]=="1"){                # if filter was used
xman<-read("fwk3")              # then to read file
#                                 # "fwk3" which contains,
       if(len(xman)==6){        # filter parameters
crh<-(encode(xman[2],xman[3],"Hz"))}
#
          if(len(xman)==8){
crh<-(encode("B.P.   FILTER",xman[3],xman[4],xman[5],"Hz"))}}
#
seis<-matrix(read("outcoh1"),ncol=3,byrow=T)
#
print("  ",quote=F)
#
i<-?missing(seis[,1])
seisn<-seis[!i,]
z<-seisn[,3]
#
if(val==0){
           se<-seisn
           y1<-se[,1]
           x1<-se[,2]
           z8<-se[,3]
}
#
if(val==1){
z1<-mean(z)   ;     ii<-c(z<z1)
se<-seisn[!ii,]
y1<-se[,1]            # (se) is the final matrix which
x1<-se[,2]            # contains only the desiered
z8<-se[,3]            # coefficients.
}
#
if(val==2){
        z1<-mean(z)   ;   zm<-max(z)
```

```
        av<-((z1+zm)/2)
        ii<-c(z<av)
        se<-seisn[!ii,]
        y1<-se[,1]
        x1<-se[,2]
        z8<-se[,3]
}
#
em<-max(z8)
jj<-c(z8<em)
mah<-se[!jj,]   # mah is the row of the max. coeff.
#
print(encode("MAX.  COEFF.  =",mah[3],"  AT  TIME=",mah[1],"
SEC."),quote=F)
print(encode("  AND  VEL.  =",mah[2],"  KM/SEC."),
quote=F)
#
tt<-NULL
vv<-NULL
for(i in unique(y1)) {          # computing max. coeff.
 scmax<-max(z8[y1==i])          # for each window
      v<-z8[y1==i  &  z8==scmax]
     vv<-c(vv,v)
      tt<-c(tt,rep(i,len(v)))
}
#
fit<-interp(x1,y1,z8)
convals<-pretty(fit$z,nint=user)
convals<-round(convals,3)
inc1<-(convals[2]-convals[1])
inc1<-round(inc1,3)
#                    (contour intervals computation)
maxc<-(max(convals)-inc1)
lmax<-(maxc-(inc1*2))
llmax<-(lmax-(inc1/2))
minc<-(min(convals)+inc1)
#
kk<-c(convals<llmax)                                    set<-
convals[!kk]
#                        (dividing contour intervals
#                         into three sets for different
#                        colours, or types)
convmen<-mean(convals)
mm<-c(convals>=convmen)
set1<-convals[!mm]
#sst<-c((max(set1)-inc1),max(set1))
msst<-c(min(set1)+inc1)
mk<-c(convals>=llmax  |  convals<convmen)
set2<-convals[!mk]
if(len(set2)==0){
         set2<-max(set1)  }
#
print(encode("MIN.  CONTOUR  =",msst),quote=F)
print(encode("MAX.  CONTOUR  =",maxc),quote=F)
print(encode("CONTOUR  INTERVAL  =",inc1),quote=F)
#
par(fig=c(0,0.78,0,1))
par(mar=c(9,4.1,4.1,2.4))
```

```
#
if(lon==1){                              #   colouring option
if(lbs==1){

par(col=2)
contour(fit,v=set,labex=1,axes=F)
par(col=3)
contour(fit,v=set2,add=T,labex=1,axes=F)
par(col=4)
contour(fit,v=set1,add=T,labex=1,axes=F)
}
#
if(lbs==0){
par(col=2)
contour(fit,v=set,labex=0,axes=F)
par(col=3)
contour(fit,v=set2,add=T,labex=0,axes=F)
par(col=4)
contour(fit,v=set1,add=T,labex=0,axes=F)
}}
#
#
if(lon==0){                  #  (different types of lines)
if(lbs==1){
par(col=2,lty=1)
contour(fit,v=set,labex=1,axes=F)
par(col=2,lty=5)
contour(fit,v=set2,add=T,labex=1,axes=F)
par(col=2,lty=4)
contour(fit,v=set1,add=T,labex=1,axes=F)
}
#
if(lbs==0){
par(col=2,lty=1)
contour(fit,v=set,labex=0,axes=F)
par(col=2,lty=5)
contour(fit,v=set2,add=T,labex=0,axes=F)
par(col=2,lty=4)
contour(fit,v=set1,add=T,labex=0,axes=F)
}}
#
#
par(col=1,lty=1)
#
naj<-tit[8]
if(naj=="0"){
               yyl<-("Time Intercept, Sec.")
                xl<-("Velocity, km/s")}
if(naj=="1"){
   yyl<-("Two-Way Time, Sec.")          #   (lables for
    xl<-("Velocity, km/s")}             #    X-Y   axes)
if(naj=="2"){
              yyl<-("Velocity gradient   km/sec./km.")
               xl<-(" Surface Velocity km/s")}
#
title(ylab=yyl)
stit<-(encode("CONTOUR  (MIN,MAX,INT)=",msst    ,maxc    ,incl))
ftit<-(encode(tit[5],tit[4]))
```

```
mtext(xl,1,2)
axis(1,label=T)
axis(2,label=T)
axis(3,label=F)
axis(4,label=F)
box(2)
#
par(fig=c(0,1,0,1))
mtext(tit[1],3,2)
par(cex=1.0,col=1)
#
mtext(tit[2],3,1)
par(adj=0)
mtext(ftit,1,4)
mtext(tit[6],1,5)
mtext(tit[7],1,6)
mtext(stit,1,7)
#
if(tit[3]=="1"){
                    mtext(crh,1,8)
}
#
#           ( plotting window peaks log section )
#
par(new=T)
par(fig=c(0.7,1,0,1))
par(mar=c(9,4.1,4.1,4.1))
par(col=1,lty=1)
#
#
maxco<-max(vv)
yll<-(encode("max.  power=  ",maxco))
#
plot(vv,tt,axes=F,type="l",xlab="  ",ylab="  ")
#
axis(1,label=T)
axis(2,label=F)
axis(3,label=F)
axis(4,label=T)
box(2)
#
par(adj=0)
#
aa1<-("  WINDOW  ")
aa2<-("PEAKS  LOG")
mtext(yll,4,3)
#
mtext(aa1,1,4)
mtext(aa2,1,5)
#
par(fig=c(0,1,0,1))
#
rm(seis,seisn,se,tit,convals,z,z8,y1)
rm(val,lbs,lon,user,incl,maxc,llmax,minc)
rm(ftit,stit,set,set1,set2,mm,kk,i)
rm(tt,v,vv,convmen,mk,naj,xl)
#
print("      ",quote=F)
```

```
print("       PROCESSING ENDS AT       ")
sys("date")
print("       ",quote=F)
#
END
```

```
MACRO  plomax
#
#      THIS MACRO WILL   PLOT THE MAX. COEFFICIENTS
#       OF THE COHERENCY COEFFICIENT
#
#
print("      ",quote=F)
#                                        * first option *
#
print("ENTER:  ",quote=F)
print("       0 TO DISPLAY MAX. COEFF. FOR GIVEN
WINDOWS",quote=F)
print("       1 TO DISPLAY MAX. COEFF. > ARITH. MEAN (MAX.
COEFF.)",quote=F)
print("       2 TO DISPLAY MAX. COEFF. > (HIGHEST MAX.
COEFF.+MEAN)/2",quote=F)
cho<-read(length=1,print=F)
print("      ",quote=F)
#                                          * second option *
#
print("ENTER TYPE OF PLOTTING :",quote=F)
print("                       l     FOR LINES ",quote=F)
print("                      p       "   POINTS",quote=F)
print("                     b       "   BOTH   ",quote=F)
dd<-read(length=1,print=F)
#
#
tit<-read("outcoh2")
#
if(tit[3]=="1"){          #      if filter was used
xman<-read("fwk3")       #      then to read file
                          #          "fwk3",
     if(len(xman)==6){    #      which contains all
#                                   parameters of the filter
crh<-(encode(xman[2],xman[3],"Hz"))}
#
      if(len(xman)==8){
crh<-(encode("B.P.  FILTER",xman[3],xman[4],xman[5],"Hz"))}}
#
seisn<-matrix(read("outcoh1"),ncol=3,byrow=T)
timf<-seisn[,1]
scf<-seisn[,3]
ssmax<-max(scf)
#
ss<-NULL
i<-?missing(timf)
timf2<-timf[!i]
for(i  in  unique(timf2)){
     scmax<-max(scf[timf==i])
     ss<-c(ss,scmax)
}
ssm<-mean(ss)
#
if(cho==0){
           sc2<-0
}
```

```
if(cho==1){
            sc2<-ssm
}
if(cho==2){
             sc2<-((ssmax+ssm)/2)
}
i<-c(scf<sc2)
seis<-seisn[!i,]
ztz<-len(seis)
#
if(ztz==3){
#
print("  ",quote=F)
print("  ",quote=F)
print("     THERE IS ONLY ONE MAX. VALUE SATISFYING YOUR
OPTION,",quote=F)
print("     SO, I'LL CHANGE YOUR   OPTION ",quote=F)
sc2<-ssm
i<-c(scf<sc2)
seis<-seisn[!i,]
ztz<-len(seis)
#
                  if(ztz==3){
print("  ",quote=F)
print("  ",quote=F)
sc2<-0
i<-c(scf<sc2)
seis<-seisn[!i,]}
}
#
if(sc2==0){
intit<-("PLOTTING ALL MAX.  COEFF.  >  0  ")}
#
if(sc2==ssm){
intit<-("PLOTTING  MAX.  COEFF.>  MEAN(MAX.  COEFF.)")}
#
if(sc2==((ssmax+ssm)/2)){
intit<-("PLOTTING  COEFF.  >  (HIGHEST  MAX.COEFF.  +  MEAN)/2")}
#
print(intit,quote=F)
print("  ",quote=F)
print("  ",quote=F)
#
tim<-seis[,1]
vel<-seis[,2]
sc3<-seis[,3]
#
em<-max(sc3)
jj<-c(sc3<em)
mah<-seis[!jj,]# mah is the row of the max. coeff.
#
print(encode("MAX.  COEFF.  =",mah[3],"  AT  TIME=",mah[1],"
SEC."),quote=F)
print(encode("  AND  VEL.  =",mah[2],"  KM/SEC."),
quote=F)
#
tt<-NULL
vv<-NULL
```

```
ww<-NULL
i<-?missing(tim)
tim2<-tim[!i]
for(i in unique(tim2)) {
     scmax<-max(sc3[tim==i])
     v<-vel[tim==i & sc3==scmax]
     vv<-c(vv,v)
          w<-sc3[tim==i & sc3==scmax]
         ww<-c(ww,w)
     tt<-c(tt,rep(i,len(v)))
}
#
#        ********************************************
#
par(fig=c(0,0.65,0,1))
par(mar=c(9,4.1,4.1,1.0))
#
par(col=2)
#
plot(vv,tt,type=dd,axes=F,xlab="  ",ylab="  ")
#
naj<-tit[8]
if(naj=="0"){
              yyl<-("Time Intercept, Sec.")
               xl<-("Velocity, km/s")}
if(naj=="1"){
        yyl<-("Two-Way Time, Sec.")       # (lables for
         xl<-("Velocity, km/s")}          #  X-Y  axes)
if(naj=="2"){
             yyl<-("Velocity gradient,  km/sec./km.")
              xl<-(" Surface Velocity, km/s")}
#
par(col=1)
title(ylab=yyl)
mtext(xl,1,2)
axis(1,label=T)
axis(2,label=T)
axis(3,label=F)
axis(4,label=F)
box(2)
#
tit[1]<-("MAXIMUM COHERENCY COEFFICIENTS DISPLAY")
ftit<-(encode(tit[5],tit[4]))
#
par(fig=c(0,1,0,1))
mtext(tit[1],3,2)
mtext(tit[2],3,1)
#
par(adj=0)
mtext(ftit,1,4)
mtext(tit[6],1,5)
mtext(tit[7],1,6)
mtext(intit,1,7)
#
if(tit[3]=="1"){
                  mtext(crh,1,8)}
#
#================================================
```

```
#
#                * plotting window peaks log section *
#
par(new=T)
par(fig=c(0.6,1,0,1))
par(mar=c(9,4.1,4.1,4.1))
par(col=2,lty=1)
#
#
plot(ww,tt,axes=F,type="l",xlab="  ",ylab="  ")
#
maxco<-max(ww)
yll<-(encode("max.  power=  ",maxco))
#
#
par(col=1)
axis(1,label=T)
axis(2,label=F)
axis(3,label=F)
axis(4,label=T)
box(2)
#
par(adj=0)
#
aa1<-("  WINDOW  ")
aa2<-("PEAKS  LOG")
#
mtext(aa1,1,4)
mtext(aa2,1,5)
mtext(yll,4,3)
#
rm(seis,seisn,tit,maxco,i)
rm(ftit,tt,v,vv,naj,xl)
#
par(fig=c(0,1,0,1))
#
END
```

```
MACRO  plospc
#
#    THIS  MACRO  WILL  DISPLAY  THE  COHERENCY
#    COIFFICIENTS  IN  ONE  FIGURE  BY  TWO  PLOTS  :
#                                    1)   VELOCITY SPECTRUM
#                                    2)   WINDOW PEAKS LOG
#
#  NOTE:
#=====         two  options  avialable;  desiered
#               coefficient  and  scaling  factor.
#
print("  THIS  MACRO  HAS  TWO  OPTIONS:  DESIERED  COEFF.
           AND  SCALING  FACTOR ",quote=F)
#
print("       ",quote=F)
print("    ON  THE  gould,  USE  HOLE  1  TO  TYPE  TITLES  ",quote=F)
print("                          USE  HOLE  2  TO  PLOT  RESULTS  ",quote=F)
print("       ",quote=F)
#                                          * first option *
print("     ENTER:      ",quote=F)
print("             0    TO  DISPLAY  ALL  COHERENCY  COEFFICIENT  VALUES
",quote=F)
#
print("            1    TO  DISPLAY  COEFFICIENTS    >    MEAN  VALUE
",quote=F)
#
print("            2    TO  DISPLAY  COEFFICIENTS    >    ( MEAN+MAX.
VALUE)   /   2",quote=F)
#
val<-read(length=1,print=F)
#
#
print("       ",quote=F)
#                                          * second option *
print("     ENTER:      ",quote=F)
print("                  SCALING  FACTOR     ",quote=F)
#
xx<-read(length=1,print=F)
nn<-c(xx/10)
#
#
tit<-read("outcoh2")
#
if(tit[3]=="1"){                    # if filter was used
          xman<-read("fwk3")        # then to read file
#                                      "fwk3",contains
      if(len(xman)==6){             # filter parameters
#
crh<-(encode(xman[2],xman[3],"Hz"))}
          if(len(xman)==8){
crh<-(encode("B.P.   FILTER",xman[3],xman[4],xman[5],"Hz"))}}
#
seis<-matrix(read("outcoh1"),ncol=3,byrow=T)
#

tm<-seis[,1]
```

```
vl<-seis[,2]
sc<-seis[,3]
#
em<-max(sc)
jj<-c(sc<em)
mah<-seis[!jj,] # mah is the row of the max. coeff.
#
print(encode("MAX. COEFF. =",mah[3]," AT TIME=",mah[1]," 
SEC."),quote=F)
print(encode(" AND VEL. =",mah[2]," KM/SEC."),
quote=F)
#
scmean<-mean(sc)
scmax<-max(sc)
#
if(val==1){xx1<-scmean
                    sc[sc<xx1]<-0}
#
if(val==2){xx1<-((scmean+scmax)/2)
                                sc[sc<xx1]<-0}
#
#
par(fig=c(0,0.78,0,1))
par(mar=c(9,4.1,4.1,2.4))
#
par(col=2)
#
tts<-NULL
          tts<-c(tm+((sc/scmax)*nn))
#
tt<-NULL
vv<-NULL
i<-?missing(tm)
yl<-tm[!i]
scl<-sc[!i]
for(i in unique(yl)) {              #   (computing max.
scmax<-max(scl[yl==i])              #    coeff. for each
     v<-scl[yl==i & scl==scmax]     #    window)
    vv<-c(vv,v)
     tt<-c(tt,rep(i,len(v)))}
#
#
plot(vl,tts,axes=F,type="l",xlab="  ",ylab="  ")
#
naj<-tit[8]
if(naj=="0"){
              yyl<-("Time Intercept, Sec.")
               xl<-("Velocity, km/s")}
if(naj=="1"){
   yyl<-("Two-Way Time, Sec.")       #   (lables for
    xl<-("Velocity, km/s")}          #    X-Y axes )
if(naj=="2"){
              yyl<-("Velocity gradient, km/sec./km.")
               xl<-("Surface Velocity, km/s")}
#
par(col=1)
title(ylab=yyl)
mtext(xl,1,2)
```

```
axis(1,label=T)
axis(2,label=T)
axis(3,label=F)
axis(4,label=F)
box(2)
#
tit[1]<-("VELOCITY  SPECTRUM  ANALYSIS")
ftit<-(encode(tit[5],tit[4]))
stt<-(encode("SCALING  FACTOR=",xx))
#
par(fig=c(0,1,0,1))
mtext(tit[1],3,2)
mtext(tit[2],3,1)
#
par(adj=0)
mtext(ftit,1,4)
mtext(tit[6],1,5)
mtext(tit[7],1,6)
mtext(stt,1,7)
#
if(tit[3]=="1"){
                  mtext(crh,1,8)}
#
#            ( plotting window peaks log section )
#
par(new=T)
par(fig=c(0.7,1,0,1))
par(mar=c(9,4.1,4.1,4.1))
par(col=2,lty=1)
#
plot(vv,tt,axes=F,type="l",xlab="  ",ylab="  ")
#
maxco<-max(vv)
yll<-(encode("max.  power=  ",maxco))
#
par(col=1)
axis(1,label=T)
axis(2,label=F)
axis(3,label=F)
axis(4,label=T)
box(2)
par(adj=0)
#
aa1<-("  WINDOW  ")
aa2<-("PEAKS  LOG")
#
mtext(aa1,1,4)
mtext(aa2,1,5)
mtext(yll,4,3)
#
par(fig=c(0,1,0,1))
#
rm(seis,seisn,se,tit,convals,z,z1,sc,y1)
rm(val,lbs,lon,user,inc1,maxc,llmax,minc)
rm(ftit,stit,set,set1,set2,mm,kk,i)
rm(tt,v,vv,convmen,mk,naj,xl)
#
END
```